EXPERIMENTAL DESIGN OF CONCRETE MIX PROPORTIONING USING SOME INDUSTRIAL BY-PRODUCTS

A Thesis
Submitted in fulfilment of the requirement
For the award of the degree of

DOCTOR OF PHILOSOPHY
IN
CIVIL ENGINEERING

Varinder Kumar Bansal
Registration No. 951102001

DEPARTMENT OF CIVIL ENGINEERING,
THAPAR INSTITUTE OF ENGINEERING & TECHNOLOGY,
(Deemed to be University), PATIALA-147004,
PUNJAB (INDIA)
2020

CERTIFICATE

This is to certify that the thesis entitled "**Experimental design of concrete mix proportioning using some industrial by-products**" being submitted by Varinder Kumar Bansal to the Thapar Institute of Engineering and Technology (Deemed University), Patiala, India, for the award of degree of Doctor of Philosophy in Civil Engineering, is a record of original bonafide research work carried out by him under our supervision and guidance. The matter embodied in this thesis has not been submitted in part or full to any other Institute or University for the award of any degree or diploma.

(Dr. Maneek Kumar)
Professor
Dept. Of Civil Engineering
Thapar Institute of Engineering & Technology (Deemed University)
Patiala-147001
INDIA

(Dr. Prem Pal Bansal)
Associate Professor
Dept. Of Civil Engineering
Thapar Institute of Engineering & Technology (Deemed University)
Patiala-147001
INDIA

(Dr. Ajay Batish)
Professor
Dept. Of Mechnical Engineering
Thapar Institute of Engineering & Technology (Deemed University)
Patiala-147001
INDIA

DECLARATION

I hereby declare that the research work presented in this thesis entitled **"Experimental design of concrete mix proportioning using some industrial by-products"** submitted for the award of degree of Doctor of Philosophy in the department of Civil Engineering, Thapar Institute of Engineering & Technology (Deemed University), Patiala is an authenticated record of my own research work carried out under the supervision and guidance of Dr. Maneek Kumar Professor, Dr. Prem Pal Bansal Associate Professor and Dr. Ajay Batish Professor.

The matter presented in this thesis has not previously been submitted in part or full to any other Institute or University for the award of any degree of diploma in India or Abroad.

(Varinder Kumar Bansal)

ACKNOWLEDGEMENT

First of all I thank the GOD Almighty, whose blessings have given me the strength which enabled me to complete this thesis successfully. I take the opportunity to express my gratitude to my supervisors, Dr. Maneek Kumar Professor, Department of Civil Engineering, Thapar Institute of Engineering & Technology (Deemed University), Patiala, Dr. Prem Pal Bansal Associate Professor, Department of Civil Engineering, Thapar Institute of Engineering & Technology (Deemed University), Patiala and Dr. Ajay Batish Professor, Department of Mechanical Engineering, Thapar Institute of Engineering & Technology (Deemed University), Patiala for their invaluable guidance, moral support and encouragement during the entire period of this research which cannot adequately be expressed in words in this acknowledgement. I extend my heartfelt thanks to my supervisors forever.

I would like to extend my acknowledgement to the entire faculty of the civil engineering department for their valuable suggestions and feedback.

The help and support provided by technical staff Er. Varinder Kumar Sharma and Sh. Ram Sumiran during the entire research period are greatly appreciated.

I also acknowledge the support of facility of SAI labs of Thapar Institute for SEM and XRD analysis.

I also extend my sincere thanks to Dr. Sawarandeep Singh Walia, Sh. Vinod Suri, Sh. Dharam Pal and Sh. Meharban Singh for their whole hearted help.

Special thanks to my wife Nisha Bansal and my sons Kabir Bansal and Gopal Bansal for their patience, understanding and constant support during the whole research work.

(Varinder Kumar Bansal)

ABSTRACT

With ever-increasing quantity of industrial by-products and waste materials being produced regularly, solid waste management has become the principal environmental concern in the world. The use of these materials makes concrete production economical and in addition, helps in resolving their disposal problems. Using varied industrial by-products individually or in combination as a partial replacement material in concrete has been accepted by many codes worldwide. These industrial by-products are known to have pozzolanic and cementitious properties. Several studies have been carried out to investigate the synergic effect of using ternary blends containing different supplementary cementitious materials (SCMs) in concrete. The shortcomings of individual SCMs in meeting multiple and often conflicting demands of concrete properties can be overcome by using combinations of two or more SCMs.

However, the current research work proposes to use a secondary as well as a tertiary combination of these industrial by-products/waste materials to take advantage of their synergic effect. The use of the design of experiments in utilizing the by-products in proportioning concrete mixes is certainly need of the hour. This study is an innovative step towards scientifically applying the Taguchi's experimental design along with Grey Relational Analysis (GRA) for concrete mix proportioning incorporating various industrial by-products in ternary combinations both as a partial replacement of cement as well as fine aggregate.

The study aims at finding the optimal use percentage of some industrial by-products such as fly ash (FA), ladle furnace slag (LFS), copper slag (CS), electric arc furnace slag (EAFS), iron slag (IS) and glass powder (GP) as substitutes to cement and fine aggregates in ternary combinations as well as investigating the effect of these industrial by-products on the strength and durability properties of concrete.

The results obtained from the experiments for strength and durability properties were analysed with ANOVA and Grey Relational Analysis (GRA) method to find the optimal industrial by-products and their percentage replacement for cement and sand. Finally the models were developed using ANN and ANFIS to predict the strength and durability properties.

The results of ANOVA study for strength properties show that the highest compressive strength was achieved by replacing 10% of cement and 30% of sand with by-products at all curing periods. Fly ash was the optimum by-product among the chosen by-products for the replacement of cement to achieve the highest compressive strength and split tensile strength. For all water to binder ratios, the percentage of by-product to be used as binder is the most significant factor that affects compressive and split tensile strengths.

The results of ANOVA for durability properties show that for lowest depth of water penetration in concrete, the optimal combination of by-products are 10% of fly ash as cement replacement and 30% of iron slag as sand replacement at w/b ratio of 0.40 and at 90 days of curing. For lowest depth of

wear in concrete, the optimal combination of by-products are 10% of fly ash and 20% of electric arc furnace slag at w/b ratio of 0.40 and applicable for 28 & 90 days of curing age. Fly-ash and glass powder are the most suitable replacements for cement and sand respectively, at 28 days curing for achieving the lowest depth of water penetration.

GRA for strength and durability properties taken together show that 10% of the fly ash is the optimal parameter for cement replacement for achieving desirable strength and durability properties at all the curing ages and water to binder ratios, whereas, 20% is the optimal replacement level of sand replacement for all the water to binder ratios and at all the curing ages. The confirmation experiment conducted to verify the optimum mix proportions of concrete made with industrial by-products resulted in higher compressive and split tensile strengths and lesser depth of water penetration and wear than all other mixes including the control mixes at 28 days of curing. This improvement in strength and durability properties is attributed to the synergic effect of optimal by-products due to their pozzolanic activity and cementitious properties. Additionally, the SEM images of the concrete containing the optimal parameters of the industrial by-products were compared with the corresponding control concrete SEM image. The microstructure of concrete made with combination of industrial by-products show denser and more uniform structure than the control concrete structure and justifies the improved strength and durability properties.

The XRD spectra shows the existence of hydrated phases such as quartz, calcium hydroxide, calcium silicate hydrates, calcium silicate, ettringites and aluminium oxide silicate. XRD analysis show that the concrete mixture containing industrial by-products has less quantity of calcium hydroxide [Ca(OH)2] than the control mix at 90 days of curing. The Ca(OH)2 present in the mix containing industrial by-products is consumed through the pozzolanic reaction of different by-products, and thus, converted this into calcium silicate hydrate gel (CSH gel) which lends strength and durability to the concrete. This fact helps in improvement of the strength and durability of concrete containing partial replacement materials of cement and fine aggregate than the control concrete.

The neural network and ANFIS models could predict the strength and durability properties of concrete containing industrial by-products with satisfactory performance owing to their distributed and parallel computing nature. The predicted values of the compressive strength of concrete from ANFIS model were found to highly accurate. Moreover, a comparison of the performance indices showed that the ANFIS model provided better results than the ANN model.

CONTENTS

CHAPTER – 1 INTRODUCTION

CHAPTER-2 LITERATURE REVIEW

CHAPTER-3 METHODLOGY & EXPERIMENTAL PROGRAM

CHAPTER-4 ANALYSIS OF RESULTS

CHAPTER-5 MULTI RESPONSE OPTIMISATION

CHAPTER-6 MATHEMATICAL MODELING

CHAPTER-7 CONCLUSIONS

LIST OF FIGURES

LIST OF TABLES

ABBREVIATIONS

Abbreviations		Meaning
ANFIS	-	Adaptive Neuro-Fuzzy Inferencing Systems
ANN	-	Artificial Neural Network
ANOVA	-	Analysis of Variance
ASTM	-	American Society for Testing and Materials
CA	-	Coarse Aggregates
CS	-	Copper Slag
DOE	-	Design of Experiments
dof	-	Degrees of Freedom
EAFS	-	Electric Arc Furnace Slag
EDS	-	Energy Dispersive Spectroscopy
FA	-	Fly Ash
FM	-	Fineness Modulus
GP	-	Glass Powder
GRA	-	Grey Relational Analysis
GRG	-	Grey Relational Grade
IS	-	Iron Slag
LFS	-	Ladle Slag Furnace
MS	-	Mean Sum of Squares
OA	-	Orthogonal Array
OPC	-	Ordinary Portland Cement
P	-	Portlandite

PC	-	Percentage Contribution
Q	-	Quartz
SCM	-	Supplementary Cementitious Materials
SEM	-	Scanning Electron Microscope
SS	-	Sum of Squares
V	-	Variance
w/b	-	Water to Binder Ratio
w/c	-	Water to Cement Ratio
XRD	-	X-Rays Diffraction

CHAPTER 1 INTRODUCTION

1.0 GENERAL

Discussing about construction materials without concrete seems impractical. Concrete has many advantages such as flexibility in shaping, high compressive strength, durability, fire resistance and ease of production and finally, less cost of production over other materials used in construction. The concrete generally consists of cement (commonly called the ordinary Portland cement or OPC), coarse aggregates (crushed gravel), fine aggregates (sand), water and admixtures. Presently, the shortage of cement and sand has been alarming. It is estimated that 5 billion metric tons of cement would be produced by 2030 throughout the world *(Imbabi et al., 2012).*

The manufacturing of OPC requires a specific procedure followed by calcinations of ingredients at 1500° Celsius, and then the grinding of gypsum with clinker. As the production of 1 ton Portland cement needs 4GJ energy approximately, it is called energy intensive process. It is estimated that 5% total worldwide industrial energy is consumed for the production of each ton of OPC. Tables 1.1 and 1.2 highlight its typical chemical and physical characteristics.

Table 1.1: Typical chemical constituents of the cement *(Etxeberria et al., 2010)*

S. No.	Chemical Composition	Value (%)
1.	SiO_2	20.19
2.	Fe_2O_3	3.68
3.	CaO	62.81
4.	Na_2O	0.15
5.	Al_2O_3	5.25

Cement basically contains limestone which on reaction with water releases 1 tonne of CO_2) into the atmosphere *(Etxeberria et al., 2010).* CO_2 being a green house gas, poses a great threat to our environment. Excess of CO_2 in atmosphere absorbs thermal radiations from the planetary surface and re-emanate in all directions in atmosphere and at the same

time directed them back towards the surface of earth. Consequently temperature gets higher than usual.

Table 1.2: Typical physical properties of Cement (as per CEM 142.5 N) ***(Papayianni and Anastasia, 2010)***

S. No.	Characteristics	Value
1.	Initial time setting (min)	125
2.	Specific Surface (m^2/g)	0.962
3.	App. density(kg/m^3)	3140
4.	Expansion(mm)	-
5.	28-day pozzolanicity index (%)	100
6.	Fineness(% retained at 45 µm)	11

The solar radiations cause warming mechanism as described in Figure 1.1. According to an estimate, about 1.6 billion tons of cement is produced all over the world resulting into about 5% global loading of CO_2 into the atmosphere. It will not be wrong to say that CO_2 emission will be 50% more from the present level by the year 2020. Keeping in view these complications, many countries agreed upon diminishing the CO_2 emissions *(Ozer and Ozkul, 2004).*

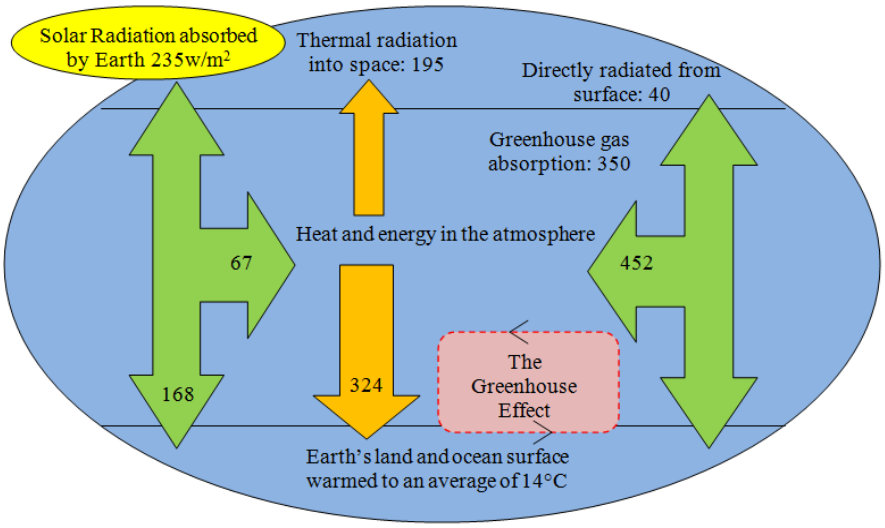

Fig. 1.1: The Green house effect

Even the cost of production of Portland cement is quite high as compared to other replacements such as fly ash, slags etc.

Mining of limestone is also quite hazardous to the environment. This leads to destruction of various landscapes. Soil texture at places near the mines is largely affected due to the processes used in mining. This leads to natural hazards such as landslides etc. These environmental concerns necessitate a reduction of clinker production in the cement industry that is possible only by using the cementitious materials, called the mineral admixtures or pozzolans (also known as supplementary cementing materials) *(Papadakis and Tsimas 2002).* Portland cement contains calcium hydroxide as a hydration product. In order to produce strength products, calcium hydroxide in the concrete is required to be consumed by the pozzolanic materials.

The proportion of C-S-H, calcium hydroxide, sulpho-aluminate and secondary phases remains at 70%, 20%, 7% and 3% respectively which are incorporated into hydrated paste of cement. Calcium hydroxide which adversely affects the properties of concrete, produced due to hydration. Due to its solubility in water and very low strength, it forms cavities *(Oner et al., 2005).* However, the use of minerals admixtures helps to positively augment the quality of concrete by reducing calcium hydroxide *(Memon et al., 2002; Papadakis and Tsimas, 2002).* The cement hydration reaction and pozzolanic reactions are described as below in Eqn. (1.1) and (1.2)

The chemical reaction of cement and water:

Cement + water → CSH gel + calcium hydroxide ---------- (1.1)

Pozzolanic Reaction:

Calcium hydroxide + Mineral admixture → CSH gel --------- (1.2)

Therefore, when mixed with the paste of Portland cement, as a partial substitution/replacement of cement, pozzolanic material reacts with calcium hydroxide; and it leads to formation of CSH gel.

The problems of OPC concrete as discussed above have motivated the researchers to consider alternative materials that are eco-friendly and helpful in developing the concrete production. The appropriate strength required to reduce the energy and the consumption of natural resources and minimum effects on environment have encouraged the

researchers to consider alternative concrete manufacturing that contains pozzolanic materials such as industrial by-products *(Wang, 2001).*These industrial by-products possess sufficient cementitious and pozzolanic properties which make them an excellent alternative material for partial substitution of cement and sand *(Siddique and Mohammad, 2011; Meyer, 2002; Mehta, 2002; Malhotra, 2000).* Hence, replacements for cement with alternative materials have become more of a rule than a choice. Some examples of grain crushed blast furnace slag, fly-ash, ladle furnace slag etc. are enough to be used as replacements for cement and sand.

Grinding has become a critical process to use slag as cementing constituents. The use of these materials will be more helpful in saving the energy which is required for the manufacturing of OPC. It has been observed that the energy consumed in production of ground crushed slag is quite less (i.e.10% approx.) then energy consumed to produce OPC *(Shi and Qian, 2000).* Using these mineral admixtures as alternative for cement in concrete mixture will not only minimise the problems, but helps to enhance the durability of concrete. It is evident from the literature that the Portland fly- ash cement has been successfully developed by using 30% fly ash *(Nazari and Riahi, 2011).* Ultimate strength can be increased with pozzolanic properties of fly-ash. Lessr water content is required by the additional amount of fly ash, therefore, it maintains early strength also. If financially cheap (low in price) and good quality of fly-ash is found, this will be more economical alternative to ordinary Portland cement *(Maslehuddin et al., 2011).*

Like cement, fine and coarse aggregates are another important ingredients in concrete and having about 70 % of volume of concrete *(Devi and Gnanavel, 2014).* Sand is the major constituent of the concrete mix than cement. Availability of fine quality of sand is very difficult because the natural deposits of sand are limited, but on other side, its demand is highly increasing day-by-day, particularly in India. So, a regular increase in demand results into scarcity of good quality sand and also creates critical environmental problem. Therefore, to overcome and control these problems, there is a need to find out other alternatives which can be used in place of sand into cement. A good concrete mixture requires aggregates which must be clean and free of absorbed chemicals *(Papayianni and Anastasia, 2010).*

Due to the increase in industries, the amount of waste material/by-products like slags is also increasing. The use of these materials makes the concrete economical and in

addition, helps in resolving their disposal problems. Using varied industrial by-products individually or in combination as a partial substitute in concrete has been accepted by many codes worldwide. *(Radlinski and Olek, 2012; Erdem, and Kirca, 2008).* The combined usage of different industry by-products in concrete has been wieldy encouraged in construction industry due to their excellent performance in term of strength and durability. This could be due to the synergic/combined effect of all the industrial by-products mixed in the concrete. *(Bagel, 1998; Pandey and Sharma, 2000; Khan and Lyndsdale, 2002).*

Many research studies have been conducted using Fly ash, Glass Powder, Ladle Furnace Slag and Copper Slag individually or in a combination of two as replacement of cement as well as sand. However, the current research work proposes to use a secondary as well as tertiary combination of these industrial by/waste products. The use of design of experiments in utilizing the by-products in proportioning concrete mixes is certainly the need of the hour. This study is a modest attempt towards scientifically applying the experimental design along with Grey Relational Analysis (GRA) for concrete mix proportioning incorporating the various industrial by-products in ternary combinations both as partial substitute of aggregate (fine) and cement.

The main objective of the present research is to find the optimal use of some industry by-products such as fly ash (FA), ladle furnace slag (LFS), copper slag (CS), electric arc furnace slag (EAFS), iron slag (IS) and glass powder (GP) as substitutes to cement and fine aggregates in ternary combinations. It also focuses on finding the effect of these industrial by-products on the split tensile strength, compressive strength and durability of concrete. Thus, the study proposes to generate and analyze the concrete data for its strength and durability using the experimental design.

For the purpose of this present investigation, cement has been partially replaced by FA, LFS and CS using 10%, 25% and 40% replacements. The sand was partially replaced by EAFS, IS and GP, each at 20%, 30% and 40% replacement levels. The experiment plan was designed using Taguchi's orthogonal array varying four factors at three levels each. In the present work, four factors, viz. (i) type of replacement as binder, i.e., FA, LFS and CS; (ii) type of replacement as fine aggregate, i.e., EAFS, IS and GP; (iii) percentage of by-product used as partial cement replacement, i.e., 10%, 25% and 40%; and (iv) percentage of by-product used as partial substitute of sand, i.e., 20%, 30% and 40% were

considered to find their effect on split tensile, compressive strength and durability properties like water permeability and abrasion resistance. The water/binder ratio of 0.40, 0.44 & 0.48; and the curing age of 7, 28 & 90 days were fixed.

1.1 SIGNIFICANCE OF RESEARCH IN INDIAN PERSPECTIVE

The accessibility of cement and superior quality aggregates is descending day-by-day owing to incredible growth in the Indian concrete industry. So, for the manufacturing of cement concrete, we require large volumes of cement and aggregates for fulfilling the demand of the rapid infrastructure development. In order to fulfil the future requirement for cement and aggregates, we will have to identify potential alternative replacement materials for cement and aggregates to fulfil the future augmentation aspiration of the Indian construction industry. Use of various industry by-products such as FA, LFS, CS, EAFS, IS and GP provides a great occasion to consume these waste materials as an option to normally available cement and aggregates. In India, the total steel fabrication is about 95.60 million tonnes, and the waste generated yearly is around 20 million tons (considerably higher than the world average), but hardly 25% is being used mainly in cement manufacture *(Ernst and Young, 2017).*

1.2 USE OF ALTERNATIVE MATERIALS

As the production of cement has badly affected the environment, it is imperative for us to look into alternatives for cement. Already, significant work has been carried out in this field, wherein, many supplementary cementing materials like ladle furnace slag, fly ash, copper slag etc., which are industrial waste materials or industrial by-products, have found their way into concrete. These SCMs possess cementitious as well as pozzolanic properties, and hence, are used as partial replacements for cement and sand which are used as a binder or fine aggregate in concrete respectively. Lot of research has gone into identifying the best alternative for substitute of cement and sand by various SCM's and their probable %age substitution of cement and sand. (SCM's), like fly ash, ladle furnace slag, copper slag, SF or glass powder are some of the most sustainable construction

materials available for use in concrete. Some researchers have even used innovative materials like bamboo as the modern construction materials *(Bhalla S., 2008).*

1.3 USE OF INDUSTRIAL BY-PRODUCTS IN CONCRETE

During the process of manufacturing in the industries, a chemical reaction takes place which leads to the generation of a secondary product called as by-product. Although a by-product is regarded as a waste, yet it is very useful and economical. Industries release a large amount of by-products at the time of manufacturing. Consequently, solid waste material is also released, which causes problems for the environment in the world *(Hisham et al., 2009).* Many alternatives ways have been explored which can be used to reduce the effect of environmental related issues such as creating awareness, inadequacy of land-fill space, its high cost etc. If we want constant development for our country then we will have to discover and find out new solutions to combat high consumption of natural resources and pollution generated in environment *(Rodriguez et al., 2009).*

Although waste materials and by-products are going to be utilized, but it is not a permanent solution to environmental problems. The use of these materials in cement and other construction work is helpful in decreasing the production cost of cement and concrete. It also reduces cost of land filling, saves energy and protects environment from effects of pollution *(Al-Jabri et al., 2011).* Apart from these, there are some other advantages of using waste material, e.g., augmenting the mechanical properties and durability properties of concrete and mortar *(Papayianni and Anastasia, 2010).*

Waste material and by-products are found, generally, in huge quantity and different shapes ranging from dust to boulders. The amount of these by-products is increasing day-by-day resulting into great complications not only for industries even for the environment also. Whereas industrialists have to face many problems in disposing of these materials; and on the other hand, these adversely affect the environment *(Al-Jabri et al., 2011).*

It is not wise to consume natural resources so rapidly despite knowing the fact that their limited quantity would cause serious environmental and socio-economic problems. Some by-products generated from industries could be used in the production of concrete which helps in preservation of natural resources and improving the mechanical properties of

final product *(Papayianni and Anastasia, 2010)*. Whereas usage of these products assists in reducing the price of concrete as well as helps in sustaining the construction materials.

1.4 ADVANTAGES OF USING INDUSTRIAL BY-PRODUCTS

Chemical reactions and manufacturing processes in industries generate the solid waste. It would not be rational to dispose of the solid wastes such as fly ash and slag kinds without their proper use *(Wang, 2001)*.

Fly-ash is an important by-product formed in the process of combustion of coal in industry. The chemical compounds of fly-ash contain mainly silica oxide and calcium oxide depending upon the source *(Maslehuddin et al., 2011)*. As coal includes trace levels of arsenic, thallium, mercury and so on, the ash produced from it will also contain these traces. So, it would not be advisable to dump it or collect it *(Yang et al., 2007)*.

Slag is considered as hyaline by-product of smelting ore separated the metal from undesirable fraction. Generally, it has the composition of metal oxides and silicon dioxide. Slags can also be utilized as an alternate of waste elimination in smelting of metal. There are some other advantages of it also. It controls the temperature of smelting, and minimises any kind of re-oxidation and utilization of solid metal.

Metal extracting industries produce slag in huge amounts. It is difficult to be free from huge amount of slag; consequently, it is of use in the making of roads. But now it is used mostly in making of concrete because of durability properties provided to the structures. Appropriate ratio of mixtures and inter-grinding OPC clinker and crushed slag are used to make slag cement.

1.5 SOURCES OF INDUSTRIAL BY-PRODUCTS/WASTES

The major sources of industrial by-products are as follows:

1. Metallurgical, steel-making industries.
2. Industrial and port/dock cleaning.
3. Mechanical and automobile industries.
4. Basic chemical industries.
5. Oil refining and recycling.

6. Chemical-related and detergents.
7. Power generation.
8. Miscellaneous.

1.6 INDUSTRIAL BY-PRODUCTS IN INDIA

A number of Indian industries produce by-products like steel slag, phosphorus slag, copper slag etc, in bulk. Indian industries such as Tata Steel Plant, Durga Steel Plant and many others as described in Table 1.3 produce a large amount of steel slag every year. Essar Steel Ltd. (Hazira, India) produces EAFS, LFS is produced by industries such as Ghanpati Meta fluxes (Vishakhapatnam, Andhra Pradesh); Cutwin Abrasive Industry (Jamnagar, Gujarat), and KBN Industry (Tirunelveli, Tamil Nadu) produce copper slag; Maalu Ferro Alloys Pvt. Ltd. (New Delhi, India) produce Ferrochromium slag in India.

Table 1.3: Plant-wise capacity of iron and steel slag in the country *(Indian Minerals Yearbook 2018 (Part- II: Metals & Alloys))* (**THM: Tonne Hot Metal)*

S. No.	Plant name	Location	Capacity ('000 tpy) (Year 2017-18)
1.	Tata Steel Ltd.	Jamshedpur, Jharkhand	2100
2.	Rashtriya Ispat Nigam Ltd.	Visakhapatnam, AP	1440
3.	Rourkela Steel Plant	Rourkela, Odisha	1570
4.	IISCO Steel Plant	Burnpur, West Bengal	400 kg per THM*
5.	Visvesvaraya Iron & Steel Plant	Bhadravati, Karnataka	400 kg per THM*
6.	Durgapur Steel Plant	Durgapur, West Bengal	566
7.	Bhilai Steel Plant	Durg, Chhattisgarh	2675
8.	JSW Steel Ltd.	Bellary, Karnataka	NA
9.	Bokaro Steel Plant	Bokaro, Jharkhand	7884
10.	Visa Steel Ltd.	Kalinganagar, Odisha	175
11.	Neelachal Ispat Nigam Ltd.	Kalinganagar, Odisha	-
12.	Sona Alloys Pvt. Ltd.	Satara, Maharashtra	100.82
13.	IDCOL Kalinga Iron Works Ltd.	Barbil, Odisha	53

1.7 DIFFERENT INDUSTRIAL BY-PRODUCTS

In the production process of concrete, main components like cement and sand are possible to be substituted by other materials like copper slag, fly-ash etc. Table 1.4 shows the detail of by-products.

Table 1.4: Various industrial by-products used as binder and fine aggregates

Basic Concrete Materials	Replacement Materials
Cement(Binder)	1. Silica-Fume 2. Fly-ash 3. Blast furnace slag 4. Metakaolin (MK) 5. Glass Powder with lithium nitrate 6. Steel-making slag 7. Rice husk ash 8. Ladle furnace slag 9. Copper slag 10.Cement kiln dust(CKD) 11.Foundry bag house dust 12.Wood ash
Fine Aggregates (sand)	1. Chemical Foundry Sand 2. Green Foundry Sand 3. Poly-Ethylene Terephthalate(PET) 4. Fine Glass Powder 5. Crushed Granite Fine 6. Fly Ash 7. Quarry dust 8. Crumb rubber 9. Copper slag 10. Phosphorus slag 11. Bottom ash 12.Boiler slag 13.Electric arc furnace slag 14. Iron slag

Of all these constituents, the by-products such as LFS, Fly ash and Copper slag have been discussed as Binder; and EAF slag, IS and Glass powder as fine aggregates.

1.8 INDUSTRIAL BY-PRODUCTS FOR REPLACEMENT AS BINDERS

1.8.1 Ladle Furnace Slag (LFS)

The ladle furnace slag is a steel industry by-product which is formed at final stage of steel-making commonly known as secondary process. This by-product contains mainly calcium oxide (CaO). Due to the presence of CaO, it has some cementing properties which project it as a cement replacement in concrete. Table 1.5 highlights the typical physical and chemical characteristics of ladle furnace slag.

Table 1.5: Typical physical and chemical characteristics of ladle furnace slag *(Manso et al., 2011)*

S. No.	Characteristics	Value	S. No.	Characteristics	Value
1.	Apparent density	2.82 Mg per m^3	7.	Fe_2O_3	2%
2.	Specific surface (Blaine value)	265 to 390 m^2 per kg	8.	$\sum$ others ($Mno+TiO_2+SO_3+Na_2O+K_2O$)	4%
3.	CaO	56%	9.	Free lime [$Ca(OH)_2$+ CaO]	11%
4.	SiO_2	17%	10.	Free MgO (periclase)	6%
5.	Al_2O_3	11%	11.	LOI	5%
6.	MgO	10%			

1.8.2 Fly-Ash

The process of coal combustion produces fly ash which is a very important and useful by-product. The fly ash can be stored in huge amount by using many techniques. According to an estimate, about 200 MT of fly ash is being produced in India annually. At the time of combustion of coal process, fly ash got separated in the exhaust gas. The fly ash grains are much finer as compared to other by- product and even finer than lime and OPC. Fly ash contains sediment particles round in shape.

On the basis of composition of the chemicals, fly-ash is, generally of two types, i.e., Class C fly-ash and Class F fly-ash. Both C and F Class fly ashes are taken from sub bituminous, but contain more than 20% calcium oxide (CaO) and less than 10% CaO

respectively. Class C fly ash is having self-cementing properties, while Class F fly ash does not hold this property. The concrete which contains 'F' fly-ash has excellent mechanical properties. Table 1.6 and table 1.7 describe the main properties of fly ash.

Table 1.6: Typical physical characteristics of fly-ash (Class F) ***(Jo et al., 2007)***

S. No.	Property	Value
1.	Sp. Gr.	2.20
2.	Bulk density	995 kg/m^3
3.	Blaine Fineness	310 m^3/kg
4.	Fineness	3150
5.	Pozzolanic activity index	75

Table 1.7: Typical chemical constituents of fly-ash (Class F) ***(Siddique, 2004)***

S. No.	Chemical composition	Value (%)	S. No.	Chemical Composition	Value (%)
1.	Na_2O	0.40	7.	Moisture	0.50
2.	CaO	6.10	8.	Loss on Ignition	0.50
3.	Al_2O_3	27.1	9.	MgO	2.00
4.	Fe_2O_3	5.40	10.	SO_3	1.40
5.	K_2O	0.60	11.	SiO_2+ Al_2O_3+ Fe_2O_3	89.8
6.	SiO_2	57.3	12.	TiO_2	1.30

1.8.3 Copper Slag

It is a by-product produced at the time of conversion of copper metal. Generally, two kinds of liquid phases are to be produced by mattes smelting (dull heating of metal. When the silica is absent, both oxides and sulphides join into ore collectively bond (covalently) Cu-Fe-O-S phase.

In order to stabilize the structure of slag, a definite quantity of aluminium and lime is added. At the temperature of 1000 to 1300° Celsius in the furnace, molten slag is discharged. Therefore, copper slag has low content of calcium oxide (CaO), and thus

having pozzolanic properties. With the increasing of CaO content it shows cementitious properties also. Copper slag is generated at 6-6.5 million tons annually in India. Table 1.8 and 1.9 present it's physical properties and chemical composition respectively.

Table 1.8 Typical physical properties of copper slag *(Brindha et al., 2010)*

S. No.	Physical Properties	Value	S. No.	Physical Properties	Value
1.	Shape of Particles	Non-regular	2.	FM	3.46
3.	Appearance	Black and glassy	4.	Hardness	6-7 mohs
5.	Type	Air cooled	6.	Water absorption	0.3 to 0.4%
7.	Specific gravity	3.91	8.	Moisture content	0.1%
9.	Percentage of voids	43.20%	10.	Fineness of copper slag	125 m^2/kg
11.	Bulk density	2.08 g/cc			

Table 1.9 Typical chemical constituents of copper slag *(Brindha et al., 2010)*

S. No.	Chemical Composition	Value (%)	S. No.	Chemical Composition	Value (%)
1.	Fe_2O_3	68.29	8.	LOI	6.59
2.	SiO_2	25.84	9.	TiO_2	0.41
3.	CaO	0.15	10.	CuO	1.20
4.	Al_2O_3	0.22	11.	Mn_2O_3	0.22
5.	Na_2O	0.58	12.	Sulphide Sulphur	0.25
6.	K_2O	0.23	13.	Insoluble residue	14.88
7.	SO_3	0.11	14.	Chloride	0.018

1.9 BY-PRODUCTS USED FOR REPLACEMENT OF FINE AGGREGATE

1.9.1 Electric Arc Furnace Slag (EAFS)

EAFS is as a by-product of steel-making, is found when the oxidizing process is over. It is of more significance when used as an aggregate in concrete composition. At present, the usage of electric arc furnaces has increased. In order to use it as an aggregate, it is treated before its use. The typical chemical composition and physical characteristics of

electric arc furnace are shown in Table 1.10 & Table 1.11 respectively.

.

Table 1.10: Typical chemical composition of electric arc furnace slag *(Manso et al., 2006)*

S. No.	Chemical Composition	Value (%)	S. No.	Chemical Composition	Value (%)
1.	∑Iron oxides	42.5	7.	SO_3	0.1
2.	SiO_2	15.3	8.	Others (P_2O_5+TiO_2+Na_2O+K_2O)	1.0
3.	CaO	23.9	9.	Free CaO	0.45
4.	$Al2O_3$	7.4	10.	Free MgO	~1.0
5.	MgO	5.1	11.	Glassy phase	<5.0
6.	MnO	4.5			

Table 1.11: Typical physical properties of EAF slag *(Manso et al., 2006)*

S. No.	Property	Coarse slag	Fine slag
1.	Absorption of water	10.5 (%)	-----
2.	Angles loss	<20 (%)	-----
3.	Proportion after primary crushing	76 (%)	24 (%)
4.	Size	4-20 (mm)	0-4 (mm)
5.	Apparent Sp. Gr.	3.35 (Mg/m^3)	3.70 (Mg/m^3)

1.9.2 Iron Slag

Iron slag is also a kind of by-product which results from the conversion of iron. As its chemical composition is not constant but highly variable, likewise its mineral composition is also not constant. Some common minerals like olivine, merwinite and others are also found in steel slag. The presence of a few common minerals confirms that iron slag is a cementitious material.

Some of the countries use iron slag as asphalt concrete aggregate. High content of free CaO may lead to the complications of volume expansion, which is found in iron slag. China has been marketing it for the last 20 years or so. There are many advantages and disadvantages of this kind of cement. Generally, steel-slag cement is used in construction

work, but specifically in production of mass concrete and pavement applications because of its unique properties. The mineral composition of iron slag is changed with its chemical composition. Table 1.12 explains the relationship found between basicity, mineral phase and its reactivity. The basicity of iron slag leads to its reactivity and free-Cao. The C_3S found in iron slag is less than in OPC. Therefore, steel slag can be considered as a weak Portland cement clinker. Its chemical compositions are explained in Table 1.13.

Table 1.12: Basicity, reactivity and mineral constituents of iron slag *(Shi and Qian, 2000)*

Reactivity	**Steel slag type**	**Basicity**		**Main mineral phase**
		$CaO/(P_2O_5+SiO_2)$	**CaO/SiO_2**	
High	C_3S	>2.5	>2.7	C_3S, C_2S, C_2F, C_4AF, and RO phase
Medium	Merwinite C_2S	1.4–1.6 1.6–2.4	1.5–2.7	RO phase C_2S, Merwinite, C_2S and RO phase
Low	Olivine	0.9–1.5	0.9–1.6	RO phase, Olivine and merwinite

Table 1.13: Typical chemical compounds of iron slag (Wang and Yan, 2007)

S. No.	**Chemical Composition**	**Value (%)**	**S. No.**	**Chemical composition**	**Value (%)**
1.	Fe_2O_3	23.86	2.	MgO	10.46
3.	SiO_2	17.09	4.	SO_3	0.00
5.	CaO	40.46	6.	TiO_2	1.00
7.	Al_2O_3	4.53	8.	Loss on Ignition	0.91
9.	Na_2O	0.42			

1.9.3 Glass Powder

The formation of glass occurs when the composition of some specific materials is melted

and then cooling process is followed during which solidification happens without crystallization. Glass is most important usable part in our daily life because a number of products used by us are made up of glass such as bottles, vacuum tubing and so on. Recycling of waste glasses is also possible as fine aggregate. When waste glass powder (WGP) is ground finer than 75 and 45 microns, then it begins to show properties of pozzolanicity and ceases to behave as an ASR aggregate consecutively. Durability of concrete can be represented by ASR. Usage of WGP as a fine aggregate is possible only at being finer than 45 micrometer. Table 1.14 highlights the typical chemical composition of waste glass, while Table 1.15 describes its physical properties.

Table 1.14: Typical properties (chemical) of waste glass *(Park et al., 2004)*

S. No.	Chemical Composition	Type		
		Flint Glass (%)	Emerald Green Glass (%)	Amber Glass (%)
1.	Silica	73.03	71.29	72.09
2.	CaO+ MgO	10.74	12.17	11.50
3.	Cr_2O_3	-----	0.44	0.01
4.	Fe_2O_3	0.05	0.60	0.33
5.	SO_3	0.22	0.053	0.13
6.	$Na_2O+ K_2O$	13.94	13.07	14.11
7.	Al_2SO_3	1.81	2.18	1.74
8.	Grain shape	Angular	Angular	Angular

Table 1.15: Typical properties (physical) of waste glass *(Park et al., 2004)*

Type	Fineness Modulus	Sp. Gr.	Water Absorption (percent)	Absolute Volume (percent)	Unit Weight (kg per m3)
Flint	3.48	2.50	0.43	62.60	1551
Emerald green	3.48	2.50	0.41	61.78	1543
Amber	3.49	2.52	0.40	61.93	1559

1.10 NEED OF TERNARY BLENDED CONCRETE

The alternative materials for Portland cement, having the qualities of strength and durability, have become a part of extensive research globally. A number of alternative materials like fly-ash, copper slag, BFS and others are considered as supplementary cementitious material is reliable and cost effective. Consequently, the use of these have resulted in the development of binary, ternary and tertiary blended concretes based on number of supplementary cementing materials (SCM's). The effect of all the SCM's are put together to make use of ternary blended concrete.

1.11 ADVANTAGES OF USING TERNARY BLENDS

The application of single supplementary cementing material (SCM) in concrete has some limitations to improve the overall performance of concrete. So, more than one SCM is required to be used for enhancing the performance of concrete in various ways. Three kinds of cementitious products are used in ternary concrete mixes. With the usage of two or more SCMs, the weakness of one SCM in improving some specific quality may be offset with the use of another SCM. Some SCMs are good for strength properties of the concrete, while others help to improve durability characteristics of concrete. In this way, the overall performance of the concrete can be improved with the use of binary or ternary SCMs. For example, the addition of an ultra-fine pozzolan, such as silica-fume (SF), to a mix containing BFS can prevent excessive bleeding problems. In a ternary combination of cement, FA and SF system, a synergistic rheological effect was observed in which the FA content offset the increased water demand typically associated with the SF use. The properties such as low permeability, sulphate resistance, and high strength can be possible with the design of ternary mixtures. Use of ternary mixtures in any concrete application, high performance concrete and masonry units is possible to a large extent. There are some examples of high profile structures made by ternary blended mixtures, i.e. New York Bridge Structure, Akashi Kaikyo bridge in Japan, etc.

If we talk about a country like India, it has started paying considerable attention on the use of blended cements for the last few years. Incorporation of SCMs like silica-fume, slag and many others on durability criteria certifies this fact. From the literature it is

found that fly ash can be used at 40%, silica fume at 5-10%, rice husk ash up to 35% and metakaolin at 5-10% replacement of cement.

The incorporation of above mentioned SCMs make the concrete achieve the objectives of sustainability, disposal of waste product from other industries and rendering the environment cleaner, decreasing the raw materials and energy requirement in cement manufacturing, decreasing the consumption of cement in concrete and making concrete durable and thus increasing the service life of construction, and much more than that it satisfies the social obligation *(Bhanumatidas and Kalidas, 2010).*

Every million ton of SCM that supplements OPC

- Reduces depleting limestone (conserves 1.5 million ton of limestone)
- Reduction of industrial waste
- Reduced CO_2 emission (reduces 1 million ton of CO_2)
- Enhancing ecological balance.

Thus, by using ternary or tertiary blends, the following concrete practices are achieved :

- Densifying the concrete by absorption of the surplus lime to form secondary hydrated mineralogy.
- Minimizing the interconnectivity of pores.
- Pore refinement and grain refinement.
- Improved impermeability to resist ingress of moisture and gases.

1.12 SIGNIFICANCE OF THE PRESENT RESEARCH

As industrial by-products and waste materials are increasing rapidly day-by-day, it has become quite difficult to manage solid waste which has posed much environmental related issues in the world. The alternatives such as recycling of by-products and others are very helpful in disposing of the waste materials. By using these materials in concrete, we can handle the disposal problems easily at less cost. Industrial by-products or wastes whether used individually or in combination as partial replacement of concrete making materials has been accepted by many codes worldwide. The use of design of experiments technique in utilizing the by-products in concrete making is certainly the need of the hour. The study is a significant step towards scientifically applying the experimental design for concrete mix proportioning incorporating the various industries by/waste products, both as partial substitution of cement as well as of sand.

1.13 ORGANIZATION OF THESIS

This research work contains seven chapters in all. An outline of every chapter is provided below:

Chapter-1 Introduction

This chapter introduces us to the thrust area by explaining the need for research, industrial by-products, physical properties and chemical composition of different industrial by-products, importance of ternary blended concrete, advantages of ternary blends, synergistic action of industrial by-products, significance of the research have been briefly discussed.

Chapter-2 Literature Review

This chapter is focused on reviewing the relevant literature for various industrial by-products used as cement and fine aggregates replacement, Literature for Taguchi design of experiments, literature related to ANN and ANFIS modeling, gaps in the research and objectives of the research.

Chapter-3 Methodology and Experimental Program

This chapter provides a detail about the design of experiments using Taguchi's method, input factors/parameters with their levels, scheme of experiments, materials used and their characterisation, concrete mixtures cast using different combinations of industrial by-products, techniques adopted for casting and testing of samples and the various test results.

Chapter-4 Analysis of Results and Discussion

This chapter presents the analysis of results using ANOVA and discussion on durability and strength properties of concrete to find the optimal parameters. It also makes experimental validation of the results.

Chapter-5 Multi Response Optimisation

This chapter presents multi response optimisation using Grey relational analysis (GRA). The four responses (split tensile strength, compressive strength, depth of wear and depth of water penetration) were optimised using GRA coupled with Taguchi design of experiments. SEM and XRD analysis has been made in support of confirmation experiments.

Chapter-6 Mathematical Modeling

This chapter takes up the development of mathematical model by artificial neural networks (ANN) and ANFIS for prediction of strength and durability properties of concrete containing industrial by-products within the range of parameters used. Artificial neural networks (ANN) and ANFIS coupled with Taguchi approach were applied for the prediction of compressive strength, split tensile strength and depth of wear of concrete.

Chapter-7 Conclusions

This chapter presents the summary of the research work by presenting the conclusions of the present study. It also gives suggestions for further work in the related area.

CHAPTER 2 LITERATURE REVIEW

2.0 INDUSTRIAL BY-PRODUCTS

There has been tremendous development in the industrial sector in India, but it has also resulted in producing large quantities of solid waste materials. The disposal of these solid waste materials has become a great environmental issue. So, we need to uset these waste materials in a more productive way rather than dumping these into the open space. Disposal of these materials need to be made without harming the environment. We must have the productive use of solid waste materials. The utilization of these materials can be maximized through their physical and chemical properties. The use of these materials in the concrete industry would be the best choice. Governments should give economic incentives for the management of the solid waste materials in a more beneficial way *(Regev et al., 2014).* These waste materials can be used as a partial substitute of cement and aggregates in cement concrete.

In the published literature, industrial by-products like fly ash (FA), ladle furnace slag (LFS) and copper slag (CS) have been targeted for their use as partial replacement of cement in manufacturing of concrete and Glass powder (GP), Electric arc furnace slag (EAFS) and Iron slag (IS) have been tried as partial substitution of fine aggregate in the production of concrete. This chapter is focused on reviewing the available literature in the area under stydy. Many of these industrial by-products have not been used in ternary combinations as a partial substitute of cement and sand, but some researchers have used certain industrial by-products in binary combinations for the same purpose.

The industrial by-products used individually or in combination as a replacement of binder, i.e., cement and fine aggregate, i.e., sand are as follows:

1. Fly Ash
2. Ladle furnace slag
3. Copper slag
4. Glass powder
5. Electric arc furnace slag
6. Iron slag.

2.1 INDUSTRIAL BY-PRODUCTS AS REPLACEMENT OF CEMENT

2.1.1 Fly Ash

Wang (2001) studied the effect of fly ash in concrete to the mechanical properties of frame concrete. Experiments were conducted for the water /binder ratios from 0.30 to 0.42 and fly ash to binder ratios from 0% to 30%, as per the theory of concrete framework model. The compressive strengths of frame concrete and corresponding mortar matrix were observed at 28/56/90 days. The 28-days compressive strengths of concrete and mortar matrix decreased with the addition of fly ash at early age, but increased at 56 & 90 days. This increase occurred because of the pozzolanic reaction of the concrete. The study provided that the optimum value of fly ash was not constant, but it depended on the water to cementitious materials (w/cm) ratio of the concrete mix.

Siddique (2004) investigated the effect of large quantities of Class F fly ash as a partial substitute of cement at 40%, 45%, & 50% level. Experiments were performed to find the fresh concrete properties such as air content, slump, temperature and unit weight. The study also determined the hardened concrete properties such as compressive, splitting tensile and flexural strengths, modulus of elasticity, and abrasion resistance till one year. It was found that with the use of high volumes of Class F fly ash as a partial substitute of cement in concrete , there was a decrease in 28-days split tensile, compressive, modulus of elasticity and flexural strength, abrasion resistance of the concrete. However, there was an increase in all these strength properties and abrasion resistance at the ages of 91 & 365 days. This increase in properties was because of the the pozzolanic reaction of fly ash. The study brought out that Class F fly ash can be effectively used up to 50% level as a cement substitute in concrete.

Jiang et al. (2004) studied the effect of large quantities of low-quality fly ash (LVLQFA) in concrete on carbonation, corrosion of steel reinforcement in concrete. The results of the test showed that the LVLQFA concrete with an activator has improved carbonation and corrosion resistances of steel reinforcement. The corrosion resistance of LVLQFA concrete is more than that of the control concrete. The concentration of CO_2 used in the experiment had a considerable effect while estimating the carbonation resistance of LVLQFA concrete. The carbonation resistance of LVLQFA concrete improved for using an activator. The carbonation resistance of LVLQFA concrete with an activator was similar to that of the control concrete.

Atis (2005) conducted laboratory experiments to assess the strength of roller compacted and superplasticised workable concrete with high-volume fly ash (HVFA); and cured at moist and dry curing conditions. Concrete mixtures were made with two different low-lime Class F fly ashes with 0%, 50% & 70% substitution of OPC. Water/binder ratios ranged between 0.28 and 0.43. The compressive and splitting tensile strengths were also measured. The relationship between the split tensile and compressive strengths was studied. The study concluded that development of high-strength concrete was possible due to high-volume fly ash. HVFA concrete was more vulnerable to dry curing conditions than normal Portland cement concrete. It was further found that HVFA concrete can be used for both structural and pavement applications.

Jo et al. (2007) investigated the properties of hardened paste of fly ash and determined its possible use in the production of lightweight aggregates. The maximum compressive strength was measured at 33.9 MPa, for paste containing 10% of NaOH, 15% of sodium silicate, and 5% of MnO_2, cured at room temperature after 24 hours of moisture curing at 500 ^{o}C. The hardened paste was grounded to make AFLA (alkali-activated fly ash lightweight aggregate). The properties of ALFA like specific gravity (SSD, OD), unit weight, water absorption and solid volume percentages of 1.85 (SSD) were 1.66 (OD), 11.8%, 972 kg/m^3, and 58.6%, respectively. The concrete made with AFLA measured a compressive strength of 26.47 MPa and good freeze–thaw resistance at 6.0% entrained air content.

Sahmaran et al. (2009) examined the mechanical properties of SCC which had more percentages of low-lime and high-lime fly ash (FA) as a replacement of cement at 30%, 40%, 50%, 60% and 70% by weight. A control SCC mixture without any FA was also produced to compare the results. The fresh properties of the SCCs like segregation ratio, slump flow time and diameter, L-box height ratio and V-funnel flow time were evaluated. The hardened properties were compressive strength, split tensile strength, drying shrinkage and transport properties (absorption, sorptivity and rapid chloride permeability tests) up to 365 days. The study found that it was possible to produce SCC with a 70% of cement substitution by both types of FA. The use of high volumes of FA in SCC led to improve the workability and transport properties. The compressive strength at 28 days was between 33 and 40 MPa. It was more than the compressive strength for normal concrete (30 MPa).

Nochaiya et al. (2010) investigated the properties of normal consistency, setting time, workability and compressive strength of Portland cement–fly ash–silica fume systems. An increase was noticed in the water requirement for normal consistency with increasing content of SF, whereas there was a decrease in initial setting time. Workability in term of slump value, was decreased with silica fume content (compared to concrete without silica fume). However, the workability of Portland cement–fly ash–silica fume concrete in most cases was more than that of the control concrete despite reduction in the slump values. The use of silica fume with fly ash increased the compressive strength of concrete at early ages (pre 28 days) at 10% silica fume. The SCM micrograph shows much denser microstructure with utilization of fly ash with silica fume, which led to increase the compressive strength.

Thomas (2011), in his research paper, reviewed that the damages resulting from alkali silica reaction can be reduced by using fly ash and other supplementary cementitious materials (SCMs) in concrete.

Bagheri et al. (2013) studied the use of fly ash (fine) in binary and ternary blends to overcome its property of slow rate of strength development in concretes containing conventional fly ashes and enhancing the durability also. They concluded that the reaction of the pozzolanic reaction of fine fly ash was slightly greater than conventional fly ash; and the water demand was also slightly reduced. The results of ternary blends showed that fine fly ash was not effective for increasing development rate of properties in concretes containing slow reacting conventional fly ashes. The results of tests conducted to check the durability of concrete such as RCPT, RCMT and electrical resistivity depicted that the use of this material failed to improve the concrete durability as can be achieved by conventional fly ash at equal replacement levels.

Anastasiou et al. (2014) examined the possibility of making concrete containing higher content of industrial by-products and secondary materials. The materials taken for the purpose were fly ash as a binder for cement replacement, recycled fine aggregate originating from mixed construction and demolition waste and steel slag as coarse aggregate replacement. Various concrete mixtures were prepared using different aggregate and binder combinations. These were tested for strength at different curing periods. The durability properties such as chloride ion penetration and freeze–thaw resistance were also investigated. The study found that the use of fine construction and demolition waste aggregate enhances porosity in concrete and also

decreases strength and durability. Concrete containing construction and demolition waste as fine aggregate and steel slag as coarse aggregate resulted in 30 MPa 28-day compressive strength. Also, concrete of sufficient strength can be made with 50% cement replacement with high calcium fly ash and use of only steel slag and recycled aggregates.

Kumar R. et al.(2014) investigated the strength and durability properties of SCC with lime stone quarry fines and fly ash as filler. The study found that there was improvement in abrasion resitance, compressive strength of SCC made with mineral admixtures than control concrete.

Wang et al. (2015) presented a numerical procedure to find the compressive strength development using high volume fly ash (HVFA) in concrete. The procedure starts with a blended hydration model considering cement hydration, fly ash reaction, and interactions between cement hydration and fly ash reaction. The hydration model was used and the hydration degree of cement and reaction degree of fly ash was determined as functions of curing period. Besides, calcium-silicate-hydrate (C-S-H) contents of hardened HVFA concrete were calculated by reaction degrees of binders and mixing proportions of concrete. The compressive strengths of HVFA concrete were ascertained using CSH contents. The numerical procedure proposed is valid for concrete with different w/b ratios and different fly ash contents.

Celik et al. (2015) studied the properties of highly flowable self-consolidating concrete (SCC) mixtures made with high proportions of fly ash as cement replacement materials and pulverized limestone instead of high dosage of a plasticizing agent. Self-consolidating concrete mixtures are extensively used for the construction of highly reinforced complex concrete elements and also in massive concrete structures e.g. dams and thick foundation. SCC mixtures with different strength values were produced by varying the proportion of Portland cement (OPC), Class F-fly ash (F), and limestone powder (L). The properties of both fresh and hardened concrete were determined. It was concluded that high volume of the OPC with F, or F and L, up to 55% by weight replacement made highly workable concrete that had high 28-day and 365-day strength, and extremely high to very high resistance to chloride penetration along with low GWP for concrete production.

Chousidis et al. (2015) investigated the effect of Greek fly ash as a partial substitution of cement, on the durability and mechanical resistance of reinforced concrete immersed in sodium chloride (NaCl) solution. The Greek fly ash was used at 5% and 10% by weight as cement replacement. The compressive strength was measured after partial immersion in 3.5% w.w

NaCl solution. Besides, the anticorrosive effect of fly ash was also determined by measuring open porosity and sorptivity, chloride concentration and mass loss of steel reinforcement embedded in cement mortars. The study concluded that the use of Greek fly ash enhances the compressive strength and elastic modulus of concrete at all ages. Further, the porosity and sorptivity were decreased in the presence of the Greek fly ash.

Rivera et al. (2015) produced high volume fly-ash concrete which maximized the use of FA in concrete as both a cement and aggregate replacement. The compressive strength was greater than 30 MPa with concrete containing as much as 728 kg of FA per cubic meter. The permeability measured was low in terms of chloride ion permeability (2300C at 56 d).

Shaikh et al. (2015) examined the effect of high volume ultrafine class F fly ash as partial substitution of cement taking into account the compressive strength and durability properties of concrete. The compressive strengths were measured at curing periods of 3, 7, 28, 56 & 90 days; and the durability properties were measured at curing periods of 28 & 90 days. The durability properties included water sorptivity, the chloride induced corrosion, volume of permeable voids, chloride ion penetration, chloride diffusivity and porosity. Microstructural analysis was also made to identify the reaction phases of calcium hydroxide in the concrete containing UFFA. It was concluded that the addition of 8 % UFFA led to highly improve the early age as well as later age compressive strengths of ordinary and HVFA concretes. All other durability properties of HVFA concretes were also improved. The HVFA concrete containing 32% fly ash and 8% UFFA showed superior durability properties than control concrete. It was also found that more C–S–H gel was produced in HVFA concrete than the control concrete by consuming calcium hydroxide (CH) in HVFA concretes.

Kapoor et al. (2016) reported the mechanical and durability properties of SCC made with mineral admixtures at 0%, 50% and 100% replacement of cement and coarse aggregates. The study showed the improvement in water penetration depth in SCC containing mineral admixtures than plain concrete.

2.1.2 Ladle Furnace Slag

Rodriguez et al. (2009) studied the effect of ladle furnace slag as a partial substitute of cement and sand in mortar. As much as 30% LFS as cement substitute and 25% LFS as sand substitute in the mortar was found by the authors from the laboratory experiments. The study established

that there was increase in the strength of mortars made by using LFS for 7 to 270 days. The additions of LFS also improved the workability in masonry mortars. This produced useful mixtures for the construction industry. Furthermore, the addition of LFS improved the volumetric efficiency of the fresh mortar by approximately 40%.

Setien et al. (2009) performed the ladle furnace slag characterization with X-ray diffraction (XRD) and scanning electron microscopy (SEM with an energy dispersive X-ray (EDX) microprobe. It was concluded that LFS had the quality of developing certain cementitious hydraulic properties; and it could be useful in construction and civil engineering applications. LFS reacts with atmospheric moisture spontaneously at room temperature. This reaction with atmospheric moisture caused its hydration and which can cause volumetric changes and strength gain. So it should be carefully used in mortars and concrete.

Papayianni and Anastasia (2010) examined the use of industrial by-products in concrete production as both binder and aggregate replacement. Cement was replaced by 50% with fly ash and sand by 30% with ladle furnace slag. The coarse and fine aggregate was replaced by Arc furnace slag. After that, tests were performed on the specimens made fron such concrete. The tests were performed for unit weight, compressive strength, splitting tensile strength, and flexural strength. Durability property tests such as Water penetration under pressure, abrasion resistance, freeze–thaw resistance, porosity and microstructure were also conducted. It was found that 28-day strength of the concrete made with 30% slag as cement replacement was the same as that of conventional concrete. The concrete mixtures containing both supplementary cementitious materials and slag aggregates showed high-strength (>70 MPa). The durability properties were also improved with the use of high volume of HCFA or LF slag as binder and EAF slag aggregates.

Manso et al. (2011) investigated the behaviour and use of ladle furnace slag in mortars in aggressive environments and compared it with the conventional mortar mixes. The mortars made with LFS were tested for density, strength, porosity, microstructure and permeability. It was found that 30% by weight replacement of cement by LFS had 7.5 MPa of mechanical strength. It was concluded that the preparation of masonry mortars, including ladle furnace slag (LFS) as a significant substitute (in this case about 22% of total mortar weight) resulted in savings of sand and cement, and produced high quality mortar which satisfied the standard requirements for masonry mortar in terms of density, strength, porosity and permeability.

So, LFS mortars showed similar behaviour as conventional mortars in different aggressive environments.

Adolfsson et al. (2011) examined the hydraulic properties of ladle furnace slag (LFS) for using LFS as a cement substitute in certain applications. The difference between LFS and basic oxygen furnace slag (BOS) is the high content of calcium aluminates present in the LFS. The aluminium is used as a de-oxidation agent which contributes in the formation of calcium aluminates like mayenite ($C_{12}A_7$), and tri-calcium aluminate (C_3A) in the solidified slag. The calcium aluminates are highly hydraulic, and react very quickly with water, especially mayenite. So, the hydration of different calcium aluminates in water formed hydrates such as C_2AH_8, C_4AH_{13}, CAH_{10}, and C_3AH_6, which gave strength to the material. Among these hydrates, only C_3AH_6 is thermodynamically stable. By doing this, all the other hydrates convert to C_3AH_6 as a final product. This conversion process can adversely affect the final strength of the material. This implies that the slag should be carefully handled in order to avoid its instant reaction with atmospheric moisture.

Saez-de-Guinoa Vilaplana et al. (2015) studied the use of Ladle Furnace slag as a raw material for the production of Portland cement. Various material compositions were used to manufacture clinker and cement at the laboratory scale. The chemical and mineralogical analysis results described that the use of Ladle Furnace slag to produce Portland cement had not affected the mineralogical properties negatively. Furthur, the compressive strength and volume expansion were positively affected while using 39.2 wt. % slag into the raw material. However, the samples containing slag required slightly higher initial setting time due to the amount of MgO in the cement. It was concluded that Ladle Furnace slag could be used as a raw material in the production of Portland cement. This could help to save the consumption of natural raw materials, energy and CO_2 emissions by the cement and concrete industry.

2.1.3 Copper Slag

Tixieret et al. (1997) attempted to find the effect of copper slag as partial substitution of cement on the mechanical properties of cementitious mixtures, and found that copper slag significantly improved the compressive strength of concrete mixtures.

Moura et al. (1999) examined the compressive and flexural strength of concrete by replacing 10% of cement by copper slag. It was found that concrete with copper slag had lesser compressive strength than that of control concrete up to 91 days. It further concluded that the flexural strength of concrete prepared with copper slag was similar to that of the concrete prepared without copper slag for water to cement ratio between 0.4 and 0.5.

Arino and Mobasher (1999) in their research work, took 15% copper slag as a cement substitute at water to binder ratio of 0.4 to prepare mortar specimens. The compressive strength of copper slag concrete was greater than ordinary Portland cement concrete, but it was more brittle than control concrete. The enhanced brittleness of concrete was because of copper slag presence which was confirmed by the fracture test. Copper slag with 19% CaO exhibited good cementitious property under the activation of NaOH. Further, the corrosion resistance of copper slag mortars was higher as compared to plain Portland cement mortars. It was found that the strength of copper slag mortar was lesser than that of the control mortar. An optimum strength performance of the copper slag mortars containing 5 to 7.5% copper slag by cement weight was reported. In another study, it was found that the replacement of 10–15% cement clinker significantly increased the abrasion resistance of the cement mortar without affecting much compressive strength.

Al-Jabri et al. (2006) investigated the effect of copper slag (CS) and cement by-pass dust (CBPD) addition on concrete properties. Two separate trial mixtures were prepared in addition to the control mixture by using different quantities of CS and CBPD. CBPD was used as an activator. As much as 5% Portland cement was replaced by copper slag in one mixture. The other mixture was prepared by taking 13.5% CS, 1.5% CBPD and 85% Portland cement. Three water-to-binder (w/b) ratios of 0.5, 0.6 and 0.7 were studied. Concrete cubes, cylinders and prisms were casted and tested for strength after 7 and 28 days of curing. The modulus of elasticity of these mixtures was also examined. It was concluded that 5% copper slag as Portland cement replacement provided the same strength as the control mixture, especially at low w/b ratios of 0.5 and 0.6. The copper slag replacement of 13.5% showed less strength values. The stydy further showed that the use of CS and CBPD as partial substitutes of Portland cement had no significant effect on the modulus of elasticity of concrete.

Al-Jabri et al. (2009) studied the effect of using copper slag as a substitute of sand on the properties of high performance concrete (HPC). Sand was replaced from 0% to 100% with

copper slag thus making eight concrete mixtures. These concrete mixes were tested to know about their workability, density, compressive strength, tensile strength, flexural strength and durability. It was found that in comparison to the control mix, there was an increase of 5% in the HPC density with the increase of copper slag content, whereas there was a sharp increase in the workability with increases in copper slag %age. The addition of up to 50% copper slag as sand substitute produced comparable strength as compared to the control mix. The study concluded that 40% by weight of copper slag could be used as a good substitute of sand.

Wu et al. (2010) revealed the optimal content of copper slag subsitution as a fine aggregate to attain a high strength concrete which could perform equally or greater than the control concrete. Mechanical properties like compressive strength, flexural and splitting tensile strength were measured by experiments. It was found that the properties of copper such as smooth glassy surface texture and low moisture absorption, and excellent compressibility can enhance the workability of concrete. The compressive, flexural and splitting tensile strength decreased due to the presence of excess water, and ferric oxide content. The study brought out that less than 40% copper slag as sand replacement can attain a high strength concrete better than the control mix.

Brindha et al. (2010) conducted their experimental study to ascertain the performance of concrete containing copper slag as partial subsitution of sand and cement. M20 grade concrete was used and compressive strength, split tensile strength tests were conducted. The sand was replaced with copper at 0%, 20%, 40%, & 60% , cement by 0%, 5%, 15% & 20% and a combination of both (85% cement+15% copper slag for cement and 60% sand + 40% copper slag for fine aggregate) in concrete. The study showed that compressive, split tensile strength of concrete increased with an increase in the percentage of slag added by weight of sand up to 40% of replacement and 15% of cement. Water absorption of S40 copper slag concrete specimens was 22% lesser than the controlled specimens. Water permeability in concrete came down up to 40% with subsitution of sand by copper slag. The resistance against sulphate attack was higher with addition of copper slag as a sand subsitution, while addition of copper slag as cement subsitution showed lesser resistance. It was observed that the concrete containing copper slag was found to be slightly low resistant to the H_2So_4 solution than the control concrete.

Al-Jabri et al. (2011) tried to find the effect of copper slag subsitution as a fine aggregate on the

strength and durability properties of cement mortars at different curing periods. The workability and density of concrete and compressive strength of concrete, tensile and flexural strength of concrete mixtures was tested. Initial surface absorption and total absorption tests were also conducted to ascertain the durability of concrete made with copper slag. Fine aggregates i.e. sand was substituted with copper slag from 0% to 100%; and accordingly, different mortar and concrete mixtures were prepared. The results concerning cement mortars showed that all mixtures with different copper slag proportions produced comparable or higher compressive strength than that of the control mixture. Further, the compressive strength of mortars with 50% copper slag replacement increased by 70% as compared to the control mixture. The workability improved significantly with an increase in copper slag percentage. A substitution of up to 40 to 50% copper slag as sand substitution yielded comparable strength to that of the control mixture. However, the strength decreased with the addition of more than 40% of copper slag. This could be due to increase in the free water content in the mix. Thus up to 40 to 50% (by weight of sand) of copper slag can be used as a substitution for fine aggregates in order to get a concrete having good strength and durability.

2.2 INDUSTRIAL BY-PRODUCTS FOR REPLACEMENT AS FINE AGGREGATE

2.2.1 Glass Powder

Shayan and Xu (2004), in their study, focused on the utilization of glass in concrete as cement and sand replacement. The research included coarse glass aggregate, fine glass aggregate and glass powder (GLP). It was found that their presence led to beneficial pozzolanic reactions in the concrete and could be used up to 30% of cement in some concrete mixtures with adequate strength development. The drying shrinkage of the concrete mixes was well below the limit of 0.075%. The study also provided that 30% GLP could be incorporated as cement or aggregate replacement in concrete. Both fine and coarse aggregates could be subsituted up to 50% in concrete of 32-MPa strength grade with required strength properties.

Chen et al. (2006) noticed a significant improvement in the compressive strength of waste E-glass having size <75 μm in concrete mixtures at later ages. The compressive strength of specimens with 40 % E-glass content increased by 17%, 27% and 43% than that of the control concrete specimen at the curing ages of 28, 91 and 365 days, respectively.

Shayan and Xu (2006) investigated the performance of glass powder (GLP) in concrete under field conditions. Field trials were conducted using 40MPa concrete mixture, having different proportions of GLP (0%, 20%, & 30%) as a cement substitute. Ten mixtures were formulated, some of which also contained sand-size crushed glass aggregate particles, to cast ten concrete slabs (1.5 × 2.5 × 0.25 m). Cylinders and prisms were also casted for ascertaining the compressive & splitting tensile strength, flexural strength, expansion, ultrasonic pulse velocity, and chloride permeability. Core samples were taken from the slabs for conducting tests as well as for micro-structural examination at various ages. It was found that up to 28 days, strength gain remained slower in GLP-bearing concrete, but at the age of 404 days all the mixtures achieved strength of about 55MPa. The results showed that glass powder can be used at 20 to 30% as a substitute of cement without harmful effects. Alkali aggregate reaction (AAR) was also mitigated with the presence of GLP. It was further revealed that both GLP and glass aggregate can be used together in 40 MPa concrete without any harmful reaction.

Shi and Zheng (2007) examined the three possible uses of waste glasses such as an aggregate, raw material for cement production and as replacement of cement in production of cement and concrete. The use of waste glass as concrete aggregates resulted in a negative effect on the workability, strength and freezing-thawing resistance of cement concrete. This could be improved by the substitution of Portland cement with pozzzolanic materials like fly ash, silica fume and metakaoline. Waste glasses could be used as raw materials for cement production as siliceous sources. Ground glass powders canbe used as a cement substitute as it exhibits very good pozzolanic reactivity. Its pozzolanic reactivity enhances with its increase in finenesses. Alkali–aggregate reaction (AAR) expansion can be decreased, if the glass powder replacement is 50% or more. Alkali–aggregate reaction can also be decreased, if it is used with other supplementary cementing materials like coal fly ash and ground blast furnace slag.

Moura et al. (2007) studied the use of copper slag as pozzolanic supplementary cementing material for use in concrete. firstly, the characterization of the copper slag was done. Then, concrete mixtures were made with copper slag additions of 20%. The properties such as specific gravity, compressive strength, splitting-tensile, absorption, absorption rate by capillary suction and carbonation were eavaluated. It was concluded that there existed a potential for the

use of copper slag as a supplementary cementing material to concrete production. The concrete mixes with copper slag addition exhibited better mechanical and durability performance.

Taha and Nounu (2008) examined the effect of lithium nitrate (Li) and pozzolanic glass powder (PGP) on the expansion induced by ASR. The test results showed that Li and PGP notably reduced the ASR expansion. The amorphous structure of the glass powder underwent pozzolanic reaction with the presence of alkaline activator which contributed to the CSH structure and hydration products. The chemistry of the cementitious materials was also studied in this experimental programme. It was concluded that 20% of pozzolanic glass powder can be utilized as a cement substitute, and 1% of lithium nitrate as chemical admixture in concrete mixes in order to mitigate the ASR.

Schwarz and Neithalath (2008) investigated the effect of a fine glass powder on cement hydration. The pozzolanicity of the glass powder and a Class F fly ash was assessed using strength activity index over a period of time. The cement pastes were made up with a water- to-binder ratio of 0.42. Cement was replaced by either glass powder or fly ash at the rates of 5%, 10%, & 20% by mass. It was found that the glass powder showed pozzolanicity levels equal to or greater than that of fly ash at all the ages studied.

Liu (2011) studied the possibility of using ground glass in SCC. The ground glass was used as a partial substitute for both the cement and fine aggregate. The objective was to produce SCC mixed with some ground glass having the same fresh properties and evaluate their corresponding hardened properties. Tests on concrete containing ground glass provided that both the fresh and hardened properties of the SCC were influenced. The usage of ground glass also reduced strength, and Ultrasonic Pulse Velocity (UPV) from early to later ages due to higher water/powder ratio and the brittle nature of glass.

Chidiac and Mihaljevic (2011) investigated the use of glass powder in high strength concrete. The study aimed to find the effect of using waste materials on the performance and production of dry-cast concrete masonry blocks. Waste Glass Powder (WGP) was used as a cement substitute; and, HDPE and LDPE polymers were used as sand substitution. The blocks were casted in an industrial plant; and their density, compressive strength, elastic modulus and bond strength was tested. It was concluded that the early strength requirement of the blocks was achieved even with 25% cement substitution. The strength development of the blocks with 10% WGP was initially slower than the control concrete, but they attained the same

compressive strength within one-year. After one-year, the blocks containing 25% WGP had a 16% lower compressive strength than the control concrete. There was no alkali silica reaction with 25% of the cement substituted with waste glass powder.

Matos et al. (2012) used waste glass powder (WGP) in mortar as a partial cement replacement at 0%, 10% and 20% to know about its applicability in concrete. An extensive experimental programme was conducted to find out pozzolanic activity, setting time, soundness, specific gravity, chemical analyses, laser particle size distribution, X-ray diffraction and scanning electron microscopy (SEM) on WGP. Also tests were conducted to find resistance to alkali silica reaction (ASR), chloride ion penetration resistance, absorption by capillarity, accelerated carbonation and external sulphate resistance on mortar containing WGP. The SEM showed that the glass particles well encapsulated into dense and mature gel. The increased durability confirmed that waste glass powder can further contribute to sustainability in construction.

Madandoust et al. (2013) used the combination of waste glass powder (GP) and rice husk ash (RHA) as replacement for Portland cement in concrete. Concrete mixtures containing 0 to 20% of GP and 0 to 20% of RHA were prepared. Compressive strength at 28-days of curing was determined to find the optimum level of replacements by GP and RHA. It was found that 10% of glass powder and 5% of rice husk ash yielded more compressive strength than the control concrete at 28 days; and the strength increased constantly with age due to the development of greater pozzolanic activity. The stydy concluded that the combination of GP and RHA can be used in concrete without any harmful effects.

Vaitkevicius et al. (2014) experimentally investigated glass powder as a complete replacement for quartz powder and silica fume in ultra high performance concrete (UHPC). The results showed that UHPC can be prepared with improved micro-structural and compressive strength properties. Glass powder undergoes low pozzolanic reaction and forms calcium silicate hydrate (C–S–H) which resulted in good mechanical and microstructural properties of UHPC. Microstructural investigation was also made by mercury intrusion porosimetry (MIP) and X-ray diffraction (XRD) analysis. The study revealed that with a combination of glass powder and silica fume, additional compressive strength of 40 MPa can be achieved.

Carsana et al. (2014) compared the behaviour of waste glass powders of different fineness with that of fly ash and silica fume. The effect of ground glass on the strength and durability performances of mortars was found out by conducting chemical analysis, compressive strength

test and durability tests. The ground glass blended with Portland cement and lime, improve the strength, resistance to chloride penetration and resistance to sulphate attack of mortars more than natural pozzolana.

Kamali et al. (2015) examined the effect of glass powder and class F fly ash as cement replacement on mechanical strength and durability of concrete. Mechanical strengths included compressive strength and flexural strength, and durability properties included alkali-silica-reactivity, electrical resistivity, chloride permeability and porosity. It was seen that there was improvement in compressive and flexural strengths as compared to the control concrete at later ages of curing. It was also found that the addition of glass powder decreased alkali-silica reaction expansions. The improvement in the mechanical strength and durability of the concrete with glass powders can be attributed to microstructure improvement due to the pozzolanic property of the glass powders.

Afshinnia et al. (2015) studied the synergic action of a finely ground glass powder in binary and ternary cementitious blends with conventional SCMs such as metakaolin, fly ash and slag. Tests were carried out to examine the pozzolanic behaviour and ASR mitigation ability. It was found that ternary mixtures consisting of finely ground soda glass with either slag or Class C fly ash performed better than the binary mixtures. The performance of binary mixtures consisting of metakaolin was better than ternary mixtures consisting of ground glass powder with metakaolin at equivalent dosage level. The maximum strength activity index and the most efficient ASR mitigation was obtained in ternary mixtures consisting of at least 10% glass powder than all the binary and ternary mixtures that contained 30% level of SCMs. The results produced by TGA studies supported these findings.

Du et al. (2014) found that concrete containing up to 100% glass sand as sand replacement had similar compressive strength to that of the control concrete after 28 days. But the 90-days compressive strength increased with this glass percentage.

Rashad (2014) found that the alkali silica reaction (ASR) expansion of mortar and concrete specimens containing glass sand can be mitigated by adding 10–30% MK, 20–50% FA, 50–60% slag, 10% SF, 1–2% Ni_2CO_3, 1% $LiNO_3$ and suitable amount of fibres. The presence of C_3S, C_2S and C_4AF in the concrete composition endorsed steel slag having cementitious properties.

Adaway et al. (2015) replaced fine aggregate with glass powder at 15%, 20%, 25%, 30% and 40% level in the concrete. An increase was observed in compressive strength up to a level of 30% replacement. At this level, the compressive strength recorded was 9% and 6% higher than the control concrete after 7 &28 days of curing respectively.

2.2.2 Electric Arc Furnace Slag

Manso Juan M. et al. (2006) presented the behaviour of slag in concrete under strict test conditions. The tests were conducted to know the chemical reactivity of slag with certain components of the cement and also its resistance to the durability of concrete. Six concrete mixtures were prepared, all having cement content of 310 kg/m3, ratio w/c: <0.6, workability between 60–90 mm (slump test) and no admixtures. The results showed that the slag concrete was having acceptable durability, though it was slightly lower than that of the control concrete. Both the mechanical strength and the durability of slag concrete were satisfactory when the mix proportions were adequate. The study brought out that EAF slag was useful when used as aggregate replacement in hydraulic concrete. Concrete prepared from EAF oxidizing slag as an aggregate produced good physical and mechanical properties.

Muhmood et al. (2009) examined the pozzolanic and cementitious behaviour of electric arc furnace steel slag. The chemical composition of electric arc furnace slag (EAFS) was almost similar to that of the cement clinker. So, it can be used partially in the place of cement clinker. It can not be used in blended cement because of less pozzolanic property. The slag blended cement was tested for compression strength and it was found that slag addition of 20 %, increased the compressive strength after 28 days. Maximum strength of 61 MPa was measured when untreated slag was substituted with treated slag at 28 days. It was found that treated electric arc furnace slag contained cementitious and pozzolanic properties.

Pellegrino et al. (2009) undertook their study to find the feasibility of using Black/Oxidizing EAFS as substitute to natural aggregates in cement concrete. There was an increase of 30% more compressive strength at 28-day period in comparison to natural aggregate concrete.

Maslehuddin et al. (2011) performed the experiments to examine the mechanical and durability properties of blended cement concrete specimens prepared from electric arc furnace dust (EAFD) and compared these with OPC conrete. The silica fume content was fixed at 8% in silica fume concrete, while 30 % fly ash was added in fly ash cement concrete. The percentage

of EAFD was kept 2% as cement substitution in the OPC concrete and in the blended cement concretes. The results also showed that the addition of EAFD improved the mechanical properties and durability of both OPC and blended cement concretes. Similarly, the workability was also increased with the addition of EAFD. The initial and final setting time also increased due to this addition. It was also observed that the strength of OPC concrete and EAFD blended cement concrete specimens was equal to or more than that of similar concrete without EAFD at 3-day period. So there was improvement in the strength and durability properties of EAFD concrete.

Ducman et al. (2011) proposed the feasibility of using EAFS as aggregate replacement in the production of refractory concrete. It was observed that when slag was heated up to a 1000 °C temperature, before its use for refractory concrete, the final product resulted good mechanical properties which were comparable to concrete made with the conventional refractory aggregate, e.g. bauxite.

Pellegrino et al. (2012) investigated the replacement of aggregates with Electric Arc Furnace (EAF) slag. Extensive experiments were performed to find the compressive and tensile strength, elastic modulus and durability characteristics of concrete containing EAF slag as aggregate. In the experimentation, concrete mixture containing EAF slag as partial replacement of fine aggregate and control mixture were designed. Hence, the values considered for both the mixtures were slump = 185 mm; water/cement ratio = 0.52; fluidifying agent = 0.4% of cement weight; aerating additive = 0.016% of cement weight; cement specific weight = 3.1 kg/l; flat air volume mainly due to aerating additive = 5%. Compressive tests were conducted on 150 mm cubes after 7,28 and 90days. The study found that EAF slag can be used as replacement for aggregates. Concrete made with EAF slag as aggregate showed better strength. The durability can be greatly improved with the addition of EAF in concrete.

Pellegrino et al. (2013) investigated the possibility of using EAF as a partial substitute of aggregates in concrete. The tests were performed to examine the physical and mechanical properties of concrete containing EAF slag as aggregate. It was concluded that higher replacement of coarse aggregates with EAF is possible without a decrease in the mechanical properties of concrete.

Arribas et al. (2014) examined the possibility of using electric-arc furnace slag as a partial substitute of aggregate in concrete. The study also investigated the durability properties of slag

concrete sulfate attack, alkali–aggregate reaction and resistance to the corrosion of steel reinforcement bars embedded in the concrete. It was found that the behaviour of the concrete with slag aggregate was similar to or better than the control concrete.

Faleschini et al. (2015) examined the possibility of using Black/Oxidizing Electric Arc Furnace slag (EAF) as replacement to coarse aggregate in High Performance Concrete (HPC). Various experimental mixes were produced, 100% replacing coarse aggregates with EAF slag. The cement content and water to cement ratio was varied. Results showed that there was improvement in the concrete strength and durability of concrete with the use of EAF slag.

2.2.3 Iron Slag

Ismail and Hashmi (2008) reported that the sand was patially substituted with waste iron at 10%, 15%, & 20% to make concrete mixtures. The tests were conducted on this concrete to find out the properties such as slump, compressive strength and flexural strength at 3, 7, 14 & 28 days of curing age. The results showed that the concrete mixes made with waste iron were having more compressive strengths than the control concrete mix. The compressive strength of the concrete improved by 22.60%, 15.90% &17.40% made with 20% waste-iron aggregate at 3, 7 & 28 days curing periods respectively.

Qasrawi et al. (2009) found that the compressive strength of concrete using steel slag as a fine aggregate was 1.1 to 1.3 times the compressive strength of control concrete.

Huang et al. (2010) prepared a cementitious material by using phosphogypsum (PG), steel slag (SS), GGBFS and limestone (LS). The results concluded that the 28 days compressive strength was more than 40 MPa with a mixture of 45% PG, 10% SS, 35% GGBFS and 10% LS. The main hydration products found in the mixture were ettringite and C–S–H gel.

Ameri et al. (2012) used the steel slag from Zob-Ahan Steel Production Factory in concrete as a partial substitute of aggregates. Compressive strength tests were conducted on specimens containing slag percentage as 0, 25, 50, 75 & 100 % and cement contents of 200, 300 and 350 kg/m^3. An improvement in the compressive strength was observed with the use of steel slag up to 25%, but after that it showed a decrease. The maximum compressive strength value occured at 25% slag substitution.

Devi and Gnanavel (2014) found the optimal percentage of partial substitution of coarse and fine aggregates with steel slag (SS) by studying its effect on the performance (strength and

durability) of M20 mix concrete. The workability of concrete lessened with an increase in steel slag. Several experiments were performed to find its compressive strength, tensile strength, flexural strength and durability tests such as acid resistance and RCPT. The compressive, tensile and flexural strength inceased with an addition of steel slag as partial substitute of fine and coarse aggregates. Finally the use of steel slag in concrete was found to be viable.

Khajuria and Siddique (2014) studied the effect of replacing sand with iron slag on compressive strength of the concrete. The iron slag replaced sand at 10%, 20% & 30%. The compressive strength of the concrete was increased by 26%, 50% and 43% after 7 , 28 and 56 days respectively with adding 10% iron slag in the mix, in comparison to the control mix. By adding 20% & 30% iron slag, the compressive strength was further icreased at 68%, 91%, 78% and 125%, 113%, 87% after 7, 28 and 56 days respectively. It was concluded that the concrete made with iron slag had more strength than that of the plain concrete.

Kothai et al. (2014) studied the effect of using steel slag as partial substitute of fine aggregates on strength properties. It was concluded that the optimum value of steel slag was 30% as sand replacement and there was an increase in the compressive and tensile strength of the concrete. He also found that there was decrease in compressive strength on further increasing the replacement of steel slag.

Ouda et al. (2017) examined the effects of oxygen furnace slag as sand substitute on the compressive strength of mortar. Cement mortar of ratio 1:3 was designed with 0%, 40%, 80% and 100% replacement of sand with iron slag. The water to cemnent was taken as 0.44 and the curing period was 90 days. The results show that the strength properties of mortars increased significantly by substituting sand partially by iron slag. The bulk density of mortar was also increased.

2.3 INDUSTRIAL BY-PRODUCTS USED IN TERNARY BLEND/MIXTURE OF CONCRETE

The usage of mineral admixtures such as FA, LFS, CS, EAFS, IS and GP has a key role in improving the engineering properties of concrete mix design (Cheng et al., 2001). Diverse research has been executed for predicting the strength of concrete when mixed with industrial

byproducts/waste both as replacement of cement as well as fine/coarse aggregate in binary combinations (Farahani et al., 2017) (Mohammed et al., 2018) (Vivek and Dhinakaran, 2017. However, very few studies have used industrial byproducts/waste in ternary combinations (Bagel, 1998) (Pandey and Sharma, 2000) (Khan and Lyndsdale, 2002). The ternary blends of concrete conataining SCM has synergic effect. The limitations of one SCM is compensated with the advantages of another SCM. So due to the synergic effect of SCM's , the resulting concrete had superior qualities related to mechanical and durability properties of concrete (Radlinski and Olek, 2012), (Erdem, and Kirca, 2008).

Gesoglu et al. (2007) examined the influence of supplementary cementing materials (SCMs) used in different combinations in concrete blends on the hardened properties of SCC. The control concrete mixture was prepared with OPC while the remaining mixtures containing fly-ash, Granulated Blast Furnace Slag (GGBFS) and SF in binary, ternary, and quaternary cementitious blends were prepared. Test results found that incorporating the mineral admixtures improve the compressive strength of concretes made with SF and GGBFS.

2.4 USE OF TAGUCHI METHOD FOR DESIGN OF EXPERIMENTS

Ozbay et al. (2009) used Taguchi's DOE methodology to find the optimal mix design parameters of high strength self compacting concrete (HSSCC). The best setting for mix proportions were proposed to maximize the properties like compressive strength, split tensile strength and to minimize the properties like depth of water permeability and water absorption values.

Alex et al. (2016) applied Taguchi approach to find the effects of parameters like RHA loading, pozzolanicity, curing period, bulk density and RHA size in concrete containing RHA as cement replacement. It was concluded that there was enhancement in mechanical strength with decreasing size of RHA. The cement replacement with 20 wt% RHA was optimum for 15 and 60 min grounded sample.

Hadi et al. (2017) used Taguchi method to design optimal composition for geopolymer concrete with GGBFS. It was estanlished that there was an improvement in the setting time the partial substitution of GGBFS with FA, MK, and SF. The Taguchi method was applied very efficiently.

2.5 MULTI- RESPONSE OPTIMIZATION BY GREY RELATIONAL ANALYSIS

Grey relational analysis is a method by which we can optimize any number of output responses rather than single response optimization as done by many optimization methods. So if the ouput responses are more than one Grey relational analysis with Taguchi method gives the set of optimal input parameters having effect on output responses.they are more than one. In present research, Grey-Taguchi relational approach based multi response optimization has been applied to maximize compressive strength, split tensile strength and to minimize wear depth and water penetration depth of concrete. Very few researchers used this method for multi response optimization in civil engineering till date. Bao et al. (2014) studied quality optimization of recycled concrete coarse aggregate based on Grey relational analysis.

2.6 PREDICTION OF STRENGTH AND DURABILITY PROPERTIES OF CONCRETE BY ARTIFICIAL NEURAL NETWORKS (ANN) AND ADAPTIVE NEURO-FUZZY INFERENCE SYSTEMS (ANFIS)

Since last few decades, many modeling methods are used for modeling which are based on artificial neural networks (ANN) and Adaptive neuro-fuzzy inference systems (ANFIS). These modeling methods are becoming very popular and are used to solve very complex problems in engineering and science. These modeling methods give very reliable results. Many researchers used ANN and ANFIS to estimate the compressive and split tensile strength of concrete containing industrial by-products very successfully. In this research work ANN and ANFIS modeling methods were used to predict the strength and durability properties of concrete containing ternary combination of by-products as replacement of cement and sand.

Topcu et al. (2008) presented the development of ANNs and fuzzy logic models for the estimation of the compressive strength of concretes consisting high-lime and low-lime fly ashes at 7, 28 and 90 days. It was concluded that the ANN and ANFIS models have strong potential for estimating the compressive strength of such concretes at 7, 28 & 90 days of curing.

Atici (2011) predicted the strength of mineral admixture concrete containing blast furnace concrete and fly ash using MRA and ANN and found that ANN is suitable for calculating nonlinear functional relationships, for which classical methods cannot be applied.

Muthupriya et al. (2011) developed ANN model for estimating the compressive strength of concrete containing metakaolin with fly ash and silica fume as partial substituent of cement and found that the ANN has a high potential for estimating the compressive strength values of such concrete very accurately.

Lif et al. (2011) developed Artificial Neural Network (ANN) for the prediction of split tensile strength of concrete containing waste marble dust as filler material and found that ANN model predicted the values of split tensile strength matching with the values obtained with experimental values.

Reddy (2012) developed the ANN model which used the back propagation algorithm for the prediction of the split tensile strength of MK blended polypropylene fiber-reinforced high performance-concrete(MK-PFRHPC). He found that the model estimated the split tensile strength of MK-PFRHPC with more accuracy.

Boga et al. (2013) studied the effects of using GGBFS and calcium nitrite-based corrosion inhibitor (CNI) on the mechanical and durability properties of concrete such as compressive strength, splitting tensile strength, chloride ion permeability. They deleloped four-layered ANN and ANFIS models to predict the mechanical properties of concrete. It was found that experimental data can be predicted very accurately via the ANN and ANFIS models.

Raif et al. (2013) predicted the mechanical properties of concrete containing GGBFS and CNI using ANN and ANFIS. It was concluded that the experimental data can be estimated very accurately using ANN and ANFIS models.

Gupta (2013) presented the ANN model developed to estimate the compressive strength of concrete at 28 days. The concrete contained nano silica as partial replacement of cement. It was resulted that the model developed for such concrete predicted the compressive strength very near to the experimental values.

Vakhshouri et al. (2014) modelled nonlinear fuction between splitting tensile strength and modulus of elasticity with compressive strength of high strength concrete using ANFIS and found that ANFIS predicted the strength properties very accurately.

Douma et al. (2014) predicted compressive strength of SCC containing fly ash using the ANFIS and resulted in the strong potential for predicting the compressive strength.

Abdul Hakeem et al. (2015) estimated the early and late composite (compression/tension) strength of self-compacting concrete (SCC) by using ANN model. It was observed from the results that SCC components can be estimated with reliable values to the experimental results using the artificial neural network (ANN) method.

Chopra et al. (2015) proposed an ANN model to estimate the compressive strength of concrete and found that Levenberg- Marquardt (LM) with tan-sigmoid activation function is best used for the estimation of the compressive strength of concrete.

Naniz et al. (2015) developed two Artificial Neural Network (ANN) models in which the compressive strength of concrete consisting Slag and Silica fume was predicted at the age of 7, 28, 90 & 180 days. It was found that ANN models had strong potential as a powerful tool for estimation of compressive strength values of concretes consisting slag and silica fume at 7, 28, 90 and 180 days

Dabhade et al.(2015) developed the Neural Network model and mathematical model by Multi-linear Regression (MLR) Method to establish a relationship between the split tensile strength of concrete and four variable parameters which were the percentage of RCA, %age of fly ash, curing age and water/cement ratio. They found that ANN modeling method predicted strength values better than MLR method.

Chithra et al. (2016) constructed models based on artificial neural networks and regression analysis to estimate the compressive strength of high-performance concrete which contained nano-silica and copper slag as partial replacement of cement and sand respectively and concluded that ANN models generated better results.

Vidivelli et al. (2016) developed a model which was based on ANN for the prediction of compressive strength of concrete containing by-products. It was found that the artificial neural network (ANN) model developed in the problem performed very well to estimate the compressive strength of HPC for different curing periods.

Gülbandılar et al. (2017) developed two different ANN models to estimate the split tensile strength of concrete having zeolite and diatomite. The results have shown that these two different ANN models have strong potential for estimating 28, 56 & 90 days the splitting tensile strength of such concrete.

Awoyera (2018) Studied the modelling of the results of laboratory experiments for the strength properties of steel slag aggregate concrete using ANN technique. It was recommendation to use this ANN model for the prediction of strength properties of steel slag aggregate concrete.

2.7 GAPS IN THE RESEARCH AREA

The following gaps were found in the research area after the review of relevant literature :

1. Significant amount of work has been carried out in the area of using Fly ash, Ladle Furnace Slag, Copper Slag, Glass Powder, Electric arc furnace slag and iron slag either individually or in a combination of two, both as replacement of cement as well as sand. However, this research work proposes to use a secondary as well as a tertiary combination of these industrial by-products or waste materials. Thus this is an innovative attempt in the area under study.
2. No procedure has yet been evolved for designing optimal mixes using these industrial by-products or waste materials as partial replacements. The current study proposes to generate and analyze the concrete data, for both strength and durability, using experimental design.

2.8 OBJECTIVES OF RESEARCH WORK

The purpose of this investigation is to establish whether there is synergistic action when the system of Indian materials is used in concrete. In other words, the answer is sought for the question whether a suitable combination of Indian industrial by- products would improve the properties of fresh and hardened concrete more than these materials when used separately. The properties have been studied not only to estimate strength characteristics of ternary concrete, but due emphasis is laid on the durability aspect of concrete as well. Keeping this basic aim in mind, the present study emphasizes on the following objectives:

1) To study the effect of some industrial by-products as partial replacement of cement and fine aggregates on strength and durability properties of concrete using statistical experimental design.
2) To determine the quantitative effect of various concrete making ingredients including industrial by-products, using experimental design methodology.
3) To develop a model for prediction of strength and durability of concrete containing industrial by-products, within the range of parameters used.

CHAPTER 3 METHODLOGY & EXPERIMENTAL PROGRAM

3.0 GENERAL

In the full factorial design method, all the possible combinations of parameters are taken into account while designing any experiment while in fractional factorial design, only some of the conditions are explored for design of the experiment if the experiment involves many dependent variables. These methods of design have some deficiencies. The deficiencies are the cost factor, time involved etc. The limitations of the full factorial design methods are taken care of by the Taguchi method. This method is very simple method and is widely used these days because it reduces the number of iterations and used to optimize the known parameter. In this method, firstly we identify all the input factors or parameters which affect the experiments. Then a number of experiments are conducted by designing the experiment using these factors. The effect of these factors on the response is worked out. Thus the optimal parameters are found which had the greatest influence on the response i.e. output.

In the present investigation, the effect of various factors/parameters like percentage of by-product used as binder, percentage of by-product to be used as fine aggregate, type of binder and type of fine aggregate were studied on resulting concrete, for strength and durability aspects, using the method developed by Taguchi *(Roy and R.K.,1990)*. The experiments were designed using the fractional factorial experiments (FFEs) design methodology of Taguchi. Taguchi method was also used to verify the optimal mixture design.

3.1 TAGUCHI METHOD

This technique was devised by Genichi Taguchi during the 1950s. This method is used to optimize the parameters which affect the experiments and thus the output response. By finding the optimal parameters, the experimental response can be obtained using these optimal parameters. This method thus helps the design engineer to find the optimum performance and cost involved *(Ozbay et al., 2009)*. The processes involved in Taguchi method are shown in Fig. 3.1. Flow graph defines the various steps of Taguchi method applying to find out the optimal mixture design *(Roy and R.K., 1990)*.

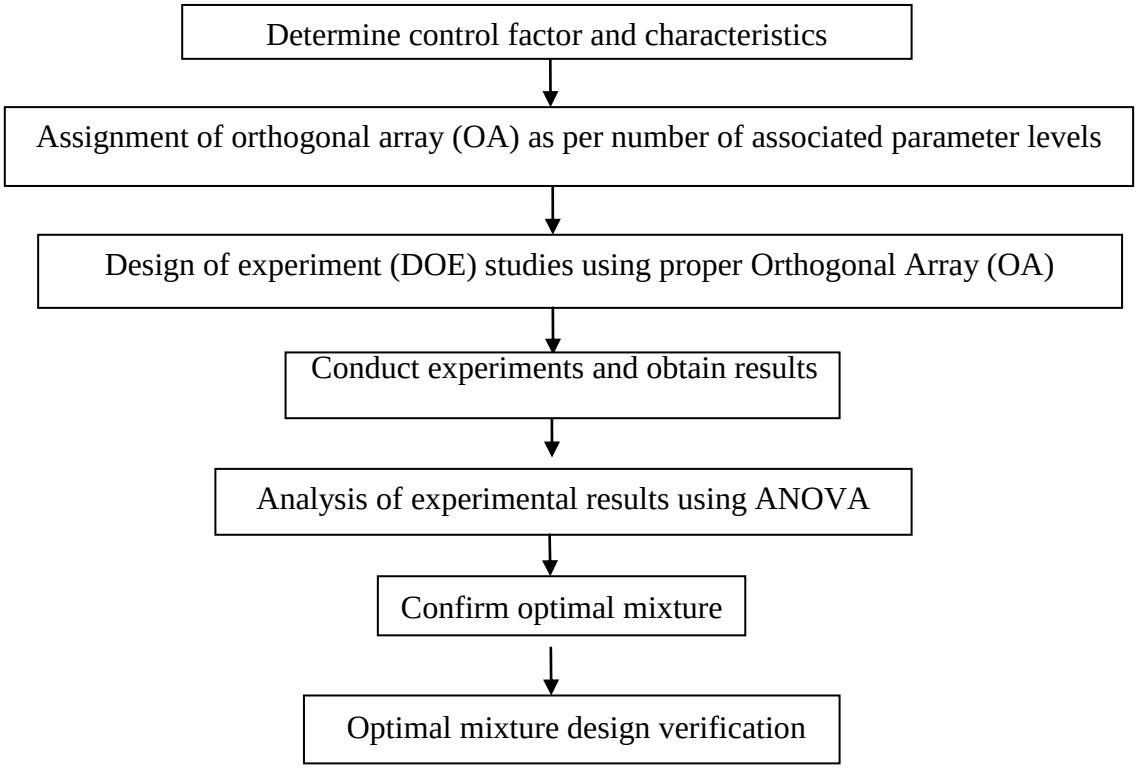

Fig. 3.1: Steps involved in Taguchi method

3.2 PROCEDURE OF EXPERIMENTAL DESIGN

The essential steps in the procedure of Taguchi method are as follows *(Roy and R.K., 1990).*

1. Establishing the response function.
2. Identification of the parameters.
3. Identifying the uncontrollable parameters as well as test conditions.
4. Indentifying the levels of the parameters.
5. Calculating the total degrees of freedom which are needed.
6. Selecting the Orthogonal Array (OA) as per the degrees of freedom.
7. Executing the tests as per the design.
8. Analysis of results.
9. Conducting the experiments for confirmation

Some of the important steps of Taguchi method used in this study are briefly explained below:-

3.2.1 Establishment of Response Functions

This study was conducted out to find the effect of industrial by-products in concrete on the following responses i.e. properties

i) Compressive Strength
ii) Split Tensile Strength
iii) Water Permeability i.e. depth of water penetration test
iv) Abrasion test i.e. depth of wear.

3.2.2 Determination of Variable Factors and their Levels

In this study, the following four controllable/variable factors with three levels each were identified; their levels are elaborated in Table 3.2

i) Percentage (%) of by-product to be partial replaced as binder i.e. cement
ii) Percentage (%) of by-product to be partial replaced as fine aggregate i.e. sand
iii) Type of replacement as binder
iv) Type of replacement as fine aggregate

3.2.3 Layout of the Taguchi's Orthogonal Array

There are two types of the Taguchi's crossed array i.e. an inner array and an array at the outer level. The array at the inner level is called as orthogonal array (OA), which is formed from the identified controllable factors taking into account their all possible levels. Here we are having four factors at three levels each. The outer array consists of all uncontrollable factors which consists of two factors i.e. water to binder ratios and curing periods each having 3 levels. So L_9 OA is used for the experiment. An L_9 OA has 4 columns, and each factor was assigned to of the four columns. L_9 allows for 9 trials to be conducted by varying the four factors at three levels each. Using full factorial method the number of experiments comes out to be 729, and to decrease the number of experiments, a standard L_9 OA was employed. Using this methodology, the total experiments have been reduced to 81 instead of 729 thus considerably saving the time and material. The details of the orthogonal array are given in the next section.

3.2.4 Execution of Trials according to Designed Orthogonal Array

According to the L_9 OA, there are nine trial experiments which are to be conducted for each of the water cement ratio and each of the curing period. These experiments were conducted for all the four response outputs.

3.2.5 Calculating Mean of the Response

The mean of the each response was calculated after the experiments were conducted and are also shown in response tables for each response and for each water to binder ratio and for each curing days. For example to calculate the mean response performance of the factor 'A' at 1^{st} level expressed as 'A1' trial run output having factor A1 in the OA were added and then divided by the number of trial run i.e. three in this case.

3.2.6 Analysis of Variance (ANOVA)

The ANOVA is done to know the optimal parameter and its contribution on the final response. It is performed by finding the (1) sum of squares (SS), (2) degrees of freedom (dof), (3) variance and (4) contribution percentage of each factor.

3.3 SELECTION OF PARAMETERS

As per the concept of experimental design, to obtain a relationship of each factor to output response, each factor must be varied at least two levels. However, it is difficult to establish a mathematical relationship between only two data points. Thus it was decided to vary each factor at a minimum of three levels. Increasing the number of levels at which each factor is varied would have made the experimental work extremely large. The sum of all the degrees of freedom of factors is the minimum dof required for the experiment. After the pilot study, four factors namely (1) percentage of by-product as a replacement of binder (percent) (2) percentage of by-product as a substitution of sand/fine aggregate (percent) (3) type of by-product used as a replacement of binder and (4) type of by-product used as a replacement of sand were identified for detailed study using the Taguchi experimental design methodology *(Ross 1995).* The levels of the factors were carefully chosen based on reported results in the literature. The percent of by-product as a replacement of binder was taken at 10%, 25% and 40% levels. As per the codal provisions, the specified cement replacement levels majorly fall in this range. Similarly the percent of by-product used as fine aggregate was varied at 20%, 30% and 40% levels. These replacement levels are by weight. Three by-products namely fly-ash, LFS and copper slag were used as a replacement of binder, whereas, glass powder, EAFS and iron slag were used as replacement of sand. The water to binder ratio was fixed at 0.40, 0.44 and 0.48 and the curing period was also fixed at &, 28 and 90 days. The water to cement/binder ratio was selected by following the Abram's law *(Singh S.B. et al., 2015).* These ratios were selected as we intended to study the effect only for such concretes

(whose strength is between 20 MPa to 60 MPa) which are commonly used in most of the construction activities. The following uncontrollable parameters/factors (Table 3.1) and controllable parameters (Table 3.2) with their levels are used for experiments are enlisted below.

Table 3.1: List of fixed/ uncontrollable parameters/factors with levels

S. No.	Parameter	Levels		
		1	2	3
1.	Water to cement ratio	0.40	0.44	0.48
2.	Curing days	7	28	90

Table 3.2: List of variable/ controllable parameters/factors and their levels

S. No.	Factor Designation	Parametric Factors	Units	Levels		
				I	II	III
1.	A	Percentage of by-product to be used as partial replacement of cement	Percentage of total cement content by weight	10%	25%	40%
2.	B	Percentage of by-product to be used as partial replacement of fine aggregate	Percentage of total fine aggregate content by weight	20%	30%	40%
3.	C	Type of replacement as binder		Fly ash(FA)	Ladle Furnace Slag(LFS)	Copper slag(CS)
4.	D	Type of replacement as Fine aggregate		Electric Arc Furnace Slag(EAFS)	Iron Slag(IS)	Glass Powder(GP)

3.4 DEGREE OF FREEDOM (dof)

The total number of dof of the entire experiment is the sum of dof of all the parameters in the experiment. The degree of freedom for each parameter is one less than its no. of levels.

In the present experiment, we have four parameters varied each at three levels. So there are two dof for each parameter thus making total degrees of freedom as eight as given in Table 3.3.

Table 3.3: Degrees of freedom (dof)

S. No.	Factor Designation (See Table 3.2)	Degrees of freedom
1.	(A)	2
2.	(B)	2
3.	(C)	2
4.	(D)	2
		Total= 8

3.5 ORTHOGONAL ARRAY (OA)

After calculating total number of dof of all the parameters, the Taguchi's orthogonal array was selected. The orthogonal array should be selected so that it should have more than or equal to 8 degrees of freedom. So that is why L_9 orthogonal array was selected for the experiment as shown in Table 3.4**.** The 9 experimental designs represent the set of values of input parameters to conduct the particular experiment. The total 9 experiment were performed with repetition to maximize or minimize the effect of uncontrollable parameters for each combination of all input parameters. The levels selected for each parameter in the present Taguchi DOE is shown in Table 3.2. Now the actual L_9 OA used in the present study for 9 experiments conducted is shown in Table 3.5.

Table 3.4: Taguchi's L_9 standard OA for 4 parameters at 3 levels

Experiment series/Trials	Parameter/ factor A	Parameter/ factor B	Parameter/ factor C	Parameter/ factor D
	Levels			
T1	1	1	1	1
T2	1	2	2	2
T3	1	3	3	3
T4	2	1	2	3
T5	2	2	3	1
T6	2	3	1	2
T7	3	1	3	2
T8	3	2	1	3
T9	3	3	2	1

Table 3.5: L_9 array used for defining the trial conditions

Trial Mixture	Parameter 'A'	Parameter 'B'	Parameter 'C'	Parameter 'D'
T1	10%	20%	Fly-ash	EAFS
T2	10%	30%	LFS	Iron Slag
T3	10%	40%	Copper slag	Glass Powder
T4	25%	20%	LFS	Glass Powder
T5	25%	30%	Copper slag	EAFS
T6	25%	40%	Fly-ash	Iron Slag
T7	40%	20%	Copper slag	Iron Slag
T8	40%	30%	Fly-ash	Glass Powder
T9	40%	40%	LFS	EAFS

3.6 EXECUTION OF EXPERIMENTS ACCORDING TO TRIAL CONDITIONS

Now the experiments were conducted as per L9 OA with all the parameters and their levels as shown in Table 3.2. Table 3.5 shows the actual trial conditions of the whole

experiment. All the nine experiments were conducted for each water to binder ratio and for each of the curing period as mentioned in the Table 3.1. The split tensile strength, compressive strength, depth of wear and water penetration depth were measured. For each concrete mix 3 specimens corresponding to above designed mix proportions for each test conducted for both strength and durability properties were cast for testing at 7, 28 & 90 days of curing.

3.7 OBJECTIVE FUNCTION (RESPONSES)

The objective of the study is to find the effect of by-products as partial replacement of cement and fine aggregates in concrete on strength and durability of concrete.

3.7.1 Compressive Strength

The maximum compressive load which the cube test specimen was able to take before failure was noted and corresponding load was reported as the compressive strength. This test was conducted on the cubical test samples of size 150mm as per IS: 516: 1959 *(BIS 516, 1959)*. At the required age of testing, the cubes were taken out from the curing tank and cleaned with dry cloth to remove the water from the surface to bring them to saturated surface dry condition. These specimens were then placed in the automatic compression testing machine (3000 KN Capacity) in a position so that it is tested at right angles to the position when it was casted. The load was applied with the hydraulic jack at the rate of 140 kg/cm^2/min till the specimen fails. In this way, the mean of three readings was taken as the compressive strength value of concrete. The specimens were cast for all the three curing periods and the test was carried out at the age of 7, 28 & 90 days. The compressive strength of the specimen is calculated as per the Eq. 3.1 as explained below.

$$\text{Compressive strength (MPa)} = \frac{P}{A} \text{x}1000 \quad \text{(3.1)}$$

where

P = Maximum load before failure of the specimen (kN)

A= X- section area (mm^2)

3.7.2 Split Tensile Strength

Split tensile strength of the concrete is the maximum tensile stress taken by the specimen before failure. It was measured by indirect test. This test was performed as per IS: 5816: 1999 *(BIS 5816, 1999)*. In this test, a cylindrical specimen of size 150 mm diameter and

300 mm of height was taken and the test specimen was placed with horizontal position between the plates of compression testing machine. The compressive load was applied along the opposite generators of concrete cylinder. Due to the applied load, a tensile stress is produced in the specimen over nearly two-third of its loaded diameter. The split tensile strength was calculated as given by Eq. 3.2 as below.

$$\text{Split Tensile Strength (MPa)} = \frac{2P}{\pi DL} \quad \text{---------- (3.2)}$$

where

P = Compressive load at failure (N)

D = Diameter of cylinder (mm)

L = Cylinder length (mm)

The mean of three readings was considered as the final split tensile strength of concrete for that particular specimen. All the specimens were tested the age of 7, 28 and 90 days.

3.7.3 Durability

Durability of concrete is its ability against acid attack, weathering action, and abrasion with no compromise with its performance. The concrete must be durable enough so that it completes its designed life span. In this study, two durability properties namely water permeability taken as depth of water penetration and abrasion strength taken as depth of wear of concrete were found and are discussed below.

(a) Water Impermeability Test

Most deterioration processes have two stages. Initially, aggressive fluids (water, solution etc.) penetrate through the capillary pore type concrete structure to reaction sites. This penetration is followed by the actual chemical or physical deterioration reactions. To access concrete durability during the first stage, tests that measure transport rates in concrete are required. The transport rate, normally called permeability of concrete, is measured in terms of flow of water through the concrete specimen. However, there is a problem with the permeability test: in good quality concrete, there is no flow of water through concrete even after some days also. In the present investigation, since mineral admixtures are used, they make the pore structure refined by reducing the size of pores. It is expected that the water permeability tests might not give any data for comparison of mixes. Therefore, water impermeability test was performed instead of water permeability

test. The test was performed as per the German Standard: DIN 1048 (Part 5) *(DIN 1048, Part 5)*. For performing the test, 150 mm cubical specimens were cast similar to the procedure adopted for casting specimens for strength tests. The specimens were subjected to all the three curing periods and the test was performed at the age of 7, 28 & 90 days. For conducting the test, the concrete specimens were subjected to a water pressure of 0.5 N per mm^2 which was acting perpendicular to the specimen position, for 72 hrs. Three cell apparatus was used for performing the test, i.e. three specimens were subjected to the said pressure at the same time. The pressure was kept constant for 72 hrs.. At the end of 72 hours, the pressure was released and the specimens were split from the center with the face which was exposed to water facing down. After about ten minutes, the maximum penetration depth was measured on each of the split halves in mm. The average of the maximum penetration depth taken from the three test specimens was considered as the representative value.

(b) Abrasion Test

Resistance to abrasion of concrete was measured as per procedure given in IS: 1237-2012 *(BIS 1237, 2012)*. First of all, the specimens were made to dry at 110 ± 5^0 Celsius for 24 hrs and then weighted to least count of 0.1 g. The original thickness of the specimen was measured at four points. After that the test specimen was put in the holding device of the machine. The abrasive powder of 20 g was spread uniformly on the surface of the machine. The machine is then started for the abrasion of the specimen. After the twenty two revolutions, the disc was stopped and the abraded powder was removed from the disc and the specimen was turned at 90 degrees about the vertical axis. The same procedure was repeated for 9 times thus giving total of 220 revolutions. After 220 revolutions the specimen was taken out and then weighted to 0.1 g. The thickness of the specimen was again measured at four points. The thickness loss was calculated from the formula given in the Eq. 3.3 as under.

$$t = \frac{(W_1 - W_2)\, V_1}{W_1 \times A} \qquad \text{---------- (3.3)}$$

Where

t = mean thickness loss (in mm)

W_1 = mass of the test sample at the start of the test (g)

W_2 = mass of the abraded specimen at the end of the test (g)

V_1 = Initial volume of the sample at the start of the test (mm^3)

A = Initial surface area of the sample (mm^2)

Abrasion resistance of control as well as concrete mixtures using industrial by-products was measured at 7, 28 & 90 days curing age. Mean wear depth of three samples were considered as wear depth of concrete mix.

3.8 MEASURING EQUIPMENTS USED

3.8.1 Automatic Compression Testing Machine (ACTM)

The fully Automatic Compression Testing Machine was used to test the specimens for compressive as well as split tensile strength. The set up of ACTM is shown in Fig. 3.2. Specifications of Automatic Compression Testing Machine:

1. Made by AIMIL Ltd, India
2. Linear Variable Differential Transducer attachment
3. Capacity- 3000 KN
4. Serial no.- 09149
5. CAT no.- AIM-320E-FA

Fig. 3.2: Automatic compression testing machine (courtesy: Structure lab TI, Patiala)

3.8.2 Water Penetration Apparatus

The equipment used for water penetration test is shown in Fig. 3.3.

Specifications of Water Penetration Test Machine:

1. Made by AIMIL Ltd, India
2. Serial no.- 05060
3. CAT no.- AIM-384

a) Test apparatus b) Specimen container c) Air compressor

Fig. 3.3: Water penetration testing machine (courtesy: Structure lab TI, Patiala)

3.8.3 Abrasion Testing Machine

The abrasion testing machine is shown in Fig. 3.4. As shown in the figure the machine comprises of rotating disc, device for holding specimen, rotating load of 30 N, automatic counter and stand.

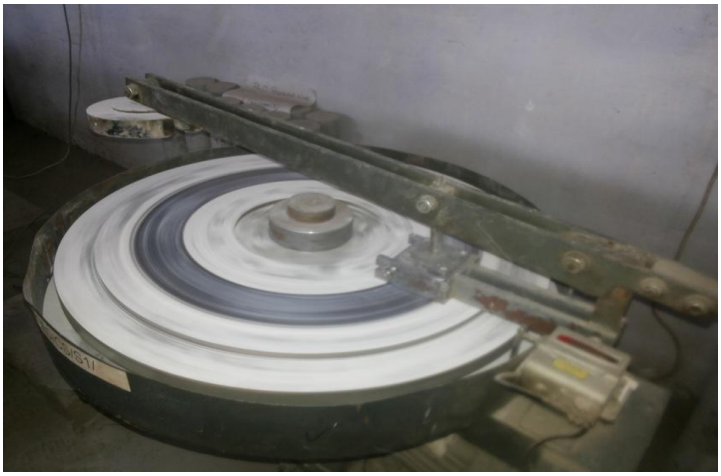

Fig. 3.4: Abrasion testing machine

3.9 ANALYSIS OF RESULTS

3.9.1 Analysis of Variance (ANOVA)

ANOVA technique was used to analyze the experimental data. ANOVA is quite helpful tool for finding the significance level of the influence of factors on a particular response. It is also used to find the contribution of each factor for the optimal response. The procedure of ANOVA consists of finding the sum of square deviations about the mean and mean square deviations as given by the Eqs. 3.4 and 3.5 below

$$SS = [\sum_{i=1}^{n} Y_i^2] - (\frac{T2}{N}) . \quad \ldots\ldots\ldots\ldots\ldots (3.4)$$

SS= Total sum of squared deviations about the mean.

Y_i = Mean value of the response for *ith* trial.

T = Sum of all values of observations

N= Total number of observations

In the ANOVA mean square deviation (MS) is calculated as:

$$MS = \frac{SS}{DOF} \quad \ldots\ldots\ldots\ldots (3.5)$$

Where, SS= Sum of squared deviations

DOF= Degree of freedom

3.10 EXPERIMENTAL PROCEDURE

The procedure devised to find the effect of substitution of cement and sand with some industrial by products. The material used for the casting of concrete samples along with the testing procedures is described herewith.

3.10.1 Characterization of the Materials

a) Cement: 43 grade OPC conformed to IS: 8112-1989 *(BIS 8112, 1989)* was used in the present study. It was tested in laboratory for finding its physical properties as per BIS code referred above. The physical properties of this cement are presented in Table 3.6.

Table 3.6: Physical Characteristics of Cement

S. No.	Characteristics	Value obtained in Lab.	Value as per IS-8112:1989
1.	Specific gravity	3.12	
2.	Fineness(% retained on90µm Sieve)	2	<10
3.	Standard consistency (%)	27.5	----
4.	Initial setting time (minutes)	125	30 (min.)
5.	Final setting time (minutes)	170	600(max.)
6.	Compressive strength (MPa)	3 days = 31.5 7 days = 40.5 28 days = 47.0	23 33 43

b) Fine Aggregate: The fine-aggregates i.e. sand used for the experiment was locally procured and conformed to Bureau of Standard Specification IS: 383-1970 *(BIS 383, 1970)*. The fineness modulus of the sand was calculated as per Table 3.7. The sand belonged to grading zone II as per IS code. The fineness modulus of fine aggregate was found to be 2.42.The sand was tested as per IS: 2386 Part III- 1963*(BIS 2386 Part-III, 1963)*.Physical characteristics of the sand are tabulated in Table 3.8. The grain size distribution curve of the sand is also given in Figure 3.5. The D50 size is 0.535mm.

Table 3.7: Calculations for fineness modulus of fine aggregates

S. No.	Size of Sieve	Weight retained (in grams)	%age retained	%age passing	Cumulative %age retained	Zone
1.	4.75 mm	1.00	0.10	99.90	0.10	II
2.	2.36 mm	50.00	5.00	94.90	5.10	II
3.	1.18 mm	153.00	15.30	79.60	20.40	II
4.	600 µ	216.00	21.60	58.00	42.00	II
5.	300 µ	373.00	37.30	20.70	79.30	II
6.	150 µ	163.00	16.30	4.40	95.60	II
7.	Pan	44.00	4.40	------	-------	------
	Total	1000		SUM=∑C	242.50	

Fineness Modulus (FM) = ∑C/100=242.50/100 = 2.42

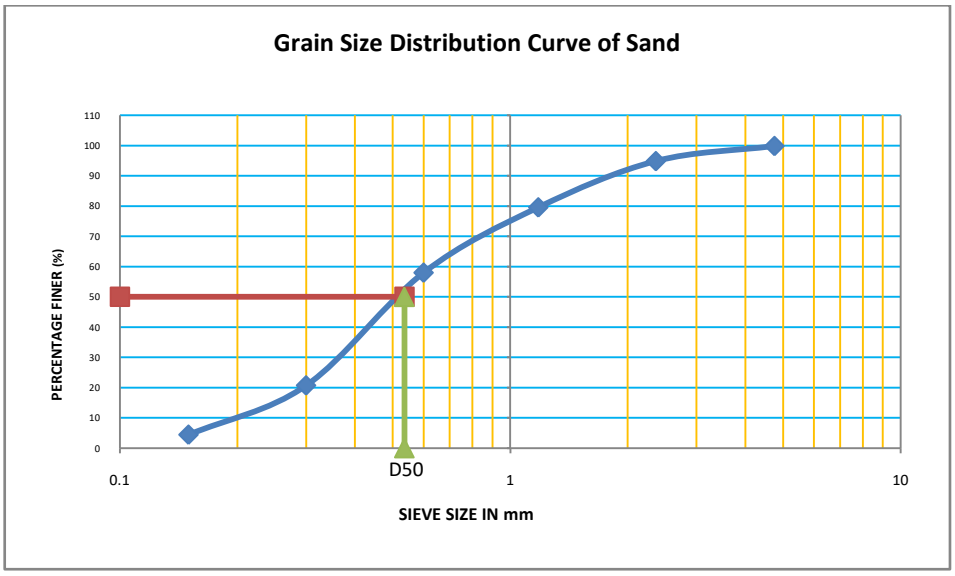

Fig. 3.5: Grain size distribution curve of sand.

Table 3.8: Physical characteristics of fine and coarse aggregates

Sr. No.	characteristic	Value for FA	Value for 10 mm CA	Value for 20 mm CA
1.	Sp. Gr.	2.73	2.72	2.69
2.	FM	2.42	6.42	7.05
3.	Water absorption	1.01%	0.8%	0.20%
4.	Grading Zone	II		

c) Coarse Aggregates: Crushed stone aggregates of 10 mm & 20 mm sizes confirming to IS: 383 1970 *(BIS 383, 1970)* specific gravity of 2.72 & 2.69, and fineness modulus of 6.42 and 7.05, respectively, were used in combination as coarse aggregates in the concrete mix. The coarse aggregates were tested as per IS: 2386 Part III-1963 *(BIS 2386 Part III, 1963)*. Physical characteristics of 20 mm & 10 mm aggregates are measured in laboratory and are shown in Table 3.8. Sieve analysis of 10 mm & 20 mm coarse aggregates are tabulated in Table 3.9 and Table 3.10 respectively.

Table 3.9: Calculations for FM of coarse aggregate (10mm)

S. No.	Size of Sieve	Mass retained (in grams)	%age mass retained	%age mass passing	Cumulative %age mass retained
1.	20 mm	0.00	0	0	0
2.	10mm	1396.00	46.53	53.47	46.53
3.	4.75 mm	1473.00	49.10	4.37	95.63
4.	2.36 mm	0	0	0	0
5.	1.18 mm	0	0	0	0
6.	600 micron	0	0	0	0
7.	300 micron	0	0	0	0
8.	150 micron	0	0	0	0
9.	Pan	131.00	4.36	------	-------
	Total	3000		SUM=∑C	142.16

Fineness Modulus (FM) = ∑C+500/100=642.16/100=6.42

Table 3.10: Calculations for fineness modulus of coarse aggregate (20mm)

S. No.	Size of Sieve	Mass retained (in grams)	%age mass retained	%age mass passing	Cumulative %age mass retained
1.	20 mm	178.00	5.93	99.87	5.93
2.	10mm	2786.00	92.90	5.45	98.83
3.	4.75 mm	36.00	1.2	0.57	100.00
4.	2.36 mm	0	0	0	0
5.	1.18 mm	0	0	0	0
6.	600 micron	0	0	0	0
7.	300 micron	0	0	0	0
9.	Pan	0	0	----	----
	Total	3000		SUM=∑C	204.76

Fineness Modulus (FM) = ∑C+500/100=704.76/100=7.05

d) Super Plasticizer: Auramix-400 is a concrete superplasticizer and is based on Polycarboxylate ether (PC) was employed as a admixture to reduce the water and also to attain the desired workability of the mixes. The dose of superplasticizer was varied between 0.5% to 2% so as to bring the workability of the mix between 50-75mm (slump

value). The general charateristics of superplasticizer are given in Table 3.11 and also confirms to IS: 9103-1999 *(BIS 9103, 1999)*.

Table 3.11: General properties of superplasticizer

S. No.	Characteristics	Value
1.	Appearance	Light yellow coloured liquid
2.	pH Value	6
3.	Volumetric mass @ 20 C	1.09 kg/ litre
4.	Chloride content	Nil
5.	Alkali content	Less than 1.5 g Na_2O equivalent / liter of admixture

e) Water: Ordinary tap water was used for the preparation of the concrete mixture and also for the curing of the specimens.

f) Industrial By-Products

A total of six industrial by-products were used as the partial replacement for cement and sand in the study as shown in Fig. 3.6 and 3.7. The sieve analysis of EAFS, IS and GP are tabulated in Tables 3.12 to Table 3.14 respectively. The sieve analysis which was done to find the fineness modulus was used to draw the grain size distribution curve and to find D50 size. The grain size distribution curve of EAFS, IS and GP is shown in Fig. 3.8 to Fig. 3.10 respectively. The specific gravity, Fineness (% retained at 90µm), Fineness modulus (FM) of by-products used as partial replacement of sand (EAFS, IS, GP) and source of each by-product are presented in the Table 3.15. Energy dispersive X-ray spectroscopy tests (EDS) and scanning electron microscopy tests (SEM) were employed to obtain the chemical properties of by-products which are shown in Fig. 3.11 to Fig. 3.16.

a) Ladle Furnace Slag (LFS) b) Fly-ash (FA) c) Copper Slag (CS)

Fig. 3.6: By-products used as cement replacement



(a) Glass powder (GP) b) Electric arc furnace slag (EAFS) (c) Iron Slag (IS)

Fig. 3.7: By-products used as sand replacement

Table 3.12: Calculations for fineness modulus of EAFS

S. No.	Size of Sieve	Weight retained (in grams)	%age retained	%age passing/finer	Cumulative %age retained
1.	4.75 mm	1.50	0.15	99.85	0.15
2.	2.36 mm	4.50	0.45	99.40	0.60
3.	1.18 mm	29.50	2.95	96.45	3.55
4.	600 µ	190.00	19.00	77.45	22.55
5.	300 µ	308.50	30.85	46.60	53.40
6.	150 µ	288.00	28.80	17.80	82.20
7.	Pan	178.00	17.80	-	-
	Total	1000		SUM=∑C	162.45

Fineness Modulus (FM) = ∑C/100=162.45 /100 = 1.62

Table3.13: Calculations for fineness modulus of IS

S. No.	Size of Sieve	Weight retained (in grams)	%age retained	%age passing/finer	Cumulative %age retained
1.	4.75 mm	2.50	0.25	99.75	0.25
2.	2.36 mm	6.00	0.60	99.15	0.85
3.	1.18 mm	49.50	4.95	94.20	5.80
4.	600 µ	158.00	15.80	78.40	21.60
5.	300 µ	324.50	32.45	45.95	54.05
6.	150 µ	265.00	26.50	19.45	80.55
7.	Pan	195.00	19.50	-	-
	Total	1000		SUM=∑C	163.10

Fineness Modulus (FM) = ∑C/100=163.10/100 = 1.63

Table 3.14: Calculations for fineness modulus of GP

S. No.	Size of Sieve	Weight retained (in grams)	%age retained	%age passing /finer	Cumulative %age retained
1.	4.75 mm	0	0	100	0
2.	2.36 mm	0	0	100	0
3.	1.18 mm	0	0	100	0
4.	600 µ	0	0	100	0
5.	300 µ	591.50	59.15	40.85	59.15
6.	150 µ	318.00	31.80	9.05	90.95
7.	Pan	90.50	9.05	-	-
	Total	1000		SUM=∑C	150.10

Fineness Modulus (FM) = ∑C/100=150.10/100 = 1.50

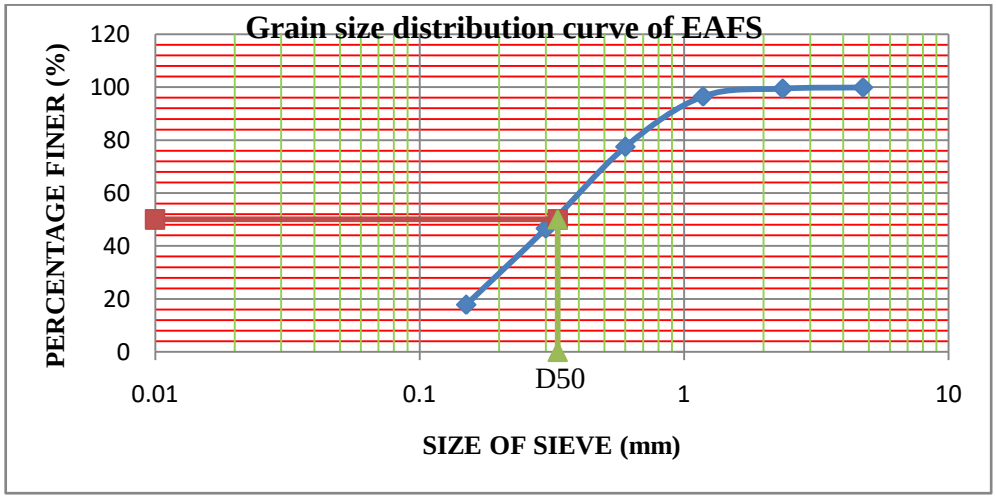

Fig. 3.8: Grain size distribution curve of EAFS

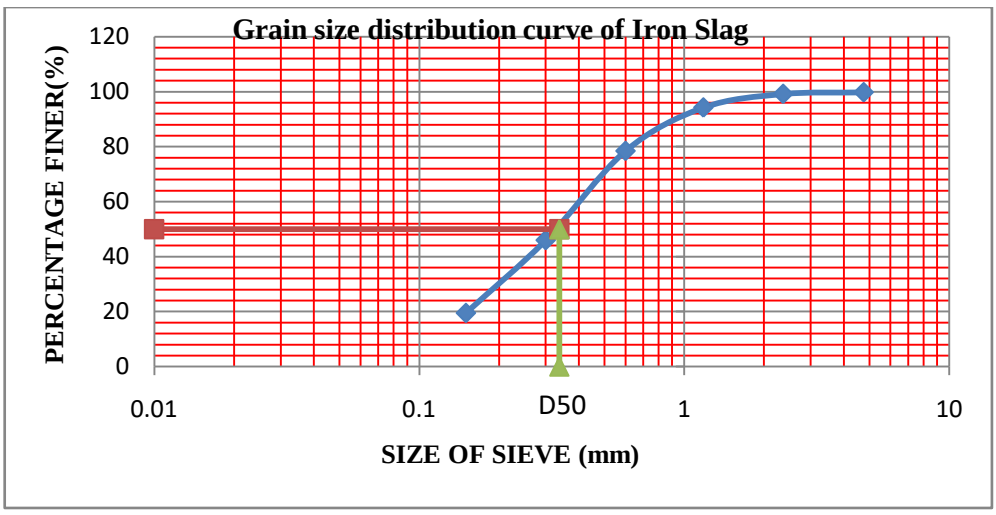

Fig. 3.9: Grain size distribution curve of Iron Slag

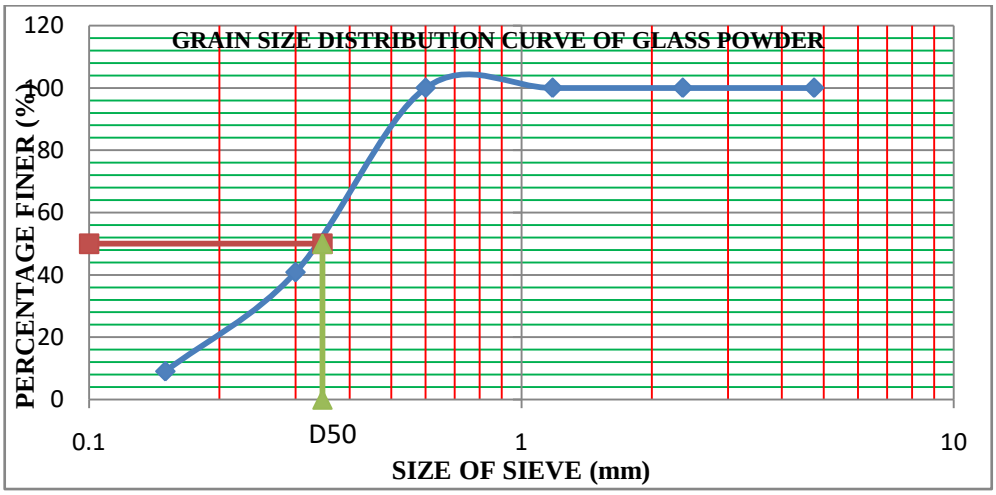

Fig. 3.10: Grain size distribution curve of Glass Powder

Table 3.15: The physical properties and source of the industrial by-products

S. No.	Name of by-product	Specific Gravity	Fineness (% retained at 90µm)	Fineness modulus (FM)	D50 Size (mm)	Source
1.	Ladle furnace slag	3.35	20	-	-	Steel Rolling Mills, Mandi Gobindgarh (Punjab)
2.	Fly-ash	2.35	0	-	-	Thermal Plant Lehra Mohabbat (Punjab)
3.	Copper Slag	3.91	85	-	-	Faridabad
4.	Glass powder	2.61	0.5	1.5	0.34	Vikas Minerals, Bareilly (Uttar Pradesh)
5.	Electric arc furnace slag	2.93	36	1.62	0.33	Steel making industries, Mandi Gobindgarh (Punjab)
6.	Iron-slag	3.35	82	1.63	0.33	Steel making industries, Mandi Gobindgarh (Punjab)

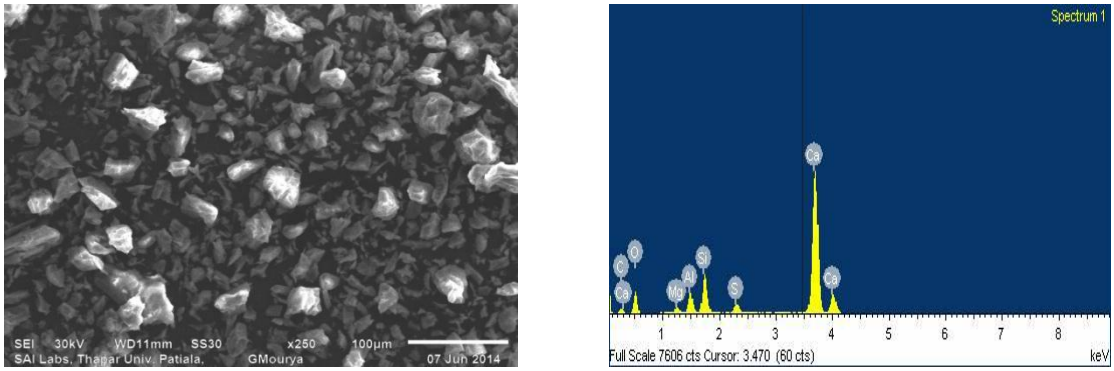

Fig. 3.11: SEM and EDS of Ladle Furnace Slag

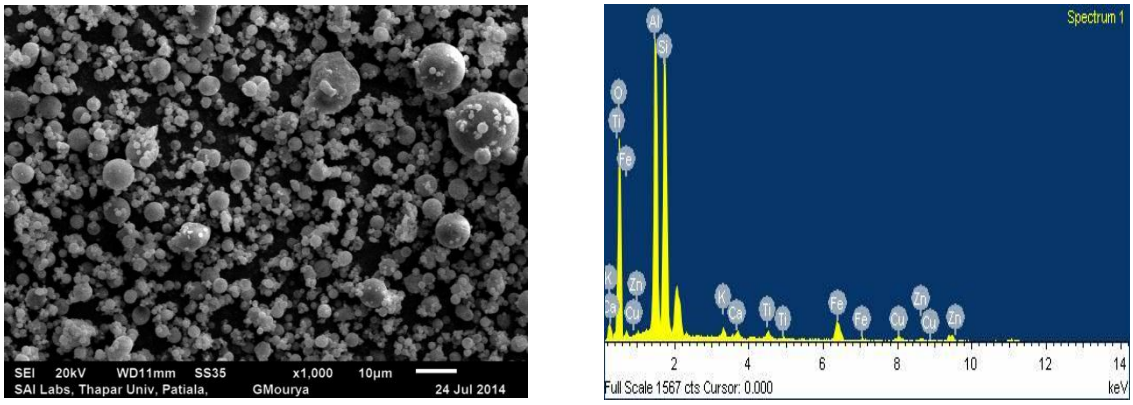

Fig. 3.12: SEM and EDS of Fly Ash

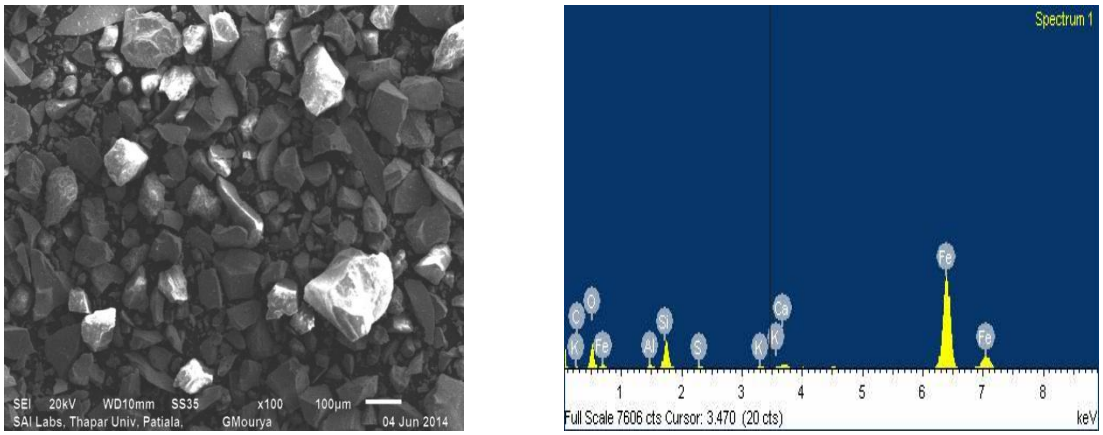

Fig. 3.13: SEM and EDS of Copper Slag

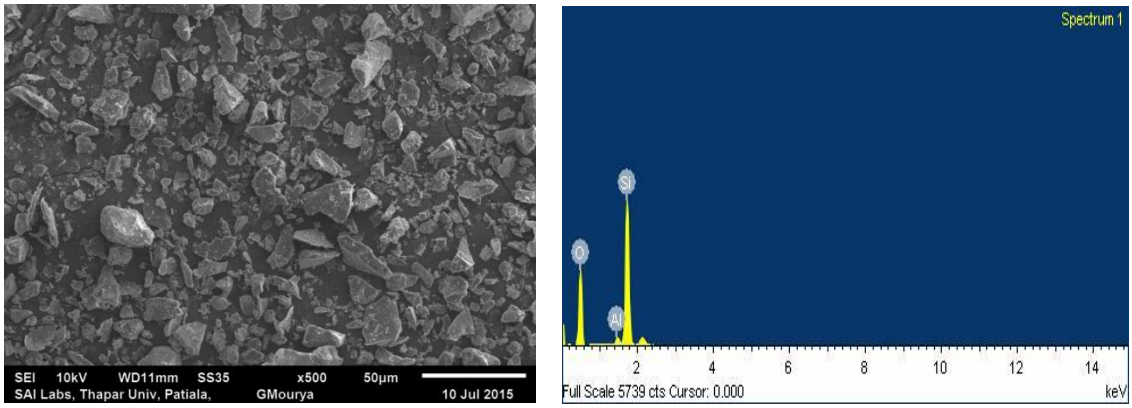

Fig. 3.14: SEM and EDS of Glass Powder

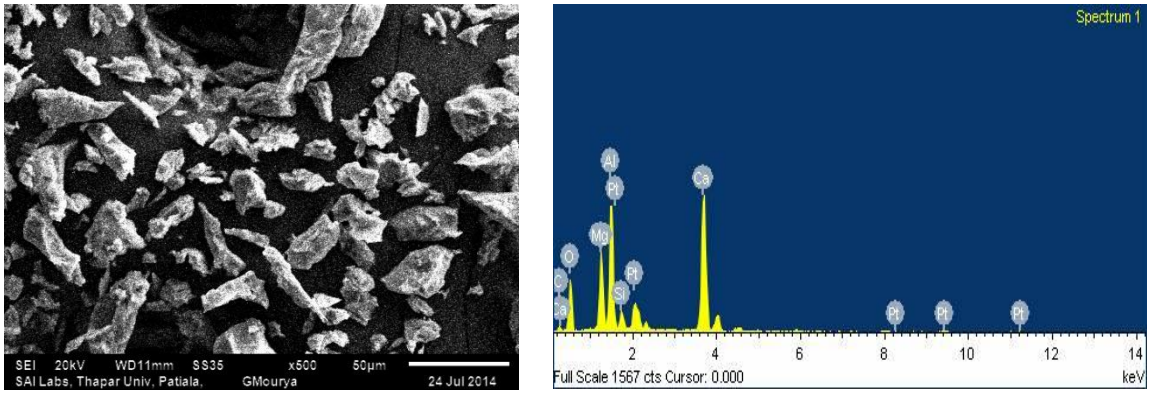

Fig. 3.15: SEM and EDS of Electric Arc Furnace Slag

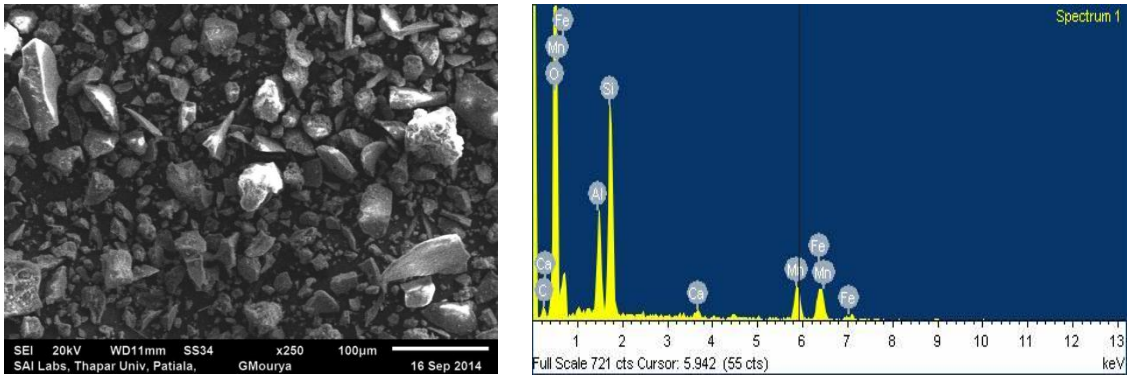

Fig. 3.16: SEM and EDS of Iron Slag

3.10.2 Chemical Composition of the Industrial By-Products Used

The Chemical composition of by-products used as partial replacement of binder and sand in this study by SEM and EDS are shown in Tables 3.16 and 3.17 respectively.

Table 3.16: Chemical composition of by-products used as a Binder by SEM and EDS

Copper Slag		Ladle Furnace slag		Fly-ash	
CaO	1.12	CaO	51.33	CaO	0.89
SiO_2	12.27	SiO_2	13.98	SiO_2	49.65
Al_2O_3	1.65	Al_2O_3	6.21	Al_2O_3	35.52
FeO	76.66	MgO	1.61	FeO	6.72
CuO	0.83	CuO	1.31	CuO	2.43
SO_3	0.73	SO_3	4.09	SO_3	---
K_2O	0.28	K_2O	---	K_2O	1.09
ZnO	2.23	ZnO	---	ZnO	2.14
CO_2	4.23	CO_2	21.46	TiO_2	1.55

Table 3.17: Chemical analysis of by-products used as a replacement of sand by SEM and EDS

Glass Powder		Electric Arc Furnace slag		Iron Slag	
CaO	----	CaO	29.92	CaO	0.85
SiO_2	97.01	SiO_2	4.33	SiO_2	30.33
Al_2O_3	2.99	Al_2O_3	24.09	Al_2O_3	12.40
MgO	----	MgO	13.45	MgO	0.75
CO_2	-----	CO_2	17.46	CO_2	34.95
K_2O	----	$\sum TiO_2 + SO_3 + MnO + Cr_2O_3$	---	TiO_2	0.60
Na_2O	----	PiO_2	10.76	MnO	9.67
				FeO	10.45

3.11 CONCRETE MIX DESIGN

3.11.1 Control Concrete

Standard high strength concrete mixes*)* were designed as per IS: 10262-2009 *(BIS* 10262*, 2009* for water/cement (w/c) ratios of 0.40, 0.44 & 0.48 and is given in Table 3.18. This was designed as control concrete specimens.

Table 3.18: Design mix for control concrete

Sr. No.	w/c	Water (kg/m^3)	Cement (kg/m^3)	Sand (kg/m^3)	CA1(20) (kg/m^3)	CA2(10) (kg/m^3)
1.	0.48	178	370.83	701.23	768.28	382.63
2.	0.44	176	400.00	678.93	769.76	383.36
3.	0.40	175	437.5	653.34	766.80	381.88

3.11.2 Concrete Mix Design Proportions Using Industrial By-Products

The proportioning of mixes for various replacements by the industrial by-products, as per the L_9 design, was carried out. The quantities of material were calculated considering the effect of variable specific gravities of the original material and its replacement by weight. The mix proportions for various trials at water/binder ratios of 0.40, 0.44 & 0.48 are given in Table 3.19 to Table 3.21 respectively.

Table 3.19: Concrete mix design proportion using specific gravity of by-products. (w/b= 0.40)

Exp. No	Water (Kg /m^3)	Binder (Kg /m^3)			Fine Aggregate (Kg /m^3)			CA (20 mm) (Kg /m^3)	CA (10 mm) (Kg /m^3)	Superplasticizer (l/m3)
		Cement	Replacement Material (%)	Amount	Sand	Replacement Material (%)	Amount			
T1	175	393.75	FA(10)	32.95	522.67	EAFS(20)	140.24	766.8	381.88	1.97
T2	175	393.75	LFS(10)	46.97	457.33	IS(30)	240.51	766.8	381.88	2.95
T3	175	393.75	CS(10)	54.83	392	GP(40)	249.85	766.8	381.88	3.93
T4	175	328.12	LFS(25)	117.44	522.67	GP(20)	124.92	766.8	381.88	3.28
T5	175	328.12	CS(25)	137.07	457.33	EAF(30)	210.36	766.8	381.88	3.28
T6	175	328.12	FA(25)	82.38	392	IS(40)	320.68	766.8	381.88	3.28
T7	175	262.5	CS(40)	219.31	522.67	IS(20)	160.33	766.8	381.88	1.31
T8	175	262.5	FA(40)	131.81	457.33	GP(30)	187.39	766.8	381.88	2.62
T9	175	262.5	LFS(40)	187.90	392	EAF(40)	280.47	766.8	381.88	5.24

(Note:- CA- Coarse Aggregates)

Table 3.20: Concrete mix design proportion using specific gravity of by-products. (w/b= 0.44)

Exp. No	Water (Kg /m^3)	Binder (Kg /m^3)			Fine Aggregate (Kg /m^3)			CA (20 mm) (Kg /m^3)	CA (10 mm) (Kg /m^3)	Superplasticizer (l/m3)
		Cement	Replacement Material (%)	Amount	Sand	Replacement Material (%)	Amount			
T1	176	360	FA(10)	30.13	543.14	EAF(20)	145.73	769.76	383.36	0.9
T2	176	360	LFS(10)	42.95	475.25	IS(30)	249.93	769.76	383.36	2.16
T3	176	360	CS(10)	50.13	407.36	GP(40)	259.63	769.76	383.36	2.7
T4	176	300	LFS(25)	107.37	543.14	GP(20)	129.82	769.76	383.36	2.25
T5	176	300	CS(25)	125.32	475.25	EAF(30)	218.6	769.76	383.36	2.25
T6	176	300	FA(25)	75.32	407.36	IS(40)	333.24	769.76	383.36	1.5
T7	176	240	CS(40)	200.51	543.14	IS(20)	166.62	769.76	383.36	0.72
T8	176	240	FA(40)	120.52	475.25	GP(30)	194.73	769.76	383.36	1.2
T9	176	240	LFS(40)	171.80	407.36	EAF(40)	291.47	769.76	383.36	4.8

Table 3.21: Concrete mix design proportion using specific gravity of by-products. (w/b= 0.48)

Exp. No	Water (Kg/m³)	Binder (Kg/m³)			Fine Aggregate (Kg/m³)			CA (20 mm) (Kg /m³)	CA (10 mm) (Kg /m³)	Superplasticizer (l/m3)
		Cement	Replacement Material (%)	Amount	Sand	Replacement Material (%)	Amount			
T1	178	333.75	FA(10)	27.93	560.98	EAF(20)	150.52	768.28	382.63	0.33
T2	178	333.75	LFS(10)	39.82	490.86	IS(30)	258.14	768.28	382.63	1.66
T3	178	333.75	CS(10)	46.47	420.74	GP(40)	267.13	768.28	382.63	1.66
T4	178	278.12	LFS(25)	99.54	560.98	GP(20)	133.56	768.28	382.63	1.39
T5	178	278.12	CS(25)	116.18	490.86	EAF(30)	225.78	768.28	382.63	1.39
T6	178	278.12	FA(25)	69.83	420.74	IS(40)	344.19	768.28	382.63	0.69
T7	178	222.5	CS(40)	185.90	560.98	IS(20)	172.1	768.28	382.63	0.44
T8	178	222.5	FA(40)	111.73	490.86	GP(30)	200.35	768.28	382.63	1.1
T9	178	222.5	LFS(40)	159.27	420.74	EAF(40)	301.04	768.28	382.63	4.44

(Note:- CA- Coarse Aggregates)

3.12 PROPERTIES INVESTIGATED

The following strength and durability tests were conducted on hardened concrete as explained earlier in section 3.7.

(a) Strength Properties: Compressive Strength test on cubes as per BIS: 516-1959 *(BIS 516, 1959)* and Split Tensile Strength test on cylinders as per IS: 5816-1999 *(BIS 5816, 1999)* were conducted to find the strength properties of the various concrete mixes. The properties were measured at the age of 7, 28 & 90 days.

(b) Durability Properties: Abrasion resistance test as per IS: 1237-2012*(BIS* 1237*, 2012)* and the test for water penetration as per IS: 3085-1987 *(BIS 3085, 1987)* were performed to find the durability properties of the concrete mixes. The properties were found at the age of 7, 28 & 90 days.

3.13 SIZES AND NUMBER OF THE VARIOUS SPECIMENS

The following are the sizes of the various specimens cast for carrying out the tests for strength and durability studies.

i) Compressive strength-150mm size cubes

ii) Split tensile strength-150 mm x 300mm cylinders

iii) Abrasion resistance test - 70.6mm x 70.6mm x 25mm tiles

iv) Water penetration test- 150mm size cubes

In this study, four factors as laid down in Table 3.2 were varied at three levels for which a possible matrix can be a 9 trial L_9 array. These trials were conducted at water/binder

ratios of 0.40, 0.44 & 0.48 and for each curing age as laid down in the Table 3.1. For each concrete mix 3 specimens corresponding to above designed mix proportions for each test conducted for both strength and durability properties were cast for testing at 7, 28 & 90 days. The details of the test matrix i.e. no. of specimens to be casted for the experimental work are presented in Table 3.22.

Table 3.22: Matrix for the tests conducted (9 combinations for each column)

Test	Water/binder = 0.40			Water/binder = 0.44			Water/binder = 0.48		
	7 days	28 days	90 days	7 days	28 days	90 days	7 days	28 days	90 days
Compressive Strength	9 x 3=27	27	27	27	27	27	27	27	27
Split Tensile Strength	27	27	27	27	27	27	27	27	27
Abrasion Test	27	27	27	27	27	27	27	27	27
Water Permeability Test	27	27	27	27	27	27	27	27	27

3.14 CASTING OF SPECIMEN

For each concrete mix, three specimens corresponding to above designed mix proportions for each test conducted for strength and durability properties were cast for testing at 7, 28 & 90 days of curing. For the casting of test samples as shown in Fig. 3.17, all the mould were cleaned and oiled properly. These moulds were properly tightened so that there is no gap between the sides of the mould. Utmost care should be observed during the batching of the materials, mixing of materials and casting operations of the samples. The casting of cubes was carried out as per IS: 10086-1982*(BIS 10086, 1982, R 2004).*

a) Loosen of mould

b) Cleaning of mould

c) Bolting of mould



d) Tighten of mould e) Oiling of mould f) Pouring of mix


g) Vibrated the mix in vibrated table h) Casted cubes

Fig. 3.17: Casting of specimens

3.15 CURING OF SPECIMEN

The moulds were loosened and the specimens were taken out very carefully after 24 hrs. as shown in the Fig.3.18 (a). After the demoulding of the specimens, these were immersed in clean water for curing for 7, 28 and 90 days as shown in Fig. 3.18 (b) at 27 ± 2 º C temperatures.



a) Opening of bolted mould b) Curing of concrete in water tank

Fig. 3.18: Curing of specimens

3.16 TESTING OF SPECIMENS

The tests were performed on the specimens for finding the compressive strength, split tensile strength, depth of water penetration and depth of wear after their curing of 7, 28 & 90 days.

3.16.1 Compressive Strength

The compressive strength tests were conducted on 150 mm cubes as per IS code 516:1979 *(BIS 516, 1979)* after curing of 7, 28 & 90 days. The mean of strength of three specimens was taken as the compressive strength of that mixture. The test was conducted in an automatic compression testing machine (ACTM) had capacity of 3000 KN as per procedure laid down in IS 516:1979 *(BIS 516, 1979)* as shown in Fig. 3.19. A uniform loading at the rate of of 5kN/Sec was applied on the specimen for the testing.

Fig. 3.19: Compressive strength measurements (ACTM) (Structure lab TI, Patiala)

3.16.2 Split Tensile Strength

The split tensile strength tests were performed on cylindrical specimens of size 150 mm x300mm as per IS 5816:1999 *(BIS 5816, 1999)* after 7, 28 and 90 days curing. The split tensile strength of the mixture was considered as the mean of strength of three cylinder specimens. An automatic compression test machine (3000KN capacity) was used to conduct the test for split tensile strength as per procedure laid down in IS 5816:1999*(BIS 5816, 1999).* The position of specimen and the type of failure in split tensile test in ACTM is shown in Fig. 3.20.

Fig. 3.20: The position of specimen and the type of failure in split tensile test in Automatic compressions testing machine (courtesy: Structure lab TI, Patiala)

3.16.3 Durability Properties

(a) Water Penetration Test

The water penetration tests were performed on cube specimens of size 150mm to find the depth of water penetration as per German standard DIN-1048 *(DIN 1048, Part5)* after 7, 28 & 90 days of curing. The depth of water penetration of the mix was taken as mean of the three tests on the samples. The testing procedure is shown in Fig. 3.21.

Fig.3.21: Depth of water penetration measurements (WPTM) (from Structure lab TI, Patiala)

(b) Abrasion Resistance Test

Resistance to abrasion of concrete as depth of wear was measured as per procedure given in BIS: 1237-2012 *(BIS 1237, 2012)*. The test samples were oven dried at 110 ± 5^0 Celsius for 24 hr and then precisely weighed to the least count of 0.1 g. Thickness at four corners

and at centre of dried specimens was measured. Fig. 3.4 shows the apparatus for measuring depth of wear of concrete specimens against abrasion. After that the test specimen was put in the holding device of the machine. The abrasive powder of 20 g was spread uniformly on the surface of the machine. The machine is then started for the abrasion of the specimen. After the twenty two revolutions, the disc was stopped and the abraded powder was removed from the disc and the specimen was turned at 90 degrees about the vertical axis. The same procedure is repeated for 9 times thus giving total of 220 revolutions. After 220 revolutions the specimen is taken out and then weighted to 0.1 g. The thickness of the specimen is again measured at four points. The thickness loss was calculated from the formula given in the Eq. 3.3.

The depth of wear of control as well concrete mixtures using industrial by-products was calculated after 7, 28 & 90 days. The depth of wear of the concrete mix was taken as mean of depth of wear on three samples.

3.16.4 Scanning Electron Microscopy (SEM)

The SEM analysis was performed on the samples to verify the results of the confirmation experiments and to evaluate the changes occurred in the concrete microstructure occurred with the addition of industrial by-products. Since the 1960s, SEM has been used for the microstructural examination of concrete. The fractured pieces of control concrete and concrete containing by-products generated from compressive strength test were first ground and then sieved through 90 μm sieve. The concrete specimens were coated with a thin layer of gold to make them electrically conductive before placing on the Scanning Electron Microscopy (SEM) stem. The working distance i.e. the distance at which the beam is focused (it is normally the distance from the final pole piece of the lens to the sample when the image is in focus) is kept between 11 to 13 mm to enable clearer images. The testing was performed in accordance with ASTM-C1723-2010 for the collected samples. It was also used to understand changes in the strength and durability characteristics of such mixes. The SEM test was conducted after 28 & 90 days and for all the three water/binder ratios i.e. 0.48, 0.44, & 0.40. From SEM images, significant amount of variations were found in the concrete microstructure with the addition industrial by-products for all the water/binder ratios. The experimental set up for scanning electron microscope is shown in Fig.3.22.

Fig. 3.22: Experimental set up for Scanning Electron Micrograph

3.16.5 X-Ray Diffraction (XRD) Analysis

The XRD technique was employed to know various phases of hardened concrete containing by-products as well as in control concrete. The XRD was carried for a diffraction angle of 2θ ranged between 5° to 80° to prepare the graph showing the angle 2θ on x-axis and relative intensities on y-axis. The diffraction peaks were shown for different compounds present in the sample. These peaks were compared with the standard peaks of compounds released by ICDD (International Centre for Diffraction Data). Fig 3.23 shows the XRD instrument.

Fig. 3.23: X-Ray diffraction (XRD) instrument

3.17 RESULTS OF THE EXPERIMENTS

3.17.1 Results of Compressive Strength Tests

As discussed in the section 3.16.1, after the experiments were conducted for control concrete and the concrete developed with partial replacement of cement and fine aggregates with industrial by products, the compressive strength of the samples was measured as explained in section 3.7.1 at different water/binder ratios and at different curing periods. The average of strength of three specimens was taken as the compressive strength of that mixture. The values of the test results which fell within the range of 10%-15% variation from the average were taken to calculate the average. The results for control concrete mixes and the concrete mixes made with the use of industrial by products are given in Table 3.23 and table 3.24 respectively.

Table 3.23: Experimental results of control concrete mixes for compressive strength

S. No.	w/c	Compressive Strength (MPa)		
		7 - Day	28 - Day	90 - Day
1	0.48	27.00	42.06	46.20
2	0.44	30.50	45.13	47.20
3	0.40	39.80	51.05	55.64

Table 3.24: Experimental results of trial mixes for compressive strength

Trial mix	Combination (See Tables 3.4 & 3.5)	Compressive strength (MPa)								
		Water/ binder = 0.48			Water/ binder = 0.44			Water/ binder = 0.40		
		7-days	28-days	90-days	7-days	28-days	90-days	7-days	28-days	90-days
T1	A1B1C1D1	28.60	46.05	57.09	30.97	47.83	61.33	41.50	53.76	72.05
T2	A1B2C2D2	28.38	45.02	55.96	31.00	45.68	56.21	39.82	50.32	64.35
T3	A1B3C3D3	26.48	39.82	45.98	29.83	40.79	48.11	30.80	46.20	51.18
T4	A2B1C2D3	21.48	30.23	38.50	26.94	37.14	43.45	27.50	39.60	44.55
T5	A2B2C3D3	22.30	33.96	41.09	28.82	37.62	45.34	29.81	40.92	46.20
T6	A2B3C1D2	22.73	39.08	56.77	30.42	46.60	60.35	31.24	49.94	66.33
T7	A3B1C3D2	16.06	23.76	31.10	19.58	27.03	33.81	21.12	31.21	36.22
T8	A3B2C1D3	21.78	31.82	44.73	25.74	37.95	51.62	29.77	49.14	64.90
T9	A3B3C2D1	17.16	24.11	32.45	23.96	28.08	36.74	25.85	30.88	39.38

3.17.2 Results of Split Tensile Strength

As discussed in the section 3.16.2, after the experiments were conducted on control concrete and the concrete developed with partial replacement of cement and fine aggregates with industrial by products, the split tensile strength of the samples was measured as explained in section 3.7.2 at different water/binder ratios and at different curing periods. The average of strength of three specimens was taken as the split tensile strength of that mixture. The values of the test results which fell within the range of 10%-15% variation from the average were taken to calculate the average. The results for control concrete and the concrete made with the use of industrial by products are given in Table 3.25 and Table 3.26 respectively.

Table 3.25: Experimental results of control concrete mix

S. No.	w/c	Split Tensile Strength (MPa)		
		7 day	28 day	90 day
1	0.48	2.21	3.45	3.81
2	0.44	2.40	3.82	4.21
3	0.40	2.97	4.47	4.89

Table 3.26: Experimental results of trial mixes

Trial mix	Combination (See Tables 3.4 & 3.5)	Split Tensile strength (MPa)								
		Water/ binder = 0.48			Water/ binder = 0.44			Water/ binder = 0.40		
		7-days	28-days	90-days	7-days	28-days	90-days	7-days	28-days	90-days
T1	A1B1C1D1	2.13	3.15	3.68	2.53	3.36	3.76	2.67	3.41	4.58
T2	A1B2C2D2	1.96	3.03	3.25	2.22	3.12	3.45	2.47	3.24	4.07
T3	A1B3C3D3	1.85	2.90	3.31	2.15	2.98	3.39	2.23	3.10	3.57
T4	A2B1C2D3	1.72	2.68	3.20	1.78	2.74	3.26	2.21	2.82	3.46
T5	A2B2C3D3	1.89	2.89	3.31	2.00	3.04	3.67	2.42	3.20	3.87
T6	A2B3C1D2	2.34	3.00	3.47	2.55	3.10	3.75	2.64	3.25	4.00
T7	A3B1C3D2	1.17	1.88	2.79	1.94	2.33	2.83	2.06	2.55	3.15
T8	A3B2C1D3	1.63	2.63	3.38	1.97	3.05	3.66	2.03	3.41	3.80
T9	A3B3C2D1	1.60	2.33	2.53	1.76	2.59	2.71	2.20	2.69	2.76

3.17.3 Results of Water Permeability of Concrete

As discussed in the section 3.16.3, after the experiments were conducted on control concrete and the concrete made with industrial by products, the water penetration depth of the concrete samples was measured as explained in section 3.7.3 at various water/binder ratios and at different curing ages. The average of water penetration depth of three specimens was taken as the water penetration depth of that mixture. The values of the test results which fell within the range of 10%-15% variation from the average were taken to calculate the average. The results for control concrete and the concrete made with industrial by products are given in Table 3.27 and Table 3.28 respectively.

Table 3.27: Experimental results of water penetration depth of control Concrete

S. No.	w/c	Water Penetration Depth (mm)		
		7-days	28-days	90-days
1	0.48	70	50	30
2	0.44	50	40	20
3	0.40	30	20	12

Table 3.28: Experimental results of water penetration depth of trial mixes

Trial mix	Combination (See Tables 3.4 & 3.5)	Water Penetration Depth (mm)								
		Water/ binder = 0.48			Water/ binder = 0.44			Water/ binder = 0.40		
		7-days	28-days	90-days	7-days	28-days	90-days	7-days	28-days	90-days
T1	A1B1C1D1	110	70	35	80	60	30	60	50	20
T2	A1B2C2D2	124	50	25	101	40	20	95	35	15
T3	A1B3C3D3	80	47	20	50	40	17	30	20	15
T4	A2B1C2D3	65	55	40	45	38	25	37	27	22
T5	A2B2C3D3	120	110	50	116	70	42	110	60	32
T6	A2B3C1D2	115	55	30	101	45	26	90	35	17
T7	A3B1C3D2	70	66	50	66	61	42	53	50	40
T8	A3B2C1D3	140	130	40	135	100	30	130	70	20
T9	A3B3C2D1	120	60	45	110	50	20	100	44	17

3.17.4 Results for the Abrasion Resistance i.e. Depth of Wear

As discussed in the section 3.16.3, after the experiments were conducted on control concrete and the concrete made with industrial by products, the depth of wear of the concrete samples was measured as explained in section 3.7.3 at various water/binder ratios and at different curing ages. The average of depth of wear of three specimens was taken as the depth of wear of that mixture. The values of the test results which fell within the range of 10%-15% variation from the average were taken to calculate the average. The results for control concrete and the concrete made with by products are given in Table 3.29 and Table 3.30 respectively.

Table 3.29: Experimental results of depth of wear of control concrete mix

S. No.	w/c ratio	Depth of wear (mm)		
		7-days	28-days	90-days
1	0.48	0.456	0.389	0.379
2	0.44	0.453	0.358	0.336
3	0.40	0.418	0.342	0.323

Table 3.30: Experimental results of depth of wear of trial mixes

Trial mix	Combination (See Tables 3.4 & 3.5)	Depth of Wear (mm)								
		Water/ binder = 0.48			Water/ binder = 0.44			Water/ binder = 0.40		
		7-days	28-days	90-days	7-days	28-days	90-days	7-days	28-days	90-days
T1	A1B1C1D1	0.422	0.383	0.352	0.364	0.265	0.246	0.362	0.263	0.224
T2	A1B2C2D2	0.387	0.370	0.347	0.385	0.330	0.313	0.339	0.321	0.312
T3	A1B3C3D3	0.470	0.394	0.340	0.382	0.352	0.315	0.326	0.322	0.314
T4	A2B1C2D3	0.392	0.365	0.339	0.387	0.360	0.250	0.376	0.356	0.234
T5	A2B2C3D3	0.357	0.328	0.313	0.331	0.317	0.288	0.330	0.306	0.240
T6	A2B3C1D2	0.458	0.363	0.340	0.394	0.358	0.339	0.335	0.316	0.275
T7	A3B1C3D2	0.503	0.370	0.341	0.426	0.337	0.293	0.345	0.323	0.289
T8	A3B2C1D3	0.491	0.380	0.351	0.440	0.365	0.294	0.342	0.336	0.285
T9	A3B3C2D1	0.572	0.498	0.409	0.504	0.374	0.355	0.476	0.355	0.330

CHAPTER 4 ANALYSIS OF RESULTS

4.0 GENERAL

The proportioning of mixes for various replacements by the industrial by-products, as per the L_9 design, was carried considering the effect of variable specific gravities of the original material and its replacement. The effect of various parameters/factors such as 1) the percentage of by-product to be used as a binder; 2) the percentage of by-product to be used as sand/fine aggregate (FA); 3) the kind of by-product to be used as cement /binder and 4) the kind of by-product to be used as FA on the strength & durability properties were evaluated using ANOVA. A confidence interval of 95% was used in this analysis. Nine trial experiments were performed using Taguchi's L_9 orthogonal array (OA). As per design of experiments, there were two fixed parameters namely water to binder ratio and curing age with three levels each. Now nine experiments were carried out for each combination of water to binder ratio and curing age, thereby resulting in a cumulative total of 81 experiments. The obtained results were analyzed to find out:

- Combination of optimal parameters.
- The percentage contribution of each parameter from ANOVA.
- Significance of each parameter.
- The theoretical predicted values of output characteristic at the optimum parameter setting.

4.1 ANALYSIS OF RESULTS FOR COMPRESSIVE STRENGTH

4.1.1 Analysis of Variance (ANOVA)

Three experiments for every 9 trial conditions as per Taguchi's L_9 matrix were completed to measure compressive strength. The mean compressive strength for each trial and for each water to binder ratios and each curing periods are presented in Table 3.24. The experimental results were analyzed with ANOVA method. The ANOVA calculations, response tables and the plots were developed using MINITAB16. The results were further analyzed for identification of the significant factors affecting the responses. The response tables for means of compressive strength for 7, 28 & 90 days are given in Tables 4.1 to 4.3 respectively for w/b ratios of 0.40,

0.44 & 0.48. Basically, if the value of mean response is large, then the quality of the product will be closer to its ideal value and vice versa. Therefore, a larger mean compressive strength is required for optimal performance. Now for example, from the Table 4.1, for 7 days of curing and at 0.48 water/ binder ratio, the optimal parameters for better compressive strength are A1 B2 C1 D3. So the optimal parameters are quantity of by-product to be used as binder (%) at level 1, quantity of by-product to be used as fine aggregate (%) at level 2, type/kind of by-product to be used as cement at level 1and type of by product to be used as sand/fine aggregate at level 3. The ANOVA data indicating sum of squares (SS), variance (V) and percentage contribution (PC) of each parameter at 95% confidence interval, at 7, 28 & 90 days of curing and for each w/b ratios of 0.40, 0.44 & 0.48 is provided in Tables 4.4 to 4.6. The larger is the percentage contribution value for a particular factor, the larger would be its effect on the output. Comparing the percentage contribution from ANOVA table for 7 days compressive strength at water to binder ratio of 0.40 (Table 4.4), the percentage of by-product used as binder (57.30% contribution) is the factor that significantly affects the compressive strength. This is followed by the type of by-product used as binder (26.93% contribution), the quantity of by-product (%) to be used as fine aggregate (9.91% contribution) and the by-product to be used as a fine aggregate (5.85% contribution).

Table 4.1: Response table for means of compressive strength for curing period of 7 Days

Level	**w/b ratio = 0.48**				**w/b ratio = 0.44**				**w/b ratio = 0.40**			
	(A)	**(B)**	**(C)**	**(D)**	**(A)**	**(B)**	**(C)**	**(D)**	**(A)**	**(B)**	**(C)**	**(D)**
1	27.82	22.05	24.37	22.69	30.60	25.83	29.04	27.92	37.37	30.04	34.17	32.39
2	22.17	24.15	22.34	22.39	28.73	28.52	27.30	27.00	29.52	33.13	31.06	30.73
3	18.33	22.12	21.61	23.25	23.09	28.07	26.08	27.50	25.58	29.30	27.24	29.36
Delta	9.49	2.11	2.76	0.86	7.51	2.69	2.97	0.92	11.79	3.84	6.93	3.03
Rank	1	3	2	4	1	3	2	4	1	3	2	4

(Note:- A, B, C and D are the control factors as listed in Table 3.2)

Table 4.2: Response table for means of compressive strength for curing of 28 Days

Level	w/b ratio = 0.48				w/b ratio = 0.44				w/b ratio = 0.40			
	(A)	(B)	(C)	(D)	(A)	(B)	(C)	(D)	(A)	(B)	(C)	(D)
1	43.63	33.35	38.98	34.71	44.77	37.33	44.13	37.84	50.09	41.52	50.95	41.85
2	34.42	36.93	33.12	35.95	40.45	40.42	36.97	39.77	43.49	46.79	40.27	43.82
3	26.56	34.34	32.51	33.96	31.02	38.49	35.15	38.63	37.08	42.34	39.44	44.98
Delta	17.07	3.59	6.47	2.00	13.75	3.08	8.98	1.93	13.02	5.27	11.50	3.13
Rank	1	3	2	4	1	3	2	4	1	3	2	4

(Note:- A, B, C and D are the control factors as listed in Table 3.2)

Table 4.3: The Response table for means of compressive strength for curing of 90 Days

Level	w/b ratio = 0.48				w/b ratio = 0.44				w/b ratio = 0.40			
	(A)	(B)	(C)	(D)	(A)	(B)	(C)	(D)	(A)	(B)	(C)	(D)
1	53.01	42.23	52.86	43.54	55.22	46.20	57.77	47.80	62.53	50.94	67.76	52.54
2	45.45	47.26	42.30	47.94	49.71	51.06	45.47	50.12	52.36	58.48	49.43	55.63
3	36.09	45.07	39.39	43.07	40.72	48.40	42.42	47.73	46.83	52.30	44.53	53.54
Delta	16.92	5.03	13.47	4.87	14.49	4.86	15.35	2.40	15.69	7.54	23.23	3.09
Rank	1	3	2	4	2	3	1	4	2	3	1	4

(Note:- A, B, C and D are the control factors as listed in Table 3.2)

Thus, it is concluded that the concrete strength properties at early age (7days) are majorly affected by the percentage replacement of the by-product used as a binder,

Table 4.4: ANOVA table for mean compressive strength at 7 days

Factor designation As per Table 3.2	dof	w/b ratio = 0.48			w/b ratio = 0.44			w/b ratio = 0.40		
		SS	V	PC	SS	V	PC	SS	V	PC
A	2	328.83	164.42	57.30343	91.53	45.77	77.1884	136.61	68.31	86.15883
B	2	56.88	28.44	9.912171	12.44	6.22	10.49081	8.561	4.28	5.399354
C	2	154.57	77.29	26.93608	13.34	6.67	11.24979	12.246	6.12	7.723454
D	2	33.56	16.78	5.84832	1.27	0.64	1.071007	1.139	0.57	0.718358
Total	8	573.84	286.92	100	118.58	59.29	100	158.556	79.278	100

(Note:- SS= Sum of squares, V = Variance, PC= %age Contribution)

Table 4.5: ANOVA table for mean compressive strength at 28 days

Factor designation As per Table 3.2	dof	w/b ratio = 0.48			w/b ratio = 0.44			w/b ratio = 0.40		
		SS	V	PC	SS	V	PC	SS	V	PC
A	2	254.3	127.15	45.03515	296.4	148.20	65.58102	437.81	218.91	80.90961
B	2	48.37	24.19	8.566065	14.59	7.30	3.228162	20.59	10.30	3.805141
C	2	247	123.50	43.74236	135.33	67.67	29.94292	76.61	38.31	14.15793
D	2	15	7.50	2.656419	5.64	2.82	1.247898	6.1	3.05	1.127312
Total	8	564.67	282.34	100	451.96	225.98	100	541.11	270.56	100

(Note:- SS= Sum of squares, V= Variance, PC= %age Contribution)

Table 4.6: ANOVA table for mean compressive strength at 90 days

Factor designation As per Table 3.2	dof	w/b ratio = 0.48			w/b ratio = 0.44			w/b ratio = 0.40		
		SS	V	PC	SS	V	PC	SS	V	PC
A	2	321.3	160.65	42.05938	321.3	160.65	42.05938	430.89	215.45	52.94074
B	2	35.53	17.77	4.651011	35.53	17.77	4.651011	38.16	19.08	4.688479
C	2	395.97	197.99	51.83396	395.97	197.99	51.83396	301.53	150.77	37.04709
D	2	11.12	5.56	1.45565	11.12	5.56	1.45565	43.33	21.67	5.323684
Total	8	763.92	381.96	100	763.92	381.96	100	813.91	406.96	100

(Note:- SS= Sum of squares, V= Variance, PC= %age Contribution)

4.1.2 Main Effects Plots for Means

The main effects plot for means of compressive strength at 7, 28 & 90 days for each of water/binder ratios are shown in Fig. 4.1 to Fig. 4.3 respectively. Main effects plot show the variation of each response with the change in factor levels. The x- axis shows the variation of each factor at its three levels and y-axis represents the change in the response (i.e. compressive strength). The horizontal line shows the mean of response. The figure depicts the extent of significance each factor has on the response. The slope of each plot is an indication of significance of each factor.

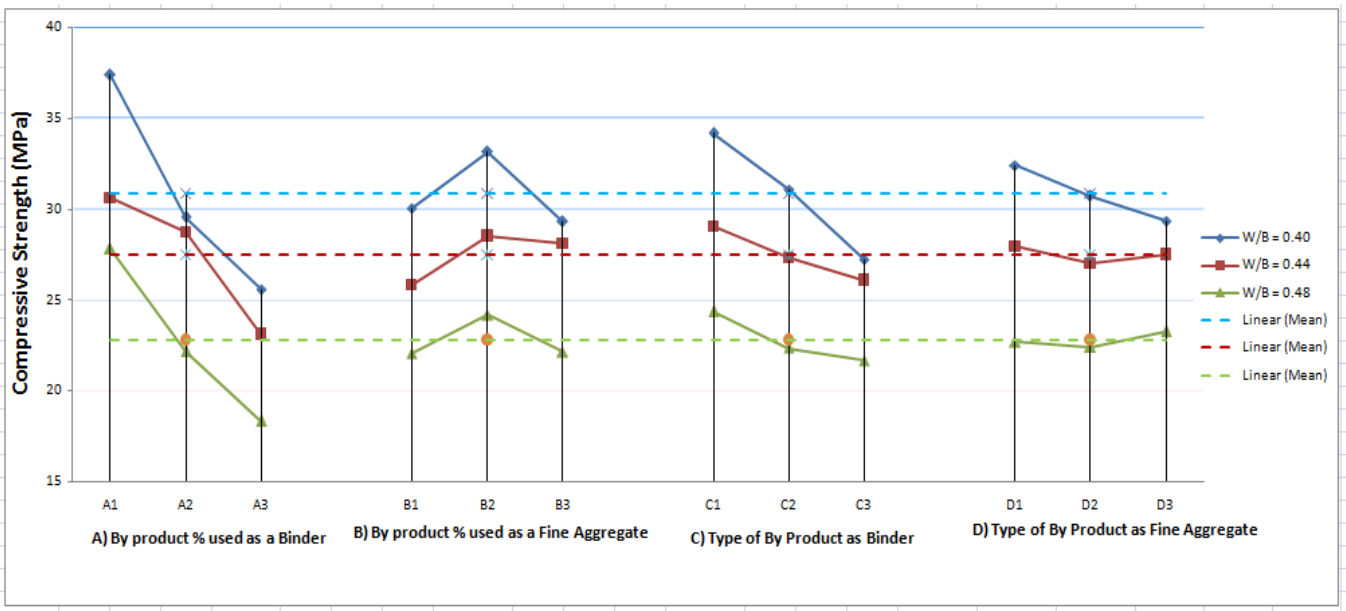

Fig. 4.1: Main effects plot for means of compressive strength at 7 days

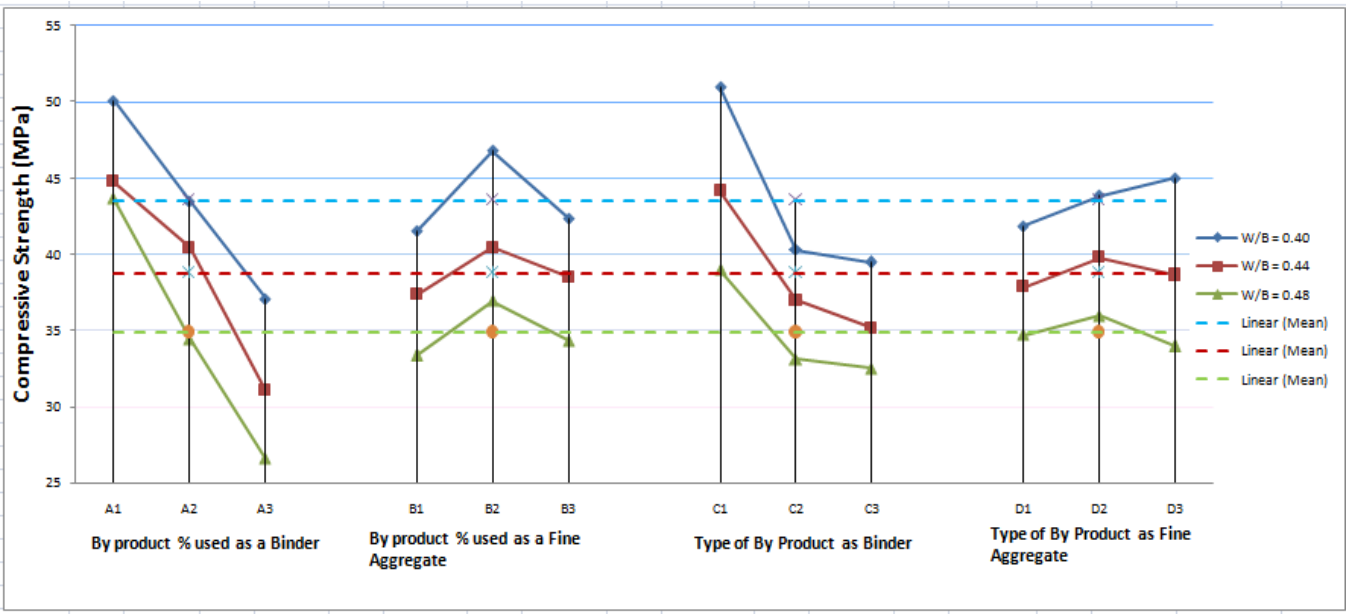

Fig. 4.2: Main effects plot for means of compressive strength at 28 days

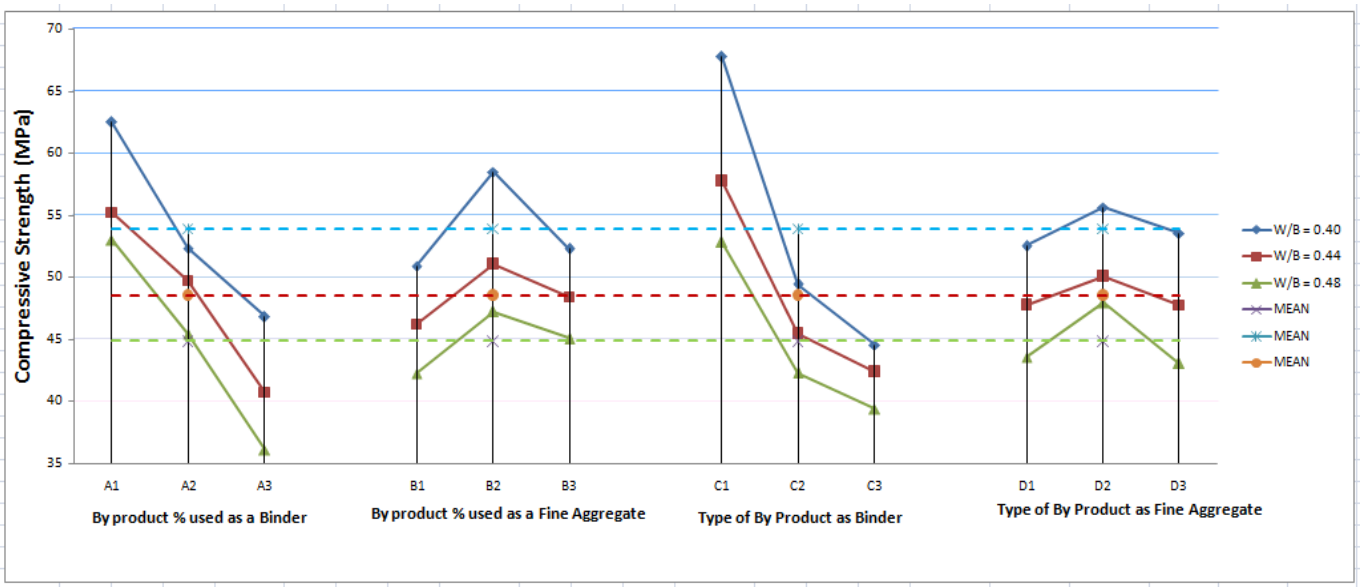

Fig. 4.3: Main effects plot for means of compressive strength at 90 days

4.1.3 Optimum Design Consideration

There could be three types of output values in any experimental analysis, which needs to be obtained with conducting experiments, which may be a 'larger is better', a 'nominal is better' or a 'smaller is better'. In the present situation compressive strength is "larger is better" type of responses. The graphs of the main effects were utilized to estimate the mean compressive strength using optimal design parameters.

4.1.4 Optimal Design Mix Parameters

The significant factors which were identified after ANOVA analysis (see Tables 4.4 to 4.6) and their graphs were used to find their most appropriate level which would increase the compressive strength. Table 4.7 to 4.9 provides the summary of the ANOVA analysis for finding the optimal mix design parameters at 7, 28 and 90 days respectively. The Tables 4.10 to 4.12 elucidates the optimal percentage replacement and the percentage contribution of each parameter towards the compressive strength of resulting concrete. The effect of curing period on optimal mix design parameters and percentage contribution of various optimal parameters towards strength at different curing periods is discussed below.

(a) Effect of curing period on optimal mix design parameters

- At curing period of 7 days (i.e. At an early age)

The optimal parameters found for compressive strength at 7 days of curing are given in Table 4.7. It is seen that at 7 days curing, for all w/b ratios, fly-ash as cement replacement gives the optimal value, whereas glass powder replacement for sand provides the optimal value of strength results, only for higher w/b of 0.48.

Table 4.7: Optimal parameters for compressive strength after 7 days of curing

Exp. No.	W/B ratio	Optimal Parameters	Optimal Parameters			
			A	B	C	D
1	0.48	A1B2C1D3	10%	30%	Fly Ash	Glass Powder
2	0.44	A1B2C1D1	10%	30%	Fly Ash	EAFS
3	0.4	A1B2C1D1	10%	30%	Fly Ash	EAFS

(Note:- A, B, C and D are the parameters defined in the Table 3.2)

However, at lower w/b of 0.44 & 0.40, electric arc furnace slag as a replacement for sand provides better results. Also, it is observed that for all water to binder ratios, 10% is the optimum %age of fly ash replacement contributing to higher compressive strength at early ages, whereas 30% of sand replacement by glass powder at w/b of 0.48 contributes positively to strength gain at an early age. For lower w/b ratios, 30% of sand replacement by electric arc furnace slag provides the optimal strength results. Thus, it can be concluded that at the early age of 7 days curing, for the replacement of cement, the replacement material (i.e. fly ash) and its percentage (i.e.10%) remains the only optimum parameters for all water binder ratios, whereas, on the other hand, for the replacement of sand, the percentage replacement remains constant (i.e. 30%) at all the water/binder ratios and the replacement material changes from glass powder to electric arc furnace slag, as the water/binder ratio reduces.

- At 28 days curing period (i.e. At normal age)

The optimal parameters for compressive strength at 28 days of curing are given in Table 4.8. On observing the tabulated analysis results at 28 days curing, for all water binder ratios, it is noticed that cement replacement by fly ash gives the optimal compressive strength, whereas, on the other

hand, replacement of sand by iron slag at higher w/b and glass powder at lower w/b gives the optimal result.

Table 4.8: Optimal parameters for compressive strength at 28 days of curing

Exp. No.	W/B ratio	Optimal Parameters	Optimal Parameters			
			A	B	C	D
1.	0.48	A1B2C1D2	10%	30%	Fly Ash	Iron Slag
2.	0.44	A1B2C1D2	10%	30%	Fly Ash	Iron Slag
3.	0.4	A1B2C1D3	10%	30%	Fly Ash	Glass Powder

(Note:- A, B, C and D are the parameters defined in the Table 3.2)

Also, it is seen that for all water/binder ratios, 10% is the optimum %age of fly ash substitution contributing to higher strength at normal age, whereas 30% of sand replacement by iron slag at water/binder ratios of 0.48 & 0.44 provides the optimal strength results. Thus, it is concluded that at normal age i.e. at 28 days of curing, the replacement material (i.e. fly ash) and its percentage (i.e.10%) remains constant at all water/binder ratios, whereas, on the other hand, for the replacement of sand, the type of material and its percentage replacement remains constant i.e. 30% iron slag at higher w/b ratios and it changes to 30% glass powder only at lower water/binder ratio.

- At curing age of 90 days

The optimal parameters for compressive strength after the curing age of 90 days are given in Table 4.9. On analyzing the results at 90 days curing, for all water/binder ratios, it is noticed that replacement of cement with fly ash gives the optimal result, whereas, on the other hand, replacement of sand by

Table 4.9: Optimal parameters for compressive strength at 90 days

Exp. No.	W/B ratio	Optimal Parameters	Optimal Parameters			
			A	B	C	D
1.	0.48	A1B2C1D2	10%	30%	Fly Ash	Iron Slag
2.	0.44	A1B2C1D2	10%	30%	Fly Ash	Iron Slag
3.	0.4	A1B2C1D2	10%	30%	Fly Ash	Iron Slag

(Note:- A, B, C and D are the parameters defined in the Table 3.2)

iron slag gives the optimal result. Also, it is observed that for all w/b ratios, 10% is the optimal %age of Fly ash replacement contributing to higher strength at 90 days age, whereas 30% of sand replacement by iron slag provides the optimal strength results. Thus, it can be concluded that at curing age of 90 days, the replacement material and its percentage replacement values for both cement as well as sand remain constant for all water-binder ratios i.e. 10% of fly ash for cement replacement and 30% of iron slag for sand replacement.

To sum up, it is found that 10% of fly ash is the optimal parameters for cement replacement for compressive strength at all the curing periods and water to binder ratios. Similarly 30% is the optimal replacement level of sand for all the w/b ratios and for all the curing ages.

(b) Percentage contribution of various optimal parameters towards compressive strength at different curing ages

The results indicating the %age contribution of optimal parameters towards concrete compressive strength at 7, 28 and 90 days are tabulated in Tables 4.10 to 4.12 respectively. The effect at different curing ages is presented below:

- At 7 days curing period (i.e. At early age)

As shown in Table 4.10, at 7 days, for all water/binder ratios, 10% of by-product to be used as a replacement of cement is the optimal parameter which contributes maximum towards strength of the resulting concrete

Table 4.10: Percentage contribution of each parameter for compressive strength after 7 days of curing age

Exp. No.	W/B ratio	Optimal Parameters				Rank				% Contribution			
		(A)	(B)	(C)	(D)	(A)	(B)	(C)	(D)	(A)	(B)	(C))	(D)
1	0.48	10%	30%	Fly Ash	GP	1	3	2	4	86.15	5.40	7.72	0.72
2	0.44	10%	30%	Fly Ash	EAFS	1	3	2	4	77.19	10.49	11.25	1.07
3	0.4	10%	30%	Fly Ash	EAFS	1	3	2	4	57.30	9.91	26.93	5.85

(Note:- A, B, C and D are the parameters defined in the Table 3.2)

It is observed that its contribution is maximum at higher water/binder ratio of 0.48, i.e.86.15% and it decreases to 57.30% as the water/binder is decreased to 0.40, whereas, the contribution of type of cement replacement material towards concrete strength, (i.e. fly ash) is maximum at 26.93% at w/b of 0.40. The %age of sand replacement, as could be seen from the Table 4.10, play a slightly better role only for lower w/b ratios whereas the type of replacement as sand does contributes very little.

- At 28 days of curing period (i.e. At normal age)

At curing of 28 days as seen from the Table 4.11, at higher w/b ratios, the %age of cement replacement material contributes the most towards the concrete strength, whereas at lower water/binder ratios, the type of cement replacement material contributes maximum towards the strength of resulting concrete.

Table 4.11: Percentage contribution of each parameter for compressive strength at 28 days of curing

Exp. No.	W/B ratio	Optimal Parameters	Optimal Parameters				Rank				% Contribution			
			(A)	(B)	(C)	(D)	(A)	(B)	(C)	(D)	(A)	(B)	(C))	(D)
1.	0.48	A1B2C1D2	10%	30%	Fly Ash	Iron Slag	1	3	2	4	80.91	3.80	14.15	1.13
2.	0.44	A1B2C1D2	10%	30%	Fly Ash	Iron Slag	1	3	2	4	65.58	3.22	29.94	1.25
3.	0.4	A1B2C1D3	10%	30%	Fly Ash	GP	1	3	2	4	45.03	8.56	43.74	2.65

(Note:- A, B, C and D are the parameters defined in the Table 3.2)

As can be observed from the table, the %age contribution towards the strength of 10% replacement of cement is maximum at 80.91% at w/b of 0.48 whereas, its value is 45.03% at water/binder ratio of 0.40.The percentage contribution of fly ash towards strength gain is 14.15% at w/b of 0.48, whereas, it is 43.74% at lower w/b of 0.40. The percentage contribution of type of sand replacement and its replacement level contributes very little at all water to binder ratios.

- At 90 days curing period

As seen from the Table 4.12, at curing of 90 days, for all water/binder ratios, the type of by-product used as material for cement replacement, which is fly ash, among the three materials, contributes maximum to the strength of resulting concrete and its contribution is maximum at 64.63% at w/b of 0.40. However, for higher w/b of 0.48 the percentage of cement replacement material contribute maximum to concrete strength. The percentage contribution of the factor, namely the percentage of cement replacement contributes maximum of 52.94% at higher w/b of 0.48 and its contribution decreases to 27.32% at lower w/b of 0.40.

The parameters, namely the type of sand replacement and its percentage replacement contributes very little towards the strength of such concrete at all water/binder ratios.

Table 4.12: Percentage contribution of each parameter for compressive strength at 90 days of curing

Exp. No.	W/B ratio	Optimal Parameters				Rank				% Contribution			
		(A)	(B)	(C)	(D)	(A)	(B)	(C)	(D)	(A)	(B)	(C))	(D)
1.	0.48	10%	30%	Fly Ash	Iron Slag	1	3	2	4	52.94	4.69	37.04	5.32
2.	0.44	10%	30%	Fly Ash	Iron Slag	2	3	1	4	42.06	4.65	51.83	1.45
3.	0.4	10%	30%	Fly Ash	Iron Slag	2	3	1	4	27.32	6.97	64.63	1.07

(Note:- A, B, C and D are the parameters defined in the Table 3.2)

From the above discussion, it also confirmed the fact that fly ash as partial cement replacement contributes maximum towards compressive strength at 90 day of curing period and not at early age although fly ash is optimal parameter at early age also.

4.2 ANALYSIS OF RESULTS FOR SPLIT TENSILE STRENGTH

4.2.1 Analysis of Variance

The mean results for the split tensile strength for each trial and for three water/ binder ratios and each curing ages are given in Table 3.26. The response tables for means of split tensile strength for nine sets of water/ binder ratios and curing periods (curing period= 7, 28, and 90 days at each w/b ratios of 0.40, 0.44 and 0.48) is given in Table 4.13 to Table 4.15. The ANOVA data indicating percentage contribution of each factor for the split tensile strength for nine sets of w/b ratio and curing period at 95% confidence interval is provided in Table 4.16 to Table 4.18. The larger is the percentage contribution value for a particular factor, the larger is its effect on the response. The ANOVA results for split tensile strength at 7 days of age and at water/binder ratio of 0.40 (Table 4.16), again show that % of by-product used as binder (53.54% contribution) is the most significant factor as is the case with compressive strength, followed by kind of by-product used as fine-aggregate (29.48% contribution) and type of by-product used as binder (15.97% contribution). The other factor namely, % of by-product used as fine aggregate with contribution of only 1% is found to be insignificant. However, rather than the type of by-product as binder, as was the case for compressive strength, kind of by-product replaced as a fine aggregate (29.48% contribution), significantly affects the tensile strength.

Table 4.13: Response table for means of split tensile strength at 7 days

Level	water/ binder ratio = 0.48				water/ binder ratio = 0.44				water/ binder ratio= 0.40			
	A	B	C	D	A	B	C	D	A	B	C	D
1	1.980	1.673	2.033	1.873	2.300	2.083	2.350	2.097	2.457	2.313	2.447	2.430
2	1.983	1.827	1.760	1.823	2.110	2.063	1.920	2.237	2.423	2.307	2.293	2.390
3	1.467	1.930	1.637	1.733	1.890	2.153	2.030	1.967	2.097	2.357	2.237	2.157
Delta	0.517	0.257	0.397	0.140	0.410	0.090	0.430	0.270	0.360	0.050	0.210	0.273
Rank	1	3	2	4	2	4	1	3	1	4	3	2

(Note:- A, B, C and D are the parameters defined in the Table 3.2)

Table 4.14: Response table for means of split tensile strength at 28 Days

Level	water/ binder ratio = 0.48				water/ binder ratio = 0.44				water/ binder ratio= 0.40			
	A	B	C	D	A	B	C	D	A	B	C	D
1	3.027	2.570	2.927	2.790	3.153	2.810	3.170	2.997	3.250	2.927	3.357	3.100
2	2.857	2.850	2.680	2.637	2.960	3.070	2.817	2.850	3.090	3.283	2.917	3.013
3	2.280	2.743	2.557	2.737	2.657	2.890	2.783	2.923	2.883	3.013	2.950	3.110
Delta	0.747	0.280	0.370	0.153	0.497	0.260	0.387	0.147	0.367	0.357	0.440	0.097
Rank	1	3	2	4	1	3	2	4	2	3	1	4

(Note:- A, B, C and D are the parameters defined in the Table 3.2)

Table4.15: Response table for means of split tensile strength at 90 Days

Level	water/ binder ratio = 0.48				water/ binder ratio = 0.44				water/ binder ratio= 0.40			
	A	B	C	D	A	B	C	D	A	B	C	D
1	3.413	3.223	3.510	3.173	3.533	3.283	3.723	3.380	4.073	3.730	4.127	3.737
2	3.327	3.313	2.993	3.170	3.560	3.593	3.140	3.343	3.777	3.913	3.430	3.740
3	2.900	3.103	3.137	3.297	3.067	3.283	3.297	3.437	3.237	3.443	3.530	3.610
Delta	0.513	0.210	0.517	0.127	0.493	0.310	0.583	0.093	0.837	0.470	0.697	0.130
Rank	2	3	1	4	2	3	1	4	1	3	2	4

(Note:- A, B, C and D are the parameters defined in the Table 3.2)

Thus, it is concluded that the strength properties of such concrete at early age (7 days) are majorly affected by the percentage replacement of the by-product used as a binder. Thus, rather than the type of the by-product, it is the percentage replacement level which significantly affects the property of concrete at early age.

Table 4.16: ANOVA table for means of split tensile strength at 7 days

Factor designation As per Table 3.2	dof	Water/ binder ratio = 0.48			Water/ binder ratio = 0.44			Water/ binder ratio= 0.40		
		(SS)	(V)	(PC)	(SS)	(V)	(PC)	(SS)	(V)	(PC)
A	2	0.5305	0.2652	58.4214	0.2526	0.1263	37.4333	0.2374	0.1187	53.5431
B	2	0.1001	0.0500	11.0206	0.0134	0.0067	1.9858	0.0044	0.0022	0.9973
C	2	0.2473	0.1236	27.2320	0.2994	0.1497	44.3687	0.0708	0.0354	15.9717
D	2	0.0302	0.0151	3.3260	0.1094	0.0547	16.2122	0.1308	0.0654	29.4878
Total	8	0.9080	0.4540	100.0000	0.6748	0.3374	100.0000	0.4434	0.2217	100.0000

(Note:- SS= Sum of squares, V= Variance, PC= %age Contribution)

Table 4.17: ANOVA for means of split tensile strength at 28 days of curing

Factor designation As per Table 3.2	dof	Water/ binder ratio = 0.48			Water/ binder ratio = 0.44			Water/ binder ratio= 0.40		
		(SS)	(V)	(PC)	(SS)	(V)	(PC)	(SS)	(V)	(PC)
A	2	0.9190	0.4595	71.3426	0.3761	0.1880	47.5913	0.2028	0.1014	25.7493
B	2	0.1198	0.0599	9.3023	0.1064	0.0532	13.4649	0.2076	0.1038	26.3673
C	2	0.2130	0.1065	16.5327	0.2755	0.1377	34.8604	0.3601	0.1800	45.7301
D	2	0.0364	0.0182	2.8224	0.0323	0.0161	4.0834	0.0170	0.0085	2.1533
Total	8	1.2881	0.6440	100.0000	0.7902	0.3951	100.0000	0.7874	0.3937	100.0000

(Note:- SS= Sum of squares, V= Variance, PC= %age Contribution)

Table 4.18: ANOVA for means of split tensile strength at 90 days of curing

Factor designation As per Table 3.2	dof	Water/ binder ratio = 0.48			Water/ binder ratio = 0.44			Water/ binder ratio= 0.40		
		(SS)	(V)	(PC)	(SS)	(V)	(PC)	(SS)	(V)	(PC)
A	2	0.4531	0.2265	46.3353	0.4619	0.2309	38.0388	1.0796	0.5398	46.9274
B	2	0.0666	0.0333	6.8112	0.1922	0.0961	15.8294	0.3367	0.1683	14.6347
C	2	0.4269	0.2134	43.6558	0.5469	0.2734	45.0393	0.8514	0.4257	37.0054
D	2	0.0313	0.0156	3.1977	0.0133	0.0066	1.0926	0.0330	0.0165	1.4325
Total	8	0.9778	0.4889	100.0000	1.2142	0.6071	100.0000	2.3006	1.1503	100.0000

(Note:- SS= Sum of squares, V= Variance, PC= %age Contribution)

4.2.2 Main Effects Plot for Means

The Main effect plot shows the variation of each response with the change in factor levels. The main effects plot for mean split tensile strength is shown in Figure 4.4 to Figure 4.6 for curing age of 7, 28 & 90 days respectively. The x- axis represents the variation of each factor at three levels and y-axis represents the net change in the response. The horizontal line shows the mean of response. The plot depicts the extent of significance each factor has on the response. The slope of each plot is an indication of significance of each factor.

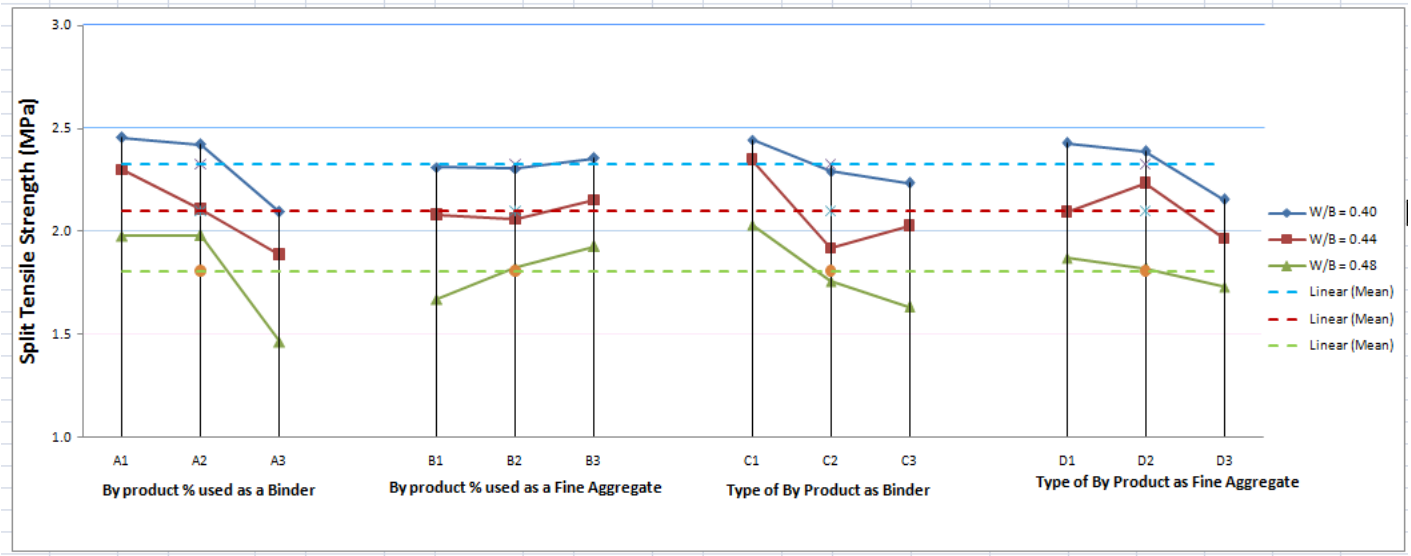

Figure 4.4: Main effects plot for mean split tensile strength at 7 days

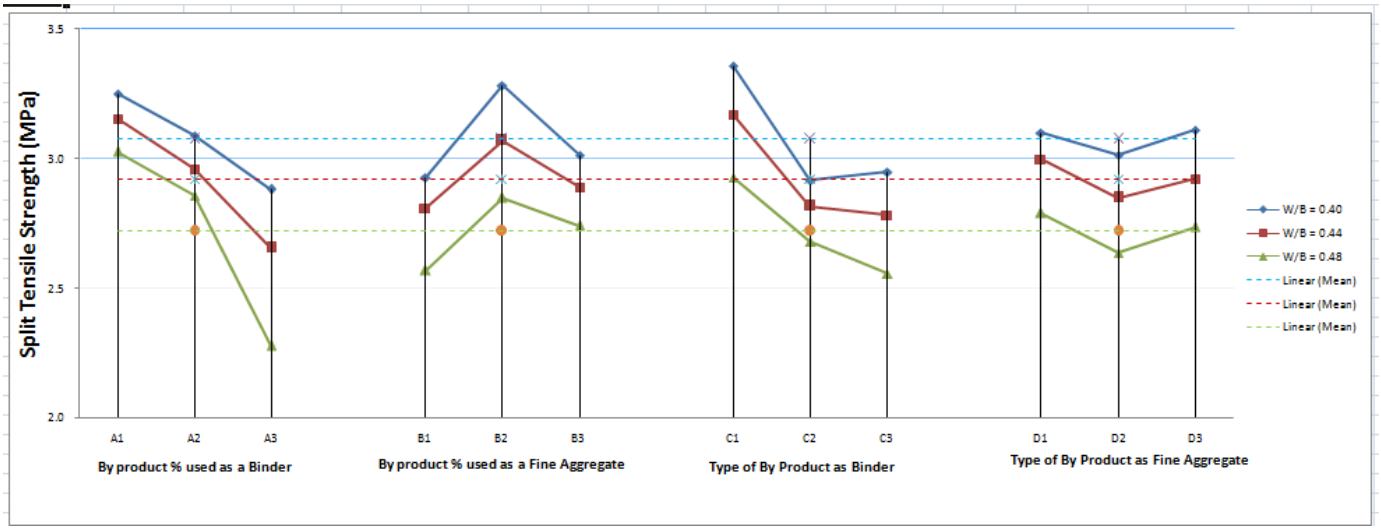

Figure 4.5: Main effects plot for mean split tensile strength at 28 days

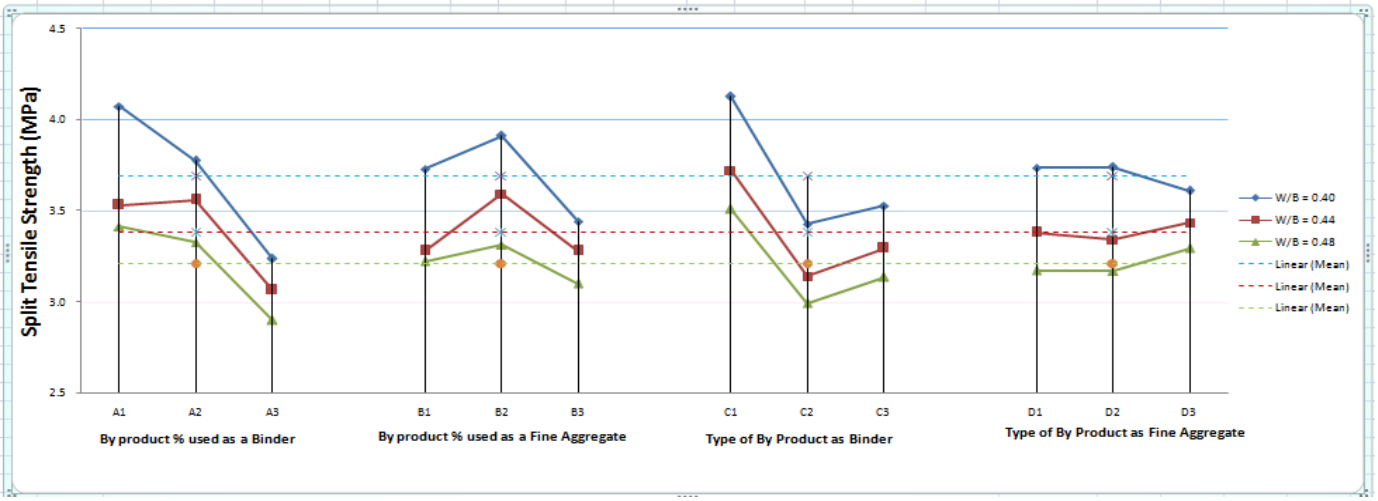

Figure 4.6: Main effects plot for mean split tensile strength at 90 days

4.2.3 Optimal Mix Design Parameters for Split Tensile Strength

The significant factors which were identified after ANOVA analysis (see Tables 4.16 to 4.18) and their graphs were used to find their most appropriate level and their percentage contribution which would increase the split tensile strength. The effect of curing age on optimal parameters and the percentage contribution of various optimal parameters towards split tensile strength at various curing ages is discussed in detail below.

(a) Effect of curing period on optimal mix design parameters

- At 7 days curing period (i.e. At early age)

It is seen from the table 4.19 that at 7 days curing, for all water binder ratios, cement replacement by fly ash gives the optimal result, whereas electric arc furnace slag replacement for sand provides the optimal strength results for w/b ratios of 0.48 & 0.40.

Table 4.19: Optimal parameters for split tensile strength after 7 days of curing

Exp. No.	W/B ratio	Optimal Parameters	Optimal Parameters			
			A	B	C	D
1.	0.48	A2B3C1D1	25%	40%	Fly Ash	Electric Arc Furnace Slag
2.	0.44	A1B3C1D2	10%	40%	Fly Ash	Iron Slag
3.	0.4	A1B3C1D1	10%	40%	Fly Ash	Electric Arc Furnace Slag

(Note:- A, B, C and D are the parameters defined in the Table 3.2)

However, at water/binder ratios of 0.44, iron slag as a replacement for sand provides better results. Also, it is found that for lower w/b ratios, 10% is the optimum %age of fly ash replacement contributing to higher split tensile strength at 7 days, whereas 40% of sand replacement by electric arc furnace slag at water/binder ratio of 0.48 & 0.40 contributes positively to strength gain at an early age. For water/binder ratio of 0.44, 40% of sand replacement by iron slag provides the optimal strength results. Thus, it can be said that at early ages, the replacement material (i.e. fly ash) and its percentage replacement of cement (i.e.10%) remains constant at lower water/binder ratios, whereas, on the other hand, for the replacement of sand, the percentage replacement remains constant (i.e. 40%) at all water binder ratios and the replacement material changes from higher w/b to lower w/b (i.e. from electric arc furnace slag to iron slag).

- At 28 days curing period (i.e. At normal age)

On observing the tabulated analysis results given in Table 4.20, at 28 days curing, for all water/binder ratios, it is seen that replacement of cement with fly ash gives the optimal result, whereas, on the other hand, replacement of sand by electric arc furnace slag at higher water/binder ratio and glass powder at lower water/binder ratio gives the optimal result.

Table 4.20: Optimal parameters for split tensile strength after 28 days of curing

Exp. No.	W/B ratio	Optimal Parameters	Optimal Parameters			
			A	B	C	D
1.	0.48	A1B2C1D1	10%	30%	FA	EAFS
2.	0.44	A1B2C1D1	10%	30%	FA	EAFS
3.	0.4	A1B2C1D3	10%	30%	FA	GP

(Note:- A, B, C and D are the parameters defined in the Table 3.2)

Also, it is seen that for all water to binder ratios, 10% is the optimum percentage of fly ash replacement contributing to higher split tensile strength at normal age, whereas 30% of sand replacement by electric arc furnace slag at water to binder ratios of 0.48 & 0.44 provides the optimal strength results. Thus, it can be summarized that at normal age, the replacement material and its percentage replacement of cement remains constant at all water/binder ratios, whereas, on the other hand, for the replacement of sand, the type of material and its percentage replacement remains constant i.e. 30% electric arc furnace slag at higher water/binder ratios and it changes to 30% glass powder only at lower water/binder ratio.

- At 90 days curing period

On analyzing the results at 90 days (Table 4.21), for all w/b ratios, it is seen that replacement of cement with fly ash gives the optimal result, whereas, on the other hand, replacement of sand by glass powder gives the optimal result at higher w/b ratios and iron slag at lower w/b ratio.

Table4.21: Optimal parameters for split tensile strength at 90 days of curing

Exp. No.	W/B ratio	Optimal Parameters	Optimal Parameters			
			A	B	C	D
1.	0.48	A1B2C1D3	10%	30%	Fly Ash	Glass Powder
2.	0.44	A2B2C1D3	25%	30%	Fly Ash	Glass Powder
3.	0.4	A1B2C1D2	10%	30%	Fly Ash	Iron Slag

(Note:- A, B, C and D are the parameters defined in the Table 3.2)

Also, it is observed that for 0.48 & 0.40 water/binder ratios, 10% is the optimum percentage of fly ash replacement contributing to higher strength at 90 days age, whereas 30% of sand replacement by glass powder provides the optimal strength results. Thus, it can be concluded that at 90 days age, the replacement material and its percentage replacement values for cement

remains constant at w/b ratio of o.48 & 0.40 and whereas for sand the replacement material and its percentage remain constant for water binder ratios of 0.48 & 0.44.

Thus, it is found that 10% of the fly ash is the optimal parameters for cement replacement for split tensile strength for all the curing periods and water/ binder ratios. Similarly 40% is the optimal replacement level of sand at water binder ratio of 0.40 and at 7 days but it changes to 30% at 28days and 90 days of curing and at 0.40 of water to binder ratio.

(b) Percentage contribution of various optimal parameters towards split tensile strength at various curing ages

The results indicating the percentage contribution of optimal parameters towards concrete split tensile strength are also tabulated in Tables 4.22 to 4.24. The effect at different curing ages is presented below:

- At curing period 0f 7 days (i.e. At early age)

As seen from the Table 4.22, at 7 days of curing, 25% of by-product to be used as partial cement replacement is the optimal parameter which contributes maximum towards split tensile strength of the resulting concrete.

Table 4.22: Percentage contribution of each parameter for split tensile strength at 7 days

Exp. No.	W/B ratio	Optimal Parameters	Optimal Parameters				Rank				% Contribution			
			(A)	(B)	(C)	(D)	(A)	(B)	(C)	(D)	(A)	(B)	(C)	(D)
1	0.48	A2B3C1D1	25%	40%	Fly Ash	EAFS	1	3	2	4	58.42	11.02	27.23	3.33
2	0.44	A1B3C1D2	10%	40%	Fly Ash	Iron Slag	2	4	1	3	37.43	1.98	44.37	16.21
3	0.4	A1B3C1D1	10%	40%	Fly Ash	EAFS	1	4	3	2	53.54	1.00	15.97	29.48

(Note:- A, B, C and D are the parameters defined in the Table 3.2)

It is observed that its contribution is maximum at higher water/binder ratio of 0.48, i.e. 58.42% and it decreases to 37.43% as the water/binder is decreased to 0.44, whereas, the contribution of type of cement replacement material towards concrete strength, (i.e. fly ash) is maximum at 44.37% at w/b of 0.44. The type of replacement as sand, as can be seen from the Table 19, play a

slightly better role only for lower w/b ratios whereas the percentage replacement as sand does contributes very little.

- At 28 days curing period (i.e. At normal age)

As seen from the Table 4.23, at curing period of 28 days, for higher water/binder ratios, the percentage of material as cement replacement contributes the most towards the concrete split tensile strength, whereas at lower w/b ratios, the type of cement replacement material contributes maximum towards the Split tensile strength of resulting concrete.

Table 4.23: Percentage contribution of each parameter for split tensile strength at 28 days

Exp. No.	W/B ratio	Optimal Parameters	Optimal Parameters				Rank				% Contribution			
			(A)	(B)	(C)	(D)	(A)	(B)	(C)	(D)	(A)	(B)	(C)	(D)
1.	0.48	A1B2C1D1	10%	30%	Fly Ash	EAFS	1	3	2	4	71.34	9.30	16.53	2.82
2.	0.44	A1B2C1D1	10%	30%	Fly Ash	EAFS	1	3	2	4	47.59	13.46	34.86	4.08
3.	0.4	A1B2C1D3	10%	30%	Fly Ash	Glass Powder	2	3	1	4	25.75	26.36	45.73	2.15

(Note:- A, B, C and D are the parameters defined in the Table 3.2)

As observed from the Table 4.23, the %age contribution towards the strength for 10% replacement of cement is maximum at 71.34% at water/binder of 0.48 whereas, its value is 25.75% at w/b of 0.40.The %age contribution of fly ash towards strength gain is maximum i.e.45.73% at w/b of 0.40, whereas, it is 16.53% at w/b of 0.48. The %age contribution of type of sand replacement and its replacement level contributes very little at all the w/b ratios.

- At 90 days curing period

As observed from the Table 4.24, at curing age of 90 days, for all water/binder ratios, the percentage of by-product used as cement replacement material, which is 10%, contributes maximum to the strength of resulting concrete and its contribution is maximum at 46.92% at w/b of 0.40.

Table 4.24: Percentage contribution of each parameter for split tensile strength at 90 days

Exp. No.	W/B ratio	Optimal Parameters	Optimal Parameters				Rank				% Contribution			
			(A)	(B)	(C)	(D)	(A)	(B)	(C)	(D)	(A)	(B)	(C)	(D)
1.	0.48	A1B2C1D3	10%	30%	Fly Ash	Glass Powder	2	3	1	4	46.33	6.81	43.65	3.20
2.	0.44	A2B2C1D3	25%	30%	Fly Ash	Glass Powder	2	3	1	4	38.03	15.83	45.04	1.10
3.	0.4	A1B2C1D2	10%	30%	Fly Ash	Iron Slag	1	3	2	4	46.92	14.63	37.00	1.43

(Note:- A, B, C and D are the parameters defined in the Table 3.2)

However, for higher w/b of 0.44, the type of cement replacement material contribute maximum to concrete strength and its contribution is 45.04%.The parameters, namely the type of sand replacement and its percentage replacement contributes very little towards the split tensile strength of such concrete at all the water/binder ratios.

From the above discussion, it is found that fly ash is contributing maximum towards the split tensile strength than all other parameters.

4.3 ANALYSIS OF RESULTS FOR WATER PERMEABILITY

4.3.1 Analysis of Variance

Three experiments for every 9 trial mixes as given by Taguchi's L_9 OA were performed to measure the water penetration depth. The mean value for the water penetration depth for each trial and for all the three water/binder ratios and each curing ages are shown in Table 3.28. The results were analyzed with ANOVA method. The ANOVA calculations and the graphs were developed using the MINITAB16 software. The results were further analyzed to identify the significant factors affecting the responses. The response tables for means of water penetration depth for 7, 28 and 90 days of curing are given in Tables 4.25 to 4.27 respectively. The ANOVA data indicating percentage contribution of each factor for each w/b ratio and curing period at 95% confidence interval is provided in Tables 4.28 to 4.30. The larger is the percentage

contribution of a particular parameter, the larger is its effect on the response. For example ANOVA for water penetration depth for 7 days of curing (See Table 4.28) and at water binder ratio of 0.40 shows that the percentage of by-product used as fine aggregate (60.73% contribution) is the most significant factor seconded by the %age of by-product to be used as a cement, kind of by product substituted as a binder and type of by product to be used sand, respectively.

Table 4.25: Response table for means of water penetration depth for curing period of 7 days

Level	Water/binder ratio= 0.48				Water/binder ratio = 0.44				Water/binder ratio = 0.40			
	(A)	(B)	(C)	(D)	(A)	(B)	(C)	(D)	(A)	(B)	(C)	(D)
1	104.67	81.67	121.67	116.67	77.00	63.67	105.33	102.00	61.67	50.00	93.33	90.00
2	100.00	128.00	103.00	103.00	87.33	117.33	85.33	89.33	79.00	111.67	77.33	79.33
3	110.00	105.00	90.00	95.00	103.67	87.00	77.33	76.67	94.33	73.33	64.33	65.67
Delta	10.00	46.33	31.67	21.67	26.67	53.67	28.00	25.33	32.67	61.67	29.00	24.33
Rank	4	1	2	3	3	1	2	4	2	1	3	4

(Note:- A, B, C and D are the parameters defined in the Table 3.2)

Table 4.26: Response table for means of water penetration depth for curing period of 28 days

Level	Water/binder ratio= 0.48				Water/binder ratio = 0.44				Water/binder ratio = 0.40			
	(A)	(B)	(C)	(D)	(A)	(B)	(C)	(D)	(A)	(B)	(C)	(D)
1	55.67	63.67	85.00	80.00	46.67	53.00	68.33	60.00	35.00	42.33	51.67	51.33
2	73.33	96.67	55.00	57.00	51.00	70.00	42.67	48.67	40.67	55.00	35.33	40.00
3	85.33	54.00	74.33	77.33	70.33	45.00	57.00	59.33	54.67	33.00	43.33	39.00
Delta	29.67	42.67	30.00	23.00	23.67	25.00	25.67	11.33	19.67	22.00	16.33	12.33
Rank	3	1	2	4	3	2	1	4	2	1	3	4

(Note:- A, B, C and D are the parameters defined in the Table 3.2)

Table 4.27 Response table for means of water penetration depth for curing period of 90 days

Level	Water/binder ratio= 0.48				Water/binder ratio = 0.44				Water/binder ratio = 0.40			
	(A)	(B)	(C)	(D)	(A)	(B)	(C)	(D)	(A)	(B)	(C)	(D)
1	26.67	41.67	35.00	43.33	22.33	32.33	28.67	30.67	16.67	27.33	19.00	23.00
2	40.00	38.33	36.67	35.00	31.00	30.67	21.67	29.33	23.67	22.33	18.00	24.00
3	45.00	31.67	40.00	33.33	30.67	21.00	33.67	24.00	25.67	16.33	29.00	19.00
Delta	18.33	10.00	5.00	10.00	8.67	11.33	12.00	6.67	9.00	11.00	11.00	5.00
Rank	1	3	4	2	3	2	1	4	3	1.5	1.5	4

(Note:- A, B, C and D are the parameters defined in the Table 3.2)

Table 4.28: ANOVA for mean depth of water penetration at 7 days of curing

Factor designation As per Table 3.2	dof	Water/binder ratio= 0.48			Water/binder ratio = 0.44			Water/binder ratio = 0.40		
		(SS)	(V)	(PC)	(SS)	(V)	(PC)	(SS)	(V)	(PC)
A	2	150.2222	75.1111	2.6773	1084.6667	542.3333	14.1972	1602.6667	801.3333	16.7328
B	2	3220.2222	1610.1111	57.3924	4344.6667	2172.3333	56.8674	5816.6667	2908.3333	60.7294
C	2	1520.2222	760.1111	27.0941	1248.0000	624.0000	16.3351	1266.0000	633.0000	13.2178
D	2	720.2222	360.1111	12.8362	962.6667	481.3333	12.6003	892.6667	446.3333	9.3200
Total	8	5610.8889	2805.4444	100.0000	7640.0000	3820.0000	100.0000	9578.0000	4789.0000	100.0000

(Note:- SS= Sum of squares, V= Variance, PC= %age Contribution)

Table 4.29: ANOVA for mean depth of water penetration at 28 days

Factor designation As per Table 3.2	dof	Water/binder ratio= 0.48			Water/binder ratio = 0.44			Water/binder ratio = 0.40		
		(SS)	(V)	(PC)	(SS)	(V)	(PC)	(SS)	(V)	(PC)
A	2	1336.222	668.1111	20.0146	952.6667	476.3333	30.0905	614.8889	307.4444	30.3166
B	2	3002.888	1501.444	44.9789	978.0000	489.0000	30.8907	731.5556	365.7778	36.0688
C	2	1387.555	693.7778	20.7835	992.6667	496.3333	31.3540	400.2222	200.1111	19.7327
D	2	949.5556	474.7778	14.2229	242.6667	121.3333	7.6648	281.5556	140.7778	13.8819
Total	8	6676.222	3338.111	100.0000	3166.000	1583.000	100.0000	2028.222	1014.111	100.0000

(Note:- SS= Sum of squares, V= Variance, PC= %age Contribution)

Table 4.30: ANOVA for mean depth of water penetration at 90 days of curing

Factor designation As per Table 3.2	dof	Water/binder ratio= 0.48			Water/binder ratio = 0.44			Water/binder ratio = 0.40		
		(SS)	(V)	(PC)	(SS)	(V)	(PC)	(SS)	(V)	(PC)
A	2	538.8889	269.4444	59.5092	144.6667	72.3333	21.8530	134.0000	67.0000	23.1034
B	2	155.5556	77.7778	17.1779	224.6667	112.3333	33.9376	182.0000	91.0000	31.3793
C	2	38.8889	19.4444	4.2945	218.0000	109.0000	32.9305	222.0000	111.0000	38.2759
D	2	172.2222	86.1111	19.0184	74.6667	37.3333	11.2790	42.0000	21.0000	7.2414
Total	8	905.5556	452.7778	100.0000	662.0000	331.0000	100.0000	580.0000	290.0000	100.0000

(Note:- SS=Sum of squares, V= Variance, PC= %age Contribution)

4.3.2 Main Effects Plots for Means

The main effects plots for water penetration depth for water/binder ratio of 0.40 and curing age of 7, 28 and 90 days are shown in Figures 4.7 to 4.9 respectively. Main effect plots represent the change in each response with the change in factor levels. The x- axis shows the three levels of each factor and y-axis represents the net change in the response. The horizontal line shows the mean of response. The three plots depict the extent of significance each factor has on the response. The slope of each plot is an indication of significance of each factor.

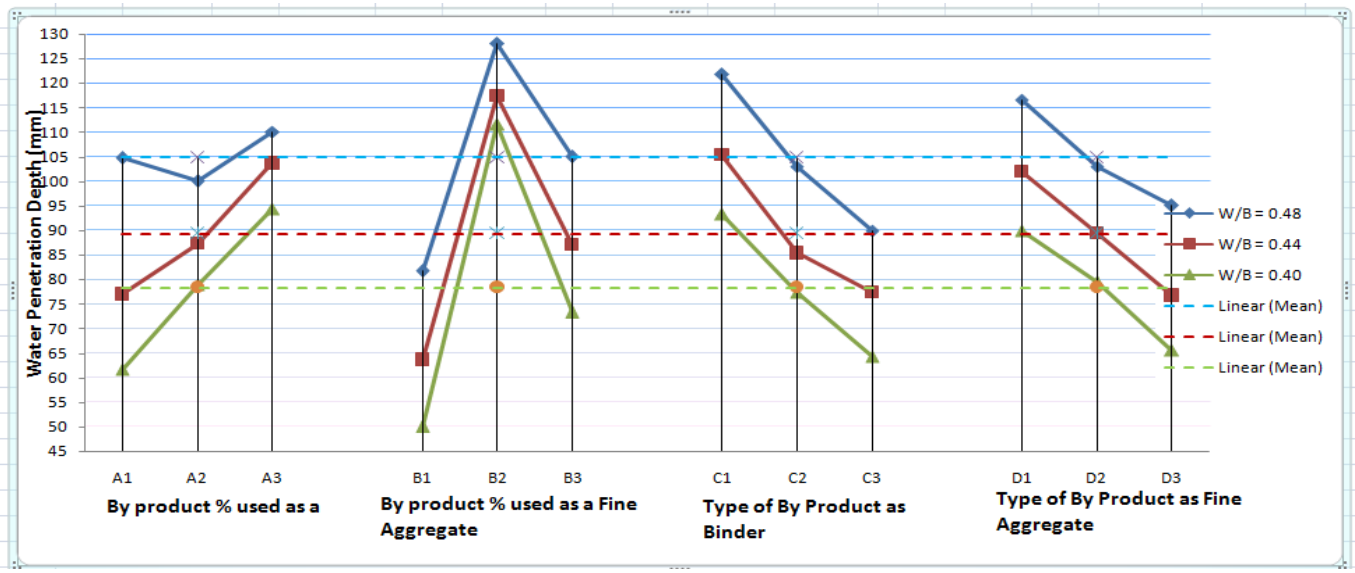

Figure 4.7: Main effects plot for mean depth of water penetration at 7 days

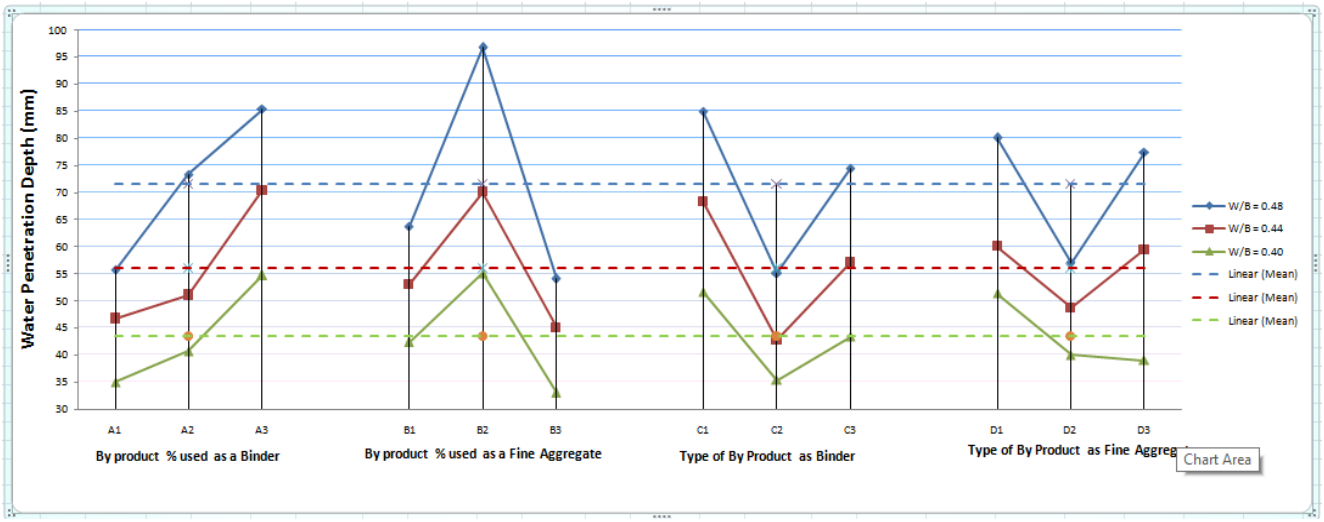

Figure 4.8: Main effects plot for mean water penetration depth at 28 days

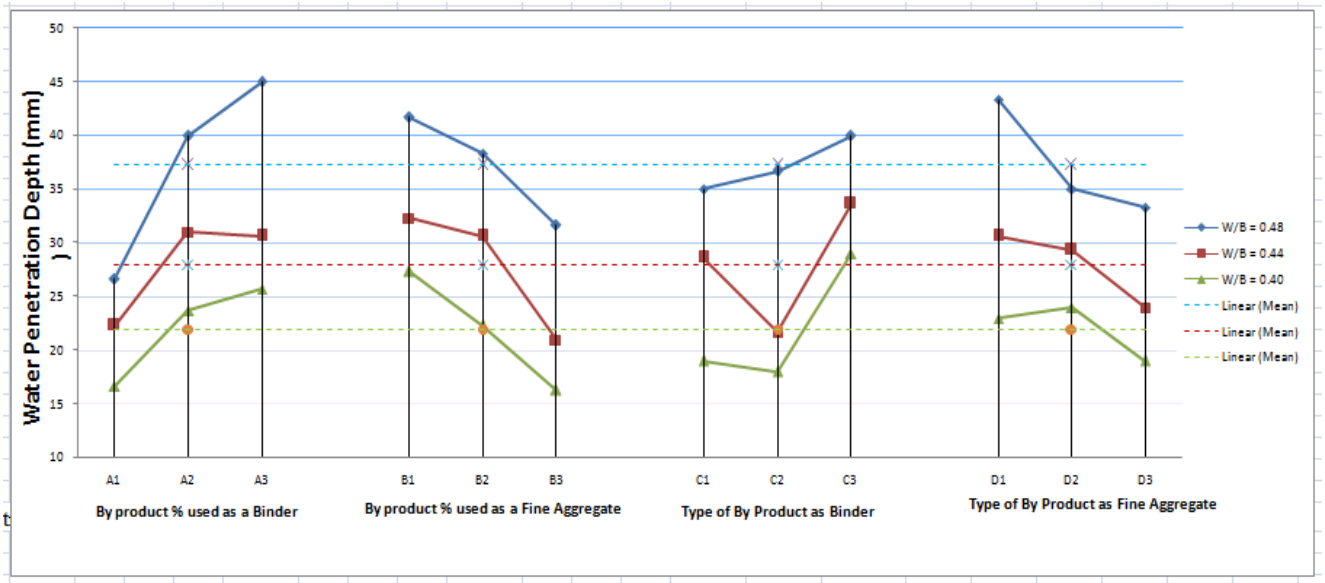

4.9: Main effects plot for mean water penetration depth at 90 days

4.3.3 Optimal Design Consideration

There could be three types of response values which needs to be obtained from the experiments. These responses could be a 'the higher is better', a 'the nominal is better' or a 'the lower is better'. In the present situation, depth of water penetration is a 'lower the best' response. The graphs of the significant factors were used for the estimation of the mean water penetration depth using optimal design parameters.

4.3.4 Optimal Mix Design Parameters

The significant factors found after ANOVA analysis (see Tables 4.28 to 4.30) and their plots were used to find their most suitable level which would decrease the depth of water penetration. Tables 4.31 to 4.33 provide the summary of the ANOVA analysis for finding the optimal mix design parameters at 7, 28 and 90 days respectively. The tables also elucidate the optimal percentage replacement and the percentage contribution of each parameter towards the water penetration depth of resulting concrete. The effect of curing age on optimal mix design parameters and percentage contribution of various optimal parameters at different curing periods is discussed below.

(a) Effect of curing age on optimal mix design parameters

- At 7 days curing period (i.e. At early age)

It is observed from the first three rows of the table 4.31 that at 7 days curing, for all water binder ratios, cement replacement by fly ash gives the optimal result, whereas glass powder replacement for sand provides the optimal parameter for lower water permeability only for higher water/binder ratio of 0.48.

Table 4.31: Optimal parameters for depth of water penetration at 7 days of curing

Exp. No.	W/B ratio	Optimal Parameters	Optimal Parameters			
			A	B	C	D
1.	0.48	A2B1C3D3	10%	30%	Fly Ash	GP
2.	0.44	A1B1C3D3	10%	30%	Fly Ash	EAFS
3.	0.4	A1B1C3D3	10%	30%	Fly-Ash	EAFS

(Note:- A, B, C and D are the parameters defined in the Table 3.2)

However, at lower w/b ratios of 0.44 & 0.40, electric arc furnace slag as a replacement for sand provides better results. Also, it is observed that for all w/b ratios, 10% is the optimum %age of fly ash replacement contributing to lower water permeability at early ages, whereas 30% of sand replacement by glass powder at w/b of 0.48 contributes positively to lower water permeability at

an early age. For lower w/b ratios, 30% of sand replacement by electric arc furnace slag provides the optimal results. Thus, it can be summarized that at early ages, the replacement material (i.e. fly ash) and its percentage replacement of cement (i.e.10%) remains constant at all water/binder ratios, whereas, on the other hand, for the replacement of sand, the percentage replacement remains constant (i.e. 30%) at all w/b ratios and the replacement material changes from higher w/b to lower w/b (i.e. from glass powder to EAFS).

- At 28 days curing period (i.e. At normal age)

On observing the Table 4.32 for results at 28 days curing, for all w/b ratios, it is seen that cement replacement by fly ash gives the optimal result, whereas, on the other hand, replacement of sand by iron slag at higher water/binder ratio and glass powder at lower w/b ratio gives the optimal result.

Table 4.32: Optimal parameters for water penetration depth at 28 days of curing

Exp. No.	W/B ratio	Optimal Parameters	Optimal Parameters			
			A	B	C	D
1.	0.48	A1B3C2D2	10%	30%	Fly Ash	Iron Slag
2.	0.44	A1B3C2D2	10%	30%	Fly Ash	Iron Slag
3.	0.4	A1B2C3D3	10%	30%	Fly Ash	GP

(Note:- A, B, C and D are the parameters defined in the Table 3.2)

Also, it is observed that for all w/b ratios, 10% is the optimal %age of Fly ash replacement contributing to lower water permeability at normal age, whereas 30% of sand replacement by iron slag at water to binder ratios of 0.48 & 0.44 provides the optimal results. Thus, it can be concluded that at normal age, the replacement material and its percentage replacement of cement remains constant at all water/binder ratios, whereas, on the other hand, for the replacement of sand, the type of material and its percentage replacement remains constant i.e. 30% iron slag at higher water to binder ratios and it changes to 30% glass powder only at lower water/binder ratio.

- At 90 days curing period

On analyzing the results at 90 days (Table 4.33), for all water/binder ratios, it is seen that cement replacement by fly ash gives the optimal result, whereas, on the other hand, replacement of sand by iron slag gives the optimal result.

Table 4.33: Optimal parameters for depth of water penetration at 90 days of curing

Exp. No.	W/B ratio	Optimal Parameters	Optimal Parameters			
			A	B	C	D
1.	0.48	A1B3C1D3	10%	30%	Fly Ash	Iron Slag
2.	0.44	A1B3C2D3	10%	30%	Fly Ash	Iron Slag
3.	0.4	A1B3C2D3	10%	30%	Fly Ash	Iron Slag

(Note:- A, B, C and D are the parameters defined in the Table 3.2)

Also, it is observed that for all water/binder ratios, 10% is the optimal %age replacement by Fly ash contributing to lower water permeability at 90 days age, whereas 30% of sand replacement by iron slag provides the optimal results. Thus, it can be concluded that at 90 days age, the replacement material and its percentage replacement values for both cement and sand remain constant for all water/binder ratios.

From the above discussion, it is found that 10% of the fly ash is the optimal parameters for cement replacement for depth of water penetration and hence water permeability at all the curing ages and water to binder ratios. Similarly 30% is the optimal replacement level of sand for all the water / binder ratios and at all the curing ages.

(b) Percentage contribution of various optimal parameters towards water permeability at different curing periods

The results indicating the percentage contribution of optimal parameters towards concrete permeability is tabulated in Tables 4.34 to 4.36.The effect at different curing ages is presented below:

- At curing of 7 days (i.e. at early age)

As seen from the Table 4.34, at the curing age 7 days, for all water/binder ratios, %age of by-product used as partial sand replacement is the optimal parameter which contributes maximum to minimize water permeability of the concrete.

Table 4.34: Percentage contribution of each parameter for depth of water penetration at 7 days of curing

Exp. No.	W/B ratio	Optimal Parameters	Optimal Parameters				Rank				% Contribution			
			A	B	C	D	A	B	C	D	A	B	C	D
1.	0.48	A2B1C3D3	10%	30%	Fly Ash	GP	4	1	2	3	2.67	57.39	27.10	12.83
2.	0.44	A1B1C3D3	10%	30%	Fly Ash	EAFS	3	1	2	4	14.19	56.86	16.33	12.60
3.	0.4	A1B1C3D3	10%	30%	Fly Ash	EAFS	2	1	3	4	16.73	60.73	13.22	9.32

(Note:- A, B, C and D are the parameters defined in the Table 3.2)

It is observed that its contribution is maximum at lower water/binder ratio of 0.40, i.e. 60.73% and it decreases to 57.39% as the water to binder ratio is increased to 0.48, whereas, the contribution of type of cement replacement material towards water permeability, (i.e. fly ash) is maximum at 27.10% at 0.48 water/binder ratio. The percentage of cement replacement, as can be seen from the Table 20, play a slightly better role only for lower w/b ratios whereas the type of replacement as sand does contributes very little.

- At 28 days curing (i.e. At normal age)

At curing of 28 days (See Table 4.35), for all w/b ratios, % of by-product to be used as partial substitution of sand is the optimal parameter which contributes maximum to minimize water permeability of the concrete.

Table 4.35: Percentage contribution of each parameter for water penetration depth after 28 days of curing period

Exp. No.	W/B ratio	Optimal Parameters	Optimal Parameters				Rank				% Contribution			
			A	B	C	D	A	B	C	D	A	B	C	D
1.	0.48	A1B3C2D2	10%	30%	Fly Ash	Iron Slag	3	1	2	4	20.01	44.98	20.78	14.22
2.	0.44	A1B3C2D2	10%	30%	Fly Ash	Iron Slag	3	2	1	4	30.09	30.89	31.35	7.66
3.	0.4	A1B2C3D3	10%	30%	Fly Ash	GP	2	1	3	4	30.31	36.06	19.73	13.88

(Note:- A, B, C and D are the parameters defined in the Table 3.2)

It is observed that its contribution is maximum at higher water/binder ratio of 0.48, i.e. 44.98% and it decreases to 30.89% as the water/binder is decreased to 0.44, whereas, the contribution of type of cement replacement material towards water permeability, (i.e. 10%) is maximum at 31.35% at 0.44 water/binder ratio. The type of replacement as sand does contributes very little.

- At 90 days curing period

At the curing of 90 days (See Table 4.36), for 0.48 water to binder ratio, the percentage of by-product to be used as cement replacement material, which is 10%, contributes maximum to minimize water permeability of resulting concrete and its contribution is maximum at 59.51%. However, for lower water to binder ratio of 0.40, the type of cement replacement material contributes maximum and its percentage contribution is 38.27%.

Table 4.36: Percentage contribution of each parameter for depth of water penetration at 90 days of curing

Exp. No.	W/B ratio	Optimal Parameters	Optimal Parameters				Rank				% Contribution			
			A	B	C	D	A	B	C	D	A	B	C	D
1.	0.48	A1B3C1D3	10%	30%	Fly Ash	Iron Slag	1	3	4	2	59.51	17.18	4.30	19.02
2.	0.44	A1B3C2D3	10%	30%	Fly Ash	Iron Slag	3	2	1	4	21.85	33.94	32.93	11.27
3.	0.4	A1B3C2D3	10%	30%	Fly Ash	Iron Slag	3	2	1	4	23.10	31.37	38.27	7.24

(Note:- A, B, C and D are the parameters defined in the Table 3.2)

The %age contribution of the parameter, namely the percentage of sand replacement contributes maximum of 33.94% at w/b of 0.44 and its contribution decreases to 17.18% at w/b ratio of 0.48. The parameters, namely the type of sand replacement contributes very little towards minimizing the water permeability of such concrete at all the water/binder ratios.

From the above discussion, it is found that fly ash as cement replacement has the maximum contribution to minimize the depth of water penetration at 90 days due to its filler effect into voids of concrete which makes the concrete impermeable and dense.

4.4 ANALYSIS OF RESULTS FOR DEPTH OF WEAR

4.4.1 Analysis of Variance

Three experiments for every 9 trial mixes as per by Taguchi's L_9 OA were performed to measure depth of wear. The mean results for the depth of wear for each trial and for all three water/binder ratios and each of three curing periods are shown in Table 3.30. The Analysis of Variance (ANOVA) calculations and the graphs were developed by MINITAB16 software. The results were further analyzed for the identification of the significant factors affecting the responses. The response tables for means of depth of wear for all water/binder ratios and curing ages are given in Tables 4.37 to 4.39. The ANOVA data indicating percentage contribution of each factor at 95% confidence interval for 7, 28 and 90 days of curing is provided in Tables 4.40 to 4.42 respectively. The larger is the percentage contribution of a particular input parameter, the greater would be its effect on the output response. For example ANOVA for depth of wear at 7 days of curing (See Table 4.40) and at water/binder ratio of 0.40 shows that type of by-product used as binder (38.77% contribution) is the most significant factor followed by type of by-product to be used as a replacement of fine aggregate, the percentage of by product used as a binder and percentage of by-product to be used as sand/fine aggregate respectively.

Table 4.37: Response table for means of depth of wear for curing period of 7 days

Level	Water/binder ratio = 0.48				Water/binder ratio = 0.44				Water/binder ratio = 0.40			
	(A)	(B)	(C)	(D)	(A)	(B)	(C)	(D)	(A)	(B)	(C)	(D)
1	0.4263	0.4390	0.4570	0.4503	0.3770	0.3923	0.3993	0.3997	0.3423	0.3610	0.3463	0.3893
2	0.4023	0.4117	0.4503	0.4493	0.3707	0.3853	0.4253	0.4017	0.3470	0.3370	0.3970	0.3397
3	0.5220	0.5000	0.4433	0.4510	0.4567	0.4267	0.3797	0.4030	0.3877	0.3790	0.3337	0.3480
Delta	0.1197	0.0883	0.0137	0.0017	0.0860	0.0413	0.0457	0.0033	0.0453	0.0420	0.0633	0.0497
Rank	1	2	3	4	1	3	2	4	3	4	1	2

(Note:- A, B, C and D are the parameters defined in the Table 3.2)

Table 4.38: Response table for means of depth of wear for curing period of 28 Days

Level	Water/binder ratio = 0.48				Water/binder ratio = 0.44				Water/binder ratio = 0.40			
	(A)	(B)	(C)	(D)	(A)	(B)	(C)	(D)	(A)	(B)	(C)	(D)
1	0.3823	0.3727	0.3753	0.4030	0.3157	0.3207	0.3293	0.3187	0.3020	0.3140	0.3050	0.3080
2	0.3520	0.3593	0.4110	0.3677	0.3450	0.3373	0.3547	0.3417	0.3260	0.3210	0.3440	0.3200
3	0.4160	0.4183	0.3640	0.3797	0.3587	0.3613	0.3353	0.3590	0.3380	0.3310	0.3170	0.3380
Delta	0.0640	0.0590	0.0470	0.0353	0.0430	0.0407	0.0253	0.0403	0.0360	0.0170	0.0390	0.0300
Rank	1	2	3	4	1	2	4	3	2	4	1	3

(Note:- A, B, C and D are the parameters defined in the Table 3.2)

Table 4.39: Response table for means of depth of wear for curing period of 90 Days

Level	Water/binder ratio = 0.48				Water/binder ratio = 0.44				Water/binder ratio = 0.40			
	(A)	(B)	(C)	(D)	(A)	(B)	(C)	(D)	(A)	(B)	(C)	(D)
1	0.3463	0.3440	0.3477	0.3580	0.2913	0.2630	0.2930	0.2963	0.2833	0.2490	0.2613	0.2647
2	0.3307	0.3370	0.3650	0.3427	0.2923	0.2983	0.3060	0.3150	0.2497	0.2790	0.2920	0.2920
3	0.3670	0.3630	0.3313	0.3433	0.3140	0.3363	0.2987	0.2863	0.3013	0.3063	0.2810	0.2777
Delta	0.0363	0.0260	0.0337	0.0153	0.0227	0.0733	0.0130	0.0287	0.0517	0.0573	0.0307	0.0273
Rank	1	3	2	4	3	1	4	2	2	1	3	4

(Note:- A, B, C and D are the parameters defined in the Table 3.2)

Table 4.40: ANOVA for mean depth of wear at 7 days of curing

Factor designation As per Table 3.2	dof	Water/binder ratio = 0.48			Water/binder ratio = 0.44			Water/binder ratio = 0.40		
		(SS)	(V)	(PC)	(SS)	(V)	(PC)	(SS)	(V)	(PC)
A	2	0.0240	0.0120	65.6991	0.0138	0.0069	69.3157	0.0037	0.0019	21.4678
B	2	0.0123	0.0061	33.5238	0.0029	0.0015	14.7666	0.0027	0.0013	15.3297
C	2	0.0003	0.0001	0.7656	0.0031	0.0016	15.8328	0.0067	0.0034	38.7770
D	2	0.0000	0.0000	0.0115	0.0000	0.0000	0.0849	0.0042	0.0021	24.4255
Total	8	0.0366	0.0183	100.0000	0.0199	0.0099	100.0000	0.0174	0.0087	100.0000

(Note:- SS= Sum of squares, V= Variance, PC= %age Contribution)

Table 4.41: ANOVA for mean depth of wear at 28 days of curing

Factor designation As per Table 3.2	dof	Water/binder ratio = 0.48			Water/binder ratio = 0.44			Water/binder ratio = 0.40		
		(SS)	(V)	(PC)	(SS)	(V)	(PC)	(SS)	(V)	(PC)
A	2	0.0061	0.0031	35.2608	0.0029	0.0014	32.4996	0.0020	0.0010	32.4324
B	2	0.0057	0.0029	32.9366	0.0025	0.0013	28.1382	0.0004	0.0002	7.0463
C	2	0.0036	0.0018	20.6967	0.0011	0.0005	11.7999	0.0024	0.0012	38.5135
D	2	0.0019	0.0010	11.1059	0.0025	0.0012	27.5622	0.0014	0.0007	22.0077
Total	8	0.0174	0.0087	100.0000	0.0089	0.0045	100.0000	0.0062	0.0031	100.0000

(Note:- SS= Sum of squares, V= Variance, PC= %age Contribution)

Table 4.42: ANOVA for mean depth of wear at 90 days of curing

Factor designation As per Table 3.2	dof	Water/binder ratio = 0.48			Water/binder ratio = 0.44			Water/binder ratio = 0.40		
		(SS)	(V)	(PC)	(SS)	(V)	(PC)	(SS)	(V)	(PC)
A	2	0.0020	0.0010	38.1007	0.0010	0.0005	9.3031	0.0041	0.0021	35.4821
B	2	0.0011	0.0005	20.7648	0.0081	0.0040	76.2813	0.0049	0.0025	42.4234
C	2	0.0017	0.0009	32.5175	0.0003	0.0001	2.4093	0.0014	0.0007	12.4515
D	2	0.0005	0.0002	8.6170	0.0013	0.0006	12.0064	0.0011	0.0006	9.6429
Total	8	0.0052	0.0026	100.0000	0.0106	0.0053	100.0000	0.0116	0.0058	100.0000

(Note:- SS= Sum of squares, V= Variance, PC= %age Contribution)

4.4.2 Main Effects Plot for Means

The main effect plots for depth of wear for 7, 28 & 90 days at w/b ratios of 0.48, 0.44 and 0.40 are shown in Figures 4.10 to 4.12. Main effect plots show the variation of response (i.e. depth of wear) with the change in factor levels. The x- axis shows the variation in three levels of each factor and y-axis represents the net change in the response. The horizontal line shows the mean of the output response. The three plots depict the extent of significance each factor has on the response. The slope of each plot is an indication of significance of each factor.

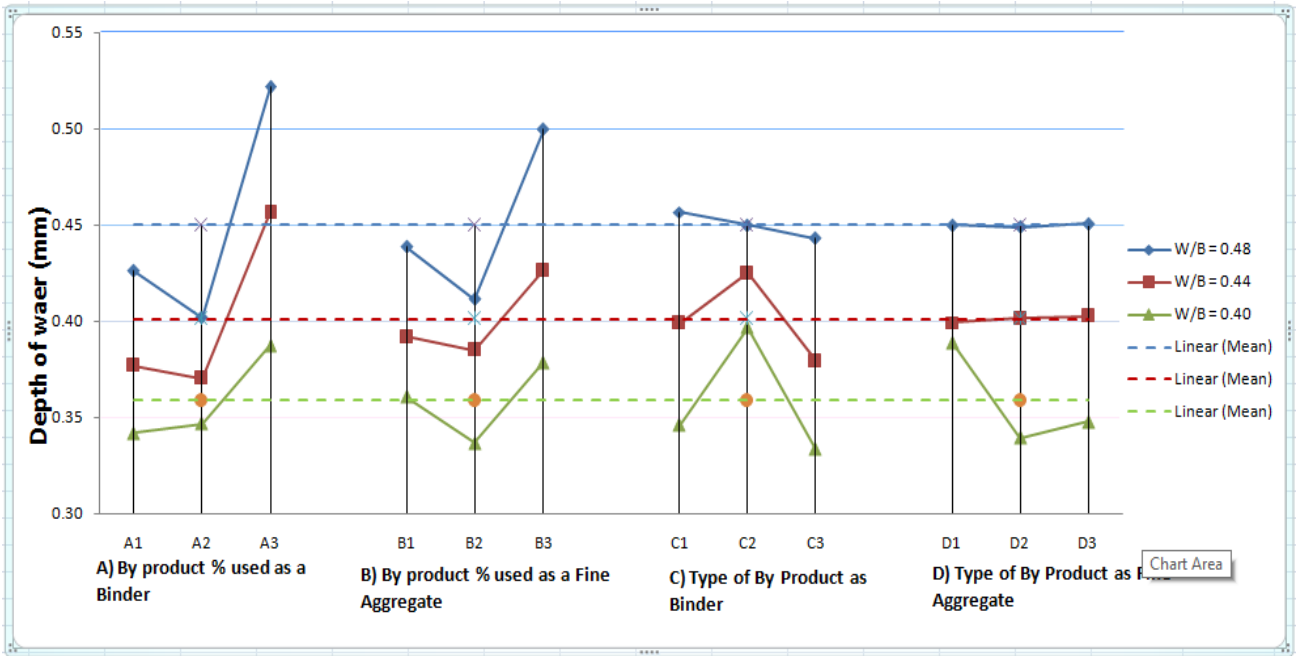

Figure 4.10: Main effects plot for mean depth of wear at 7 days

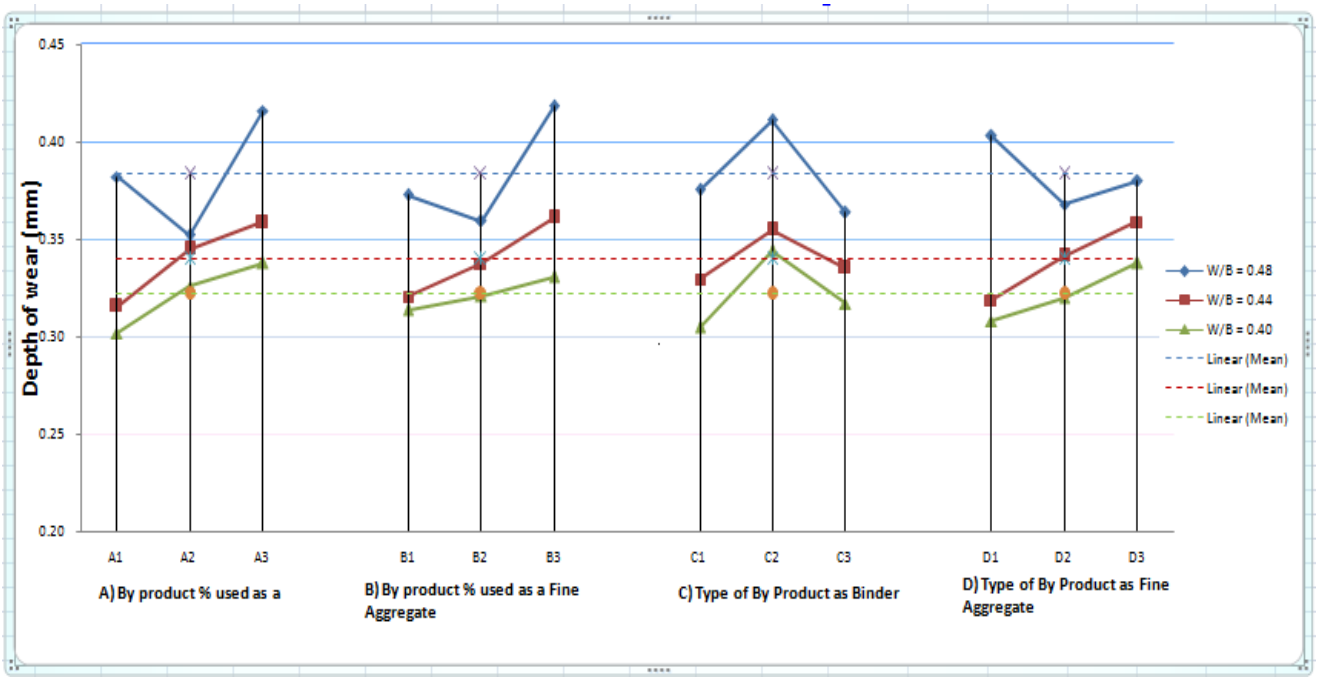

Figure 4.11: Main effects plot for mean depth of wear at 28 days

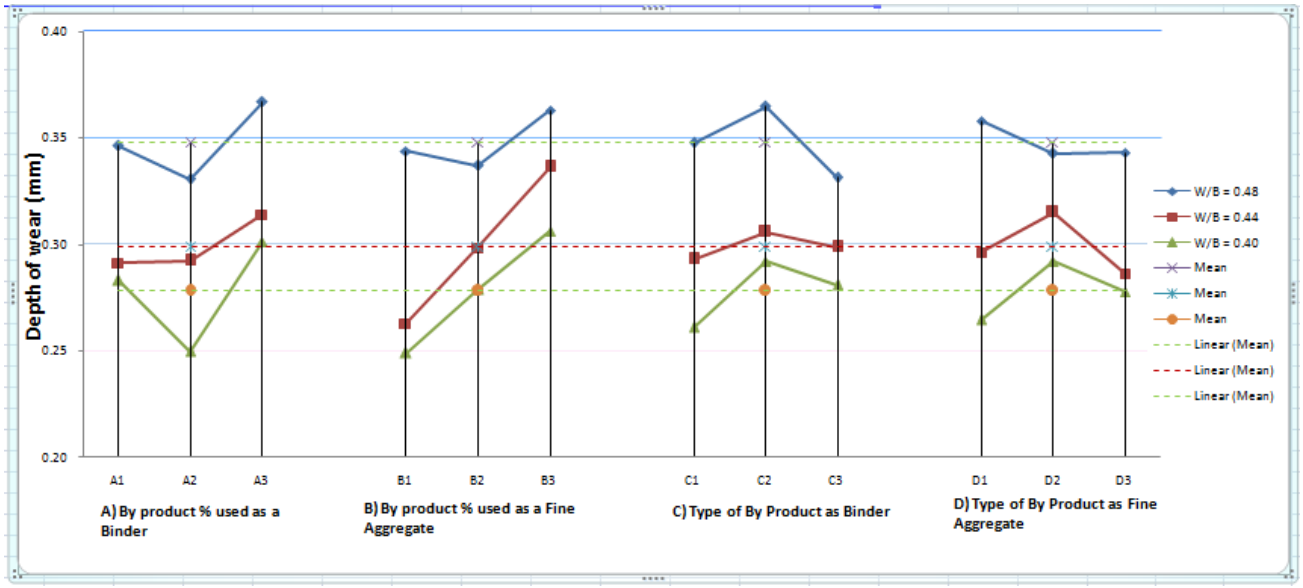

Figure 4.12: Main effects plot for mean depth of wear at 90 days

4.4.3 Optimal Design Consideration

There could be three types of output response values in any experimental analysis, which could be a 'the higher is better', a 'the nominal is better' or a 'the lower is better'. In the present situation depth of wear is a 'lower the best' response. The graphs of the main effects were used to calculate the mean depth of wear with optimal design parameters.

4.4.4 Optimal Mix Design Parameters for Depth of Wear

The significant factors identified after ANOVA analysis and their plots were used to establish their most appropriate level which would decrease the depth of wear. Tables 4.43 to 4.45 provide the summary of the ANOVA analysis for finding the optimal mix design parameters for 7, 28 and 90 days of curing periods respectively. The Tables 4.46 to 4.48 elucidates the optimal percentage replacement and the percentage contribution of each parameter towards the depth of wear of resulting concrete. The effect of curing age on optimal mix design parameters and the percentage contribution of various optimal parameters towards water permeability at different curing periods is discussed below.

(a) Effect of curing age on optimal mix design parameters

- At 7 days curing period (i.e. At early age)

It is seen from the Table 4.43 that at 7 days of curing, copper slag is the optimal replacement material for cement replacement at all the water/binder ratios, whereas for the sand replacement, iron slag is the optimal material at water to binder ratios of 0.48 and 0.40 and electric arc furnace slag at w/b of 0.44.

Table 4.43: Optimal parameters for depth of wear at 7 days of curing

Exp. No.	W/B ratio	Optimal Parameters	Optimal Parameters			
			A	B	C	D
1.	0.48	A2B2C3D2	25	30	Copper Slag	Iron Slag
2.	0.44	A2B2C3D1	25	30	Copper Slag	Electric Arc Furnace Slag
3.	0.4	A1B2C3D2	10	30	Copper Slag	Iron Slag

(Note:- A, B, C and D are the parameters defined in the Table 3.2)

Also, it is seen from the table that at higher w/b ratios of 0.48 and 0.44, 25% is the optimal %age of cement replacement by copper slag which contributes to lower depth of wear at early ages, whereas, 10% is the optimal value of cement replacement by copper slag at lower w/b of 0.40. Also 30% is the optimal value of sand replacement by iron slag at water/binder ratios of 0.48 and 0.40 and by electric arc furnace slag at w/b ratio of 0.44 which contributes positively to lower depth of wear at an early age. Thus, it can be concluded that at early ages, the material for cement replacement (i.e. copper slag) and its percentage replacement (i.e.25%) remains constant at higher water binder ratios but at lower water binder ratio, its %age replacement decreases to 10% whereas, on the other hand, for the replacement of sand, the percentage replacement remains constant (i.e. 30%) at all w/b ratios and the replacement material changes from higher w/b to lower w/b (i.e. from iron slag to EAFS).

- At 28 days curing period (i.e. At normal age)

On observing the tabulated analysis results given in Table 4.44 at curing age of 28 days, it is seen that replacement of cement with copper slag gives the optimal result at higher water to binder ratio of 0.48 and fly ash gives the optimal result at lower w/b of 0.40, whereas, substitution of

sand by iron slag at higher water/binder ratio and electric arc furnace slag at lower water/binder ratio gives the optimal result.

Table 4.44: Optimal parameters for depth of wear at 28 days of curing

Exp. No.	W/B ratio	Optimal Parameters	Optimal Parameters			
			A	B	C	D
1.	0.48	A2B2C3D2	25	30	Copper Slag	Iron Slag
2.	0.44	A1B1C1D1	10	20	Fly Ash	Glass Powder
3.	0.4	A1B1C1D1	10	20	Fly Ash	Electric Arc Furnace Slag

(Note:- A, B, C and D are the parameters defined in the Table 3.2)

Also, it is seen that 25% is the optimum %age replacement by copper slag at 0.48 water to binder ratio and 10% is the optimum percentage replacement by fly ash at 0.44 & 0.40 w/b ratios contributing to lower depth of wear at normal age, whereas 30% of sand replacement by iron slag at water/binder ratios of 0.48 & 20% of sand replacement by electric arc furnace slag at 0.44 & 0.40 water/binder ratio provides the optimal results. Thus, it can be concluded that at normal age, the material for cement replacement (i.e. fly ash) and its percentage replacement (i.e.10%) remains constant at lower water/binder ratios but at higher w/b ratio, the replacement material changes to copper slag and its %age replacement increases to 25% whereas, on the other hand, for the sand replacement, the material for sand replacement (i.e. EAFS) and its percentage replacement (i.e.20%) remains constant at lower w/b ratios but at higher w/b ratio, the replacement material changes to iron slag and its %age replacement increases to 30%.

- At curing period of 90 days

On observing the tabulated analysis results given in Table 4.45 at curing period of 90 days, it is seen that replacement of cement by copper slag gives the optimal result at higher w/b of 0.48 and fly-ash gives the optimal result at lower water to binder ratio of 0.40, whereas, replacement of sand by iron slag at higher water/binder ratio and electric arc furnace slag at lower water/binder ratio gives the optimal result.

Table 4.45: Optimal parameters for depth of wear at 90 days of curing

Exp. No.	W/B ratio	Optimal Parameters	Optimal Parameters			
			A	B	C	D
1.	0.48	A2B2C3D2	25	30	Copper Slag	Iron Slag
2.	0.44	A1B1C1D3	10	20	Fly Ash	Glass Powder
3.	0.4	A1B1C1D1	10	20	Fly Ash	Electric Arc Furnace Slag

(Note:- A, B, C and D are the parameters defined in the Table 3.2)

Also, it is observed that 25% is the optimum %age replacement by copper slag at 0.48 water/binder ratio and 10% is the optimum percentage replacement by fly ash at 0.44 & 0.40 w/b ratios contributing to lower depth of wear at normal age, whereas 30% of sand replacement by iron slag at water to binder ratios of 0.48 & 20% of sand replacement by electric arc furnace slag at w/b of 0.40 provides the optimal results. Thus, it can be concluded that at normal age, the material for cement replacement (i.e. fly ash) and its percentage replacement (i.e.10%) remains constant at lower w/b ratios whereas at higher w/b ratio, the replacement material changes to copper slag and its %age replacement increases to 25% whereas, on the other hand, for the sand replacement , the material for sand replacement (i.e. EAFS) and its percentage replacement (i.e.20%) remains constant at lower w/b ratios but at higher w/b ratio, the replacement material changes to iron slag and its %age replacement increases to 30%.

From the above discussion, it is found that 25 % of copper slag as cement replacement is the optimal parameter to minimize the depth of wear for abrasion after 7 & 28 days but at curing of 90 days, the optimal parameter for cement replacement changes to 10 % of fly ash because of its slow pozzolanic reaction with cement.

(b) Percentage contribution of various optimal parameters towards depth of wear at different curing periods

The results indicating the percentage contribution of optimal parameters towards concrete abrasion are also tabulated in Tables 4.46 to 4.48. The effect at different curing ages is presented below:

- After 7 days curing age (i.e. At early age)

At 7 days of curing age (See Table 4.46), for higher w/b ratio of 0.48, the percentage of by-product used as cement replacement material, which is 25%, contributes maximum to minimize depth of wear of resulting concrete and its contribution is maximum at 65.69%.

Table 4.46: Percentage contribution of each parameter for depth of wear at 7 days of curing

Exp. No.	W/B ratio	Optimal Parameters	Optimal Parameters				Rank				% Contribution			
			A	B	C	D	A	B	C	D	A	B	C	D
1.	0.48	A2B2C3D2	25	30	CS	IS	1	2	3	4	65.69	33.52	0.76	0.01
2.	0.44	A2B2C3D1	25	30	CS	EAFS	1	3	2	4	69.31	14.77	15.83	0.08
3.	0.4	A1B2C3D2	10	30	CS	IS	3	4	1	2	21.47	15.33	38.77	24.43

(Note:- A, B, C and D are the parameters defined in the Table 3.2)

However, for lower w/b of 0.40, the type of cement replacement material contribute maximum and its %age contribution is 38.77%. The %age contribution of the parameter, namely the percentage of sand replacement contributes maximum of 33.52% at 0.48 water/binder ratio and its contribution decreases to 14.77% at 0.44 water/binder ratio. The parameters, namely the type of sand replacement contributes very little towards minimizing the depth of wear of such concrete at all the water/binder ratios.

- At 28 days of curing period (i.e. At normal age)

At the curing of 28 days (See Table 4.47), for higher w/b of 0.48, the percentage of by-product used as cement replacement material, which is 25%, contributes maximum to minimize depth of wear of resulting concrete and its contribution is maximum at 35.26%.

Table 4.47: Percentage contribution of each parameter for depth of wear at 28 days of curing

Exp. No.	W/B ratio	Optimal Parameters	Optimal Parameters				Rank				% Contribution			
			A	B	C	D	A	B	C	D	A	B	C	D
1.	0.48	A2B2C3D2	25	30	CS	IS	1	2	3	4	35.26	32.93	20.69	11.1
2.	0.44	A1B1C1D1	10	20	FA	EAFS	1	2	4	3	32.5	28.13	11.8	27.56
3.	0.4	A1B1C1D1	10	20	FA	EAFS	2	4	1	3	32.43	7.04	38.51	22

(Note:- A, B, C and D are the parameters defined in the Table 3.2)

However, for lower w/b of 0.40, the type of cement replacement material contribute maximum and its percentage contribution is 38.51%. The percentage contribution of the factor, namely the percentage of sand replacement contributes maximum of 32.93% at 0.48 water/binder ratio and its contribution decreases to 7.04% at w/b of 0.40. The parameters, namely the type of sand replacement contributes very little towards minimizing the depth of wear of such concrete at 0.48w/b ratio.

- At 90 days curing period

At the curing age of 90 days (See Table 4.48), for higher w/b of 0.48, the percentage of by-product used as cement replacement material, which is 25%, contributes maximum to minimize depth of wear of resulting concrete and its contribution is maximum at 38.1%.

Table 4.48: Percentage contribution of each parameter for depth of wear at 90 days of curing

Exp. No.	W/B ratio	Optimal Parameters	Optimal Parameters				Rank				% Contribution			
			A	B	C	D	A	B	C	D	A	B	C	D
1.	0.48	A2B2C3D2	25	30	CS	IS	1	3	2	4	38.1	20.76	32.51	8.62
2.	0.44	A1B1C1D3	10	20	FA	GP	3	1	4	2	9.3	76.28	2.4	12
3.	0.4	A1B1C1D1	10	20	FA	EAFS	2	1	3	4	35.48	42.42	12.45	9.64

(Note:- A, B, C and D are the parameters defined in the Table 3.2)

However, for lower water/binder ratio of 0.44, the percentage of by-product used as sand replacement material contribute maximum and its percentage contribution is 76.28%. The %age contribution of the factor, namely the type of cement replacement contributes maximum of 32.51% at water/binder ratio of 0.48 and its contribution decreases to 2.4% at w/b ratio of 0.44. The contribution of the parameters, namely the type of sand replacement is significant at water/binder ratio of 0.44 and contributes maximum of 12% towards minimizing the depth of wear of such concrete.

4.5 FURTHER ANALYSIS - SIGNIFICANT FACTORS FOR OPTIMAL SETTINGS

The ANOVA results show that % of by-product used as binder has the biggest impact on the compressive and split tensile strength and in fact its magnitude is so large that the effect of the other factors has been dwarfed to a large extent. An additional analysis of results was completed to study the effect of factors other than % of by-product used as binder. For each response, nine trial condition results were available for each curing period (7, 28 & 90 days) and for each of the water/binder ratios (0.40, 0.44 & 0.48). The data was analyzed by breaking up the data for the four responses as per the curing days used. This data split as per the curing days used was analyzed for studying the effect of the by-products replaced for cement or sand.

4.5.1 Estimated Mean of Compressive Strength

Compressive strength is a “Higher the better” type response. In this experimental analysis, the response table for means of compressive strength given in Tables 4.1 to 4.3 is used for the estimation of the mean compressive strength with optimal design parameters. The estimated mean compressive strength all the optimal mixes is calculated and is given in Table 4.49. For example, we calculate the estimated compressive strength for optimal mix of one set of w/b=0.40 and curing age =7 days and is given by:

$$\mu_{A1, B2, C1} = \overline{A_1} + \overline{B_2} + \overline{C_1} - 2\overline{T}$$

$$= 37.37+33.13+34.17 -2*30.82$$

$$= 43.03 \text{ N/mm}^2$$

Where μ is the mean value of compressive strength for the optimal settings of each factor. $\overline{T}$ is the mean of all responses (Refer Table 3.24).

Therefore, the estimated mean of compressive strength is 43.03 N/mm^2.

The average of compressive strength obtained at this setting of optimal mix (A1B2C1D1) was 44.5 N/mm^2, which is very near to the estimated value. The detail modeling to predict compressive strength using these results with ANN and ANFIS approach is presented in chapter-6, section-6.1 and 6.2, respectively.

Table 4.49: Estimated mean compressive strength for 7days, 28 days and 90 days

Exp. No.	Curing Period (Days)	W/B ratio	Optimal Parameters	Optimal Parameters				Estimated Mean Compressive Strength (MPa)
				A	B	C	D	
1	7 Days	0.48	A1B2C1D3	10%	30%	Fly Ash	GP	30.80
2		0.44	A1B2C1D1	10%	30%	Fly Ash	EAFS	33.21
3		0.4	A1B2C1D1	10%	30%	Fly Ash	EAFS	43.03
4	28 Days	0.48	A1B2C1D2	10%	30%	Fly Ash	Iron Slag	50.80
5		0.44	A1B2C1D2	10%	30%	Fly Ash	Iron Slag	51.82
6		0.4	A1B2C1D3	10%	30%	Fly Ash	GP	60.72
7	90 Days	0.48	A1B2C1D2	10%	30%	Fly Ash	Iron Slag	63.42
8		0.44	A1B2C1D2	10%	30%	Fly Ash	Iron Slag	66.93
9		0.4	A1B2C1D2	10%	30%	Fly Ash	Iron Slag	80.95

(Note:- A, B, C and D are the parameters defined in the Table 3.2)

4.5.2. Significant Factors for Optimal Compressive Strength Based on Estimated Mean

From the data given in Table 4.49, it was noticed that highest compressive strength could be measured for the optimal mix after 90 days of curing having 10% fly ash as partial replacement of binder, 30% iron slag used as replacement of fine aggregate and water/binder ratio was 0.40. Similarly, for a curing period of 28 days, the compressive strength was highest with water to binder ratio of 0.40, 10% Fly-ash as a binder and 30% glass powder as a fine aggregate were selected. For 7 days the highest compressive strength was highest when water to cement ratio was 0.40, 10% fly ash used as cement replacement and 30% EAF slag as a fine aggregate material to be selected.

From the discussion given above, it is found that highest compressive strength can be arrived with 10% of fly-ash as cement replacement at all the curing periods and at 0.40 w/b ratio. This could be attributed to the very fine particles of the fly ash which fills the air voids thus making the concrete denser than other by-products. But in case of sand replacement, highest compressive strength can be achieved by using 30% of electric arc furnace slag, 30% of glass powder and 30% of iron slag at 7, 28 & 90 days of curing respectively.

4.5.3 Estimated Mean of Split Tensile Strength

We know that split tensile strength is a "Higher the better" type response. In this experimental analysis, the response tables for means of split tensile strength in Tables 4.13 to 4.15 is used for the estimation of the mean split tensile strength with optimal mix design parameters. The estimated mean tensile strength all the optimal mixes is calculated and is given in Table 4.50. For example, we calculate the estimated tensile strength for optimal mix with w/b of 0.40 and curing of 7 days and is given by:

$$\mu_{A1, B3, C1} = \overline{A_1} + \overline{B_3} + \overline{C_1} - 2\overline{T}$$
$$= 2.457+2.447+2.430 -2*2.325$$
$$= 2.684 \text{ N/mm}^2$$

Where μ is the mean split tensile strength at the optimal settings of factors. $\overline{T}$ is the mean of all responses (Refer Table 3.26).

Therefore, the estimated mean value of split tensile strength is 2.684 N/mm^2.

The average value of split tensile strength obtained at this setting of (A1B3C1D1) was 2.72 N/mm^2, which is very near to the predicted value. The detail modeling to predict split tensile strength using these results with ANN and ANFIS approach is presented in chapter-6, section-6.1 and 6.2 respectively.

Table 4.50: Estimated mean split tensile strength after 7, 28 & 90 days

Exp. No.	Curing age (Days)	W/B ratio	Optimal Parameters	Optimal Parameters				Estimated Mean Split Tensile Strength (MPa)
				A	B	C	D	
1	7 Days	0.48	A2B3C1D1	25%	40%	Fly Ash	EAFS	2.326
2		0.44	A1B3C1D2	10%	40%	Fly Ash	IS	2.687
3		0.4	A1B3C1D1	10%	40%	Fly Ash	EAFS	2.684
4	28 Days	0.48	A1B2C1D1	10%	30%	Fly Ash	EAFS	3.364
5		0.44	A1B2C1D1	10%	30%	Fly Ash	EAFS	3.553
6		0.4	A1B2C1D3	10%	30%	Fly Ash	GP	3.75
7	90 Days	0.48	A1B2C1D3	10%	30%	Fly Ash	GP	3.81
8		0.44	A2B2C1D3	25%	30%	Fly Ash	GP	4.10
9		0.4	A1B2C1D2	10%	30%	Fly Ash	Iron Slag	4.73

(Note:- A, B, C and D are the parameters defined in the Table 3.2)

4.5.4 Significant Factors for Optimal Split Tensile Strength Based on Estimated Mean

From the data provided in Table 4.50, it was observed that highest split tensile strength could be measured for a curing of 90 days when water/ binder ratio is 0.40, 10% fly ash is used as partial replacement of cement and 30% iron slag is used as replacement of sand. Similarly, for a curing period of 28 days, highest split tensile strength was measured with 0.40 water/ binder ratio, 10% Fly-ash as a cement replacement and 30% glass powder as a fine aggregate material were selected. For 7 days the highest split tensile strength could be achieved when water/ binder ratio is 0.44, 10% fly ash as binder and 40% iron slag as fine aggregate to be selected.

From the above discussion, it is found that highest split tensile strength could be achieved with 10% of fly ash as replacement of cement at all the curing ages and at 0.40 water/binder ratio. But in case of sand replacement, highest split tensile strength would be by using 40% of electric arc furnace slag, 30% of glass powder and 30% of iron slag at 7, 28 & 90 days of curing respectively.

4.5.5 Estimated Mean of Water Penetration Depth

Water penetration depth is a "Lower the better" type response. In this experimental analysis, the response tables for means of water penetration depth given in Tables 4.25 to 4.27 is used to calculate the mean water penetration depth with optimal mix design parameters. The estimated mean water penetration depth all the optimal mixes is calculated and is given in Table 4.51. For example, we calculate the estimated water penetration depth for optimal mix with w/b ratio of 0.40 and curing of 7 days and is given by:

$$\mu_{A1, B1, C3} = \overline{A_1} + \overline{B_1} + \overline{C_3} - 2\overline{T}$$
$$= 61.67+50+64.33 -2*78.33$$
$$= 19.34 \text{ mm}$$

Where μ is the mean water penetration depth at the optimal settings of each factor. $\overline{T}$ is the mean of all responses (Refer Table 3.28).

Therefore, the estimated mean of depth of water penetration is 19.34 mm. The average value of depth of water penetration obtained at this setting of (A1B1C3D3) was 19.20 mm, which is very close to the predicted value.

Table 4.51: Estimated mean depth of water penetration for 7, 28 & 90 days

Exp. No.	Curing Age (Days)	W/B ratio	Optimal Parameters	Optimal Parameters				Estimated mean depth of water penetration (mm)
				A	B	C	D	
1	7 Days	0.48	A2B1C3D3	10%	30%	Fly Ash	GP	56.91
2		0.44	A1B1C3D3	10%	30%	Fly Ash	EAFS	39.34
3		0.4	A1B1C3D3	10%	30%	Fly Ash	EAFS	19.34
4	28 Days	0.48	A1B3C2D2	10%	30%	Fly Ash	Iron Slag	21.79
5		0.44	A1B3C2D2	10%	30%	Fly Ash	Iron Slag	22.34
6		0.4	A1B2C3D3	10%	30%	Fly Ash	GP	16.45
7	90 Days	0.48	A1B3C1D3	10%	30%	Fly Ash	Iron Slag	17.23
8		0.44	A1B3C2D3	10%	30%	Fly Ash	Iron Slag	9.0
9		0.4	A1B3C2D3	10%	30%	Fly Ash	Iron Slag	7.0

(Note:- A, B, C and D are the parameters defined in the Table 3.2)

4.5.6 Significant Factors for Optimal Depth of Water Penetration Based on Estimated Mean

From the data provided in Table 4.51, it was seen that lowest depth of water penetration can be achieved for curing age of 90 days when water/ binder ratio is 0.40, 10% fly ash is used as partial replacement of binder and 30% iron slag is used as replacement of fine aggregate. Similarly, for a curing age of 28 days, lowest depth of water penetration can be achieved with w/b ratio of 0.40, 10% Fly-ash as cement and 30% glass powder as a fine aggregate were selected. For 7 days the lowest depth of water penetration could be achieved when water /binder ratio is 0.40, 10% fly-ash used as a binder material and 30% EAFS as a fine aggregate to be selected.

From the above discussion, it is found that lowest water penetration depth can be achieved with 10% of fly ash is to be used as replacement of cement at all the curing periods and at 0.40 water/binder ratio. This is attributed to the fineness of the fly ash which fills the air voids thus making the concrete denser than other by-products. But in case of sand replacement, lowest depth of water penetration can be achieved by using 30% of electric arc furnace slag, 30% of glass powder and 30% of iron slag at 7, 28 & 90 days of curing respectively and at 0.40 water/binder ratio.

4.5.7 Estimated Mean of Depth of Wear

Depth of wear is a "Lower the better" type of response. In this experimental analysis, the response table for means of depth of wear given in Tables 4.37 to 4.39 is used to calculate the mean depth of wear with optimal mix design parameters. The estimated mean depth of wear for all the optimal mixes is calculated and is given in Table 4.52. For example, we calculate the estimated mean of wear depth for optimal mix at w/b of 0.40 and curing of 7 days and is given by:

$\mu_{A1, B2, C3} = \overline{A_1} + \overline{B_2} + \overline{C_3} - 2\overline{T}$

$= 0.334+0.339+0.342 -2*0.36$

$= 0.296$ mm

Where μ is the mean depth of wear at the optimal settings of each factor. $\overline{T}$ is the mean of all responses (Refer Table 3.30).

Therefore, the estimated mean of depth of wear is 0.296 mm. The average value of depth of wear obtained at this setting of (A1B2C3D2) was 0.290 mm, which is very near to the estimated value. The detail of modeling to predict the depth of wear using these results with ANN approach is presented in chapter-6, section-6.3.

Table 4.52: Estimated mean depth of abrasion for 7, 28 & 90 days

Exp. No.	Curing Age (Days)	W/B ratio	Optimal Parameters	Optimal Parameters				Estimated mean depth of abrasion (mm)
				A	B	C	D	
1	7 Days	0.48	A2B2C3D2	25	30	CS	IS	0.357
2		0.44	A2B2C3D1	25	30	CS	EAFS	0.334
3		0.4	A1B2C3D2	10	30	CS	IS	0.296
4	28 Days	0.48	A2B2C3D2	25	30	CS	IS	0.310
5		0.44	A1B1C1D1	10	20	FA	EAFS	0.275
6		0.4	A1B1C1D1	10	20	FA	EAFS	0.339
7	90 Days	0.48	A2B2C3D2	25	30	CS	IS	0.303
8		0.44	A1B1C1D3	10	20	FA	GP	0.240
9		0.4	A1B1C1D1	10	20	FA	EAFS	0.204

(Note:- A, B, C and D are the parameters defined in the Table 3.2)

4.5.8 Significant Factors for Optimal Depth of Wear Based on Estimated Mean

From the data provided in Table 4.52, it was observed that lowest depth of wear can be achieved for curing age of 90 days when water / binder ratio is 0.40, 10% fly-ash is used as binder replacement and 20% EAF slag is used as fine aggregate replacement. Similarly, for 28 days of curing, lowest depth of abrasion could be measured with w/b of 0.44, 10% Fly ash as a binder and 20% electric arc furnace slag as a fine aggregate were selected. For 7 days the lowest depth of abrasion could be achieved when water/ binder ratio is 0.40, 10% copper slag as a binder and 30% iron slag as a fine aggregate to be selected.

4.5.9 Summary of Significant Factors for Optimal Compressive Strength, Split Tensile Strength, Water Penetration Depth and Depth of Wear

The optimal settings of each of the factors after 7, 28 & 90 days of curing for compressive strength, split tensile strength, water penetration depth and depth of wear are presented in Table 4.53.

Table 4.53 Significant factors for optimal compressive strength, split tensile strength, water penetration depth and depth of wear

Factors	Compressive Strength			Split Tensile Strength			Depth of Water Penetration			Depth of wear		
	Best Level setting			Best Level setting			Best Level setting			Best Level setting		
	Curing age (Days)			Curing age (Days)			Curing age (Days)			Curing age (Days)		
	7	28	90	7	28	90	7	28	90	7	28	90
w/b ratio	0.40	0.40	0.40	0.40	0.40	0.40	0.40	0.40	0.40	0.40	0.44	0.40
% By-product as Binder	10 %	10 %	10 %	10 %	10 %	10 %	10 %	10 %	10 %	10%	10%	10%
% By-product as Fine aggregate	30 %	30 %	30 %	40 %	30 %	30 %	30 %	30 %	30 %	30%	20%	20%
By-product as Binder	FA	FA	FA	FA	FA	FA	FA	FA	FA	Copper Slag	FA	FA
By-product as Fine Aggregate	EAFS	Glass Powder	Iron Slag	EAFS	Glass Powder	Iron Slag	EAFS	Glass Powder	Iron Slag	Iron Slag	EAFS	EAFS

As seen from the above table, it is concluded that 10% of fly-ash to be used as cement replacement is the most significant factor for the optimal strength and durability of the concrete under consideration at w/b of 0.40 and at all the curing of 7, 28 & 90 days. For the sand replacement, EAF slag, glass powder and iron slag are the most significant factor for optimal compressive strength, split tensile strength and water penetration depth at 7, 28 and 90 days of curing respectively and at w/b of 0.40. For the best abrasion strength, the most significant factor for sand replacement is iron slag at 7 days of curing and it is electric arc furnace slag at 28 & 90 days of curing and for 0.40 water/binder ratio.

4.6 VALIDATION OF RESULTS

The 9 trials as per L_9 array were repeated for 7 days of curing by varying all the other factors considered in the earlier experimentation. The compressive strength was measured for cubes cast after each trial and analyzed using ANOVA. It was seen from the results that for all w/b ratios, % of the by-product to be used as partial replacement of cement is the most significant factor that affects concrete compressive strength, followed by the type of by-product used as replacement of binder and % of by-product used as replacement of fine aggregates. On the other hand, the type of by-product to be used as a fine-aggregate was found to be insignificant. The optimal mixture resulted in more compressive as well as split tensile strength in comparison to the control mix at all the water/binder ratios and at all the curing periods. The increase in compressive and split tensile strength is attributed to the synergic effect and pozzolanic activity of the optimal percentages of the industrial by-products.

CHAPTER 5 MULTI RESPONSE OPTIMISATION

5.0 GREY RELATIONAL ANALYSIS (GRA); A MULTIPLE OPTIMIZATION TECHNIQUE

5.1 INTRODUCTION

Grey relational analysis technique was first presented by Deng (1989) and is now widely used by many researchers for the optimization of process parameters which have multi-responses by Grey relational grade. GRA technique is very effective in optimising the multiple response characteristics. The Grey systems have a lack of information in GRA. The Grey Relational Grade (GRG) which is a ranking scheme used to rank the order of the grey relationship between the dependent and independent variables. In this chapter, multi-response optimisation of compressive strength, split tensile strength, water penetration depth and depth of wear was carried out with the help of GRA technique. The objective is to maximise compressive and split tensile strength; while minimising water penetration depth and depth of wear. In other words, multi response parameters are entirely different from single optimization of response. The following are the steps followed for the optimization of the input factors with multiple output responses using GRA with Taguchi method as in Fig. 5.1

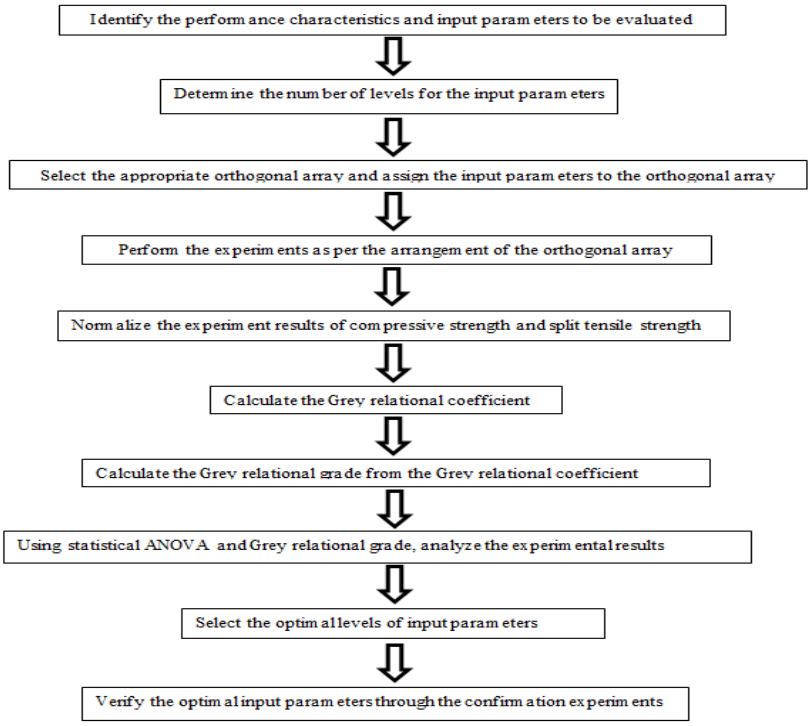

Fig. 5.1: Steps followed in Grey relational analysis with Taguchi method

5.2 MULTI RESPONSE OPTIMIZATION USING GRA FOR STRENGTH PROPERTIES

In this study, GRA was used to optimize the strength properties which include compressive as well as split tensile strength. The best possible levels of partial binder replacement and fine aggregate replacement in the mix proportions were found with the use of Grey relational analysis (GRA) technique coupled with Taguchi. The performance characteristics for "the larger the better" is taken to maximize the strength properties of concrete. For detailed calculations, the response data for one set of water/binder ratio and curing period (water/binder = 0.40 and curing age = 90 days), as given in the Tables 5.5, was analyzed using ANOVA method at significance level of 0.05, to determine the change in the properties of the concrete. Concrete mix design proportions given in Table 5.1 were selected as independent factors, whereas strength properties of the concrete mixtures were the dependent variables. GRA method is used to find statistically the significant parameters, and the response table for grey relation grade is shown in Table 5.5. This method finally gives the percentage contribution of each control factor shown in Table 5.6. The %age contribution (PC) of each factor gives an idea of its quantum of contribution to the output response. If the percentage contribution of the factor is more, than the contribution of the factor for that response is more and vice versa. The summary of the GRA for all the combinations of water/binder ratios of 0.48, 0.44 & 0.40 and curing ages of 7, 28 & 90 days were performed in a similar manner. The following are the stages involved in the approach.

5.2.1 Normalisation of Data

In GRA, the first step is to normalise the random data and make all the data as dimensionless. Thus, the original data is converted into the useful data for comparison. We can normalise the original data with different methods. As we know, the compressive strength (CS) and split tensile strength (STS) are “larger-the-better” properties of concrete; the original sequence can be normalized by using the Eqn. (5.1):

$$x_i^*(k) = \frac{x_i(k) - min\ x_i(k)}{max\ \ x_i(k) - min\ x_i(k)} \quad ---------- \qquad (5.1)$$

Where, $x_i(k)$ and $x_i^*(k)$ are the original values and values after the data normalisation respectively, and k=1 and 2 for CS & STS, respectively; i = 1 to 9 for trial numbers 1 to 9. All the order values after data normalisation using Eqn. (5.1) are given in Table 5.2.

Table 5.1: Experimental detail using Taguchi's L_9 OA and response results (for w/b= 0.40 and curing period=90 days)

Exp. No.	Levels of parameters				Compressive Strength (MPa)	Split Tensile Strength (MPa)
	Parameter [A]	Parameter [B]	Parameter [C]	Parameter [D]		
1	10%	20%	FA	EAFS	72.05	4.58
2	10%	30%	LFS	IS	64.35	4.07
3	10%	40%	CS	GP	51.18	3.57
4	25%	20%	LFS	GP	44.55	3.46
5	25%	30%	CS	EAFS	46.20	3.87
6	25%	40%	FA	IS	66.33	4
7	40%	20%	CS	IS	36.22	3.15
8	40%	30%	FA	GP	64.9	3.8
9	40%	40%	LFS	EAFS	39.38	2.76

(Note:- A, B, C and D are the control parameters defined in Table 3.2)

Table 5.2: The normalised values of each concrete property

Trial No.	Compressive strength	Split tensile strength
	1.0000	**1.0000**
1	1.0000	1.0000
2	0.7851	0.7198
3	0.4175	0.4451
4	0.2325	0.3846
5	0.2785	0.6099
6	0.8404	0.6813
7	0.0000	0.2143
8	0.8004	0.5714
9	0.0882	0.0000

The deviation order values $\delta_{0i}(k)$ is calculated using the expression as shown in Eqn.(5.2).

$$\delta_{0i}(k) = |x_0^*(k) - x_i^*(k)| \qquad \ldots\ldots\ldots\ldots \qquad (5.2)$$

Where $x_0^*(k)$ is the reference value which is 1 and $x_i^*(k)$ is the normalised value. The values of all δ_{0i} for i from 1 to 9 are given in Table 5.3.

Table 5.3: The deviation order values

Exp. No.	Deviation order values	
	Compressive strength	Split tensile strength
	1.0000	**1.0000**
1	0.0000	0.0000
2	0.2149	0.2802
3	0.5825	0.5549
4	0.7675	0.6154
5	0.7215	0.3901
6	0.1596	0.3187
7	1.0000	0.7857
8	0.1996	0.4286
9	0.9118	1.0000

5.2.2 Calculation of the Grey Relational Coefficients

The Grey relational coefficients for all the experiments of the L_9 OA are calculated using Eqn. (5.3).

$$\zeta_i(k) = \frac{\Delta_{min} + \zeta\Delta_{max}}{\Delta_{0i}(k) + \zeta\Delta_{max}} \quad - - - - - - - - - - \qquad (5.3)$$

Where δ_{0i} (k) = the deviation order value among reference sequence $x_0^*(k)$ and comparability value $x_i^*(k)$, and ζ = the identification coefficient and its value is taken as 0.5 *(Deng, 1989).* The values of the Grey relational coefficients are shown in Table 5.4.

Table 5.4: Grey relational coefficients and Grey relational grades

Exp. no.	Grey relational coefficients		Grey relational grades $\Upsilon_i=½(\zeta_i(1)+\zeta_i(2))$	Rank
	CS	STS		
	$\zeta_i(1)$	$\zeta_i(2)$		
1	1.0000	1.0000	1.0000	1
2	0.6994	0.6408	0.6701	3
3	0.4619	0.4740	0.4679	6
4	0.3945	0.4483	0.4214	7
5	0.4093	0.5617	0.4855	5
6	0.7580	0.6107	0.6844	2
7	0.3333	0.3889	0.3611	8
8	0.7147	0.5385	0.6266	4
9	0.3542	0.3333	0.3437	9

(Note- CS- Compressive Strength, STS- Split Tensile Strength)

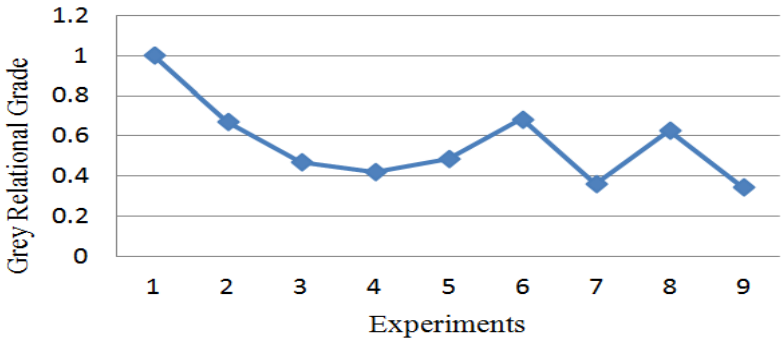

Fig. 5.2: The graph showing the GRG of each experiment

The Grey relational grade (GRG) is now calculated by taking mean of the Grey relational coefficients of each response and is given by the expression in Eqn. (5.4).

$$\Upsilon_i = \frac{1}{n}\sum_{k=1}^{n} \zeta_i\,(k) \quad ---------- \quad (5.4)$$

Where Υ_i is the GRG for the i_{th} experiment, n = the number of responses. Table 5.4 presents the GRG for each of the experiment conducted as per L_9 OA. If the value of the GRG is higher than it indicates that the experimental value is close to the normalized value and vice versa. As observed from Table 5.4, it can be said that experiment 1 is having best multiple response value among all the nine experiments as it is having the highest GRG. Thus, it can be observed that in the GRA, the optimization of the multiple responses of concrete has been converted into the optimization of one GRG only.

Now, due to the orthogonality of experimental design, it is possible to find the effect of each individual factor on the GRG at each level. Table 5.5 shows the mean of the GRG for each level of the parameters/ factors. The total mean of the GRG for all the nine experiments is 0.5623.

Table 5.5: Response table for GRG

Symbol	Parameters	Grey relational grade (GRG)			Main effect (max.-min.)	Rank
		Level 1	Level 2	Level 3		
A	By-product used as a binder (%)	0.7127	0.5304	0.4438	0.2689	2
B	By-product used as FA (%)	0.5941	0.5942	0.4987	0.0955	4
C	Type of by-product as a binder	0.7703	0.4784	0.4382	0.3321	1
D	Type of by-product used as FA	0.6098	0.5719	0.5053	0.1045	3
	Optimal Parameters = A1 B2 C1 D1					

Fig. 5.3 shows the GRG for various parameters at their different levels. The horizontal line represents the mean of the GRG for each parameter. Basically, a larger value of the GRG shows that it is very close to its ideal value. Thus, we require a larger GRG for optimum response value. Therefore, the optimal parameters for better compressive and split tensile strength are A1 B2 C1 D1 as shown in Table 5.5. So the optimal parameters are quantity of by-product to be used as binder (%) at level 1, quantity of by-product to be used as fine aggregate (%) at level 2, kind of by-product to be used as cement at level 1and type of by-product to be used as sand at level 1.Thus, it can be concluded that most optimum results can be obtained with 10% of cement replacement with fly ash along with 30% of fine aggregates replacement by EAFS.

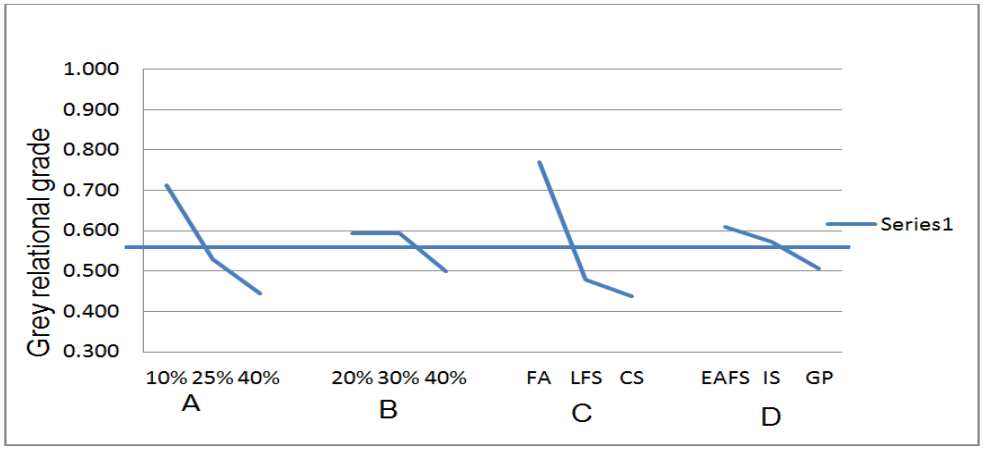

Fig. 5.3: Effect of factors on the GRG

In addition, ANOVA analysis was applied on GRG to obtain the contribution of each factor that affects the two output responses, i.e. compressive and split tensile strength jointly and is discussed below.

5.2.3 Analysis of Variance (ANOVA)

The aim of ANOVA is to find which parameter has maximum effect on the strength properties of such concrete. ANOVA for GRG is shown in Table 5.6. Fig. 5.4 shows the percentage contributions of each parameter which affects the GRG. It clearly shows that the type of by-product used as a binder is the parameter which contributes maximum in improving the compressive & split tensile strength at 90 days curing age.

Table 5.6: ANOVA table for Grey relational grades

Parameter	DOF	SS	MS	PC
[A] By-Product Used as Binder (%)	2	0.1130	0.0565	32.74
[B] By-Product Used as FA (%)	2	0.0182	0.0091	5.28
[C] Type of By-Product used as Binder	2	0.1971	0.0986	57.12
[D] Type of By-Product used as FA	2	0.0168	0.0084	4.86
TOTAL	8	0.3451	0.1726	100.00

(Note:- DOF-Degrees of freedom; SS- Sum of Squares; MS-Mean sum of squares; PC-Percentage Contribution)

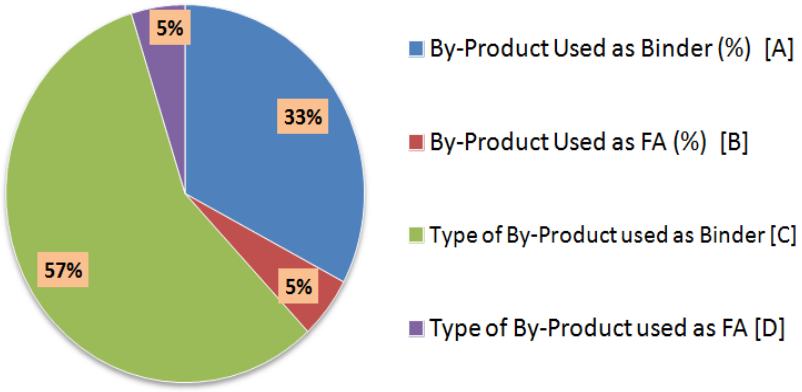

Fig. 5.4: Percentage contributions of each factor towards the Strength Properties

The results of Grey relational analysis for all other combinations of water to binder ratios and curing periods were performed in a similar manner as above.

5.2.4 Results and Discussion

The optimal parameters for strength properties at 7, 28 & 90 days are presented in Tables 5.7 to 5.9 respectively. The effect of curing age on the optimal mix design parameters and the percentage contribution of various optimal parameters towards the strength at different curing periods are discussed below:

(a) Effect of curing period on optimal mix design parameters

- At curing age of 7 days (i.e. at early age)

It is observed from the Table 5.7 that at 7 days curing, for all water-binder ratios, cement replacement by fly ash gives the optimal result, whereas iron slag replacement for sand provides the optimal strength results only for higher w/b ratios of 0.44 & 0.48. However, at a lower w/b of 0.40, electric arc furnace slag as a replacement for sand provides better results.

Table 5.7: Optimal parameters for strength properties at curing of 7 days

Exp. No.	W/B ratio	Optimal Parameters	Optimal Parameters			
			A	B	C	D
1.	0.48	A1B3C1D2	10	40	Fly Ash	Iron Slag
2.	0.44	A1B3C1D2	10	40	Fly Ash	Iron Slag
3.	0.4	A1B1C1D1	10	20	Fly Ash	Electric Arc Furnace Slag

(Note:- A, B, C and D are the control parameters defined in Table 3.2)

Also, it is observed that for all water binder ratios, 10% is the optimal %age of fly ash replacement contributing to higher strength at early ages, whereas 40% of sand replacement by iron slag at 0.48 & 0.44 w/b ratios contributes positively to strength gain at an early age. For lower water/binder ratio, 20% of sand replacement by electric arc furnace slag provides the optimal strength results. Thus, it can be concluded that at early ages, the replacement material and its percentage replacement of cement remains constant at all water/ binder ratios, whereas, on the other hand, for the replacement of sand, the type of material and its percentage replacement remains constant i.e. 40% iron slag at higher w/b ratios and it changes to 20% electric arc furnace slag only at lower w/b ratios.

- At 28 days of curing age (i.e. at normal age)

On observing the tabulated analysis results at 28 days curing (See Table 5.8), for all water binder ratios, we see that the cement replacement by fly ash gives the optimal result than other materials, whereas, on the other hand, replacement of sand by electric arc furnace slag gives the optimal result than other materials.

Table 5.8: Optimal parameters for strength properties at 28 days of curing

Exp. No.	W/B ratio	Optimal Parameters	Optimal Parameters			
			A	B	C	D
1.	0.48	A1B2C1D1	10	30	Fly-Ash	EAFS
2.	0.44	A1B2C1D1	10	30	Fly-Ash	EAFS
3.	0.4	A1B2C1D1	10	30	Fly-Ash	EAFS

(Note:- A, B, C and D are the control parameters defined in Table 3.2)

Also, it is observed that for all water binder ratios, 10% is the optimal %age of fly ash for substitution as cement contributing to higher strength at a normal age, whereas 30% of sand replacement by electric arc furnace slag provides the optimal strength results. Thus, it can be concluded that at curing of 28 days, the replacement material and its percentage replacement values for both cement and sand remain constant for all water binder ratios.

- At curing period of 90 days

On analyzing the results at 90 days curing (See Table 5.9), for all water binder ratios, it is found that cement replacement by fly ash gives the optimal result, whereas, iron slag replacement for sand provides the optimal strength results only for higher w/b ratio of 0.48.

Table 5.9: Optimal parameters for strength properties at 90 days of curing

Exp. No.	W/B ratio	Optimal Parameters	Optimal Parameters			
			A	B	C	D
1.	0.48	A1B2C1D2	10	30	Fly-Ash	Iron Slag
2.	0.44	A1B2C1D1	10	30	Fly-Ash	EAFS
3.	0.4	A1B2C1D1	10	30	Fly-Ash	EAFS

(Note:- A, B, C and D are the control parameters defined in Table 3.2)

However, at lower w/b ratios of 0.44 & 0.40, electric arc furnace slag as sand replacement provides better results. Also, it is seen that for all water binder ratios, 10% is the optimal %age of fly ash replacing binder contributing to higher strength, whereas 30% of sand replacement by iron slag at w/b= 0.48 contributes positively to strength gain. For lower w/b ratios, 30% of sand replacement by electric arc furnace slag provides the optimal strength results. Thus, it can be concluded that at 90 days, the replacement material and its percentage replacement for cement remains constant at all water/binder ratios, whereas on the other

hand, for the replacement of sand, the type of material and its percentage replacement remains constant (i.e. 30% iron slag) at higher w/b of 0.48. However, it changes to 30% electric arc furnace slag only at lower water/binder ratios of 0.40 & 0.44.

To sum up, it is found that 10% of the fly-ash is the optimal parameters for cement replacement for compressive and split tensile strength at all the curing periods and water to binder ratios. Similarly 30% is the optimal replacement level of sand for all the water binder ratios and at all the curing periods. The optimal parameter for sand replacement material changes from iron slag at 7 days curing to electric arc furnace slag at 90 days curing.

(b) Percentage contribution of various optimal parameters towards the strength at different curing periods

The results indicating the percentage contribution of optimal parameters towards concrete strength are tabulated in Tables 5.10 to 5.12 for 7, 28 & 90 days curing period respectively. Their effect at different curing ages is presented below:

- At 7 days curing period (i.e. at an early age)

As see from the Table 5.10, at curing of 7 days, for all water/binder ratios, 10% of by-product to be used as partial cement replacement is the optimal parameter which contributes maximum towards the strength of resulting concrete. It is observed that its contribution is maximum at higher w/b ratio of 0.48, i.e.72.13% and it decreases to 48.72% as the w/b is decreased to 0.40, whereas, at lower water/binder ratios, the contribution of type of binder replacement material towards concrete strength, (i.e. fly ash) starts increasing, which is 29.32% at w/b of 0.40.

Table 5.10: Percentage contribution of each parameter for strength properties at 7 days of curing

Exp. No.	W/B ratio	Optimal Parameters	Optimal Parameters				Rank				% Contribution			
			A	B	C	D	A	B	C	D	A	B	C	D
1.	0.48	A1B3C1D2	10	40	FA	IS	1	4	2	3	72.13	1.06	21.15	5.3
2.	0.44	A1B3C1D2	10	40	FA	IS	1	4	2	3	56.45	2.19	31.21	10.16
3.	0.4	A1B1C1D1	10	20	FA	EAFS	1	4	2	3	48.72	1.65	29.32	20.3

(Note:- A, B, C and D are the control parameters defined in Table 3.2)

The percentage of sand replacement, as can be observed from the Table 5.10, contributes very little and almost remains constant at all the water/binder ratios, whereas the type of replacement as sand does play a slightly better role only for lower w/b ratios.

➢ At curing period of 28 days

At curing period of 28 days (See Table 5.11), for higher water/binder ratios, the percentage of material as cement replacement contributes the most towards the concrete strength, but at lower w/b ratios, the type of cement replacement product contributes maximum towards the strength of resulting concrete.

Table 5.11: Percentage contribution of each parameter for strength properties at 28 days of curing

Exp. No.	W/B ratio	Optimal Parameters	Optimal Parameters				Rank				% Contribution			
			A	B	C	D	A	B	C	D	A	B	C	D
1.	0.48	A1B2C1D1	10	30	FA	EAFS	1	4	2	3	77.14	1.64	16.5	4.73
2.	0.44	A1B2C1D1	10	30	FA	EAFS	1	4	2	3	53.01	1.01	41.15	4.83
3.	0.4	A1B2C1D1	10	30	FA	EAFS	2	3	1	4	26.82	10.72	61.99	0.47

(Note:- A, B, C and D are the control parameters defined in Table 3.2)

As can be observed from the Table 5.11, the percentage contribution towards the strength of 10% replacement of cement is maximum at 77.14% at w/b of 0.48 whereas, its value is 26.82% at w/b of 0.40. The %age contribution of fly-ash towards strength gain is 16.50% at w/b of 0.48; whereas, it is 61.99% at lower at w/b of 0.40. The %age contribution of the parameters, namely the type of sand replacement and its percentage replacement contributes very little at all the water/binder ratios.

➢ At curing period of 90 days

At curing of 90 days (See Table 5.12), for all water/binder ratios, the type of by-product used as material for cement replacement, which is fly-ash, among three materials, contributes the maximum to the strength of resulting concrete and its contribution is maximum at 65.43% at w/b of 0.44.

Table 5.12: Percentage contribution of each parameter for strength properties at 90 days of curing

Exp. No.	W/B ratio	Optimal Parameters	Optimal Parameters				Rank				% Contribution			
			A	B	C	D	A	B	C	D	A	B	C	D
1.	0.48	A1B2C1D2	10	30	FA	IS	2	4	1	3	45.7	0.4	49.1	4.8
2.	0.44	A1B2C1D1	10	30	FA	EAFS	2	4	1	3	28.9	2.32	65.43	3.35
3.	0.4	A1B2C1D1	10	30	FA	EAFS	2	4	1	3	32.74	5.28	57.12	4.86

(Note:- A, B, C and D are the control parameters defined in Table 3.2)

However, for higher w/b of 0.48 both the percentage and types of cement replacement material contribute almost equally to concrete strength. The parameter, namely the percentage of cement replacement contributes maximum to the strength i.e. 45.7% at higher w/b of 0.48, and its contribution decreases to 32.74% at lower w/b of 0.40. The parameters, namely the type of sand replacement and its percentage replacement contributes very little towards the strength of such concrete at all the water to binder ratios.

From the above discussion, it also confirmed the fact that fly ash as partial cement replacement contributes maximum towards strength at 90 day of curing and not at early age although fly ash is optimal parameter at early age also.

(c) Confirmation experiment to verify optimum mix-design proportions

The optimum mixes were designed using optimal parameters obtained by the Grey-Taguchi relational analysis. These optimal parameters were verified by conducting an experiment to verify whether the compressive and split tensile strength comes out to be maximum with the use of these optimal mixes. Same materials and the same conditions were used in the experiment for the comparison of the results. Twelve 150 mm cube samples and 150x300 mm size cylinders were cast as per the optimum mix design proportions derived from the Taguchi method. The compressive and split tensile strength tests were conducted to measure the results at 28 days using the related standards. Table 5.13 shows the measured results. It is observed that the mixture resulted in more compressive and split tensile strength than all other mixtures and control mixes. The verification experiment results showed that proposed optimal mix design proportions satisfied with maximum values for compressive & split tensile strength.

The optimum combination of control factors for confirmation experiment at curing age of 28

days and for all the w/b ratios is as given below.

- Percentage of replacement as binder-- 10 %
- Percentage of replacement as fine aggregate--30 %
- Type of replacement as binder---Fly ash
- Type of replacement as Fine aggregate--- Electric arc furnace slag

Table 5.13: Results of confirmation experiment at 28 days

Exp. No.	W/B ratio	Optimal Parameters	Optimal Parameters				Control Mix Results		Trial Mix Results	
			A	B	C	D	Compressive strength (MPa)	Split tensile strength (MPa)	Compressive strength (MPa)	Split tensile strength (MPa)
1	0.48	A1B2C1D1	10	30	FA	EAFS	42.06	3.45	47.15	3.46
2	0.44	A1B2C1D1	10	30	FA	EAFS	45.13	3.82	48.79	3.87
3	0.40	A1B2C1D1	10	30	FA	EAFS	51.05	4.47	54.15	4.48

(Note:- A, B, C and D are the control parameters defined in Table 3.2)

(d) SEM and XRD analysis to verify the results of the confirmation experiments

The SEM and XRD analysis was performed on the samples of the confirmation experiments to verify the results of the confirmation experiments and to evaluate the changes in the micro-structure of concrete with the addition of industrial by-products. Since the 1960s, SEM has been used for the micro-structural examination of concrete. The small pieces of control concrete and concrete containing by-products generated from compressive strength test were made to powder with grinding and then sieved through 90 μm sieve. The concrete specimens were coated with a thin layer of gold to make them electrically conductive before placing on the Scanning Electron Microscopy (SEM) stem. The testing was performed in accordance with ASTM-C1723-2010 for the collected samples. It was also used to understand changes in the strength and durability properties of such mixes. The SEM and XRD test was performed at 28 days of curing ages for the three w/b ratios i.e. 0.48, 0.44, & 0.40. From SEM images, significant amount of variations were found in the concrete microstructure with the addition of industrial by-products for all the water/binder ratios.

The SEM images of the control concrete at w/c ratios of 0.48, 0.44 & 0.40 at 28 days of curing are given in Fig.5.5 to Fig.5.7 respectively. The existence of calcium hydroxide (CH) and C-S-H gel is also shown in SEM images. SEM micrograph of optimal mix concrete

having 10% of fly ash as replacement of cement and 30% of electric arc furnace slag as sand replacement for w/b=0.48 at 28 days of curing period is presented in Fig. 5.8. Similarly Fig.5.9 shows the SEM micrograph of optimal mix concrete consisting 10% fly ash as replacement of cement and 30% electric arc furnace slag as sand replacement for w/b=0.40 at curing period of 28 days. The SEM images of the concrete having the optimal parameters of the industrial by-products were compared with the corresponding control concrete SEM image. The micro-structure of the concrete mixed with combination of industrial by-products show denser and more uniform structure than the control concrete structure. The strength properties of the concrete made with industrial by-products improved significantly than the control concrete as shown in Table 5.13. The improved strength and durability of concrete containing industrial by-products in ternary combinations could be due to the synergic effect of the industrial by-products and due to their pozzolanic and comentitious properties.

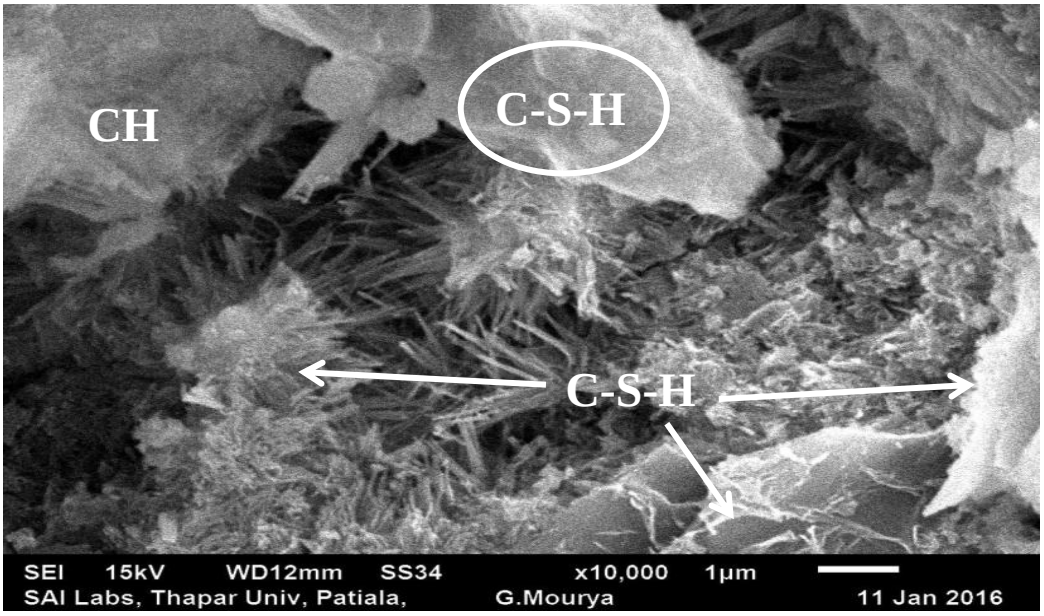

Fig.5.5: SEM of control concrete for w/c of 0.48 at 28 days curing age

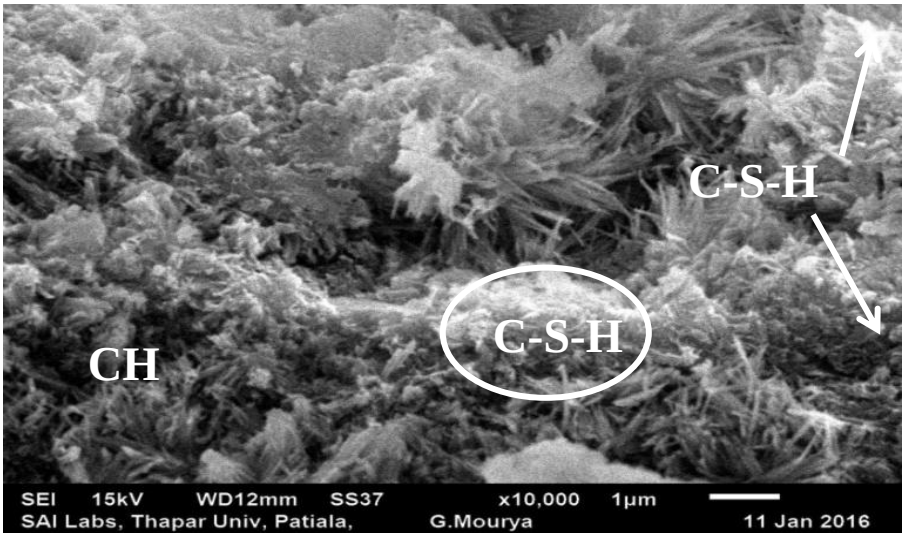

Fig. 5.6: SEM of control concrete for w/c of 0.44 at 28 days curing age

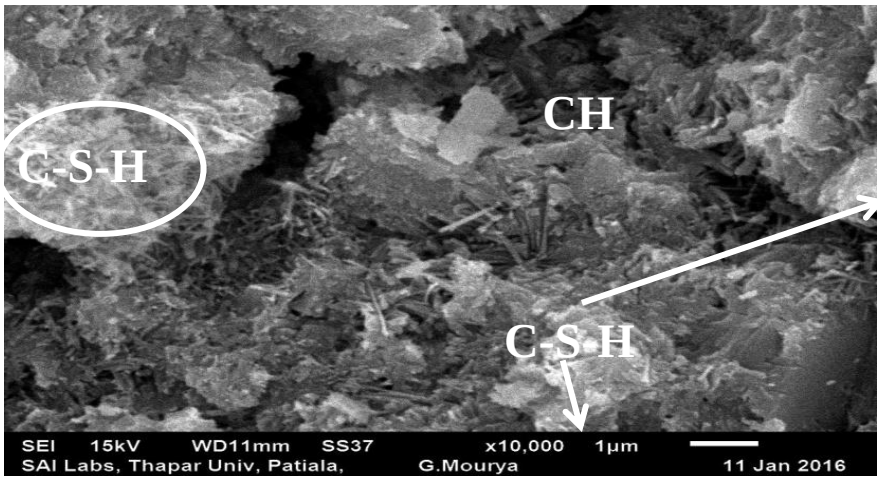

Fig. 5.7: SEM of control concrete for w/c of 0.40 at 28 days curing age

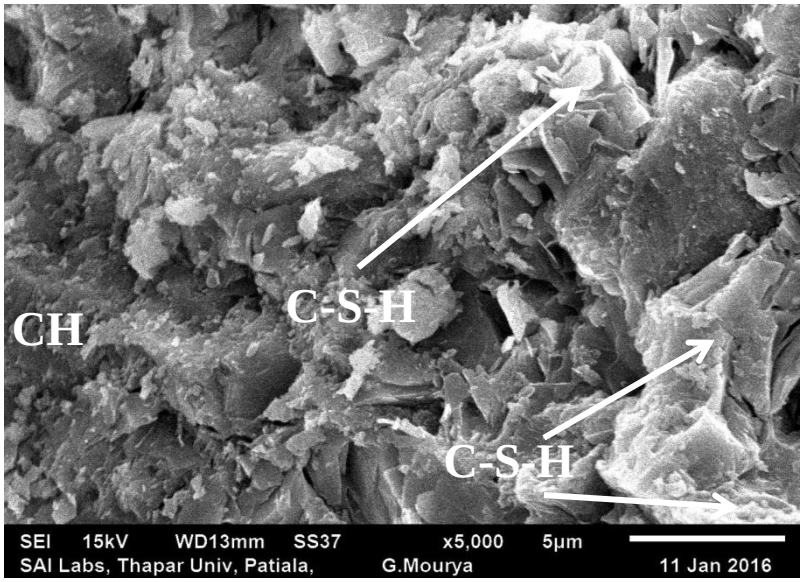

Fig. 5.8: SEM of optimal mix concrete consisting of 10% fly-ash and 30% electric arc furnace slag for w/b=0.48 at 28 days curing age

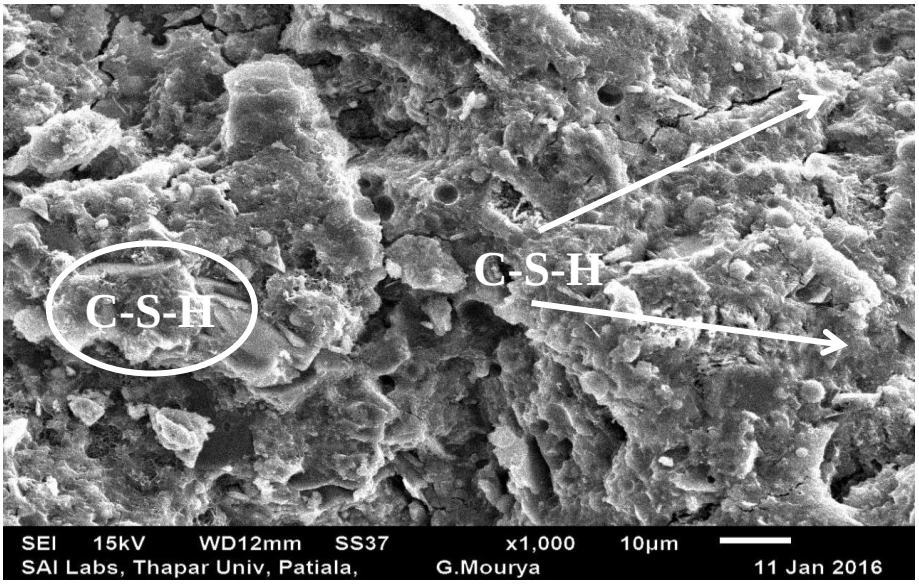

Fig. 5.9: SEM of optimal mix concrete which contains 10% fly-ash and 30% electric arc furnace slag for w/b=0.40 at curing age of 28 days

The X-ray diffraction (XRD) technique was also used to know various phases and compounds present in the concrete which contained industrial by-products and in standard concrete without by-products. The XRD was carried for diffraction angle of 2θ and the total range was between 5° and 80° to prepare the graph. The x-axis represents the angle 2θ and y-axis represents relative intensities. The diffraction peaks were shown for different compounds present in the sample. The comparison of these peaks was done with the peaks of standard compounds released by International Centre for Diffraction Data (ICDD).

The Fig. 5.10 to Fig.5.12 presents the XRD spectra of control concrete for water/cement=0.48, 0.44 & 0.40 respectively at 28 days of curing age. Similarly X-ray spectra of optimal mix concrete which contains 10% of fly ash as replacement of cement and 30% electric arc furnace slag as sand replacement for w/b=0.48 at 28 days of curing age and X-ray diffractogram of optimal mix concrete containing 10% fly-ash as cement replacement and 30% electric arc furnace slag as sand replacement for w/b=0.40 at 28 days curing age is displayed in Fig.5.13 and Fig.5.14 respectively.

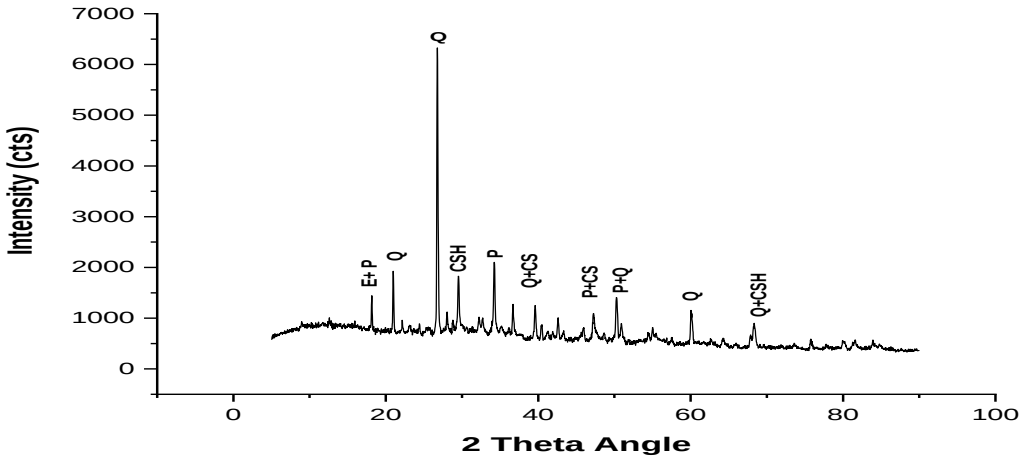

Fig.5.10: X-ray spectra of control concrete for w/c=0.48 at 28 days. (Note: CSH = Calcium Silicate Hydrates; E = Ettringites; CS = Calcium Silicate; P = Calcium hydroxide; Q = Quarts.)

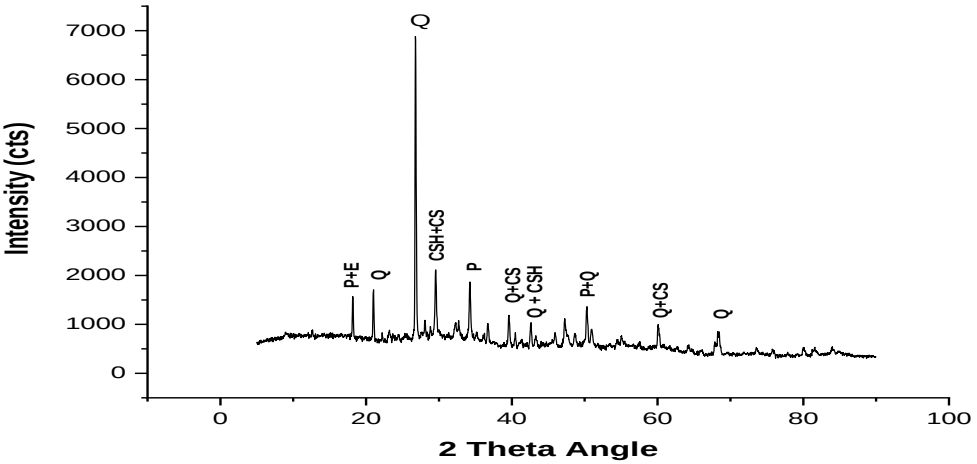

Fig.5.11: X-ray spectra of control concrete for w/c=0.44 at curing age of 28 days. (Note: CSH = Calcium Silicate Hydrates; E = Ettringites; CS = Calcium Silicate; P = Calcium hydroxide; Q = Quarts.)

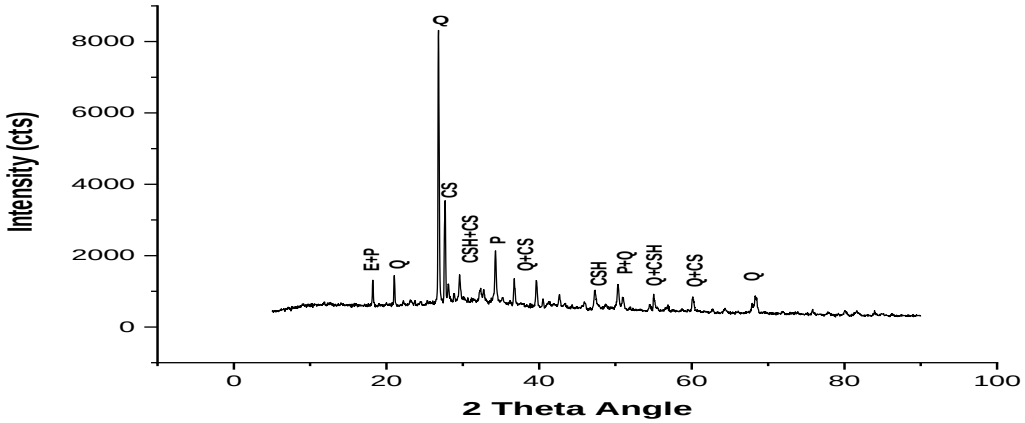

Fig. 5.12: X-ray spectra of control concrete for w/c=0.40 at 28 days of curing age. (Note: CSH = Calcium Silicate Hydrates; E = Ettringites; CS = Calcium Silicate; P = Calcium hydroxide; Q = Quarts.)

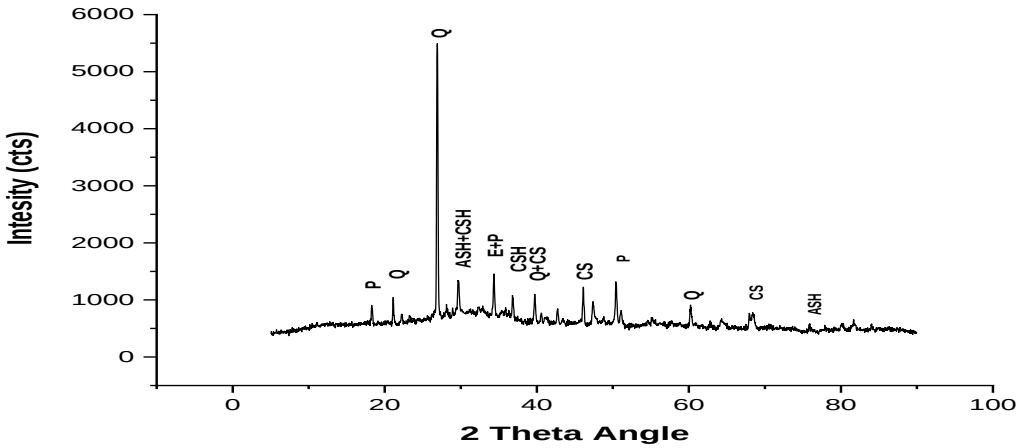

Fig. 5.13: X-ray diffractogram of optimal mix concrete which contains 10% of fly ash as replacement of cement and 30% electric arc furnace slag as sand replacement for w/b=0.48 at 28 days of curing age. (Note: CSH = Calcium Silicate Hydrates; E = Ettringites; CS = Calcium Silicate; P = Calcium hydroxide; Q = Quarts; ASH = Aluminium silicate hydrate)

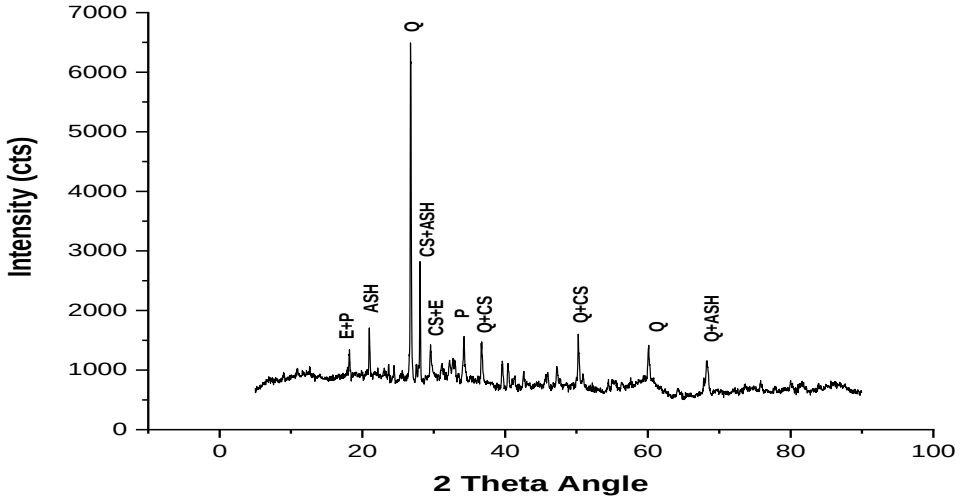

Fig.5.14: X-ray spectra of optimal mix concrete which contains 10% fly-ash as replacement of cement and 30% electric arc furnace slag as sand replacement for w/b=0.40 at 28 days 0f curing age. (Note: CSH = Calcium Silicate Hydrates; E = Ettringites; CS = Calcium Silicate; P = Calcium hydroxide; Q = Quarts; ASH = Aluminium silicate hydrate)

The XRD spectra shows the existence of hydrated phases of compounds such as quartz, $Ca(OH)_2$, CSH, CS, ettringites and aluminium oxide silicate. XRD analysis also show that the concrete mixture containing industrial by-products has smaller quantity of Ca $(OH)_2$ (calcium hydroxide) than in the control mix at curing of 28 days as shown in the Table 5.14. The industrial by-products present in the concrete mix consumed Ca $(OH)_2$ by their pozzolanic reaction and thus, converted this into calcium silicate hydrate gel (CSH gel) which lends strength and durability to the concrete. This fact helps to improve the strength and durability of concrete containing partial replacement of cement and sand than the control concrete.

Table 5.14: Quantity of calcium hydroxide in specimens of control concrete and the concrete containing industrial by-products at 28 days

S. No.	Type of Mix	Quantity of Ca $(OH)_2$ (%)
1	Control concrete for w/c= o.48	6
2	Control concrete for w/c= o.40	5
3	Concrete having 10% fly-ash as cement replacement and 30% electric arc furnace slag as sand replacement for w/b=0.48	3
4	Concrete having10% fly-ash as cement replacement and 30% electric arc furnace slag as sand replacement for w/b=0.40	2

5.3 GREY RELATIONAL ANALYSIS FOR DURABILITY PROPERTIES

The nine sets of experiments were carried out for each w/b ratios of 0.48, 0.44 & 0.40 and for each curing age of 7, 28 & 90 days to find the depth of water penetration and depth of wear, however, the detailed calculations for one set of nine experiments, i.e. for w/b=0.40 and curing period of 90 days has only been presented here. The optimal parameters are found with these detailed calculations. The optimal parameters for all other combinations of experiments for water/binder ratios and curing ages are found in the similar manner. Table 5.15 gives the experimental layout and results of compressive and split tensile strength for w/b=0.40 and for curing period of 90 days.

5.3.1 Data Normalization

The data was pre-processed to normalise the values in order to bring it to dimensionless quantities. Here the depth of wear and water penetration depth are "lower-the-better" properties of the concrete. For the "lower-the-better "characteristics, the original data can be normalized by Eqn. (5.5).

$$X_i^*(k) = \frac{maxX_i(k) - X_i(k)}{maxX_i(k) - minX_i(k)} \quad \text{(5.5)}$$

Where, $X_i(k)$ and X_i^*(k) are the comparability sequence and sequence after the data normalisation respectively and k=1 and 2 for depth of wear and depth of water penetration respectively; i=1, 2, 3…... 9 for experiment numbers 1 to 9. All the sequences after data pre-processing using Eqn. (5.5) are presented in Table 5.16.

Table 5.15: Experimental layout using an L_9 OA and performance results (For w/c= 0.40 and curing period=90 days)

Expt No.	Levels of parameters				Depth of Wear (mm)	Depth of Water Penetration (mm)
	Parameter [A]	Parameter [B]	Parameter [C]	Parameter [D]		
1	10%	20%	FA	EAFS	0.224	20
2	10%	30%	LFS	IS	0.312	15
3	10%	40%	CS	GP	0.314	15
4	25%	20%	LFS	GP	0.234	22
5	25%	30%	CS	EAFS	0.24	32
6	25%	40%	FA	IS	0.275	17
7	40%	20%	CS	IS	0.289	40
8	40%	30%	FA	GP	0.285	20
9	40%	40%	LFS	EAFS	0.33	17

(Note:- A, B, C and D are the control parameters defined in Table 3.2)

Table 5.16: The sequences of each response after data normalisation

Expt. No.	Depth of Wear	Depth of Water Penetration
Reference Sequence	**1.0000**	**1.0000**
1	1.0000	0.8000
2	0.1698	1.0000
3	0.1509	1.0000
4	0.9056	0.7200
5	0.8490	0.3200
6	0.5188	0.9200
7	0.3867	0.0000
8	0.4245	0.8000
9	0.0000	0.9200

The value of the deviation sequence $\Delta_{0i}(k)$ is calculated using the expression as shown in Eqn. (5.6).

$$\Delta_{0i}(k) = |x_0^*(k) - x_i^*(k)| \quad ---------- \quad (5.6)$$

Where $x_i^*(k)$ is the comparability sequence and $x_0^*(k)$ is the reference sequence. The results of all Δ_{0i} for i = 1 to 9 are presented in Table 5.17.

Table 5.17: The Deviation Sequences of the responses

Comparability Sequence	Reference Sequence	
	Depth of Wear	**Depth of Water Penetration**
Exp. No.	**1.0000**	**1.0000**
1	0.0000	0.2000
2	0.8301	0.0000
3	0.8490	0.0000
4	0.0943	0.2800
5	0.1509	0.6800
6	0.4811	0.0800
7	0.6132	1.0000
8	0.5754	0.2000
9	1.0000	0.0800

5.3.2 Computing the Grey Relational Coefficients

The Grey relational coefficients for all the experiments of the L_9 OA can be calculated using Eqn. (5.7).

$$\zeta_i(k) = \frac{\Delta_{min} + \zeta\Delta_{max}}{\Delta_{0i}(k) + \zeta\Delta_{max}} \quad - - - - - - - - - - - - - \quad (5.7)$$

Where $\Delta_{0i}(k)$ = the deviation sequence among reference sequence $x_0^*(k)$ and comparability sequence $x_i^*(k)$, and ζ = is the identification coefficient and its value is taken as 0.5 *(Deng, 1989)*. The Grey relational coefficients are given in Table 5.18.

Table 5.18: Grey relational coefficients and GRG

TRIAL NO.	GREY RELATIONAL COEFFICIENTS		GREY RELATIONAL GRADE ϒ;=½(ζ;(1)+ζ;(2))	RANK
	Depth of Wear	Depth of Water Penetration		
	ζ;(1)	ζ;(2)		
1	1.0000	0.7142	0.8571	1
2	0.3758	1.0000	0.6879	3
3	0.3706	1.0000	0.6853	5
4	0.8412	0.6410	0.7411	2
5	0.7681	0.4237	0.5959	7
6	0.5096	0.8620	0.6858	4
7	0.4491	0.3333	0.3912	9
8	0.4649	0.7142	0.5896	8
9	0.3333	0.8620	0.5977	6

The grey relational grade (GRG) is calculated by taking mean value of the grey relational coefficients related to each response and is calculated from the Eqn. (5.8).

$\Upsilon; = \frac{1}{n}\sum \zeta;(k)$ ---------- (5.8)

Where ϒ; the GRG for the i_{th} experiment and n is the number of responses. Here the value of n is 2. The GRG for each experiment using L9 OA is also given in Table 5.18. If the value of the GRG is higher than it indicates that the experimental value is near to the normalized value

and vice versa. So in this case experiment 1 is having best multiple response value than all other nine experiments because it has the highest GRG.

Thus, it can be derived that in the GRA, the optimization of the multiple responses of concrete has been converted into the optimization of one GRG only.

Due to the orthogonality of the design, it is possible to find out the effect of each individual factor on the GRG at each level. The mean of the GRG for each level of the factors/parameters is shown in the response Table 5.19.

Table 5.19: Response table of the GRG

Symbol	Parameter	Grey Relational Grade			Main effect (max-min)	Order
		Levels				
		1	2	3		
A	By-Product Used as Binder (%)	0.7435*	0.6743	0.5262	0.2173	1
B	By-Product Used as FA (%)	0.6632*	0.6245	0.6563	0.0387	4
C	Type of By-Product used as Binder	0.7109*	0.6756	0.5575	0.1534	2
D	Type of By-Product used as FA	0.6836*	0.5883	0.6720	0.0952	3
Optimal Paratmeters = A1 B1 C1 D1						

Basically, a larger value of the GRG shows that it is more close to its ideal value. Thus, we require a larger GRG for optimum response value. Therefore, the optimal parameters for abrasion resistance and water permeability are A1 B1 C1 D1 as presented in Table 5.19. So the optimal parameters are quantity of by-product used as binder(%) at level 1, quantity of by-product as fine aggregate (%) at level 1, type of by-product as binder at level 1 and type of by-product as fine aggregate at level 1.

The GRG were analysed with ANOVA to find out the contribution of each factor affecting the depth of wear for abrasion strength and depth of water penetration for water permeability.

5.3.3 Analysis of Variance (ANOVA)

With ANOVA technique, we can find which parameter mostly affects the responses. ANOVA analysis for GRG is shown in Table 5.20. The %age contribution of each factor is shown in Fig. 5.15. The figure clearly reveals that the percentage of by-product used as binder is the parameter which contributes maximum in improving abrasion strength as well as water permeability of the resulting concrete.

Table 5.20: ANOVA table for GRG

Factor/Parameter	DOF	SS	MS	PC
[A] By-Product Used as Binder (%)	2	0.0739	0.0370	56.26
[B] By-Product Used as FA (%)	2	0.0026	0.0013	1.94
[C] Type of By-Product used as Binder	2	0.0387	0.0194	29.46
[D] Type of By-Product used as FA	2	0.0162	0.0081	12.33
TOTAL	**8**	**0.1314**	**0.0657**	**100.00**

(Note:- DOF-Degrees of freedom; SS- Sum of Squares; MS-Mean sum of squares; PC-Percentage Contribution)

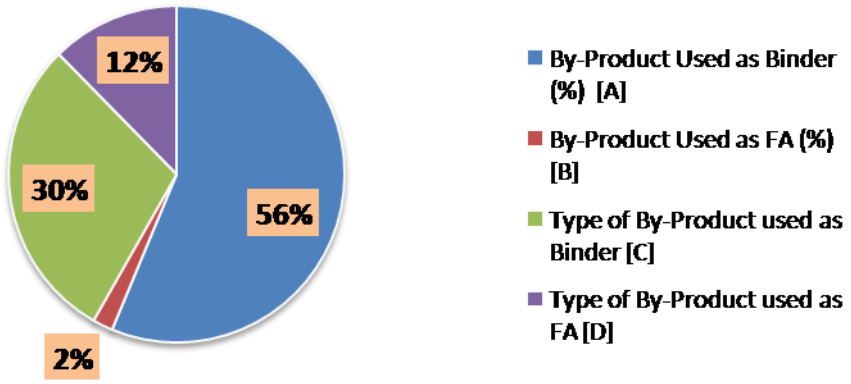

Fig. 5.15: Percentage contributions of each factor towards durability properties

The results of Grey relational analysis for all other combinations of w/b ratios and curing periods were performed in a similar manner as above.

5.3.4 Results and Discussion

The GRA for all the combinations of w/b ratios of 0.48, 0.44 & 0.40 and curing ages of 7, 28 & 90 days were performed in the similar manner. The optimal parameters for durability properties is shown in Tables 5.21 to 5.23 and their contribution towards durability is shown in tables 5.24 to 5.26 for 7, 28 & 90 days of curing periods respectively. The effect of curing age on optimal mix design parameters and the percentage contribution towards the durability of various optimal parameters at different curing periods is discussed below:

(a) Effect of curing period on optimal mix design parameters

- At curing period of 7 days (i.e. at an early age)

It is observed from the Table 5.21 that at 7 days curing, for all water-binder ratios, replacement of cement by copper slag gives the optimal result. Whereas replacement of sand with glass powder provides the optimal results for better durability at all w/b ratios.

Table 5.21: Optimal parameters for durability properties at 7 days of curing

Exp. No.	W/B ratio	Optimal Parameters	Optimal Parameters			
			A	B	C	D
1.	0.48	A2B1C3D3	25	20	Copper Slag	Glass Powder
2.	0.44	A2B1C3D3	25	20	Copper Slag	Glass Powder
3.	0.4	A1B1C3D3	10	20	Copper Slag	Glass Powder

(Note:- A, B, C and D are the control parameters defined in Table 3.2)

Also, it is observed that for 0.48 & 0.44 water/binder ratios, 25% is optimum %age of cement replacement with copper slag contributing to better durability at early ages, whereas 10% of cement replacement with copper slag at 0.40 w/b ratio contributes positively to durability at an early age. For the sand replacement by glass powder, 20% is the optimum percentage replacement at all w/b ratios. Thus, it could be concluded that at early ages, the cement replacement material and its percentage replacement remains constant at higher water/binder ratios, whereas, for the replacement of sand, the type of material and its percentage

replacement remains constant at all w/b ratios.

- At 28 days of curing period (i.e. at normal age)

On observing the tabulated analysis results given in Table 5.22 at 28 days curing, for higher water to binder ratios, we see that the replacement of cement with copper slag gives the optimal result, and for lower water-binder ratio cement replacement by fly ash gives the optimal result than other materials whereas, on the other hand, sand replacement by iron slag gives the optimal result at higher water-binder ratio and by glass powder at lower water-binder ratio.

Table 5.22: Optimal parameters for durability properties at 28 days of curing

Exp. No.	W/B ratio	Optimal Parameters	Optimal Parameters			
			A	B	C	D
1.	0.48	A2B3C3D2	25	40	Copper Slag	Iron Slag
2.	0.44	A1B1C2D1	10	20	Ladle Furnace Slag	Electric Arc Furnace Slag
3.	0.4	A1B1C1D3	10	20	Fly-ash	Glass Powder(GP)

(Note:- A, B, C and D are the control parameters defined in Table 3.2)

Also, it is observer that for higher water/binder ratio, 25% is optimal %age of replacement of cement with copper slag contributing to better durability at a normal age, whereas 40% of sand replacement by iron slag provides the optimal strength results. Thus, it can be concluded that at a normal age, curing of 28 days, the percentage replacement values for both cement and sand changes from 25% to 10% and from 40% to 20% respectively from higher to lower w/b ratios whereas the replacement material also changes from higher water-binder ratio to lower water to binder ratio for both cement and sand.

- At curing period of 90 days

On analyzing the results at 90 days curing given in Table 5.23, for higher water/ binder ratio, it is observed that cement replacement by copper slag gives optimal result and for lower water-binder ratio, cement replacement by fly ash gives the optimal values for durability properties.

Table 5.23: Optimal parameters for durability properties at 90 days of curing

Exp. No.	W/B ratio	Optimal Parameters	Optimal Parameters			
			A	B	C	D
1.	0.48	A1B2C3D3	10	30	Copper Slag	Glass Powder
2.	0.44	A1B1C2D3	10	20	Ladle Furnace Slag	Glass Powder
3.	0.4	A1B1C1D1	10	20	Fly-ash	EAFS

(Note:- A, B, C and D are the control parameters defined in Table 3.2)

Whereas, the glass powder replacement for sand provides the optimal strength results only for higher w/b ratios of 0.48 & 0.44, however, at lower w/b of 0.40, EAFS as a replacement for sand provides better results. Also, it is seen that for all water binder ratios, 10% is the optimal %age of binder replacement material contributing to better durability, whereas 30% of sand replacement by glass powder at w/b ratio of 0.48 contributes positively to durability. For lower w/b ratios, 20% of sand replacement by electric arc furnace slag provides the optimal durability properties. Thus, it is concluded that at 90 days, the percentage replacement for cement i.e. 10% remains constant at all water binder ratios, whereas, for the replacement of sand, the type of material and its percentage replacement remains constant (i.e. 30% of glass powder) at higher water/binder ratios of 0.48. However, it changes to 20% electric arc furnace slag only at lower w/b of 0.40.

From the discussion given above, it is found that 25% of the copper slag is the optimal parameters for cement replacement for durability properties at 7 & 28 days of curing ages and at all water to binder ratios. But at 90 days of curing, 10 % copper slag, 10% ladle furnace slag and 10% fly ash are the optimal parameters at water to binder ratios of 0.48, 0.44 & 0.40 respectively. Similarly 20% glass powder is the optimal replacement level of sand for all the water binder ratios and at 7 days of curing age. The optimal parameter for sand replacement material changes from glass powder at 7 days curing to electric arc furnace slag at 90 days curing.

(b) Percentage contribution towards the durability of various optimal parameters at different curing periods

The results indicating the percentage contribution of optimal parameters towards concrete durability are tabulated in Tables 5.24 to 5.26. The effect at different curing ages is presented below:

➢ At curing period of 7 days (i.e. at an early age)

At curing age of 7 days (See Table 5.24), for higher water/binder ratios, 25% of by-product to be used as partial cement replacement is the optimal parameter which contributes maximum towards the durability of the resulting concrete. It is observed that its contribution is maximum at lower water/binder ratio of 0.44, i.e. 48.19% and it decreases to 33.62% as the water/binder is increased to 0.48.

Table 5.24: Percentage contribution of various optimal parameters at 7 days curing

Exp. No.	W/B ratio	Optimal Parameters	Optimal Parameters				Rank				% Contribution			
			A	B	C	D	A	B	C	D	A	B	C	D
1	0.48	A2B1C3D3	25	20	CS	GP	1	2	3	4	33.62	32.91	27.987	5.48
2	0.44	A2B1C3D3	25	20	CS	GP	1	3	2	4	48.19	18.62	22.53	10.66
3	0.4	A1B1C3D3	10	20	CS	GP	3	4	1	2	28.53	4.66	36.23	30.58

(Note:- A, B, C and D are the control parameters defined in Table 3.2)

Also, at higher water/binder ratios, contribution of %age of sand replacement material towards concrete durability, (i.e. 20%) starts increasing, which is 32.91% at w/b of 0.48. The type of cement replacement material, as can be seen from the Table 5.23, contributes very little and almost remains constant at all the water/binder ratios, whereas the type of replacement as sand does play a slightly better role only for lower w/b ratios.

➢ At curing period of 28 days

At curing of 28 days (See Table 5.25), for all water/binder ratios, the percentage of cement replacement material contributes the most towards the concrete durability. As can be observed from the Table 5.25, 10% of cement replacement material contributes maximum of 73.48% at w/b of 0.40 whereas, its value is 69.12% at w/b of 0.44.

Table 5.25: Percentage contribution of various optimal parameters at 28 days curing

Exp. No.	W/B ratio	Optimal Parameters	Optimal Parameters				Rank				% Contribution			
			A	B	C	D	A	B	C	D	A	B	C	D
4	0.48	A2B3C3D2	25	40	CS	IS	1	4	3	2	58.65	2.76	14.95	23.63
5	0.44	A1B1C2D1	10	20	LFS	EAFS	1	2	3	4	69.12	21.52	7.09	2.26
6	0.4	A1B1C1D3	10	20	FA	GP	1	2	3	4	73.48	22.67	2.16	1.69

(Note:- A, B, C and D are the control parameters defined in Table 3.2)

The percentage contribution of fly ash towards durability is 2.16% at w/b of 0.40; whereas, the percentage contribution of copper slag is 14.95% at higher w/b of 0.48. The percentage contribution of parameters, namely the %age of sand replacement contributes very little at all the water binder ratios, whereas the type of sand replacement material does play a slightly better role at higher water to binder ratio of 0.48.

- At curing period of 90 days

At 90 days (See Table 5.26), for all water binder ratios, the %age of material for cement replacement contributes the most towards the concrete durability and its contribution is maximum at 56.63% for w/b of 0.48. But, for lower w/b of 0.44, both the percentage of sand replacement and types of sand replacement material contribute almost equally to concrete durability.

Table 5.26: Percentage contribution of various optimal parameters at 90 days curing

Exp. No.	W/B ratio	Optimal Parameters	Optimal Parameters				Rank				% Contribution			
			A	B	C	D	A	B	C	D	A	B	C	D
1.	0.48	A1B2C3D3	10	30	CS	GP	1	4	2	3	56.63	10.68	21.35	11.34
2.	0.44	A1B1C2D3	10	20	LFS	GP	1	4	3	2	41.93	15.86	16.33	25.88
3.	0.4	A1B1C1D1	10	20	FA	EAFS	1	4	2	3	56.26	1.94	29.46	12.33

(Note:- A, B, C and D are the control parameters defined in Table 3.2)

The parameter, namely the type of cement replacement material contributes 29.46% at lower w/b of 0.40, and its contribution decreases to 21.35% at higher w/b of 0.48. The percentage contribution of parameters, namely the percentage of sand replacement contributes very little at all the water binder ratios, whereas the type of replacement as sand does play a slightly better role for all water/binder ratios.

From the discussion given above, it is found that percentage of by-product as cement replacement material and not the type of by-product as cement replacement as in case of strength properties, is the optimal parameter which contributes maximum to enhance the durability properties of concrete.

(c) Confirmation experiment to verify optimum mix-design proportions

Optimal mix-design proportions found using the Grey-Taguchi relational analysis was

verified by conducting an experiment to check whether the depth of wear and depth of water penetration can really be minimised by the proposed optimum mix design proportions. Same materials and the same conditions were used in the experiment to compare the results. Twelve 150 mm cube samples and 150x300 mm size cylinders were cast according to the experiments designed as per Taguchi method with optimal mix proportions. These specimens were tested for depth of wear and depth of water penetration at 90 days. The results are tabulated in Table 5.27, and it is seen that the mixture resulted in less depth of wear and water penetration depth than all other mixes and control mixes. The results of the verification study showed that the optimal mix proportions resulted the maximization for abrasion strength and minimisation of water permeability. The SEM and XRD tests were also performed on the samples of confirmation experiments to verify these results.

The optimum combination of control factors for confirmation experiment at 90 days of curing period and for w/b ratios of 0.40 is as given below.

(1) Percentage of by-product to be used as cement replacement --10 %

(2) Percentage of by-product to be used as fine aggregate replacement --20 %

(3) Type of replacement as binder---Fly Ash

(4) Type of replacement as Fine aggregate---Electric arc furnace slag

Table 5.27 Results of the confirmation experiment at 90 days of curing age.

Exp. No.	W/B ratio	Optimal Parameters	Optimal Parameters				Control Mix Results		Trial Mix Results	
			A	B	C	D	Depth of water penetration (mm)	Depth of wear (mm)	Depth of water penetration (mm)	Depth of wear (mm)
1	0.48	A1B2C3D3	10	30	CS	GP	27	0.368	18	0.303
2	0.44	A1B1C2D3	10	20	LFS	GP	18	0.330	15	0.212
3	0.40	A1B1C1D1	10	20	FA	EAFS	11	0.318	11	0.201

(Note:- A, B, C and D are the control parameters defined in Table 3.2)

(d) SEM and XRD analysis to verify the results of the confirmation experiments

The SEM and XRD analysis was performed on the samples of the confirmation experiments to verify the results of the confirmation experiments for durability properties and to evaluate the modifications in the micro-structure of concrete with the addition of industrial by-

products. The small pieces of control concrete and concrete containing by-products generated from compressive strength test were made to powder with grinding and then sieved through 90 μm sieve. The concrete specimens were coated with a thin layer of gold to make them electrically conductive before placing on the Scanning Electron Microscopy (SEM) stem. The testing was performed in accordance with ASTM-C1723-2010 for the collected samples. It was also used to understand changes in the strength and durability properties of such mixes. The SEM and XRD tests were carried at 90 days of curing ages for the three water to binder ratios i.e. 0.48, 0.44, & 0.40. From SEM images, significant amount of variations were found in the concrete microstructure with the addition of industrial by-products for all the water/binder ratios.

The SEM images of the control concrete at water to cement ratio of 0.48 & 0.40 and at 90 days of curing are given in Fig.5.16 and Fig.5.17. The existence of calcium hydroxide (CH) and C-S-H gel is also shown in SEM images. SEM micrograph of optimal mix concrete containing 10% copper slag as replacement of cement and 30% glass powder as replacement of sand for w/b=0.48 at 90 days curing age is displayed in Fig. 5.18. The Fig. 5.19 displays the SEM micrograph of optimal mix concrete containing 10% LFS as replacement of cement and 20% glass powder as replacement of sand for w/b=0.44 at 90 days of curing period. Similarly Fig.5.20 shows the SEM micrograph of trial mix concrete which contains 10% of fly ash as cement substitution and 20% electric arc furnace slag as sand replacement for w/b=0.40 at 90 days of curing age. The SEM images of the concrete containing the optimal parameters of the industry by-products were compared with the corresponding control concrete SEM image. The micro-structure of the concrete made with combination of industrial by-products show denser and more uniform structure than the control concrete structure. This confirms the improvement in durability properties of concrete made with industrial by-products caused by their synergic effect and pozzolanic property.

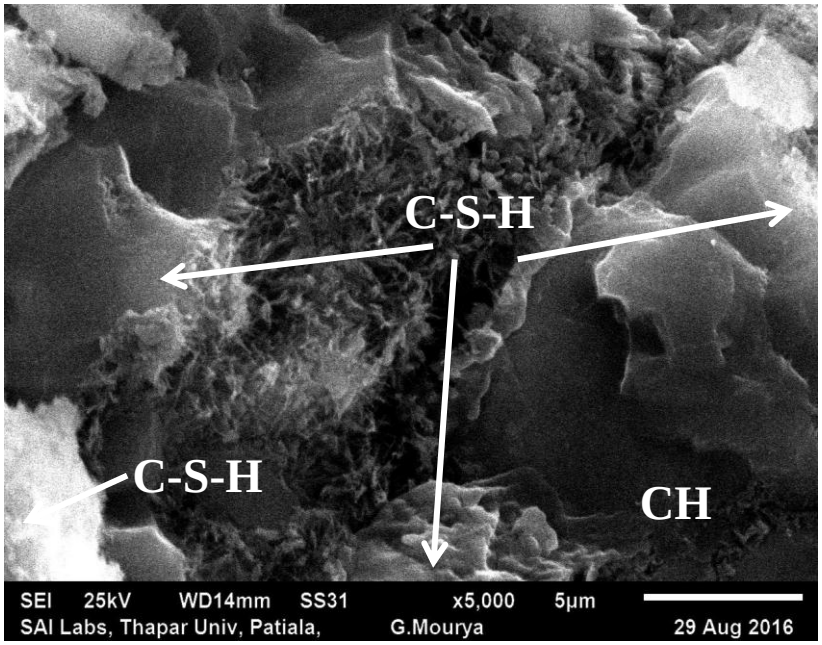

Fig. 5.16: SEM of control concrete for w/c=0.48 at 90 days curing age

Fig. 5.17: SEM of control concrete for w/c=0.40 at 90 days curing age

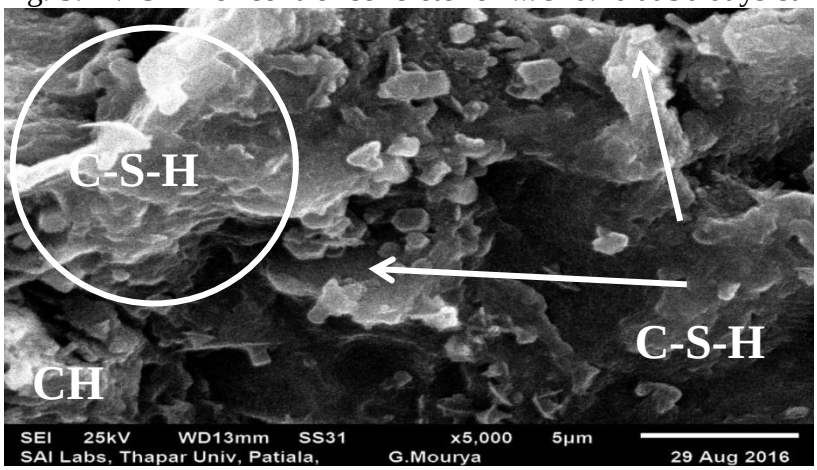

Fig. 5.18: SEM of optimal mix concrete containing 10% copper slag as replacement of cement and 30% glass powder as replacement of sand for w/b=0.48 at 90 days curing age

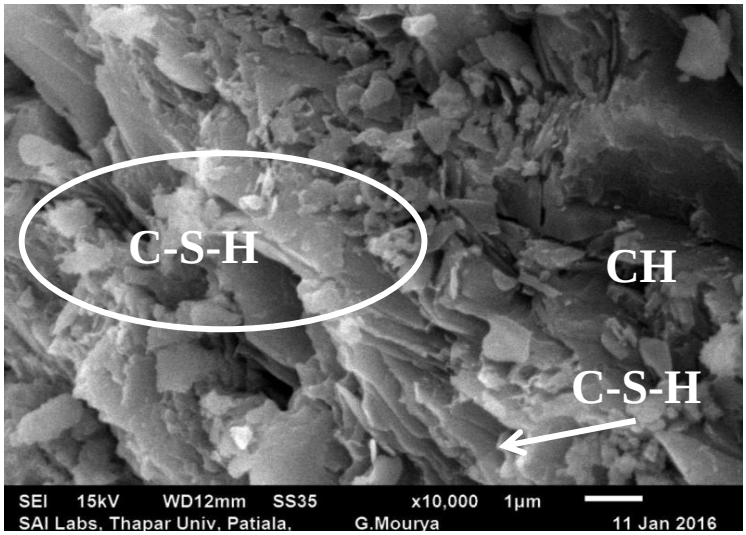

Fig.5.19: SEM of optimal mix concrete containing 10% LFS as replacement of cement and 20% glass powder as replacement of sand for w/b=0.44 at 90 days curing age

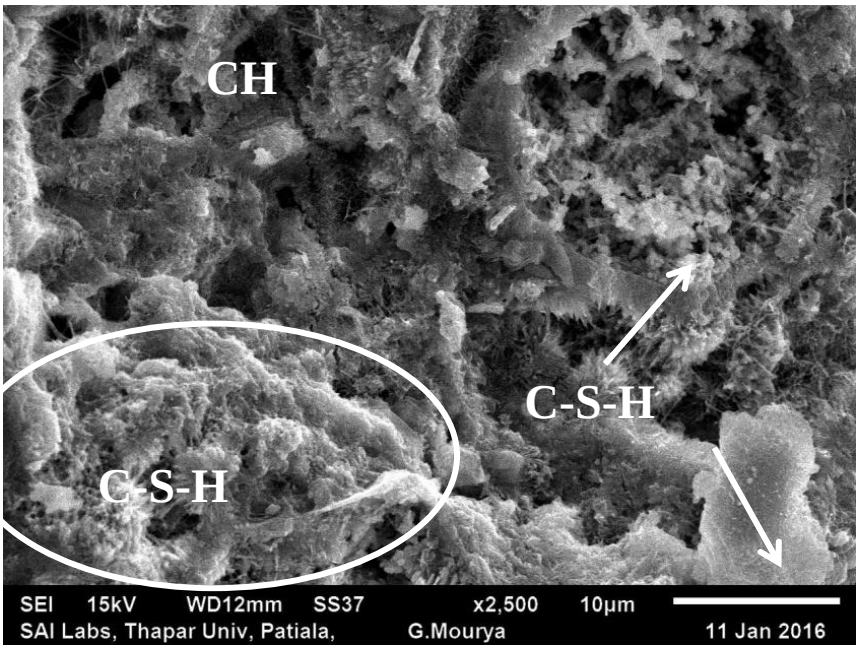

Fig. 5.20: SEM of trial mix concrete consisting of 10% fly-ash as cement replacement and 20% electric arc furnace slag as sand replacement for w/b=0.40 at 90 days of age.

The X-ray diffraction (XRD) technique was also used to know different phases and compounds exist in the concrete which contained industrial by-products and in standard concrete without by-products. The XRD was carried for diffraction angle of 2θ and the total range was between 5° and 80° to prepare the graph. The x-axis represents the angle 2θ and y-axis represents relative intensities. The diffraction peaks were shown for different compounds present in the sample. The comparison of these peaks was done with the peaks of standard compounds released by ICDD.

The Fig. 5.21 and Fig.5.22 shows the XRD spectra of the control concrete for w/c=0.48 and 0.40 respectively at 90 days of curing age. Similarly the XRD spectra of optimal mix concrete containing 10% copper slag as binder replacement and 30% glass powder as fine aggregate replacement for w/b=0.48 at 90 days curing age and XRD spectra of optimal mix concrete which contains 10% fly-ash as cement replacement and 20% electric arc furnace slag as sand replacement for w/b=0.40 at 90 days curing age is displayed in Fig.5.23 and Fig.5.24, respectively.

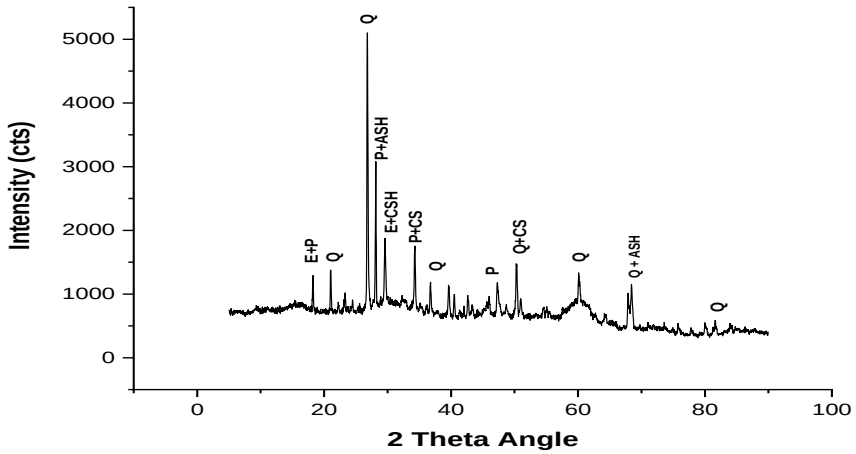

Fig.5.21: X-ray spectra of control concrete for w/c=0.48 at 90 days of curing age. (Note: CSH = Calcium silicate hydrates; E = Ettringites; CS = Calcium silicate; P = Calcium hydroxide; Q = Quarts; ASH = Aluminium silicate hydrate)

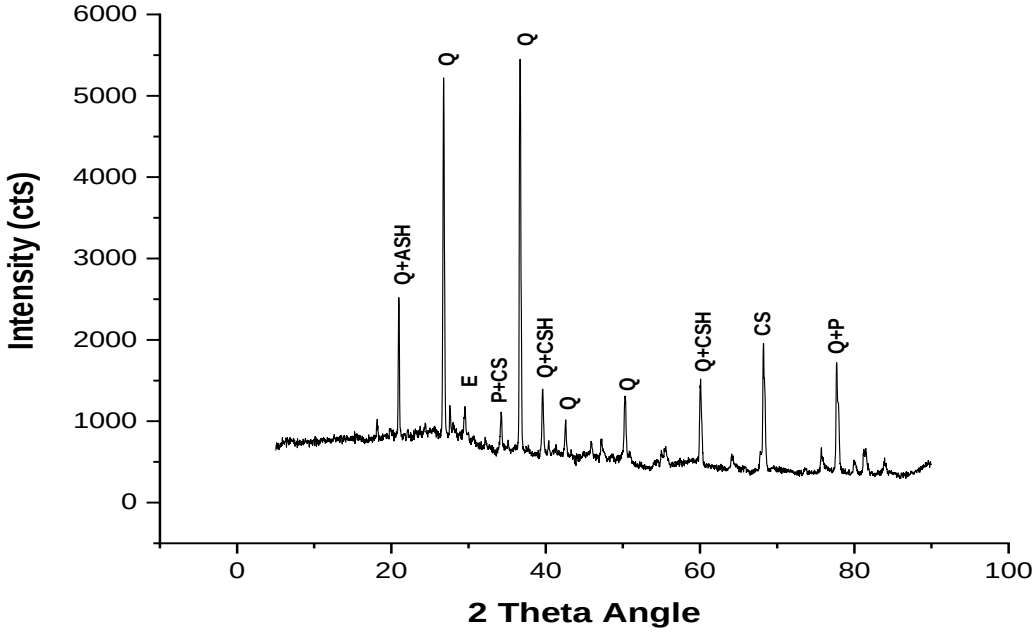

Fig. 5.22: X-ray spectra of control concrete for w/c=0.40 at 90 days of curing age. (Note: CSH = Calcium silicate hydrates; E = Ettringites; CS = Calcium silicate; P = Calcium hydroxide; Q = Quarts; ASH = Aluminium silicate hydrate)

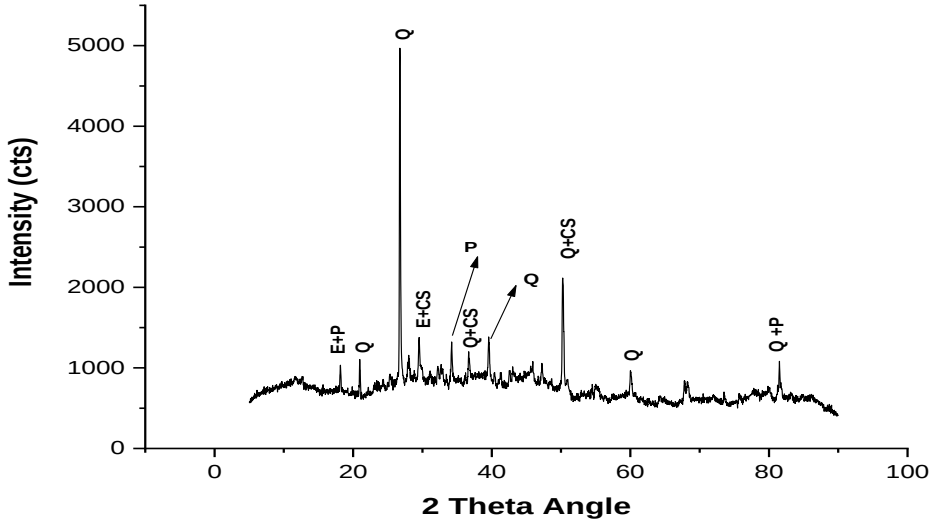

Fig. 5.23: X-ray spectra of optimal mix concrete containing 10% copper slag as replacement of cement and 30% glass powder as replacement of sand for w/b=0.48 at 90 days of curing period. (Note: CSH = Calcium silicate hydrates; E = Ettringites; CS = Calcium silicate; P = Calcium hydroxide; Q = Quarts; ASH = Aluminium silicate hydrate)

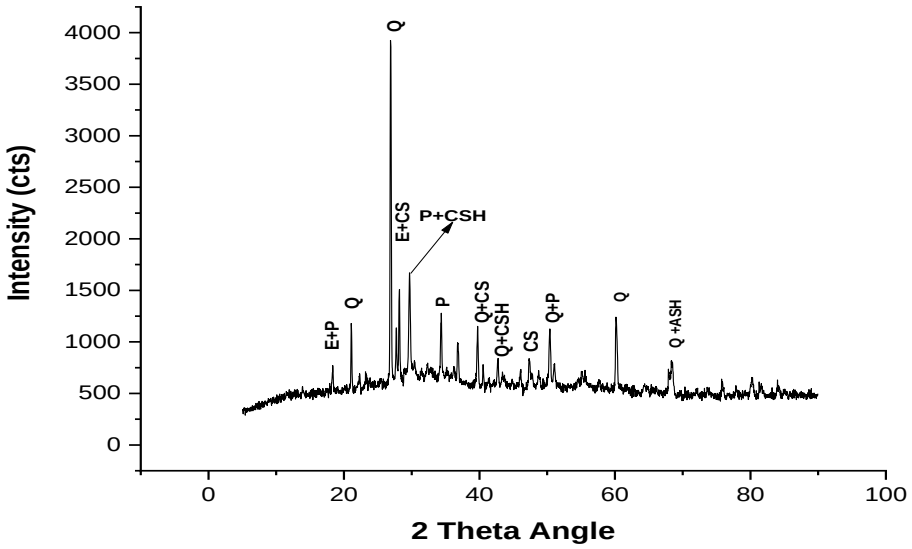

Fig.5.24: X-ray spectra of optimal mix concrete which contains 10% fly ash as replacement of cement and 20% electric arc furnace slag as replacement of sand for w/b=0.40 at 90 days of curing age. (Note: CSH = Calcium silicate hydrates; E = Ettringites; CS = Calcium silicate; P = Calcium hydroxide; Q = Quarts; ASH = Aluminium silicate hydrate)

The XRD spectra shows the existence of hydrated phases such as quartz, calcium hydroxide ($Ca(OH)_2$), calcium silicate hydrates (CSH), calcium silicate (CS), ettringites and aluminium oxide silicate. The XRD and EDS analysis also show that the concrete mixture containing industrial by-products has less quantity of calcium hydroxide $Ca(OH)_2$ than the control mix at 90 days of curing period as presented in Table 5.28. The quantity of $Ca(OH)_2$ present in the mix containing industrial by-products has been decreased by the pozzolanic reaction of the different by-products and thus converted this into calcium silicate hydrate gel (CSH gel) which is primarily responsible for the strength and durability of the concrete. This fact confirmed the enhancement taken place in strength and durability of concrete containing industrial by-products as partial replacement of cement and sand than in the control concrete.

Table 5.28: Quantity of calcium hydroxide in specimens of control concrete and the concrete consisting industrial by-products at 90 days

S. No.	Type of Concrete Mix	% Quantity of Ca $(OH)_2$
1	Control mix at w/c= 0.48	3
2	Control mix at w/c= 0.40	2
3	Concrete containing 10% copper slag as cement replacement and 30% glass powder as sand replacement for w/b=0.48	1
4	Concrete containing 10% fly ash as cement replacement and 20% electric arc furnace slag as sand replacement for w/b=0.40	1

5.4 MULTI RESPONSE OPTIMIZATION USING GRA FOR STRENGTH AND DURABILITY PROPERTIES TAKEN TOGETHER

In this study, GRA was used to optimize the strength as well as durability properties taken together. The strength properties include split tensile and compressive strength whereas durability properties include depth of water penetration for water permeability and wear depth for abrasion strength. The best possible levels of replacement of binder and fine aggregates in mix proportions were investigated for strength properties to be maximum and durability properties to be minimum using the Taguchi based Grey relational analysis (GRA). The performance statistics of "the larger the better" situations are found for maximisation of the strength properties of concrete and “the smaller the better” situations are found for minimisation of durability properties of concrete. For detailed calculations, the response data for one set of water/binder ratio and curing age (w/b = 0.40 and curing age = 90 days), as given in the Tables 5.29, was also analyzed using ANOVA technique. GRA was applied to determine statistically the significant parameters. This analysis finally gives the %age

contribution of each factor towards the strength and durability properties.

Table 5.29: Experimental design using an L_9 OA and response results (For w/b= 0.40 and curing period=90 days)

Expt No.	Levels of parameters				Compressive strength (MPa) (CS)	Split tensile strength (MPa) (STS)	Depth of Wear (mm) (DW)	Depth of Water Penetration (mm) (DWP)
	By-Product Used as Binder (%) [A]	By-Product Used as FA (%) [B]	Type of By-Product as Binder [C]	Type of By-Product as FA [D]				
1	10%	20%	FA	0.224	72.05	4.58	0.224	20
2	10%	30%	LFS	0.312	64.35	4.07	0.312	15
3	10%	40%	CS	0.314	51.18	3.57	0.314	15
4	25%	20%	LFS	0.234	44.55	3.46	0.234	22
5	25%	30%	CS	0.24	46.20	3.87	0.24	32
6	25%	40%	FA	0.275	66.33	4	0.275	17
7	40%	20%	CS	0.289	36.22	3.15	0.289	40
8	40%	30%	FA	0.285	64.9	3.8	0.285	20
9	40%	40%	LFS	0.33	39.38	2.76	0.33	17

(Note:- A, B, C and D are the control parameters defined in Table 3.2)

The experimental results given in table 5.29 is normalised in order to bring the data to a dimensionless quantity. Since "the larger the better" characteristics is used for both the strength properties and "the smaller the better" characteristics is used for durability properties i.e. depth of wear and depth of water penetration. The equations (5.9) and (5.10) are used for strength and durability properties respectively to normalise the data as given below:

$$x_i^*(k) = \frac{x_i(k) - min\ x_i(k)}{max\ x_i(k) - min\ x_i(k)} \quad \text{----------} \quad (5.9)$$

$$x_i^*(k) = \frac{max\ x_i(k) - x_i(k)}{max\ x_i(k) - min\ x_i(k)} \quad \text{----------} \quad (5.10)$$

Where, $x_i(k)$ and x_i^*(k) are the comparability sequence and sequence after data normalisation respectively, i=1, 2, 3….. 9 for each of experiment from 1 to 9. All the sequences after data normalisation using Eqn. (5.9) and Eqn. (5.10) are given in Table 5.30.

Table 5.30: The sequences of each response after data normalisation

Expt. No.	Compressive strength	Split tensile strength	Depth of Wear	Depth of Water Penetration
Reference Sequence	**1.0000**	**1.0000**	**1.0000**	**1.0000**
1	1.0000	1.0000	1.0000	0.8000
2	0.7851	0.7198	0.1698	1.0000
3	0.4175	0.4451	0.1509	1.0000
4	0.2325	0.3846	0.9056	0.7200
5	0.2785	0.6099	0.8490	0.3200
6	0.8404	0.6813	0.5188	0.9200
7	0.0000	0.2143	0.3867	0.0000
8	0.8004	0.5714	0.4245	0.8000
9	0.0882	0.0000	0.0000	0.9200

The deviation sequence $\Delta_{0i}(k)$ for each of the performance characteristics is calculated using Eqn.(5.11) as given below:

$$\Delta_{0i}(k) = |x_0^*(k) - x_i^*(k)| \qquad ------ \qquad (5.11)$$

Where $x_0^*(k)$ = reference sequence and $x_i^*(k)$ = comparability sequence. The results of all Δ_{0i} for i = 1 to 9 are given in Table 5.31.

Table 5.31: The deviation sequences

Comparability sequence	Deviation sequence			
	CS	**STS**	**DW**	**DWP**
Exp. No.	1.0000	1.0000	1.0000	1.0000
1	0.0000	0.0000	0.0000	0.2000
2	0.2149	0.2802	0.8301	0.0000
3	0.5825	0.5549	0.8490	0.0000
4	0.7675	0.6154	0.0943	0.2800
5	0.7215	0.3901	0.1509	0.6800
6	0.1596	0.3187	0.4811	0.0800
7	1.0000	0.7857	0.6132	1.0000
8	0.1996	0.4286	0.5754	0.2000
9	0.9118	1.0000	1.0000	0.0800

(Note:- CS- Compressive Strength, STS- Split Tensile Strength, DW- Depth of Water, DWP- Depth of Water Penetration)

The Grey relational coefficient for all the experiments of the L_9 OA was determined using Eqn. (5.12).

$$\zeta_i(k) = \frac{\Delta_{min} + \zeta\Delta_{max}}{\Delta_{0i}(k) + \zeta\Delta_{max}} \quad ---------- \qquad (5.12)$$

Where $\Delta_{0i}(k)$ = deviation sequence among reference sequence $x_0^*(k)$ and comparability sequence $x_i^*(k)$, and ζ = identification coefficient and its value is taken as 0.5 *(Deng, 1989)*.

The Grey relational coefficient is presented in Table 5.32.

The Grey relation grade (GRG) is calculated by taking mean of grey relation coefficients of each of the response and is given by the Eqn. (5.13).

$$\Upsilon_i = 1/4\ (\zeta_i(1) + \zeta_i(2) + \zeta_i(3) + \zeta_i(4)) \text{----------} (5.13)$$

Table 5.32 presents the GRG for individual experiment conducted as per L_9 OA.

Table 5.32: The GRG and its rank

Exp. no.	Grey relational coefficient				GRG $\Upsilon_i=1/4(\zeta_i(1)+\zeta_i(2)+\zeta_i(3)+\zeta_i(4))$	Rank
	CS	STS	DW	DWP		
	$\zeta_I(1)$	$\zeta_I(2)$	$\zeta_I(3)$	$\zeta_I(4)$		
1	1.0000	1.0000	1.0000	0.7142	0.928571	1
2	0.6994	0.6408	0.3758	1.0000	0.679037	3
3	0.4619	0.4740	0.3706	1.0000	0.576627	6
4	0.3945	0.4483	0.8412	0.6410	0.581266	5
5	0.4093	0.5617	0.7681	0.4237	0.54072	7
6	0.7580	0.6107	0.5096	0.8620	0.685102	2
7	0.3333	0.3889	0.4491	0.3333	0.37617	9
8	0.7147	0.5385	0.4649	0.7142	0.608086	4
9	0.3542	0.3333	0.3333	0.8620	0.470734	8

(Note:- CS- Compressive Strength, STS- Split Tensile Strength, DW- Depth of Water, DWP- Depth of Water Penetration)

After calculating GRG for all the 9 experiments, response table is generated by averaging each level of parameter as per the Taguchi L_9 standard table. The response table is given in

Table 5.33. Now we require larger GRG for the optimal factor. So from the Table 5.33, we see that the optimal parameters are A1B1C1D1 i.e. quantity of by-product used as binder (%) at level 1, quantity of by-product to be used as fine aggregate (%) at level 1, type of the byproduct to be used as binder material at level 1and the by-product to be used as fine aggregate at level 1.Thus, it can be concluded that most optimum results can be obtained with 10% replacement of cement by FA along with 20% replacement of fine aggregates by EAFS.

Table 5.33: Response table for GRG

Symbol	Parameter	Grey relational grade			Main effect (max-min)	Rank
		Level 1	Level II	Level III		
A	By-product used as a binder (%)	0.728078 *	0.6024	0.4850	0.2431	1
B	By-product used as fine aggregate (%)	0.628669 *	0.609281	0.577488	0.0512	4
C	Type of by-product as a binder	0.740586 *	0.577012	0.497839	0.2427	2
D	Type of by-product as fine aggregate	0.646675 *	0.580103	0.58866	0.0666	3
	Total average value of all the Grey relational grades = 0.605146 Optimal Parameters = A1 B1 C1 D1					

Now for finding the %age contribution of each optimal parameter, ANOVA has been applied on grey relation grades. The ANOVA calculations are shown in the Table 5.34. The table clearly depicts that the by-product used as the binder is the most optimal parameter and has the maximum contribution for maximum split tensile and compressive strength and minimum wear depth and depth of water penetration.

Table 5.34: ANOVA table for GRG

Parameter	DOF	SS	MS	PC
[A] By-Product Used as Binder (%)	2	0.089	0.044	46.062
[B] By-Product Used as Fine Aggregate (%)	2	0.004	0.002	2.081
[C] Type of By-Product used as Binder	2	0.092	0.046	47.768
[D] Type of By-Product as Fine Aggregate	2	0.008	0.004	4.089
TOTAL	8	0.192		100.000

(Note:- DOF-Degrees of freedom; SS- Sum of Squares; MS-Mean sum of squares; PC-Percentage Contribution)

The Grey relational analysis for all the combinations of 0.48, 0.44 & 0.40 w/b ratios and curing of 7, 28 & 90 days was performed in a similar manner, and the summary of the analysis is presented in results and discussion.

5.4.1 Results and Discussion

The effect of curing period on optimal mix design parameters and their percentage contribution towards the strength and durability properties at different curing periods is discussed below:

(a) Effect of curing period on optimal mix design parameters

- At curing period of 7 days (i.e. at an early age)

It is observed from the Table 5.35 that at 7 days curing, replacement of cement by ladle furnace slag gives the optimal result for higher water/binder ratio and by fly-ash at lower w/b ratios of 0.44 & 0.40. Whereas replacement of sand with iron slag provides the optimal results for better strength and durability at all w/b ratios.

Table 5.35: Optimal parameters for strength and durability properties at 7 days of curing

Exp. No.	W/B ratio	Optimal Parameters	Optimal Parameters			
			A	B	C	D
1.	0.48	A1B1C2D2	10	20	Ladle Furnace Slag (LFS)	Iron Slag (IS)
2.	0.44	A1B1C1D2	10	20	Fly- ash (FA)	Iron Slag (IS)
3.	0.4	A1B1C1D2	10	20	Fly Ash (FA)	Iron Slag (IS)

(Note:- A, B, C and D are the control parameters as defined in Table 3.2)

It is also seen that for all water binder ratios, 10% is the optimal %age of cement replacement contributing to higher strength and durability at early ages, whereas 20% of sand replacement

by iron slag at all w/b ratios contributes positively to strength gain and durability at an early age. Thus, it is summarised that at 7 days, the percentage replacement of cement remains constant at all water/binder ratios and the replacement material changes from ladle furnace slag at water/binder ratio of 0.48 to fly ash at water/binder ratios of 0.44 and 0.40, whereas, on the other hand, for the replacement of sand, the type of material and its percentage replacement remains constant i.e. 20% iron slag at all water binder ratios.

- At 28 days of curing period (i.e. at normal age)

It is observed from the table 5.36 that at 28 days curing, for all water binder ratios, replacement of cement by fly-ash gives the optimal result, whereas sand replacement by iron slag provides the optimal strength and durability results only for higher w/b ratio of 0.48. But, at a lower w/b of 0.44 and 0.40, electric arc furnace slag as sand replacement provides better results.

Table 5.36: Optimal parameters for strength & durability properties at 28 days of curing time

Exp. No.	W/B ratio	Optimal Parameters	Optimal Parameters			
			A	B	C	D
1.	0.48	A1B2C1D2	10	30	Fly Ash	Iron Slag
2.	0.44	A1B1C1D1	10	20	Fly Ash	EAFS
3.	0.4	A1B2C1D1	10	30	Fly Ash	EAFS

(Note:- A, B, C and D are the control parameters as defined in Table 3.2)

Also, it is observed that for all water binder ratios, 10% is the optimum %age of fly ash replacement contributing to higher strength and durability at early ages, whereas 30% of sand replacement by iron slag at 0.48 w/b ratios contributes positively to strength and durability at an early age. For lower w/c ratios, 20% of sand replacement by electric arc furnace slag provides the optimal strength results. Thus, it can be concluded that at early ages, the replacement material and its percentage replacement of cement remains constant at all water/binder ratios, whereas, on the other hand, for the replacement of sand, the type of material and its percentage replacement remains constant i.e. 30% iron slag at higher w/b ratios and it changes to 20% electric arc furnace slag only at lower w/b ratios.

- At 90 days of curing period

It is observed from the Table 5.37 that at 90 days curing period, for all water-binder ratios, cement replacement by fly ash gives the optimal result, whereas sand replacement by iron

slag provides the optimal strength and durability results only for higher w/b ratios of 0.48. However, at a lower w/b of 0.44 and 0.40, electric arc furnace slag as sand replacement provides better results.

Table 5.37: Optimal parameters for strength & durability properties at 90 days of curing time.

Exp. No.	W/B ratio	Optimal Parameters	Optimal Parameters			
			A	B	C	D
1.	0.48	A1B2C1D2	10	30	Fly Ash	Iron Slag
2.	0.44	A1B1C1D1	10	20	Fly Ash	EAFS
3.	0.4	A1 B1 C1 D1	10	20	Fly Ash	EAFS

(Note:- A, B, C and D are the control parameters as defined in Table 3.2)

Also, it is observed that for all water binder ratios, 10% is the optimum %age of fly ash replacement contributing to higher strength and durability at early ages, whereas 30% of sand replacement by iron slag at 0.48 w/b ratios contributes positively to strength and durability at an early age. For lower w/c ratios, 20% of sand replacement by electric arc furnace slag provides the optimal results. Thus, it can be concluded that at early ages, the replacement material and its percentage replacement of cement remains constant at all water/binder ratios, whereas, on the other hand, for the replacement of sand, the type of material and its percentage replacement changes from 30% iron slag at higher w/b ratios to 20% electric arc furnace slag only at lower w/b ratios.

(b) Percentage contribution towards the strength and durability of various optimal parameters at different curing periods

The results indicating the percentage contribution of optimal parameters towards concrete strength and durability are also tabulated in Tables 5.38 to 5.40 for curing age of 7, 28. 90 days respectively. The effect at different curing ages is presented below:

- At curing age of 7 days

At the age of 7 days (See Table 5.38), for all water/binder ratios, 10% of by-product used as cement replacement is the optimal parameter which contributes maximum towards the strength & durability of the resulting concrete. It is also seen that its contribution is maximum at higher water/binder ratio of 0.48, i.e.88.97% and it decreases to 79.48% as the w/b is

decreased to 0.40, whereas, at lower w/b ratios, the contribution of type of cement replacement material towards concrete strength, (i.e. fly ash) starts increasing, which is 14.31% at 0.40 water/binder ratio.

Table 5.38: Percentage contribution of various optimal parameters at 7 days curing

Exp. No.	w/b ratio	Optimal parameters	Optimal parameters				Rank				% Contribution			
			A	B	C	D	A	B	C	D	A	B	C	D
1.	0.48	A1B1C2D2	10	20	LFS	IS	1	2	4	3	88.97	9.68	0.03	1.32
2.	0.44	A1B1C1D2	10	20	FA	IS	1	3	2	4	86.71	4.01	8.49	0.71
3.	0.4	A1B1C1D2	10	20	FA	IS	1	3	2	4	79.48	3.89	14.31	2.32

(Note:- A, B, C and D are the control parameters as defined in Table 3.2)

The type of replacement as sand, as can be observed from the Table 5.38, contributes very little at all the water/binder ratios, whereas percentage of sand replacement does play a slightly better role only for higher w/b ratios.

- At curing period of 28 days (i.e. at normal age)

At 28 days (See Table 5.39), for all water to binder ratios, 10% of by-product used as partial cement replacement is the optimal parameter which contributes maximum towards the strength & durability of the resulting concrete. Also it is seen that its contribution is maximum at higher w/b ratio of 0.48, i.e.90.86% and it decreases to 57.28% as the water/binder is decreased to 0.40, whereas, at lower w/b ratios, the contribution of type of cement replacement material towards concrete strength, (i.e. fly ash) starts increasing, which is 41.12% at 0.40 water/binder ratio.

Table 5.39: Percentage contribution of various optimal parameters at 28 days curing

Exp. No.	w/b ratio	Optimal parameters	Optimal parameters				Rank				% Contribution			
			A	B	C	D	A	B	C	D	A	B	C	D
1.	0.48	A1B2C1D2	10	30	FA	IS	1	4	3	2	90.86	0.112	2.714	6.31
2.	0.44	A1B1C1D1	10	20	FA	EAFS	1	4	2	3	73.50	2.95	18.93	4.6
3.	0.4	A1B2C1D1	10	30	FA	EAFS	1	4	2	3	57.28	0.57	41.12	1.03

(Note:- A, B, C and D are the control parameters as defined in Table 3.2)

The percentage of sand replacement, as can be observed from the Table 5.39, contributes very little at all the water/binder ratios, whereas the type of replacement as sand does play a slightly better role only for higher water/binder ratios.

- At 90 days curing period

At curing of 90 days (See Table 5.40), for all water binder ratios, 10% of by-product used as partial cement replacement is the optimal parameter which contributes maximum towards the strength & durability of the resulting concrete. Also it is observed that its contribution is maximum at higher water/binder ratio of 0.48, i.e.72.34% and it decreases to 46.06% as the w/b is decreased to 0.40, whereas, at lower w/b ratios, the contribution of type of cement replacement material towards concrete strength, (i.e. fly ash) starts increasing, which is 47.77% at w/b of 0.40.

Table 5.40: Percentage contribution of various optimal parameters at 90 days curing

Exp. No.	w/b ratio	Optimal parameters	Optimal parameters				Rank				% Contribution			
			A	B	C	D	A	B	C	D	A	B	C	D
1.	0.48	A1B2C1D2	10	30	FA	IS	1	4	2	3	72.34	2.16	22.81	2.68
2.	0.44	A1B1C1D1	10	20	FA	EAFS	1	4	2	3	52.80	0.74	44.53	1.92
3.	0.4	A1 B1 C1 D1	10	20	FA	EAFS	1	4	2	3	46.06	2.08	47.77	4.09

(Note:- A, B, C and D are the control parameters as defined in Table 3.2)

The percentage of sand replacement, as can be observed from the Table 5.40, contributes very little and almost remains constant at all the water/binder ratios, whereas the type of replacement as sand does play a slightly better role only for lower w/b ratios.

(c) Confirmation experiment to verify optimum mix-design parameters

Optimal mix-design proportions from the Grey-Taguchi relational analysis was verified by conducting an experiment to check whether the strength and durability properties can actually be optimized by the proposed optimum mix design proportions. Same materials and the same conditions were used in the experiment in order to compare the results. Twenty four 150 mm cube samples, 150x300 mm size cylinders and 70.6x70.6x25 mm tiles were cast according to

the optimal mix design proportions evaluated from the Grey-Taguchi method. The tests were conducted on specimens for split tensile strength, compressive strength, depth of wear and depth of water penetration at 7 days. The measured values of the strength properties are tabulated in Table 5.41, and it is concluded that the optimal mixture resulted in more compressive & split tensile strength and less water penetration depth & depth of wear than all other mixes and control mixes. The results of verification study also showed that proposed optimal mixture design proportions also satisfied the expected maximisation of compressive & split tensile strength and minimisation of water penetration depth & wear depth.

Table 5.41: Results of the confirmation experiment at 7 days curing age

Exp. No.	W/B ratio	Optimal Parameters	Optimal Parameters				Control Mix Results		Trial Mix Results	
			A	B	C	D	Compressive strength (MPa)	Split tensile strength (MPa)	Compressive strength (MPa)	Split tensile strength (MPa)
1	0.48	A1B1C2D2	10	20	LFS	IS	27.00	2.21	28.70	2.31
2	0.44	A1B1C1D2	10	20	FA	IS	30.50	2.40	31.10	2.62
3	0.40	A1B1C1D2	10	20	FA	IS	39.80	2.97	41.70	3.10

(Note:- A, B, C and D are the control parameters as defined in Table 3.2)

The optimum combination of control factors for confirmation experiment after 7 days of curing age and for all the water to binder ratios is as given below.

- Percentage of by-product to be used as partial replacement of cement-- 10 %
- Percentage of by-product used as partial replacement of fine aggregate--20 %
- Type of replacement as binder---Fly ash
- Type of replacement as Fine aggregate--- Iron slag

CHAPTER 6 MATHEMATICAL MODELING

6.0 INTRODUCTION

The results obtained after the experimental analysis were utilised for the development of mathematical models. The models were developed for prediction of strength as well as durability characteristics of concrete incorporating industrial by-products, within the range of parameters used using ANN and ANFIS methods. Subsequently, the experimental outcomes were compared with predicted values for the validation of the model. The ANN and ANFIS were also compared for their performance.

6.1 PREDICTION OF COMPRESSIVE AND SPLIT TENSILE STRENGTH USING ARTIFICIAL NEURAL NETWORK (ANN) MODELING TECHNIQUE

Artificial Neural networks are the modelling techniques which are capable of modelling very complex functions. ANN can represent both linear and nonlinear relationships and they can learn from the input data itself. The ANN is trained first from the input data and then the problem is solved *(Muthupriya et al., 2011)*. Artificial Neural Network consists the elements called neurons, which are similar to biological neurons, which interact with each other using their weights which are assigned to them. The ANN comprises of three different layers namely 1. input layer, 2. hidden layer and 3. output layer as shown in Fig. 6.1.The data is fed through input layer and then this data is processed in hidden layer and finally the results are available at output layer.

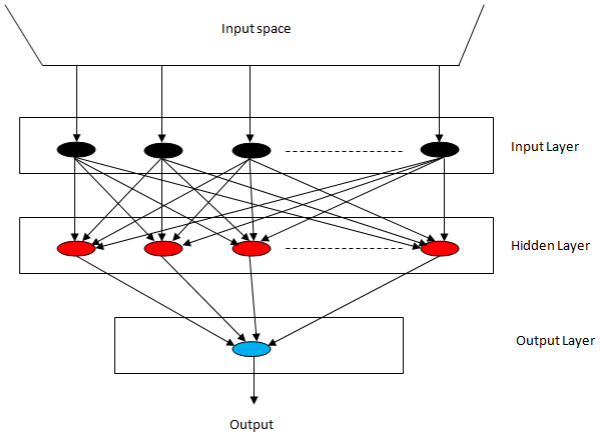

Fig. 6.1: Artificial neural network (ANN)

6.1.1. Architecture of Neural Networks (ANN)

There are many types of algorithms which could be used in ANN Modelling. Out of the different available algorithms, Levenberg-Marquardt back propagation (LMBP) algorithm is used most commonly for training of the network. This choice is due to its speed and robustness *(Kermani et al., 2005)*. Hence, LMBP algorithm has been applied in this problem. This algorithm uses feed-forward networks which are multi layered, in which, the neurons are placed in layers, signals are to be sent forward and errors are to be sent backwards (Fig.6.2). The weights are assigned to each input parameter. An epoch is the number of iterations required by the neural network model to converge. In this way weights were re-initialized unless a best model has been obtained with minimum error.

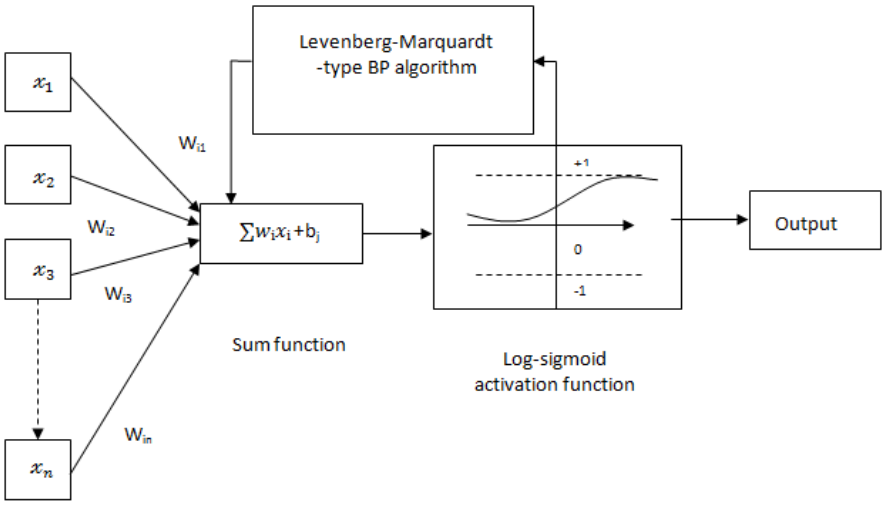

Fig. 6.2: A typical ANN model

6.1.2. Model Structure and Parameters of Neural Network

The neural network model used herein was developed using MATLAB software. The network consisted of an input layer with 9 neurons, a hidden layer with 20 neurons and an output layer with one neuron as shown in Fig.6.3. The nine input parameters in the input layer were water to binder ratio, curing period, amount of cement, type of cement replacement material, percentage of cement replacement, amount of sand, type of sand replacement material, percentage of sand replacement and superplasticizer.

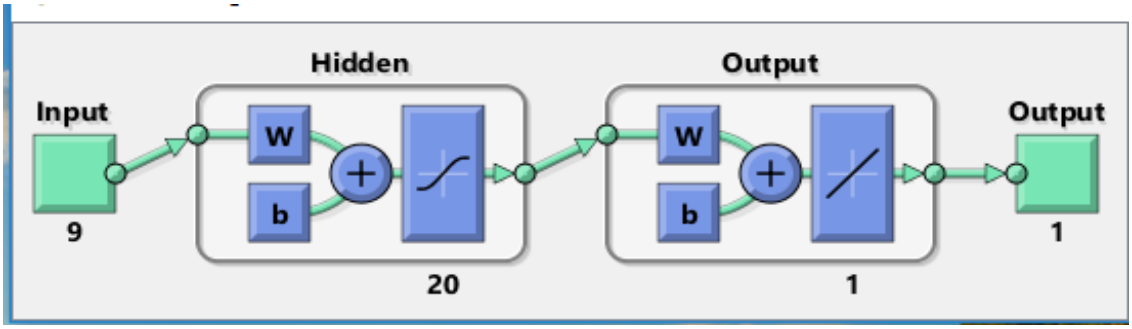

Fig. 6.3: The ANN network

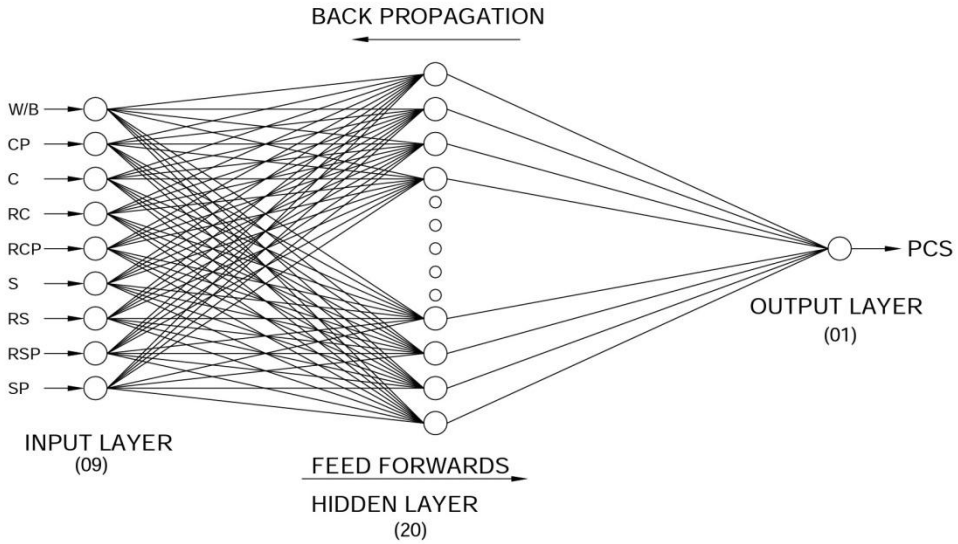

Fig. 6.4: The FFBP ANN for the concrete on the response compressive strength

(Note: W/B= Water/ binder ratio, CP= Curing Period, C= Amount of Cement, RC= Type of cement replacement material, RCP= Percentage of cement replacement, S= Amount of Sand, RS= Type of sand replacement material, RSP= Percentage of sand replacement, SP= Superplasticizer, PCS= Predicted Compressive Strength)

The FFBP neural network architecture used in this study has been shown in Fig.6.4. The neurons of neighbouring layers are inter-connected with each other by some weights. The neurons of output layer produces the network output i.e. prediction of compressive or the split tensile strength as the case may be. Table 6.1 shows the actual experimental outcomes and ANN predicted values for the output i.e. compressive or split tensile strength. Out of the total data, around 70% of the data has been taken for the training of network, 15% data has been considered for testing and remaining 15% data has been considered for validation of the network. The gradient decent method is used for learning the FFBP algorithm. The network

adjusts automatically its threshold and weight values while training so that the variation between the outputs and target is minimum. The error goal and learning rate were kept as 0.001 and 0.3 respectively. The transfer function used in hidden layer was *transig* and in output layer was *purelin (Patowari et al., 2010)*. The MATLAB software program used for ANN is given at annexure A.

The *transig* and *purelin* transfer functions shown by equations (6.1) and (6.2) evaluate the output values as given below:

$$transig\ (n) = \frac{2}{1+exp^{-2n}} - 1 \qquad \text{----------(6.1)}$$

$$purelin\ (n) = n \qquad \text{----------(6.2)}$$

Where 'n' is input value to the function.

Table 6.1: ANN predicted outcomes for compressive & split tensile strengths

S. No.	Concrete mix Design as depicted in Table 3.15 to 3.18	Curing Age (Days)	W/B Ratio	Compressive Strength (MPa)		Split Tensile Strength (MPa)	
				Experimental Values	ANN Predicted Values	Experimental Values	ANN Predicted Values
1.	1	7	0.40	41.50	39.989566	2.67	2.60425
2.	2	7	0.40	39.82	39.820000	2.47	2.46986
3.	3	7	0.40	30.80	30.800003	2.23	2.75362
4.	4	7	0.40	27.50	27.500002	2.21	2.20998
5.	5	7	0.40	29.81	29.810002	2.42	2.41980
6.	6	7	0.40	31.24	31.239999	2.64	2.63990
7.	7	7	0.40	21.12	19.754387	2.06	2.42953
8.	8	7	0.40	29.77	32.691878	2.03	2.02995
9.	9	7	0.40	25.85	25.850001	2.20	2.19969
10.	Control	7	0.40	39.80	39.799996	2.97	2.97285
11.	1	7	0.44	30.97	30.970000	2.53	2.53022

12.	2	7	0.44	31.00	31.000000	2.22	2.21982
13.	3	7	0.44	29.83	27.707924	2.15	2.10156
14.	4	7	0.44	26.94	26.940001	1.78	1.98800
15.	5	7	0.44	28.82	28.820001	2.00	2.22885
16.	6	7	0.44	30.42	26.594765	2.55	2.54984
17.	7	7	0.44	19.58	19.580000	1.94	1.93988
18.	8	7	0.44	25.74	25.975034	1.97	1.96984
19.	9	7	0.44	23.96	23.960000	1.76	1.75989
20.	Control	7	0.44	30.50	30.499999	2.40	2.40193
21.	1	7	0.48	28.60	26.479998	2.13	2.53022
22.	2	7	0.48	28.38	16.671810	1.96	2.21982
23.	3	7	0.48	26.48	22.300000	1.85	2.10156
24.	4	7	0.48	21.48	22.729999	1.72	1.98800
25.	5	7	0.48	22.30	16.453694	1.89	2.22885
26.	6	7	0.48	22.73	21.780000	2.34	2.54984
27.	7	7	0.48	16.06	17.046537	1.17	1.93988
28.	8	7	0.48	21.78	49.338063	1.63	1.96984
29.	9	7	0.48	17.16	53.759997	1.60	1.75989
30.	Control	7	0.48	27.00	27.000000	2.21	2.20961
31.	1	28	0.40	53.76	44.279377	3.41	3.51579
32.	2	28	0.40	50.32	39.600002	3.24	3.06398
33.	3	28	0.40	46.20	36.961750	3.10	3.09967
34.	4	28	0.40	39.60	45.590843	2.82	2.82002
35.	5	28	0.40	40.92	23.554584	3.20	2.88736
36.	6	28	0.40	49.94	49.139999	3.25	3.24999
37.	7	28	0.40	31.21	30.880000	2.55	2.54979
38.	8	28	0.40	49.14	45.130000	3.41	2.97165
39.	9	28	0.40	30.88	45.915692	2.69	2.68977
40.	Control	28	0.40	51.05	55.728579	4.47	4.46962
41.	1	28	0.44	47.83	40.789999	3.36	3.36041
42.	2	28	0.44	45.68	37.140001	3.12	3.11986
43.	3	28	0.44	40.79	37.620000	2.98	2.97957

44.	4	28	0.44	37.14	37.465128	2.74	2.77099
45.	5	28	0.44	37.62	22.694384	3.04	3.03975
46.	6	28	0.44	46.60	37.949999	3.10	3.25757
47.	7	28	0.44	27.03	28.080000	2.33	2.32994
48.	8	28	0.44	37.95	42.059999	3.05	3.04986
49.	9	28	0.44	28.08	44.196961	2.59	2.58989
50.	Control	28	0.44	45.13	45.679997	3.82	3.57768
51.	1	28	0.48	46.05	39.819998	3.15	3.13895
52.	2	28	0.48	45.02	30.230001	3.03	3.02991
53.	3	28	0.48	39.82	33.960000	2.90	2.89984
54.	4	28	0.48	30.23	28.600000	2.68	2.67995
55.	5	28	0.48	33.96	28.379998	2.89	2.88968
56.	6	28	0.48	39.08	39.079997	3.00	2.97679
57.	7	28	0.48	23.76	23.760000	1.88	1.88010
58.	8	28	0.48	31.82	34.055203	2.63	2.62990
59.	9	28	0.48	24.11	24.110001	2.33	2.33017
60.	Control	28	0.48	42.06	45.019998	3.45	2.85641
61.	1	90	0.40	72.05	72.049990	4.58	4.40301
62.	2	90	0.40	64.35	66.023759	4.07	4.07016
63.	3	90	0.40	51.18	51.179999	3.57	3.56999
64.	4	90	0.40	44.55	54.179090	3.46	4.25787
65.	5	90	0.40	46.20	42.883348	3.87	3.87002
66.	6	90	0.40	66.33	66.329993	4.00	3.99990
67.	7	90	0.40	36.22	36.219998	3.15	3.14982
68.	8	90	0.40	64.90	64.899995	3.80	3.80003
69.	9	90	0.40	39.38	41.579578	2.76	2.76002
70.	Control	90	0.40	55.64	55.639989	4.89	4.88885
71.	1	90	0.44	61.33	61.329993	3.76	3.76075
72.	2	90	0.44	56.21	56.209996	3.45	3.29669
73.	3	90	0.44	48.11	48.110000	3.39	3.27951
74.	4	90	0.44	43.45	43.449999	3.26	3.26024
75.	5	90	0.44	45.34	45.339999	3.67	3.69597

76.	6	90	0.44	60.35	60.349992	3.75	3.75008
77.	7	90	0.44	33.81	26.944606	2.83	2.82987
78.	8	90	0.44	51.62	51.619995	3.66	3.65996
79.	9	90	0.44	36.74	36.739999	2.71	2.61556
80.	Control	90	0.44	47.20	47.199988	4.21	4.20898
81.	1	90	0.48	57.09	48.706684	3.68	3.27835
82.	2	90	0.48	55.96	44.628577	3.25	3.25005
83.	3	90	0.48	45.98	45.979999	3.31	3.30992
84.	4	90	0.48	38.50	38.499998	3.20	3.20001
85.	5	90	0.48	41.09	42.656702	3.31	3.51965
86.	6	90	0.48	56.77	56.769991	3.47	3.46981
87.	7	90	0.48	31.10	31.099998	2.79	2.79004
88.	8	90	0.48	44.73	44.729996	3.38	3.77621
89.	9	90	0.48	32.45	32.449997	2.53	2.18537
90.	Control	90	0.48	46.20	46.199992	3.81	3.19872

The target and predicted compressive and split tensile strength verses all data samples from the FFBP neural network is compared and exhibited in figures 6.5 and 6.6 respectively, which displays a close relationship between the two results.

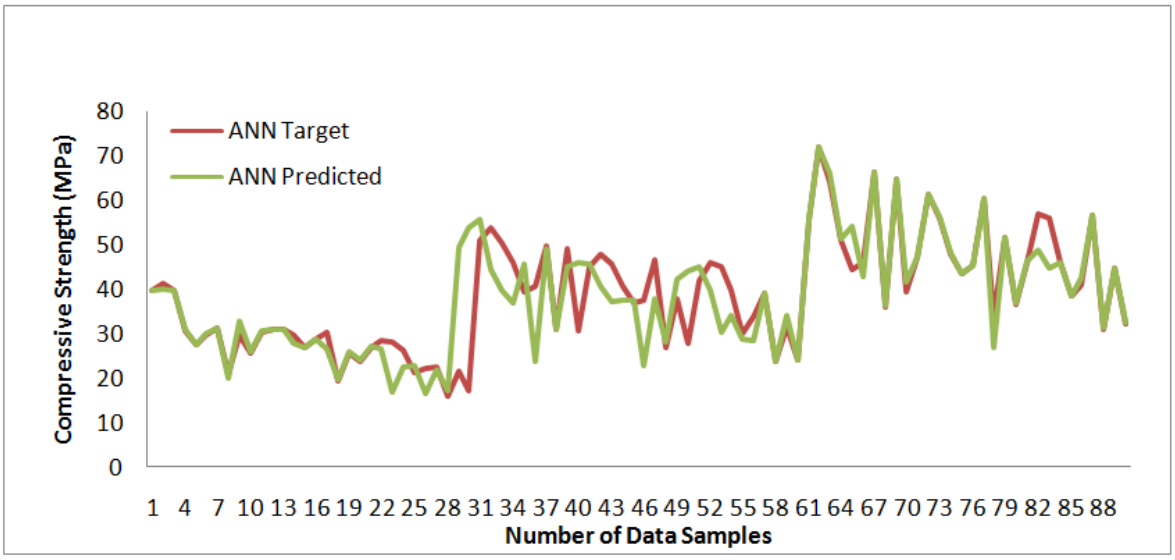

Fig. 6.5: The comparison of the Experimental/Target and predicted compressive strength verses all data samples for ANN modelling

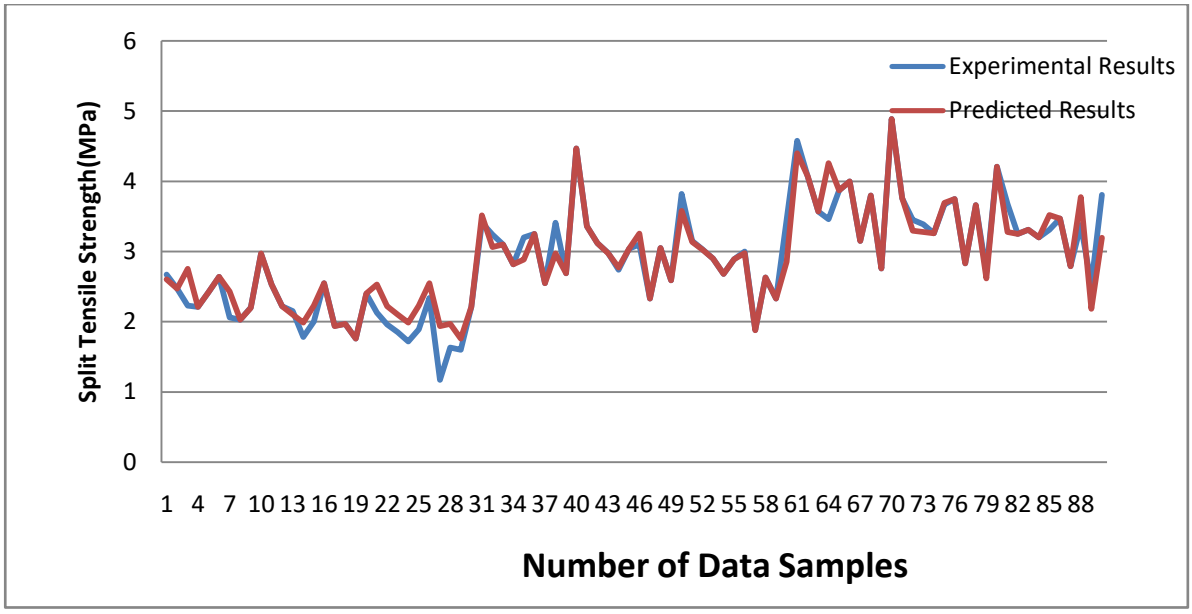

Fig. 6.6: The comparison of the predicted and experimental/target split tensile strength verses all data samples for ANN modelling

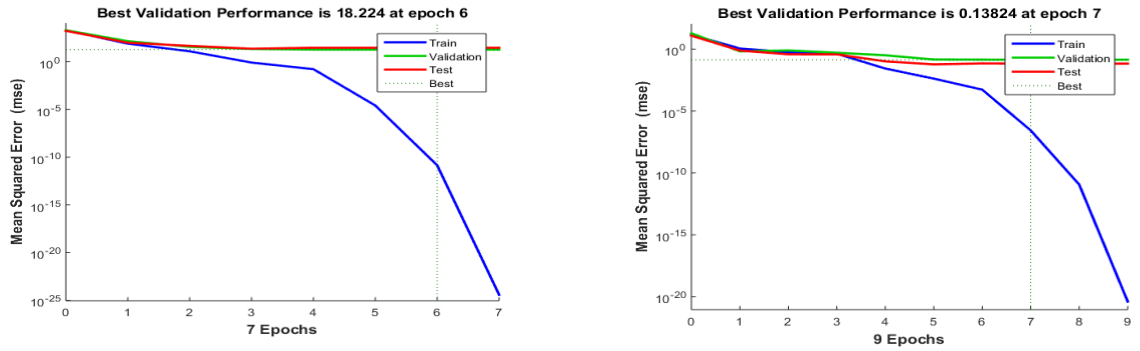

(a) Compressive strength (b) Split Tensile Strength

Fig. 6.7: The performance of FFBP algorithm

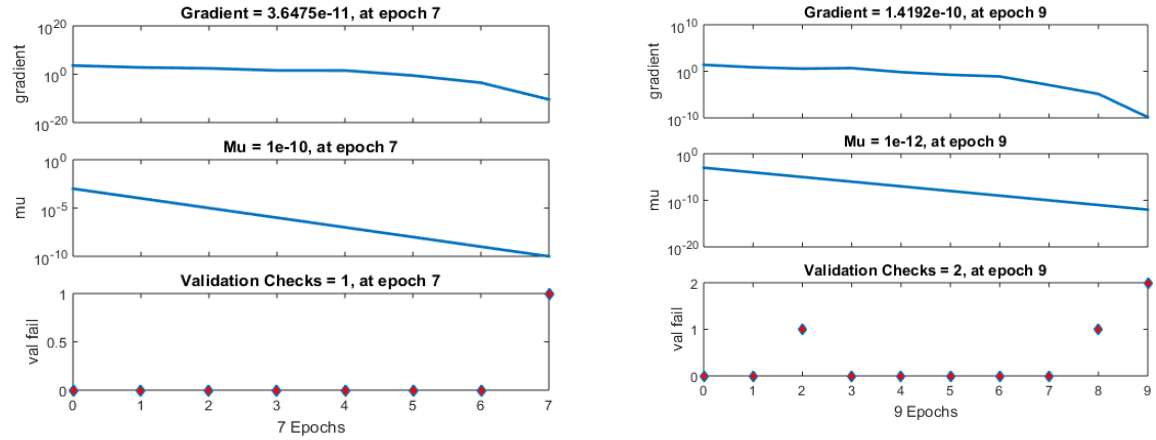

(a) Compressive strength (b) Split Tensile Strength

Fig. 6.8: Learning behaviour of the neural network model

The best results have been shown from the performance graph of the result after training of the model. The best validation performance of the network for compressive strength was 18.224 at epoch 6 and the model is completed in 7 epochs as depicted in Fig. 6.7. Fig. 6.8 displays the learning behaviour of the neural network model for compressive & split tensile strength with the no. of epochs during training of the neural network.

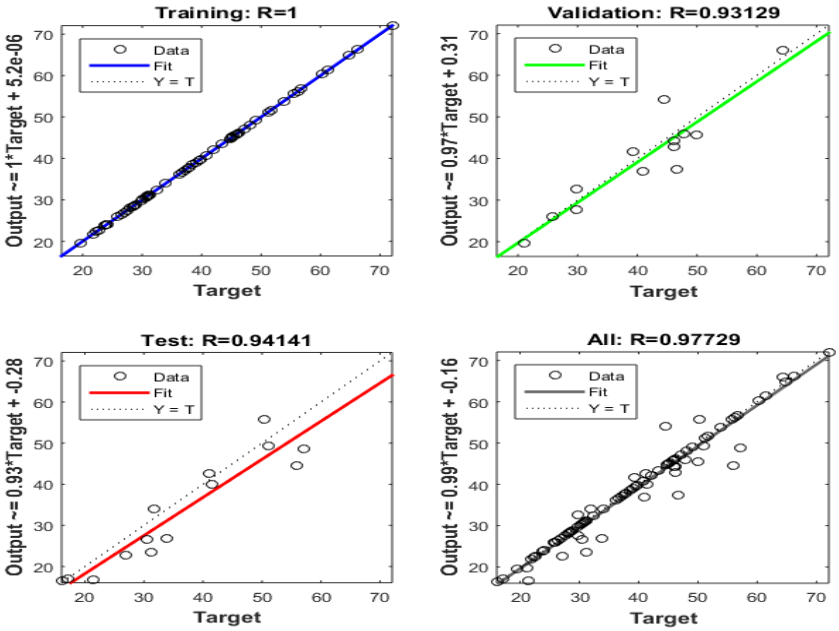

Fig. 6.9: The correlation between the ANN estimated values and experimental values of compressive strength for training, testing, validation and all data.

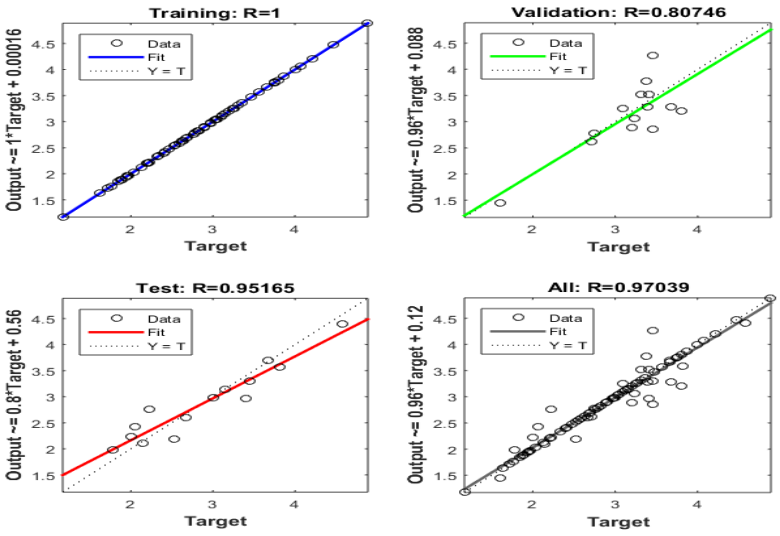

Fig. 6.10: The correlation between the ANN estimated values and experimental values of split tensile strength for training, testing, validation and all data.

The ANN model developed in the current work was utilised for prediction of the compressive & split tensile strength of concrete containing industrial by-products. In addition, a linear

regression was also performed between the output response of the network and the experimental/target value. In this case, the experimental values of compressive and split tensile strength were input to the model for training, testing and validation to perform the regression. The comparison between the experimental results and predicted outcomes for training, testing and the whole data of each model are shown in Fig.6.9 and Fig.6.10 for compressive and split tensile strength respectively. It is clearly observed that the estimated values of the training and testing in both the ANN models are very near to the target values. Therefore, these types of models show good potential for predicting the split tensile as well as compressive strength of concrete containing ternary combination of industrial by-products.

The performance indices to evaluate the performance of the ANN models for testing and training data sets were determined. These indices are the root mean squared error (RMSE), determination coefficients (R^2), Mean absolute percentage error (MAPE), Integral absolute error (IAE) and mean absolute error (MAE) and are given in Table 6.2. It is considered that a prediction is better if the values of RMSE, MAPE, and IAE are close to zero and R^2 is close to one. From the performance indicators shown in Table 6.2, it is observed that the calculated values of above mentioned performance indices are very close to the permissible limits and hence ANN models predicted the compressive and split tensile strength very accurately.

Where t and o are the target and the predicted value of the network respectively, and n is the total number of patterns and $\bar{t}$ is the average of the target values.

Table 6.2: Performance indices of ANN models

S. No.	Performance indices	Formula	Compressive strength model	Split tensile model
			Value	Value
1	RMSE	RMSE = $\sqrt{\frac{1}{n}\sum_{i=1}^{n}(ti-oi)^2}$	0.717	0.1787
2	R^2	$R^2 = 1 - \frac{\sum_{i=1}^{n}(ti-oi)^2}{\sum_{i=1}^{n}(ti-\bar{t}i)^2}$	0.659	0.9412
3	MAPE	MAPE = $\frac{1}{n}\left[\frac{\sum_{i=1}^{n}\lvert ti-oi\rvert}{\sum_{i=1}^{n} ti} \times 100\right]$	0.1047%	0.0301
4	IAE	IAE = $\frac{\sum_{i=1}^{n}\left[(ti-oi)^2\right]^{1/2}}{\sum_{i=1}^{n} ti} \times 100$	1.946%	0.6534
5	MAE	MAE = $\frac{1}{n}[\sum_{i=1}^{n}\lvert ti-oi\rvert]$	3.661	0.0781

The regression equations and coefficient of correlation (R) for training, testing, validation and all data for the ANN models both for compressive & split tensile strength is shown in Table 6.3. From this table, we see that the overall value of the correlation factor (R) for the ANN model developed for compressive strength is 0.97729 and for split tensile strength is 0.97039. It is established that the network is considered more precise and meaningful from statistical angle if the value of coefficients of correlation approaches near to one. Therefore, it is observed from the table that the value of R for both the strength properties is very close to one. Therefore it is concluded that there is no significant difference in the experimental values and its predicted values at 95% confidence level for compressive & split tensile strength.

Table 6.3: The values of the correlation coefficient (R)

S. No.	Type of data	Regression Equations		Correlation Coefficient (R)	
		Compressive strength model	Split tensile strength model	Compressive strength model	Split tensile model
1.	Training data	Output= 1xTarget+5.2e-06	Output= 1xTarget+0.00016	1	1
2.	Testing data	Output= 0.93xTarget-0.28	Output= 0.8xTarget+0.56	0.94141	0.9516
3.	Validation data	Output= 0.97xTarget+0.31	Output= 0.96xTarget+0.088	0.93129	0.80746
4.	Overall data	Output= 0.99xTarget-0.16	Output= 0.96xTarget-0.12	0.97729	0.97039

6.2 MODELING FOR THE PREDICTION OF COMPRESSIVE AND SPLIT TENSILE STRENGTH USING ADAPTIVE NEURO-FUZZY INFERENCING SYSTEMS (ANFIS) TECHNIQUE

Jang (1993) was the first to introduce the adaptive neuro-fuzzy inference systems (ANFIS). ANFIS has the capability of the human-like reasoning by using input and output sets of data

and IF-THEN fuzzy rules. However, its adaptability to deal with a changing external environment is very limited. Therefore learning concepts of neural network have been introduced in ANFIS. The back-propagation is the basic algorithm for the learning of the model, the aims of which is minimization of the prediction error. So in ANFIS, the reasoning capabilities of fuzzy logic and the learning capabilities of a neural network were combined together *(Yuan et al., 2014).*

Fig. 6.11 shows the structure of a typical ANFIS model with two input variables.

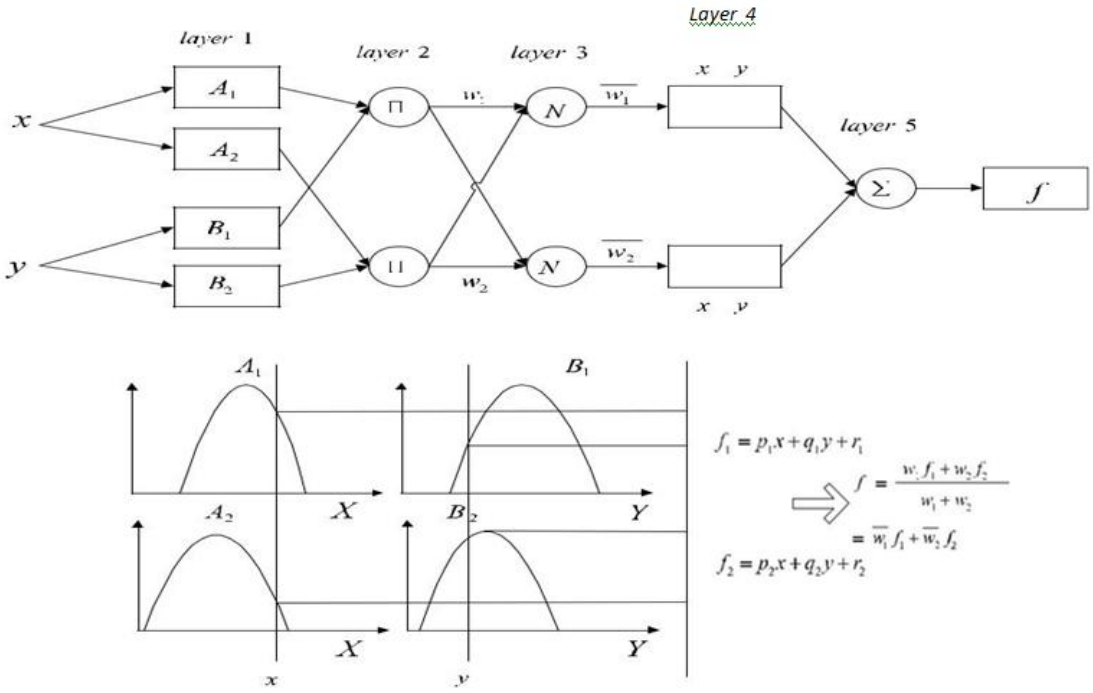

Fig. 6.11: The Structure and reasoning flow of ANFIS model

As shown in the Figure 6.11, the model consists of five layers, which are 1.Input layer, 2. Input membership function layer, 3. Rule 4. The output membership function and 5. Out-put layer. The ANFIS model developed in this study was used to estimate the compressive & split tensile strength of concrete containing industrial by-products. MATLAB software with ANFIS toolbox was used to develop the model. Subtractive clustering method was used to build the model. The MATLAB software program used for this ANFIS model is given in annexure-B.

The comparison of the Experimental and predicted compressive strength verses all data, test data and training data samples for ANFIS modelling is presented in Fig. 6.12 to Fig. 6.14 respectively. Similarly the comparison of the estimated and experimental value of split tensile strength verses all data, test data and training data samples for ANFIS modelling is shown in

Fig. 6.15 to Fig. 6.17 respectively. It clearly shows that the estimated values for the training and testing of the ANFIS model is very near to the experimental values for both the compressive & split tensile strength. Therefore, these models show good potential for predicting the compressive strength & split tensile strength of concrete containing industrial by-products.

The correlation graph between the ANFIS estimated values and the experimental outcomes of compressive & split tensile strength for training data, testing data and all data is exhibited in figures 6.18 and 6.19 respectively. Table 6.4 shows the actual experimental results and ANFIS predicted results for compressive and split tensile strength.

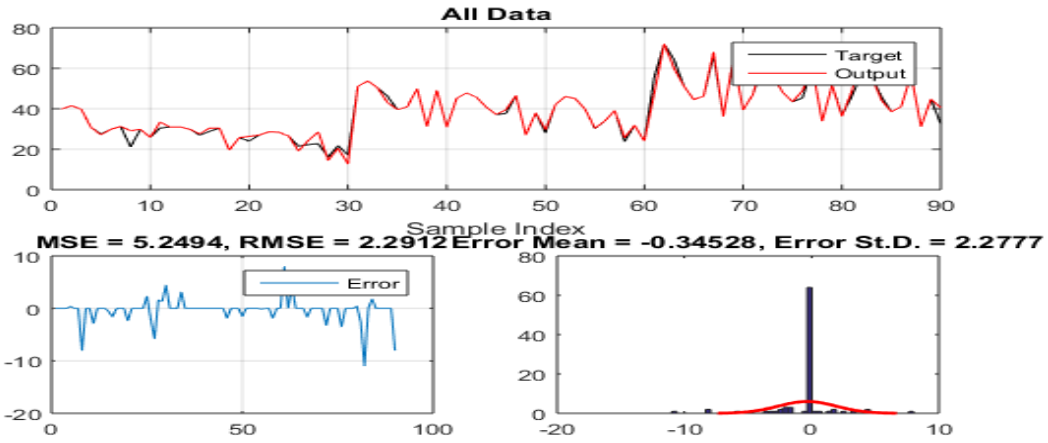

Fig. 6.12: The comparison of the predicted and experimental values of compressive strength verses all data samples for ANFIS modelling.

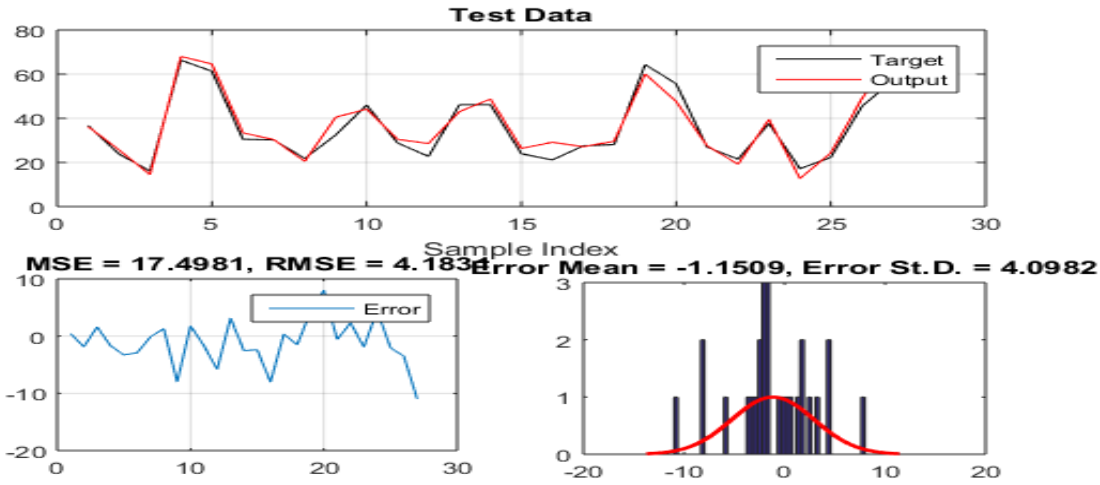

Fig. 6.13: The comparison of the target and output compressive strength verses test data samples for ANFIS modelling

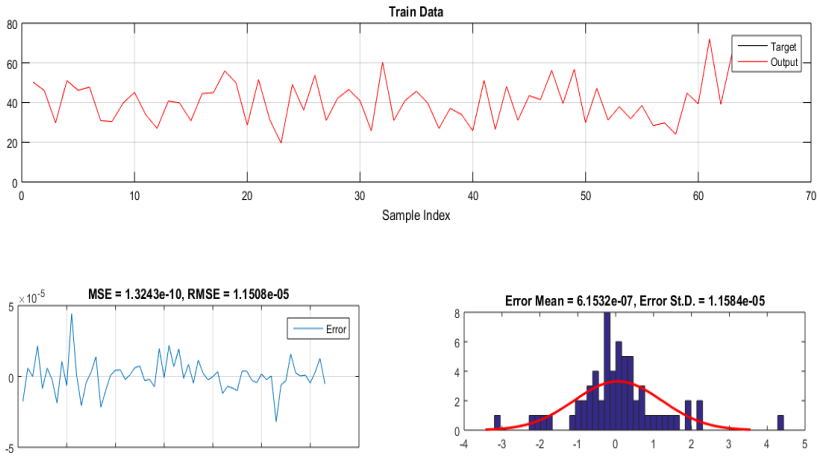

Fig. 6.14: The comparison of the output and target compressive strength verses training data samples for ANFIS modelling.

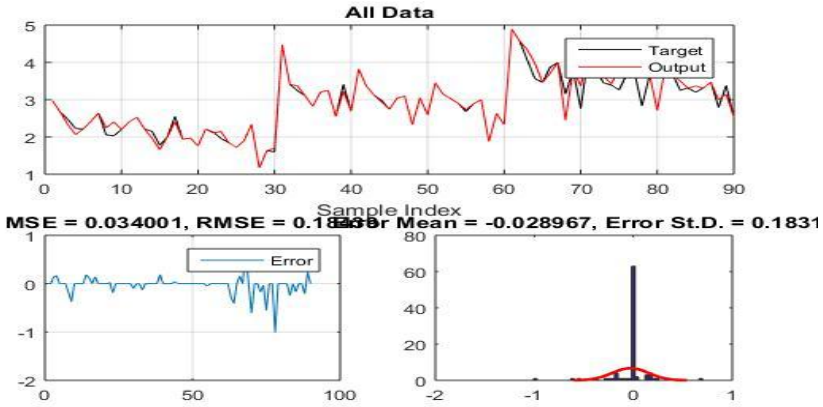

Fig. 6.15: The comparison of the output and target split tensile strength verses all data samples for ANFIS modelling.

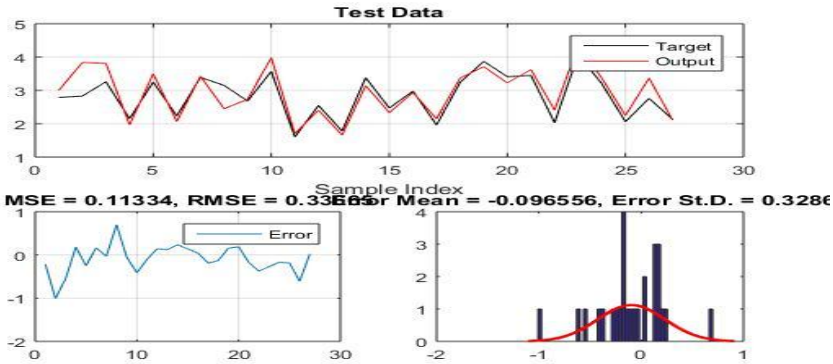

Fig. 6.16: The comparison of the output and target values of the split tensile strength verses test data samples for ANFIS modelling

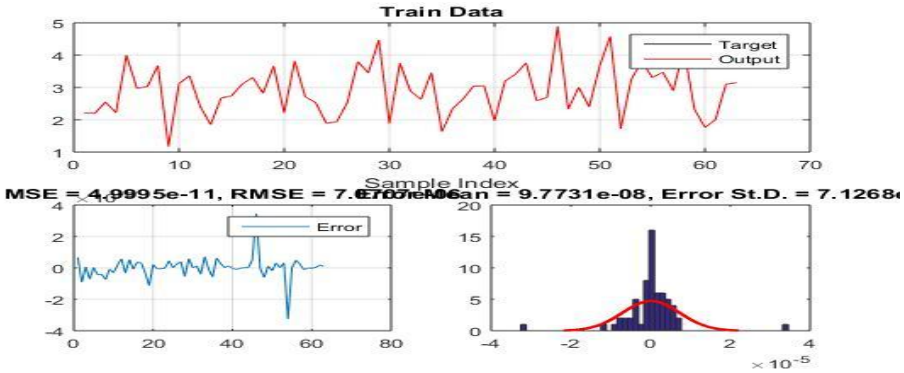

Fig. 6.17: The comparison of the output and target values of the split tensile strength verses training data samples for ANFIS modelling.

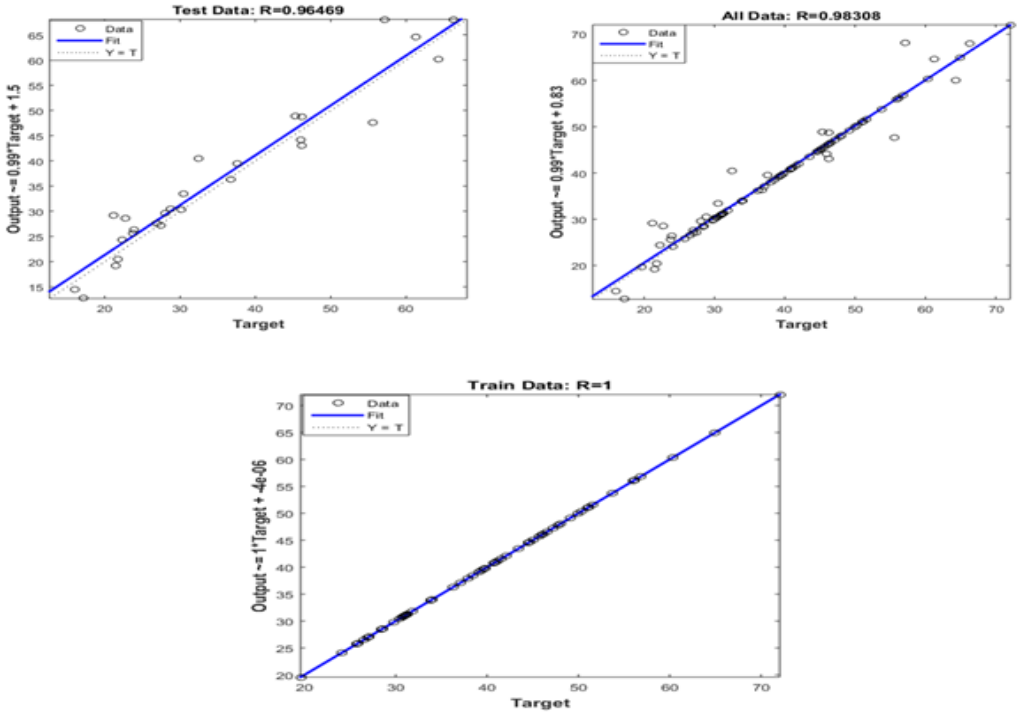

Fig. 6.18: The correlation between the ANFIS output and target values of compressive strength for training, testing and all data.

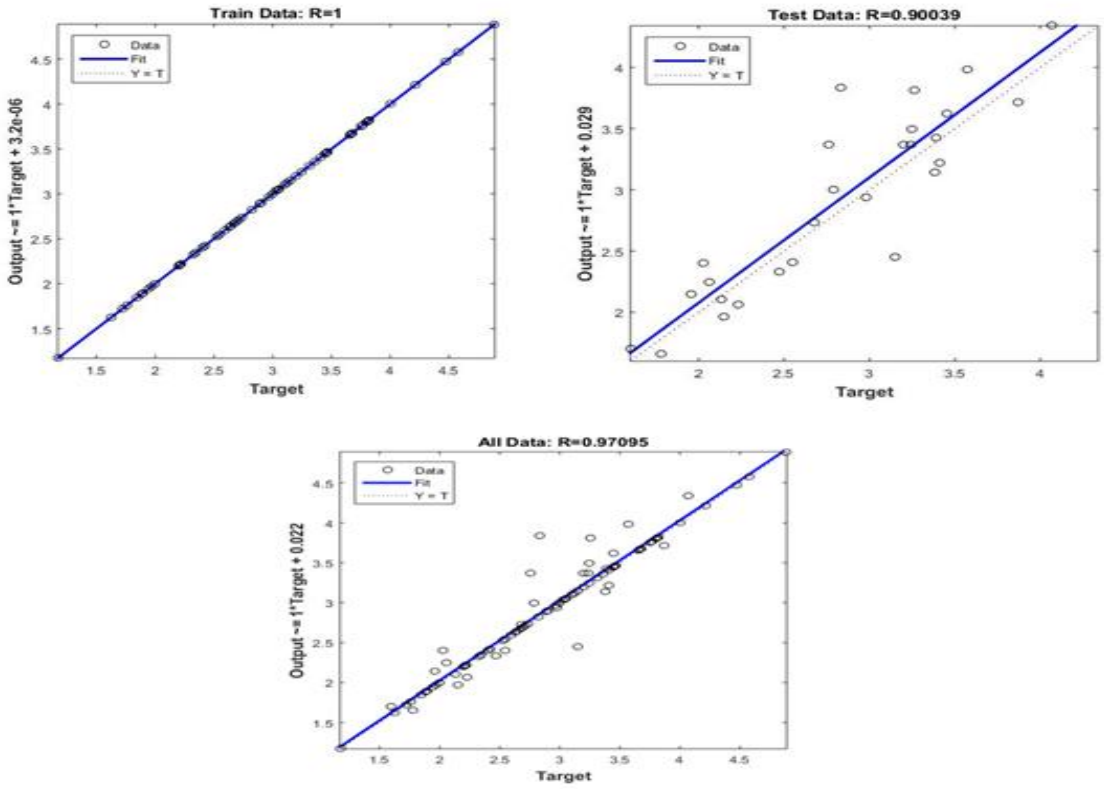

Fig. 6.19: The correlation between the ANFIS output and target values of split tensile strength for training, testing and all data.

Table 6.4: Predicted compressive and split tensile strength by ANFIS Model

S. No.	Concrete mix Design as depicted in Table 3.15 to 3.18	Curing Age (Days)	W/B Ratio	Compressive Strength (MPa)		Split Tensile Strength (MPa)	
				Experimental Values	ANFIS Predicted Values	Experimental Values	ANFIS Predicted Values
1.	1	7	0.40	41.5	41.49999613	2.67	2.669994765
2.	2	7	0.40	39.82	39.82000425	2.47	2.330243385
3.	3	7	0.40	30.80	30.79999696	2.23	2.065046676
4.	4	7	0.40	27.50	27.12873173	2.21	2.209997883
5.	5	7	0.40	29.81	29.80999746	2.42	2.419994215
6.	6	7	0.40	31.24	31.24000215	2.64	2.63999719

7.	7	7	0.40	21.12	29.16179349	2.06	2.244988768
8.	8	7	0.40	29.77	29.77000004	2.03	2.403617507
9.	9	7	0.40	25.85	25.85000016	2.20	2.200009151
10.	Control	7	0.40	39.80	39.80000469	2.97	2.970004457
11.	1	7	0.44	30.97	30.97000205	2.53	2.530000075
12.	2	7	0.44	31.00	30.99998052	2.22	2.22000723
13.	3	7	0.44	29.83	29.82999822	2.15	1.965949323
14.	4	7	0.44	26.94	27.55248073	1.78	1.657882815
15.	5	7	0.44	28.82	30.45885392	2.00	1.999999737
16.	6	7	0.44	30.42	30.4200188	2.55	2.406227333
17.	7	7	0.44	19.58	19.57999882	1.94	1.939999899
18.	8	7	0.44	25.74	25.73997815	1.97	1.970000262
19.	9	7	0.44	23.96	26.33263902	1.76	1.760000123
20.	Control	7	0.44	30.50	33.41261392	2.40	2.399998721
21.	1	7	0.48	28.60	28.59999569	2.13	2.10761529
22.	2	7	0.48	28.38	28.37998411	1.96	2.14674038
23.	3	7	0.48	26.48	26.48001205	1.85	1.850003248
24.	4	7	0.48	21.48	19.14868068	1.72	1.719999903
25.	5	7	0.48	22.30	24.33765098	1.89	1.889995564
26.	6	7	0.48	22.73	28.55074418	2.34	2.33999372
27.	7	7	0.48	16.06	14.4415056	1.17	1.170000815
28.	8	7	0.48	21.78	20.47791822	1.63	1.630005819
29.	9	7	0.48	17.16	12.69583832	1.60	1.702073353
30.	Control	7	0.48	27.00	26.99998849	2.21	2.209993467
31.	1	28	0.40	53.76	53.76000289	3.41	3.410000132
32.	2	28	0.40	50.32	50.3200175	3.24	3.369027273
33.	3	28	0.40	46.20	43.03396048	3.10	3.099998174
34.	4	28	0.40	39.60	39.60000262	2.82	2.820003248
35.	5	28	0.40	40.92	40.92000093	3.20	3.200001055
36.	6	28	0.40	49.94	49.93999909	3.25	3.249996841
37.	7	28	0.40	31.21	31.20999964	2.55	2.549999402
38.	8	28	0.40	49.14	49.13999366	3.41	3.221519161

39.	9	28	0.40	30.88	30.88000231	2.69	2.689995131
40.	Control	28	0.40	51.05	51.04997835	4.47	4.469994196
41.	1	28	0.44	47.83	47.82999415	3.36	3.359998435
42.	2	28	0.44	45.68	45.67999143	3.12	3.120003088
43.	3	28	0.44	40.79	40.7900207	2.98	2.937065152
44.	4	28	0.44	37.14	37.13999775	2.74	2.740000776
45.	5	28	0.44	37.62	39.52500224	3.04	3.039999787
46.	6	28	0.44	46.60	46.59998026	3.10	3.099996276
47.	7	28	0.44	27.03	27.02999856	2.33	2.330000084
48.	8	28	0.44	37.95	37.95003201	3.05	3.0499988
49.	9	28	0.44	28.08	29.61307114	2.59	2.589999871
50.	Control	28	0.44	45.13	45.13000651	3.82	3.820000632
51.	1	28	0.48	46.05	46.04999408	3.15	3.149999041
52.	2	28	0.48	45.02	45.02002183	3.03	3.03000405
53.	3	28	0.48	39.82	39.81998935	2.90	2.899997627
54.	4	28	0.48	30.23	30.33379373	2.68	2.732340694
55.	5	28	0.48	33.96	33.9600024	2.89	2.890004042
56.	6	28	0.48	39.08	39.07998729	3.00	3.000006151
57.	7	28	0.48	23.76	25.63011707	1.88	1.879999878
58.	8	28	0.48	31.82	31.82000591	2.63	2.629992937
59.	9	28	0.48	24.11	24.10999968	2.33	2.330000375
60.	Control	28	0.48	42.06	42.06000725	3.45	3.450005521
61.	1	90	0.40	72.05	72.04999705	4.58	4.579996893
62.	2	90	0.40	64.35	60.08588752	4.07	4.339463024
63.	3	90	0.40	51.18	51.17999667	3.57	3.980757292
64.	4	90	0.40	44.55	44.54998601	3.46	3.460000801
65.	5	90	0.40	46.20	46.20000851	3.87	3.711423156
66.	6	90	0.40	66.33	68.01360399	4.00	3.999999759
67.	7	90	0.40	36.22	36.2199927	3.15	2.450267922
68.	8	90	0.40	64.90	64.90000517	3.80	3.799996141
69.	9	90	0.40	39.38	39.38000457	2.76	3.36948454
70.	Control	90	0.40	55.64	47.62513745	4.89	4.8899655

71.	1	90	0.44	61.33	64.60448713	3.76	3.759999864
72.	2	90	0.44	56.21	56.20999636	3.45	3.623821339
73.	3	90	0.44	48.11	48.11000698	3.39	3.423509633
74.	4	90	0.44	43.45	43.45000999	3.26	3.810406197
75.	5	90	0.44	45.34	48.8551834	3.67	3.670001793
76.	6	90	0.44	60.35	60.3499932	3.75	3.749998848
77.	7	90	0.44	33.81	33.80995568	2.83	3.838009131
78.	8	90	0.44	51.62	51.61999544	3.66	3.660011297
79.	9	90	0.44	36.74	36.28834618	2.71	2.710000436
80.	Control	90	0.44	47.20	47.20000225	4.21	4.210001115
81.	1	90	0.48	57.09	68.07460176	3.68	3.680007421
82.	2	90	0.48	55.96	55.9600099	3.25	3.498430096
83.	3	90	0.48	45.98	44.17953859	3.31	3.310000084
84.	4	90	0.48	38.50	38.5000029	3.20	3.3664596
85.	5	90	0.48	41.09	41.09000139	3.31	3.3099969
86.	6	90	0.48	56.77	56.77000444	3.47	3.469995091
87.	7	90	0.48	31.10	31.10000814	2.79	3.000738882
88.	8	90	0.48	44.73	44.72999902	3.38	3.143916044
89.	9	90	0.48	32.45	40.47576797	2.53	2.529997557
90.	Control	90	0.48	46.20	48.72752419	3.81	3.810032547

To examine the performance of the ANFIS model, five indices were determined from the ANFIS predicted values both for compressive & split tensile strength. These indices are 1.Root mean squared error (RMSE), 2. Determination coefficients (R^2), 3.Mean absolute percentage error (MAPE), 4. Integral absolute error (IAE) and 5. Mean absolute error (MAE) between the predicted values and experimental values calculated using the equations given in the Table. 6.5. Where t and o are the target and the predicted value of the network respectively, and n is the total number of patterns and $\bar{t}$ is the average of the target values. It is considered that a prediction is better if the values of RMSE, MAPE, and IAE are close to zero and R^2 is close to one. From the performance indices shown in Table 6.5, it is observed that the calculated values of above mentioned performance indices are very close to the permissible limits and hence ANFIS models predicted the compressive and split tensile strength very accurately.

Table 6.5: Performance Indices of ANFIS model

S. No.	Performance indices	Formula	For compressive Strength	For Split Tensile Strength
			Value	Value
1	RMSE	$\text{RMSE} = \sqrt{\frac{1}{n}\sum_{i=1}^{n}(ti - oi)^2}$	0.2911	0.1844
2	R^2	$R^2 = 1 - \frac{\sum_{i=1}^{n}(ti-oi)^2}{\sum_{i=1}^{n}(ti-\bar{t}\bar{i})^2}$	0.9652	0.9374
3	MAPE	$\text{MAPE} = \frac{1}{n}\left[\frac{\sum_{i=1}^{n}\lvert ti-oi\rvert}{\sum_{i=1}^{n} ti} \times 100\right]$	0.02755%	0.0292
4	IAE	$\text{IAE} = \frac{\sum_{i=1}^{n}[(ti-oi)^2]^{1/2}}{\sum_{i=1}^{n} ti} \times 100$	0.6219%	0.6741
5	MAE	$\text{MAE} = \frac{1}{n}[\sum_{i=1}^{n}\lvert ti - oi\rvert]$	0.9627	0.0757

Table 6.6: Regression equations and the values of the correlation coefficient (R)

S. No.	Type of data	Regression Equations		Correlation coefficient (R)	
		Compressive strength model	Split tensile strength model	Compressive Strength model	split tensile strength model
1.	Training data	Output= 1xTarget+4e-06	Output= 1xTarget+3.2e-06	1	1
2.	Testing data	Output= 0.99xTarget+1.5	Output= 1.0xTarget+0.029	0.96469	0.90039
3.	Overall data	Output= 0.99xTarget+0.83	Output= 1xTarget+0.022	0.98308	0.97095

The regression equations and coefficient of correlation (R) calculated for training, testing, and validation for the whole data for the compressive & split tensile strength is shown in Table. 6.6. The correlation coefficients are 1.00 for training, 0.96469 for testing and 0.98308 for all data in predicting the compressive strength, whereas these are 1.00 for training, 0.90039 for testing and 0.97095 for all data in predicting the split tensile strength as shown in Table 6.6. It is established that the network is considered more precise and meaningful from the statistical angle if the value of coefficients of correlation approaches near to one. From this table, we see that the overall values of the correlation coefficients (R) are close to one. Therefore, it is concluded that there is no significant variation between the experimental values and ANFIS predicted values at 95% confidence level.

6.3 MODELING TO PREDICT DEPTH OF WEAR FOR ABRASION STRENGTH USING ANN APPROACH

By following the same procedure described in section 6.1, ANN was applied to the input parameters and output response to develop model for the prediction of the depth of wear for abrasion strength. A total of 90 readings were taken to measure depth of wear of concrete made with different level settings of input parameters. Table 6.7 shows the actual experimental data and ANN predicted values. The comparison between the predicted results from the FFBP neural network and the experimental results for depth of wear is shown in Fig. 6.20 which shows a close relationship between the two results for depth of wear. Fig. 6.21 displays the learning behaviour of the FFBP neural network model and Fig. 6.22 shows mean square error (MSE) gradient for depth of wear with the 11 epochs during training of the this network model.

Table 6.7: Experimental data and ANN predicted results for depth of wear

S. No.	Concrete mix Design as depicted in Table 3.15 to 3.18	Curing Age (Days)	W/B Ratio	Depth of wear (mm)	
				Experimental Values	Predicted Values by ANN Model
1.	1	7	0.40	0.418	0.39872
2.	2	7	0.40	0.362	0.35893
3.	3	7	0.40	0.339	0.35897
4.	4	7	0.40	0.326	0.32252
5.	5	7	0.40	0.376	0.35468
6.	6	7	0.40	0.330	0.32979
7.	7	7	0.40	0.335	0.34028
8.	8	7	0.40	0.345	0.36257
9.	9	7	0.40	0.342	0.36142
10.	Control	7	0.40	0.476	0.47406
11.	1	7	0.44	0.453	0.43116
12.	2	7	0.44	0.364	0.36948
13.	3	7	0.44	0.385	0.38759

14.	4	7	0.44	0.382	0.38036
15.	5	7	0.44	0.387	0.39662
16.	6	7	0.44	0.331	0.34314
17.	7	7	0.44	0.394	0.42821
18.	8	7	0.44	0.426	0.41708
19.	9	7	0.44	0.440	0.44646
20.	Control	7	0.44	0.504	0.48134
21.	1	7	0.48	0.456	0.45480
22.	2	7	0.48	0.422	0.46286
23.	3	7	0.48	0.387	0.39066
24.	4	7	0.48	0.470	0.45762
25.	5	7	0.48	0.392	0.40582
26.	6	7	0.48	0.357	0.40760
27.	7	7	0.48	0.458	0.45152
28.	8	7	0.48	0.503	0.49596
29.	9	7	0.48	0.491	0.46725
30.	Control	7	0.48	0.572	0.58203
31.	1	28	0.40	0.342	0.33915
32.	2	28	0.40	0.263	0.26573
33.	3	28	0.40	0.321	0.32251
34.	4	28	0.40	0.322	0.32522
35.	5	28	0.40	0.356	0.33048
36.	6	28	0.40	0.306	0.29536
37.	7	28	0.40	0.316	0.30996
38.	8	28	0.40	0.323	0.32060
39.	9	28	0.40	0.336	0.33176
40.	Control	28	0.40	0.355	0.37097
41.	1	28	0.44	0.358	0.36534
42.	2	28	0.44	0.265	0.28423
43.	3	28	0.44	0.330	0.32218
44.	4	28	0.44	0.352	0.37395
45.	5	28	0.44	0.360	0.33734

46.	6	28	0.44	0.317	0.30581
47.	7	28	0.44	0.358	0.35806
48.	8	28	0.44	0.337	0.34563
49.	9	28	0.44	0.365	0.37491
50.	Control	28	0.44	0.374	0.39430
51.	1	28	0.48	0.389	0.39349
52.	2	28	0.48	0.383	0.37714
53.	3	28	0.48	0.370	0.31569
54.	4	28	0.48	0.394	0.40138
55.	5	28	0.48	0.365	0.31845
56.	6	28	0.48	0.328	0.33150
57.	7	28	0.48	0.363	0.36598
58.	8	28	0.48	0.370	0.40301
59.	9	28	0.48	0.380	0.38713
60.	Control	28	0.48	0.498	0.49614
61.	1	90	0.40	0.323	0.29528
62.	2	90	0.40	0.224	0.23672
63.	3	90	0.40	0.312	0.30803
64.	4	90	0.40	0.314	0.28965
65.	5	90	0.40	0.234	0.23305
66.	6	90	0.40	0.240	0.24741
67.	7	90	0.40	0.275	0.28290
68.	8	90	0.40	0.289	0.28554
69.	9	90	0.40	0.285	0.24557
70.	Control	90	0.40	0.330	0.32614
71.	1	90	0.44	0.336	0.33441
72.	2	90	0.44	0.246	0.24581
73.	3	90	0.44	0.313	0.32344
74.	4	90	0.44	0.315	0.32163
75.	5	90	0.44	0.250	0.25334
76.	6	90	0.44	0.288	0.28218
77.	7	90	0.44	0.339	0.32274

78.	8	90	0.44	0.293	0.29451
79.	9	90	0.44	0.294	0.29197
80.	Control	90	0.44	0.355	0.36600
81.	1	90	0.48	0.379	0.38184
82.	2	90	0.48	0.352	0.33246
83.	3	90	0.48	0.347	0.33645
84.	4	90	0.48	0.340	0.33879
85.	5	90	0.48	0.339	0.29373
86.	6	90	0.48	0.313	0.30897
87.	7	90	0.48	0.340	0.34611
88.	8	90	0.48	0.341	0.34464
89.	9	90	0.48	0.351	0.35052
90.	Control	90	0.48	0.409	0.40859

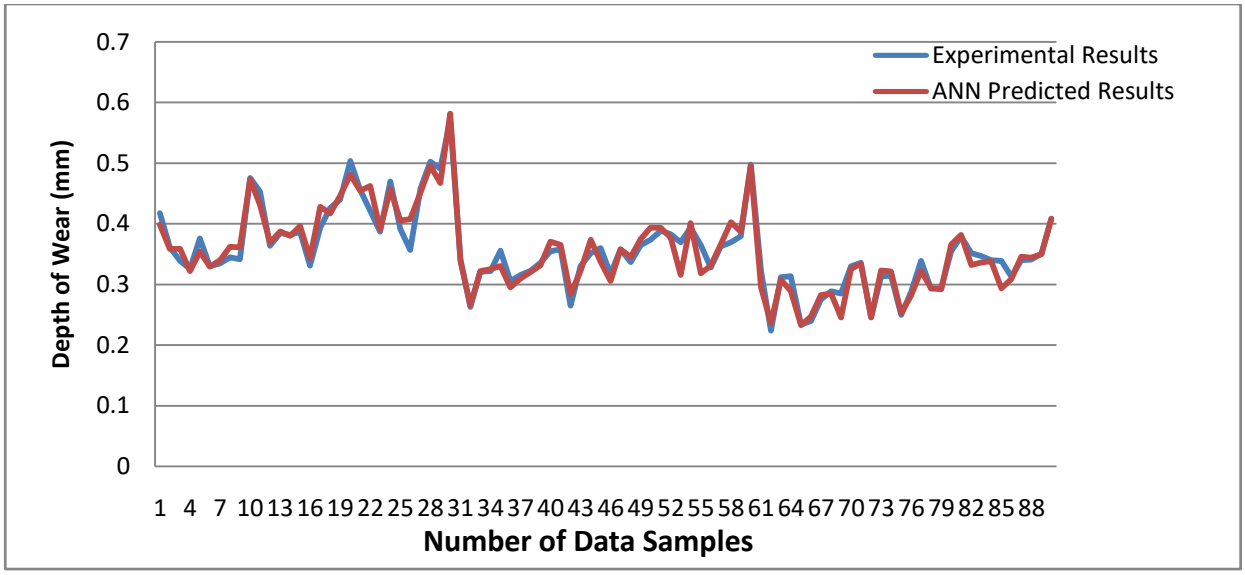

Fig. 6.20: The comparison of the predicted and experimental/target depth of wear verses all data samples for ANN modelling

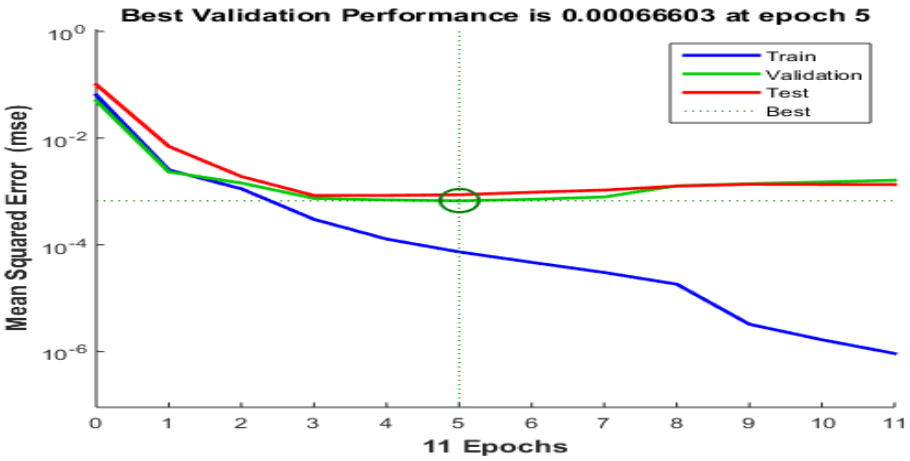

Fig. 6.21: Learning behaviour of the FFBP neural network model for depth of wear

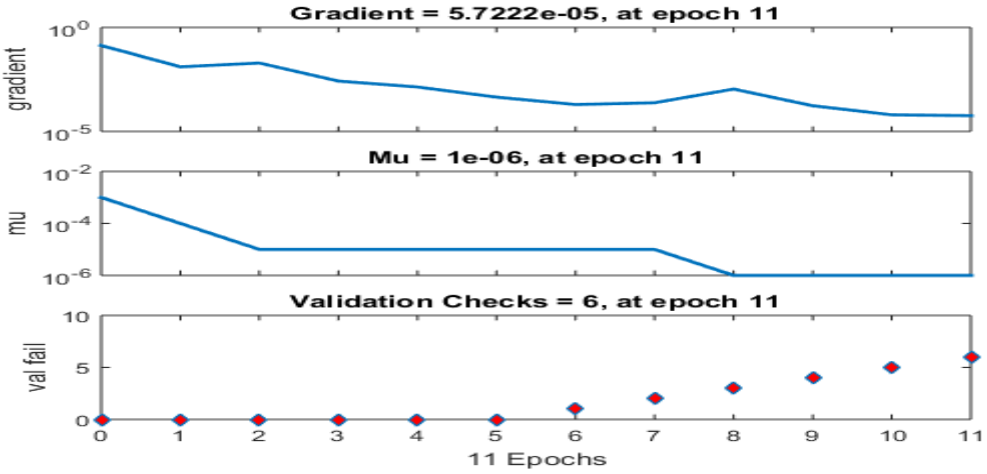

Fig. 6.22: The performance results of FFBP algorithm

In addition, to find the performance of the network, a linear regression between the network output response values and the target values was performed. In the present model, the whole data of depth of wear were fed to the model for training, validation and testing to perform the regression analysis. The obtained results from the regression have been given separately for the output, which are shown in Fig. 6.23. The coefficients of correlation are 0.993 for training data, 0.898 for validation data, 0.849 for testing data and 0.965 for overall data for predicting the depth of wear are shown in Table 6.8. From the statistical point of view, the network is considered more accurate and powerful if the value of correlation coefficients is near to one. Therefore, it is concluded that there is no significant variation between the experimental outcomes and ANN estimated value at 95% confidence level.

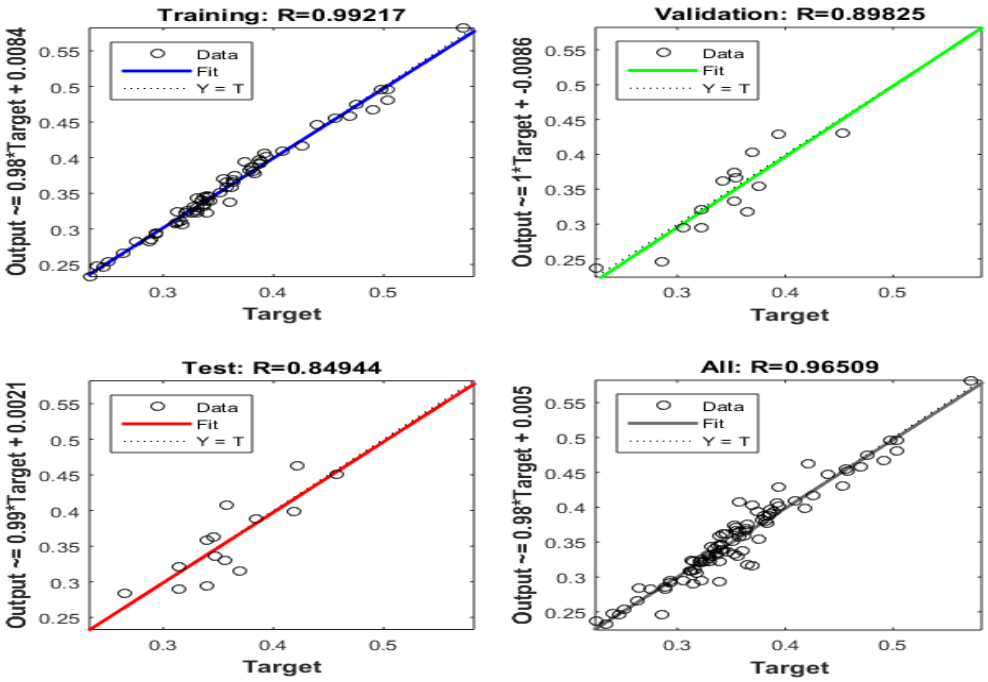

Fig. 6.23: The correlation between the FFBP-ANN predicted values and experimental values of depth of wear for training, testing, validation and all data.

Table 6.8: Regression equations and values of the correlation coefficient (R)

S. No.	Type of data	Regression equations	Correlation Coefficient (R)
1.	Training data	Output= 0.98xTarget+0.0084	0.993
2.	Testing data	Output= 0.99xTarget+0.0021	0.849
3.	Validation data	Output= 1xTarget+0.0086	0.898
4.	Overall data	Output= 0.98xTarget+0.005	0.965

Five indices were found to calculate the performance factors of the ANN model in predicting depth of wear. These indices are the root mean squared error (RMSE), determination coefficients (R^2), mean absolute percentage error (MAPE), integral absolute error (IAE) and mean absolute error (MAE) which are calculated using the equations given in the Table 6.9 for the predicted and experimental results. Where t and o are the target and the predicted value of the network respectively, and n is the total number of experiments and $\bar{t}$ is the average of the target values. The predicted value is considered better when the value of RMSE, MAPE, and IAE is near to zero and the value of R^2 is near to one. From the statistical

values of the indices shown in Table 6.9, it is seen that the ANN model predicted the depth of wear very accurately.

Table 6.9: Statistical values of proposed ANN model

S. No.	Performance indices	Formula	Value
1	RMSE	$\text{RMSE} = \sqrt{\frac{1}{n}\sum_{i=1}^{n}(ti - oi)^2}$	0.017
2	R^2	$R^2 = 1 - \frac{\sum_{i=1}^{n}(ti-oi)^2}{\sum_{i=1}^{n}(ti-\bar{t})^2}$	0.928
3	MAPE	$\text{MAPE} = \frac{1}{n}\left[\frac{\sum_{i=1}^{n}\lvert ti-oi\rvert}{\sum_{i=1}^{n} ti} \times 100\right]$	0.0368
4	IAE	$\text{IAE} = \frac{\sum_{i=1}^{n}[(ti-oi)^2]^{1/2}}{\sum_{i=1}^{n} ti} \times 100$	0.502
5	MAE	$\text{MAE} = \frac{1}{n}[\sum_{i=1}^{n}\lvert ti - oi\rvert]$	0.0118

6.4 COMPARISION OF ANN AND ANFIS MODELS

6.4.1 COMPRESSIVE STRENGTH

The ANN and ANFIS models which were developed in the current work were used to predict the compressive strength of concrete containing industrial by-products. These two models were compared to know which model is better predicting the compressive strength. So to compare these two models, five indices which were determined for evaluating the performance of the ANN and ANFIS models in predicting compressive strength in the previous section were compared and are given in Table 6.10. These indices are the root mean squared error (RMSE), determination coefficients (R^2), Mean absolute percentage error (MAPE), Integral absolute error (IAE) and mean absolute error (MAE) between the predicted and experimental results. The t and o are the target and the predicted value of the network respectively, and n is the total number of experiments and $\bar{t}$ is the average of the target values. From the statistical point of view, predicted value is considered better when the values of RMSE, MAPE, and IAE is near to zero and the value of R^2 is near to one. So comparing the values of indices from the Table 6.10 for ANN and ANFIS models, it is observed that better results have been shown by ANFIS model for all the performance indices than the ANN model.

Table 6.10: Statistical results of proposed ANN and ANFIS models

S. No.	Performance indicators	Formula	ANN	ANFIS
1	RMSE	$\text{RMSE} = \sqrt{\frac{1}{n}\sum_{i=1}^{n}(ti - oi)^2}$	0.717	0.2911
2	R^2	$R^2 = 1 - \frac{\sum_{i=1}^{n}(ti-oi)^2}{\sum_{i=1}^{n}(ti-\bar{t}i)^2}$	0.659	0.9652
3	MAPE	$\text{MAPE} = \frac{1}{n}\left[\frac{\sum_{i=1}^{n}\lvert ti-oi\rvert}{\sum_{i=1}^{n} ti} \times 100\right]$	0.1047%	0.02755%
4	IAE	$\text{IAE} = \frac{\sum_{i=1}^{n}\left[(ti-oi)^2\right]^{1/2}}{\sum_{i=1}^{n} ti} \times 100$	1.946%	0.6219%
5	MAE	$\text{MAE} = \frac{1}{n}[\sum_{i=1}^{n}\lvert ti - oi\rvert]$	3.661	0.9627

The correlation coefficient (R) found for the ANN and ANFIS models for training data, validation data, testing data and all data is presented in Table.6.11.

Table 6.11: The values of the coefficient of correlation (R)

Model	Training Data	Testing Data	Validation Data	Overall Data
ANN	1	0.94141	0.93129	0.97729
ANFIS	1	0.96469	-	0.98308

From this table, again we see that the overall value of the correlation factor (R) for the ANN model is 0.97729 and while for the ANFIS model is 0.98308, which is better and closer to one. It was concluded that the prediction of the compressive strength is better by the ANFIS model than the ANN model.

CHAPTER 7 CONCLUSIONS

The followings are the conclusions which could be derived from the experimental and analytical work and are presented here:

7.1 STRENGTH PROPERTIES ANALYSED WITH ANOVA

- The highest compressive strength is achieved by partially replacing 10% of cement and 30% of sand with industry by-products at all curing periods.
- Fly ash is the optimal by-product among the chosen by-products for the partial replacement of cement to achieve the highest compressive and split tensile strength.
- Iron slag may be used as fine aggregate partial replacement material for 90 days of curing to achieve highest compressive and split tensile strength.
- Fly-ash and glass powder are good replacements for cement and sand, respectively at 28 days curing for achieving the highest compressive and tensile strengths of concrete.
- Concrete with high compressive strength of up to 80 MPa could be manufactured using the optimum ternary combinations of industrial by-products.
- Electric arc furnace slag as partial replacement material for sand, gives the maximum compressive strength and split tensile strength for 7 days of curing but as the curing period increases to 28 days, glass powder as the sand replacement material gives the maximum compressive and split tensile strength.
- For all the water/binder ratios, the percentage of by-product to be used as binder is the most significant factor that affects compressive and split tensile strength followed by the type of by-product used as partial replacement of binder and percentage of by-product used as partial replacement of fine aggregates. The effect of type of by-product used as a fine-aggregate was found to be insignificant.
- The confirmation experiment conducted to verify the optimum mix proportions of concrete made with industrial by-products resulted in more compressive and split tensile strengths than all other mixes and control mixes at 28 days of curing. This increase in compressive and split tensile strength is attributed to the synergic effect of optimal by-products due to their pozzolanic activity and cementitious properties.

7.2 DURABILITY PROPERTIES ANALYSED WITH ANOVA

- For lowest depth of water penetration in concrete, the optimal combination of by-products are 10% of fly ash as cement replacement and 30% of iron slag as sand replacement at w/b ratio of 0.40 and at 90 days of curing.
- For lowest depth of wear in concrete, the optimal combination of by-products are 10% of fly ash and 20% of electric arc furnace slag at w/b ratio of 0.40 and 90 days of curing age.
- Fly-ash and glass powder are the most suitable partial replacements for cement and sand respectively, at 28 days curing for achieving the lowest depth of water penetration.
- 10% fly ash as cement replacement material and 20% electric arc furnace slag as sand replacement are the optimal parameters for achieving lowest depth of wear at 28 days of curing.
- The confirmation experiments conducted to verify the optimum mix proportions show that there is improvement in durability properties of the concrete mixture made with industrial by-products over the control concrete mix at all the w/b ratios and curing ages.

7.3 MULTI RESPONSE OPTIMIZATION OF STRENGTH PROPERTIES BY GREY RELATIONAL ANALYSIS

- Taguchi method with Grey relational analysis can be used efficiently and economically for designing the experiments and for multi-response optimization for strength properties.
- Fly ash at 10% level of the binder replacement content is the most optimum parameter which positively affects the strength characteristics of concrete at all water/binder ratios and at all curing ages.
- The optimal parameter for the replacement of cement at 7 and 28 days of curing period is the percentage of by-product as partial replacement i.e. 10 %, which contributes maximum to the compressive as well as split tensile strength.
- The optimal parameter for the replacement of cement at 90 days of curing period is the type of by-product i.e. Fly ash, which has the maximum contribution towards

strength gain, proving that Fly ash as a binder replacement contributes towards the strength gain at later ages due to its slow pozzolanic reaction.

- The optimal parameter for the replacement of fine aggregate is iron slag at 7 days of curing, but as curing period increases to 90 days, electric arc furnace slag contributes more to the strength characteristics in comparison to other parameters.
- The optimum percentage of the replacement for fine aggregate is 40% at 7 days curing, but it reduces to 30% at 28 and 90 days of curing.
- As water to binder ratio decreases from 0.48 to 0.40, the optimal by-product used as a replacement of fine aggregate changes from iron slag to electric arc furnace slag.
- The major contributor towards strength gain is the type of by-product used as a replacement for cement and not the type of by-product used as a replacement of fine aggregate.

7.4 MULTI RESPONSE OPTIMIZATION OF DURABILITY PROPERTIES BY GREY RELATIONAL ANALYSIS

- The optimal parameter for partial replacement of cement at 7, 28 & 90 days of curing period is the percentage of by-product as partial cement replacement i.e. 10 %, which contributes maximum to the durability of concrete.
- For more durable concrete, the optimal parameters for the replacement of cement and sand at 90 days of curing period and at water/binder ratio of 0.40 are 10% fly ash and 20% electric arc furnace slag respectively.
- The optimal durability parameters for partial replacement of cement and sand at 28 days of curing period and at water/binder ratio of 0.40 are 10% fly ash as cement replacement and 20% glass powder, respectively.
- As seen from the results of the confirmation experiment, the improvement in durability of the concrete i.e. less depth of water penetration and less depth of wear of concrete made with industrial by-products is due to the synergic effect of ternary combination of by-products

.

7.5 MULTI RESPONSE OPTIMIZATION OF STRENGTH AND DURABILITY PROPERTIES BY GREY RELATIONAL ANALYSIS

- 10% of the fly ash is the optimal parameter for cement replacement for more strength and durability properties at all the curing ages and water to binder ratios.
- 20% is the optimal replacement level of sand replacement for all the water to binder ratios and at all the curing ages.
- The optimal parameter for sand replacement material changes from iron slag at 7 days curing to electric arc furnace slag at 90 days curing.
- The percentage of cement replacement material parameter i.e. 10%, contributes maximum towards the strength and durability of concrete at 7 and 28 days but at 90 days, it is the type of cement replacement material parameter i.e. fly ash, which contributes maximum. This change is attributed to the slow pozzolanic reaction of the fly ash at early ages.
- The confirmation experiment conducted to verify the optimum mix proportions of concrete made with ternary combination of industrial by-products resulted in more compressive and split tensile strength and less depth of water penetration and wear than all other mixes and control mixes at 28 days of curing. This improvement in strength and durability properties is attributed to the synergic effect of optimal by-products due to their pozzolanic activity and cementitious properties.

7.6 MODELING BY ANN AND ANFIS

- The neural network and ANFIS models could predict the strength and durability properties of concrete containing ternary combination of industrial by-products with satisfactory performance results.
- The predicted values of the compressive strength of concrete from ANFIS model are highly accurate. Moreover, the comparison of the performance indices showed that the ANFIS model provided better estimates than the ANN model.
- In general, the proposed ANN and ANFIS models are highly applicable and reliable for predicting the compressive strength of concrete containing ternary combination of industrial by-products as partial replacement of cement and sand.

7.7 SCOPE FOR FURTHER WORK

- The present research work can be further expanded by taking other alternative industrial by-products and waste materials to be replaced as cement and fine aggregates.
- The replacement percentage of the by-products can be varied to other levels.
- The other properties of strength and durability of the concrete could be taken for further investigation.

LIST OF PUBLICATIONS

1. Bansal V.K., Kumar M., Bansal P.P. and Batish A., "Utilisation of industrial by-products in concrete applications by adopting Grey Taguchi method for optimisation." ***International Journal of Structural and Construction Engineering***, 12 (2018): 1165-1176.
2. Bansal V.K., Kumar M., Bansal P.P. and Batish A., "Predicting compressive strength of concrete containing ternary combination of industrial by-products as partial replacement of cement and fine aggregates using ANN and ANFIS." ***International Journal of Latest Trends in Engineering and Technology,*** 11 (2018): 42-57.

ANNEXURE- A

```
% ANN Advance Script
% Solve an Input-Output Fitting problem with a Neural Network
% Script generated by Neural Fitting app
% This script assumes these variables are defined:
%
%   Inputs - input data.
%   Targets - target data.
data=xlsread('C:\Users\VK Bansal\Desktop\Normalized data.xlsx');
Inputs= data(1:1:end,1:9);
Targets=data(1:1:end,11);
x = Inputs';
t = Targets';

% Choose a Training Function
% For a list of all training functions type: help nntrain
% 'trainlm' is usually fastest.
% 'trainbr' takes longer but may be better for challenging problems.
% 'trainscg' uses less memory. Suitable in low memory situations.
trainFcn = 'trainlm';  % Levenberg-Marquardt backpropagation.

% Create a Fitting Network
hiddenLayerSize = 20;
net = fitnet(hiddenLayerSize,trainFcn);

% Choose Input and Output Pre/Post-Processing Functions
% For a list of all processing functions type: help nnprocess
net.input.processFcns = {'removeconstantrows','mapminmax'};
net.output.processFcns = {'removeconstantrows','mapminmax'};

% Setup Division of Data for Training, Validation, Testing
% For a list of all data division functions type: help nndivide
```

```
net.divideFcn = 'dividerand';  % Divide data randomly
net.divideMode = 'sample';  % Divide up every sample
net.divideParam.trainRatio = 70/100;
net.divideParam.valRatio = 15/100;
net.divideParam.testRatio = 15/100;

% Choose a Performance Function
% For a list of all performance functions type: help nnperformance
net.performFcn = 'mse';  % Mean Squared Error

% Choose Plot Functions
% For a list of all plot functions type: help nnplot
net.plotFcns = {'plotperform','plottrainstate','ploterrhist', ...
    'plotregression', 'plotfit'};

% Train the Network
[net,tr] = train(net,x,t);

% Test the Network
y = net(x);
e = gsubtract(t,y);
performance = perform(net,t,y)

% Recalculate Training, Validation and Test Performance
trainTargets = t .* tr.trainMask{1};
valTargets = t .* tr.valMask{1};
testTargets = t .* tr.testMask{1};
trainPerformance = perform(net,trainTargets,y)
valPerformance = perform(net,valTargets,y)
testPerformance = perform(net,testTargets,y)

% View the Network
view(net)
```

```
% Plots
% Uncomment these lines to enable various plots.
figure, plotperform(tr)
figure, plottrainstate(tr)
figure, ploterrhist(e)
figure, plotregression(t,y)
figure, plotfit(net,x,t)

% Deployment
% Change the (false) values to (true) to enable the following code blocks.
% See the help for each generation function for more information.
if (false)
    % Generate MATLAB function for neural network for application
    % deployment in MATLAB scripts or with MATLAB Compiler and Builder
    % tools, or simply to examine the calculations your trained neural
    % network performs.
    genFunction(net,'myNeuralNetworkFunction');
    y = myNeuralNetworkFunction(x);
end
if (false)
    % Generate a matrix-only MATLAB function for neural network code
    % generation with MATLAB Coder tools.
    genFunction(net,'myNeuralNetworkFunction','MatrixOnly','yes');
    y = myNeuralNetworkFunction(x);
end
if (false)
    % Generate a Simulink diagram for simulation or deployment with.
    % Simulink Coder tools.
    gensim(net);
end
```

ANNEXURE-B

```
% ANFIS Program
clc;
clear;
close all;

data=xlsread('C:\Users\VK Bansal\Desktop\Normalized data.xlsx');
Inputs= data(1:1:end,1:9);
Targets=data(1:1:end,11);

nData = size(Inputs,1);

%Targets = Targets(:,2); % Select 1st Output to Model

%% Shuffling Data

PERM = randperm(nData); % Permutation to Shuffle Data

pTrain=0.70;
nTrainData=round(pTrain*nData);
TrainInd=PERM(1:nTrainData);
TrainInputs=Inputs(TrainInd,:);
TrainTargets=Targets(TrainInd,:);

pTest=1-pTrain;
nTestData=nData-nTrainData;
TestInd=PERM(nTrainData+1:end);
TestInputs=Inputs(TestInd,:);
TestTargets=Targets(TestInd,:);

%% Selection of FIS Generation Method
```

```
Option{1}='Grid Partitioning (genfis1)';
Option{2}='Subtractive Clustering (genfis2)';
Option{3}='FCM (genfis3)';

ANSWER=questdlg('Select FIS Generation Approach:',...
            'Select GENFIS',...
            Option{1},Option{2},Option{3},...
            Option{3});
pause(0.01);

%% Setting the Parameters of FIS Generation Methods

switch ANSWER
   case Option{1}
      Prompt={'Number of MFs','Input MF Type:','Output MF Type:'};
      Title='Enter genfis1 parameters';
      DefaultValues={'5', 'gaussmf', 'linear'};

      PARAMS=inputdlg(Prompt,Title,1,DefaultValues);
      pause(0.01);

      nMFs=str2num(PARAMS{1});    %#ok
      InputMF=PARAMS{2};
      OutputMF=PARAMS{3};

      fis=genfis1([TrainInputs TrainTargets],nMFs,InputMF,OutputMF);

   case Option{2}
      Prompt={'Influence Radius:'};
      Title='Enter genfis2 parameters';
      DefaultValues={'0.3'};

      PARAMS=inputdlg(Prompt,Title,1,DefaultValues);
      pause(0.01);
```

```
        Radius=str2num(PARAMS{1});  %#ok

        fis=genfis2(TrainInputs,TrainTargets,Radius);

    case Option{3}
        Prompt={'Number fo Clusters:',...
            'Partition Matrix Exponent:',...
            'Maximum Number of Iterations:',...
            'Minimum Improvemnet:'};
        Title='Enter genfis3 parameters';
        DefaultValues={'13', '9', '200', '1e-5'};

        PARAMS=inputdlg(Prompt,Title,1,DefaultValues);
        pause(0.01);

        nCluster=str2num(PARAMS{1});        %#ok
        Exponent=str2num(PARAMS{2});        %#ok
        MaxIt=str2num(PARAMS{3});           %#ok
        MinImprovment=str2num(PARAMS{4});   %#ok
        DisplayInfo=1;
        FCMOptions=[Exponent MaxIt MinImprovment DisplayInfo];

        fis=genfis3(TrainInputs,TrainTargets,'sugeno',nCluster,FCMOptions);
end

%% Training ANFIS Structure

Prompt={'Maximum Number of Epochs:',...
        'Error Goal:',...
        'Initial Step Size:',...
        'Step Size Decrease Rate:',...
        'Step Size Increase Rate:'};
Title='Enter genfis3 parameters';
```

```
DefaultValues={'200', '0', '0.01', '0.9', '1.1'};

PARAMS=inputdlg(Prompt,Title,1,DefaultValues);
pause(0.01);

MaxEpoch=str2num(PARAMS{1});              %#ok
ErrorGoal=str2num(PARAMS{2});             %#ok
InitialStepSize=str2num(PARAMS{3});       %#ok
StepSizeDecreaseRate=str2num(PARAMS{4});  %#ok
StepSizeIncreaseRate=str2num(PARAMS{5});  %#ok
TrainOptions=[MaxEpoch ...
        ErrorGoal ...
        InitialStepSize ...
        StepSizeDecreaseRate ...
        StepSizeIncreaseRate];

DisplayInfo=true;
DisplayError=true;
DisplayStepSize=true;
DisplayFinalResult=true;
DisplayOptions=[DisplayInfo ...
         DisplayError ...
         DisplayStepSize ...
         DisplayFinalResult];

OptimizationMethod=1;
% 0: Backpropagation
% 1: Hybrid

fis=anfis([TrainInputs
TrainTargets],fis,TrainOptions,DisplayOptions,[],OptimizationMethod);



%% Apply ANFIS to Data
```

```
Outputs=evalfis(Inputs,fis);
TrainOutputs=Outputs(TrainInd,:);
TestOutputs=Outputs(TestInd,:);

%% Error Calculation

TrainErrors=TrainTargets-TrainOutputs;
TrainMSE=mean(TrainErrors.^2);
TrainRMSE=sqrt(TrainMSE);
TrainErrorMean=mean(TrainErrors);
TrainErrorSTD=std(TrainErrors);

TestErrors=TestTargets-TestOutputs;
TestMSE=mean(TestErrors.^2);
TestRMSE=sqrt(TestMSE);
TestErrorMean=mean(TestErrors);
TestErrorSTD=std(TestErrors);

%% Plot Results

figure(5);
PlotResults(TrainTargets,TrainOutputs,'Train Data');

figure(6);
PlotResults(TestTargets,TestOutputs,'Test Data');

figure(7);
PlotResults(Targets,Outputs,'All Data');

% if ~isempty(which('plotregression'))
%     figure;
%     plotregression(TrainTargets, TrainOutputs, 'Train Data', ...
%                    TestTargets, TestOutputs, 'Test Data', ...
```

```
%                   Targets, Outputs, 'All Data');
%     set(gcf,'Toolbar','figure');
% end
if ~isempty(which('plotregression'))
    figure;
    plotregression(TrainTargets, TrainOutputs, 'Train Data');
    figure
     plotregression(TestTargets, TestOutputs, 'Test Data');
     figure
     plotregression(Targets, Outputs, 'All Data');
    set(gcf,'Toolbar','figure');
end

figure;
gensurf(fis, [1 2], 1, [30 30]);
xlim([min(Inputs(:,1)) max(Inputs(:,1))]);
ylim([min(Inputs(:,2)) max(Inputs(:,2))]);
```

REFERENCES

Abdul Hakeem Zakariyya and Adeola A. Adedeji, (2015): "Artificial neural network estimation of self-compacting concrete in tension and compressive strengths", Webs journal of science and engineering application, vol. 5, pp. 276-285.

Adaway M. and Wang Y., (2015): "Recycled glass as a partial replacement for fine aggregate in structural concrete-effects on compressive strength", Electronic Journal of Structural Engineering, Vol. 14, pp. 116-122.

Adolfsson D., Ryan R., Fredrik E. and Bo B., (2011): "Influence of mineralogy on the hydraulic properties of ladle slag", Cement and Concrete Research, Vol. 41, pp. 865-571.

Afshinnia K. and Rangaraju P.R., (2015): "Efficiency of ternary blends containing fine glass powder in mitigating alkali–silica reaction", Construction and Building Materials, Vol. 100, pp. 234-245.

Alex J., J. Dhanalakshmi and B. Ambedkar, (2016): "Experimental investigation on rice husk ash as cement replacement on concrete production", Construction and Building Materials, Vol. 127, pp. 353–362.

Al-Jabri K.S., Hisada M., Al-Oraimi S.K. and Al-Saidy A.H., (2009): "Copper slag as sand replacement for high performance concrete", Cement & Concrete Composites, Vol. 31, pp. 483-488.

Al-Jabri K.S., Taha R.A., Al-Hashmi A. and Al-Harthy A.S., (2006): "Effect of copper slag and cement by-pass dust addition on mechanical properties of concrete", Construction and Building Materials, Vol. 20, pp. 322-331.

Al-Jabri, K.S., Al-Saidy A.H. and Taha, R., (2011): "Effect of copper slag as a fine aggregate on the properties of cement mortars and concrete", Construction & Building Material, Vol. 25, pp. 933-938.

Ameri M., Kazemzadehazad.S., (2012): "Evalution of the use of steel slag in concrete". 25th ARRB Conference – Shaping the future: Linking policy, research and outcomes, Perth, Australia.

Anastasiou, E., Filikas, K.G. and Stefanidou, M., (2014): "Utilization of fine recycled aggregates in concrete with fly ash and steel slag", Construction and Building Materials, Vol. 50, pp. 154-161.

Arino, A.M. and Mobasher, B. (1999): "Effect of ground copper slag on strength and toughness of cementitious mixes", ACI Materials Journal, Vol. 96, No. 1, pp. 68-73.

Arribas I., Vegas I., San-Jose J.T. and Manso J.M., (2014): "Durability studies on steelmaking slag concretes", Materials and Design, Vol. 63, pp. 168-176.

Atici U., (2011): "Prediction of strength of mineral admixture concrete using multivariate regression analysis and an artificial neural network", Expert Systems with Applications, Vol. 38, pp. 9609-9618.

Atis C.D., (2005): "Strength properties of high-volume fly ash roller compacted and workable concrete and influence of curing condition", Cement & Concrete Research, Vol. 35, pp. 1112-1121.

Awoyera Paul O., (2018): "Predictive models for determination of compressive and split-tensile strengths of steel slag aggregate concrete", Materials Research Innovations, Vol. 22, Issue 5.

Bagel L., (1998): "Strength and Pore Structure of Ternary Blended Cement Mortars Containing Blast Furnace Slag and Silica Fume," Cement and Concrete Research, Vol. 28, pp. 1011-1020.

Bagheri A., Zanganeh H., Alizadeh H., Shakerinia M. and Marian M.A.S., (2013): "Comparing the performance of fine fly ash and silica fume in enhancing the properties of concretes containing fly ash", Construction and Building Materials, Vol. 47, pp. 1402-1408.

Bao Xue-ying,Wang Qi-cai and Zhang Lei, (2004): "Study on Quality Optimization of Recycled Concrete Coarse Aggregate Based on Grey Relational Analysis", Bulletin of the Chinese Ceramic Society, Vol. 4.

Bhalla S., Gupta, S., Puttaguna, S. and Suresh, R. (2008): "Bamboo as Green Alternative to Concrete and Steel for Modern Structures", Journal of Environmental Research and Development, Vol. 3, No. 2, (Oct-Dec), pp. 362-370.

Bhanumatidas N. And Kalidas N., (2000): "Durability of concrete role of complementary cementing material", Proceeding of seminar on eco friendly blended cements for economical and durable concrete in the new millennium, organized by Maharastra India Chapter of ACI and ACC, pp. 141-154.

BIS: 10086 (1982-R2004): "Specification for moulds for use in tests of cement and concrete", Bureau of Indian Standards, New Delhi, India.

BIS: 10262 (1982): "Recommended guidelines for concrete mix design", Bureau of Indian Standards, New Delhi, India;

BIS: 1237 (2012 -R2016): "Cement concrete flooring tiles – specification", Bureau of Indian Standards, New Delhi, India.

BIS: 2386 (1963-Part III): “Indian standard methods of test for aggregate for concrete. Part III – specific gravity, density, voids, absorption and bulking”, Bureau of Indian Standards, New Delhi, India.

BIS: 383 (1970): “Indian standard specification for coarse and fine aggregates from natural sources for concrete”, Bureau of Indian Standards, New Delhi, India.

BIS: 516 (1959): “Indian standard methods of test for strength of concrete”, Bureau of Indian Standards, New Delhi, India.

BIS: 5816 (1999): “Indian standard splitting tensile strength of concrete-test method”, Bureau of Indian Standards, New Delhi, India.

BIS: 8112 (1989): “Indian standard 43 Grade ordinary Portland cement specification”, Bureau of Indian Standards, New Delhi, India.

BIS: 9103 (1999): “Indian standard concrete admixtures specification (First Revision)”, Bureau of Indian Standards, New Delhi, India.

BIS: 3085 (1965-R2002): “Method of test for permeability of cement mortar and concrete”, Bureau of Indian Standards, New Delhi, India;

Boga A., R., Murat Ö. and İlker Bekir Topçuc, (2013): “Using ANN and ANFIS to predict the mechanical and chloride permeability properties of concrete containing GGBFS and CNI”, Composites Part B: Engineering Vol. 45, pp. 688-696.

Brindha D. Baskaran T. and Nagan S., (2010): “Assessment of corrosion and durability characteristic of copper slag admixed concrete”, International journal of civil and structural engineering, Vol. 1, No 2, pp.192-211.

Carsana M., Frassoni M. and Bertolini L., (2014): “Comparison of ground waste glass with other supplementary cementitious materials”, Cement and Concrete Composites, Vol. 45, pp. 39-45.

Celik K., Meral C., Petek Gursel A., Mehta P.K., Horvath A. and Monteiro P.J.M., (2015): “Mechanical properties, durability, and life-cycle assessment of self consolidating concrete mixtures made with blended Portland cements containing fly ash and limestone powder”, Cement and Concrete Composites, Vol. 56, pp. 59-72.

Chen C. H., Wu J. K. and Yang C. C., (2006): “Waste E-glass particles used in cementitious mixtures”, Cement Concrete Research, Vol. 36, No. 3, pp. 449–56.

Cheng P. K., Peng Y. N. and Hwang C. L., (2001): "A Design consideration for durability of high-performance concrete", Cement and Concrete Composites, Vol. 23, No.(4-5), pp. 375-380.

Chidiac S.E. and Mihaljevic S.N., (2011): “Performance of dry cast concrete blocks containing waste glass powder or polyethylene aggregates”, Cement & Concrete Composites, Vol. 33, pp. 855-863.

Chithra S., Kumar SRRS., Chinnaraju K. and Ashmita F.A., (2016): “A comparative study on the compressive strength prediction models for high performance concrete containing nano silica and copper slag using regression analysis and artificial neural networks”, Construction and Building Materials,Vol. 114, pp. 528-535.

Chopra P., Sharma R.K. and Kumar M., (2015): “Artificial neural networks for the Prediction of Compressive Strength of Concrete”, International Journal of Applied Science and Engineering, Vol. 13, pp. 187-204.

Chousidis N., Rakanta E., Ioannou I. and Batis G., (2015): “Mechanical properties and durability performance of reinforced concrete containing fly ash”, Construction and Building Materials, Vol. 101, pp. 810-817.

Dabhade A.N, Chaudhari S.R, Gajbhiye A.R., (2015): “Modeling Split Tensile Strength of Recycled Aggregate Concrete Using Regression and Neural Network”, International Journal of Research in Advent Technology (Special Issue 1st International Conference on Advent Trends in Engineering, Science and Technology) Vol. 08.

Deng J. L., (1989): "Basic methods of the grey system", Journal of Grey Systems, Vol. 1, pp. 1-24.

Devi S. and Gnanavel B.K., (2014): “Properties of concrete manufactured using steel slag, 12th Global Congress on Manufacturing and Management, GCMM 2014”, Procedia Engineering, Vol. 97, pp. 95-104,.

DIN: 1048 (part-5): German Standard for determination of Permeability of Concrete.

Douma O.B., Boukhatem B. and Ghrici M., (2014): “Prediction compressive strength of self-compacting concrete containing fly ash using fuzzy logic inference system.”, International Journal of Civil, Environmental, Structural, Construction and Architectural Engineering, Vol. 8, pp. 1265-1269.

Du H. and Tan K.H., (2014): “Concrete with recycled glass as fine aggregates”, ACI materials Journal, Vol. 111, No.05, pp. 47-58.

Ducman V. and Mladenovic A., (2011): “The potential use of steel slag in refractory concrete”, Materials Characterization, Vol. 62, pp. 716-723.

Erdem T. K. and Kirca O., (2008): “Use of binary and ternary blends in high strength concrete”, Construction and Building Materials, Vol. 22, No. 7, pp. 1477-1483.

Ernst and Young, (2017) : World steel association, J. P. Morgan.

Etxeberria M., Pacheco C., Meneses J.M., and Berridi I., (2010): "Properties of concrete using metallurgical industrial by-products as aggregates", Construction and Building Material, Vol. 24, No.9, pp. 1594-1600.

Faleschini F., Alejandro Fernandez-Ruiz M., Zanini M.A., Brunelli K., Pellegrino C. and Hernandez-Montes E., (2015): "High performance concrete with electric arc furnace slag as aggregate: Mechanical and durability properties", Construction and Building Materials, Vol. 101, pp. 113-121.

Farahani J. N., Shafigh P., Alsubari B. and Mahmud H., (2017): "Engineering properties of lightweight aggregate concrete containing binary and ternary blended cement", Journal of Cleaner Production, Vol. 149, pp. 976-988.

Gesoglu M. and Ozbay E., (2007): "Effects of mineral admixtures on fresh and hardened properties of self-compacting concretes: binary, ternary and quaternary systems", Materials and Structures, Vol. 40, No.9, pp. 923-937.

Gülbandılar E. and Koçak Y., (2017): "Prediction of Splitting Tensile Strength of Concrete Containing Zeolite and Diatomite by ANN", International Journal of Economic and Environment Geology, Vol. 8(1), pp. 32-40.

Gupta S., (2013): "Using artificial neural network to predict the compressive strength of concrete containing nano-silica", Civil Engineering and Architecture, Vol. 1, pp. 96-102.

Hadi Muhammad N.S., Nabeel A. Farhan and M. Neaz Sheikh, (2017): "Design of geopolymer concrete with GGBFS at ambient curing condition using Taguchi method", Construction and Building Materials, Vol.140, pp. 424–431.

Huang Y and Liu Z.S., (2010): "Investigation on phosphogypsum–steel slag–granulated blast-furnace slag-limestone cement", Construction and Building Materials, Vol. 24, pp. 1296-1301.

Imbabi M.S., Carrigan C. and McKenna S., (2012): "Trends and developments in green cement and concrete technology", International Journal of Sustainable Built Environment, Vol. 1, No.2, pp. 194-216.

Indian Minerals Yearbook, (2017), (Part- II: Metals & Alloys), Indian Bureau of Mines, Ministry of Mines, Government of India.

Ismail Z.Z. and AL-Hashmi E.A., (2008): "Reuse of waste iron as a partial replacement of sand in concrete, Waste Management", Vol. 28, No. 11, pp. 2048-2053.

Jang J.S., (1993): "ANFIS-Adaptive network-based fuzzy inference system", IEEE Transactions on Systems, Man and Cybernetics, Vol. 23(3). pp. 665-685.

Jiang L., Liu Z. and Ye Y., (2004): “Durability of concrete incorporating large volumes of low-quality fly ash”, Cement and Concrete Research, Vol. 34, pp. 1467-1469.

Jo B., Park S. and Park J., (2007): “Properties of concrete made with alkali-activated fly ash lightweight aggregate (AFLA)”, Cement & Concrete Composites, Vol. 29, pp. 128-135.

Kamali M. and Ghahremaninezhad A., (2015): “Effect of glass powders on the mechanical and durability properties of cementitious materials”, Construction and Building Materials, Vol. 98, pp. 407-416.

Kapoor K., Singh S.P. and Singh B. (2016): “Durability of self- compacting concrete made with recycled concrete aggregates and mineral admixtures “, Construction and Building Materials, Vol. 128, pp. 67-76.

Kermani B.G., Schiffman S.S. and Nagle H.T., (2005): “Performance of the Levenberg–Marquardt neural network training method in electronic nose applications”, Sensors and Actuators B: Chemical, Vol. 110, pp.13-22.

Khajuria C. and Siddique R., (2014): “Use of Iron Slag as Partial Replacement of Sand to Concrete”, International Journal of Science, Engineering and Technology Research, Vol. 3, No. 6.

Khan M.I. and Lyndsdale C.J., (2002): “Strength, permeability and carbonation of high-performance concrete”, Cement and Concrete Research, Vol. 32, pp.123-131.

Kothai P.S. and Malathy R., (2014): “Utilization of steel slag in concrete as a partial replacement material for fine aggregate”, International journal of innovative research in science, engineering and technology, Vol. 3, pp. 11585-11592.

Kumar R., Madan S.K., Devgan N.P. and Lal Roshan (2014): “An experimental study on performance of self compacting concrete containing lime stone quarry fines and fly ash”, Asian journal of civil engineering, Vol. 15, No. 3, pp. 421-433.

Lif C., Atık., Tozu B., Yapay Sinir Agı and Yarmada Cekme Dayanımı, (2011): “Estimation Of Splitting Tensile Strength Of Concretes With Waste Marble Dust And Glass Fibre By Artificial Neural Network“, E-Journal of New World Sciences Academy, Vol. 6, Number: 4.

Liu M., (2011): “Incorporating ground glass in self-compacting concrete”, Construction & Building Material, Vol. 25, pp. 919-925.

Madandoust R. and Ghavidel R., (2013): “Mechanical properties of concrete containing waste glass powder and rice husk ash”, Biosystems Engineering, Vol. 116, No. 2, pp. 113-119.

Malhotra V.M., (2000): “Role of Supplementary Cementing Materials in Reducing Greenhouse Gas Emissions”, Concrete Technology for a Sustainable Development in the 21st Century, London.

Manso J.M., Angel R., Angel A. and Javier J.G., (2011): “The durability of masonry mortars made with ladle furnace slag”, Construction and Building Materials, Vol. 25, pp. 3508-3519.

Manso J.M., Polanco J.A., Losanez M. and Gonzalez J.J., (2006): “Durability of concrete made with EAF slag as aggregate”, Cement & Concrete Composites, Vol. 28, No. 6, pp. 528-534.

Maslehuddin M., Sharif A.M., Shameem M., Ibrahim M. and Barry M., (2003): “Comparison of properties of steel slag and crushed limestone aggregate concretes”, Construction and Building Materials, Vol. 17, pp. 105-112.

Matos A.M. and Sousa-Coutinho J., (2012): “Durability of mortar using waste glass powder as cement replacement”, Construction and Building Materials, Vol. 36, pp. 205-215.

Mehta P.K., (2002): “Greening of the Concrete Industry for Sustainable Development”, Concrete International, pp. 23-28.

Memon, A.H., Radin, S.S., Zain, M.F.M. and Trottier, J.F. (2002): “Effect of mineral and chemical admixtures on high-strength concrete in sea water”, Cement and Concrete Research, Vol. 32, pp. 373-377.

Meyer C., (2002): “Concrete and Sustainable Development”, Special Publication ACI 206, pp. 1-12.

Mohammed S. M., Ismail A., El-Gamal S. and Fitrian H., (2018): “Performances evaluation of binary concrete designed with silica fume and metakaolin”, Construction and Building Materials, Vol. 166, pp. 400–412.

Moura W., Masuero A., Molin D. and Vilela A., (1999): “Concrete Performance with Admixtures of Electrical Steel Slag and Copper Slag Concerning Mechanical Properties”, American Concrete Institute, Vol. 186, pp. 81-100.

Moura W.A., Gonçalves J.P. and Lima M.B.L., (2007): “Copper Slag Waste as a Supplementary Cementing Material to Concrete”, Journal of Materials Science, March, Vol. 42, No. 7, pp. 2226-2230.

Muhmood L., Vitta S. and Venkateswaran D., (2009): “Cementitious and Pozzolanic Behavior of Electric arc Furnace Steel Slags”, Cement and Concrete Research, Vol. 39, No. 2, pp. 102-109.

Muthupriya P, Subramanian K, Vishnuram BG, (2011): “Prediction of compressive strength and durability of high performance concrete by artificial neural networks”, International journal of optimization in civil engineering, Vol. 1, pp. 189-209.

Najimi M., Sobhani J. and Pourkhorshidi A.R., (2011): “Durability of copper slag contained concrete exposed to sulfate attack”, Construction & Building Material, Vol. 25, pp. 1895-1905.

Naniz O.A., Tajar S.F. and Trighat A., (2015): “Utilization of artificial neural network (ANN) to predict the compressive strength of concrete containing slag and silica fume”, International Journal of Material Science Innovations, Vol. 3, pp. 6-15.

Nazari A. and Riahi S. (2011): “Splitting tensile strength of concrete using ground granulated blast furnace slag and SiO2 nanoparticles as binder”, Energy and Building, Vol. 43, No.4, pp. 864-872.

Nochaiya T., Watcharapong W. and Chaipanich A., (2010): “Utilization of fly ash with silica fume and properties of Portland cement–fly ash–silica fume concrete”, Fuel, Vol. 89, pp. 768-774.

Oner, A., Akyuz, S. and Yildiz, R. (2005): “An experimental study on strength development of concrete containing fly ash and optimum usage of fly ash in concrete”, Cement and Concrete Research, Vol. 35, pp. 1165-1171.

Ouda A.S. and Gawwad H.A., (2017): “The effect of replacing sand by iron slag on physical, mechanical and radiological properties of cement mortar”, HBRC Journal, Vol. 13, No. 3, pp. 255-261.

Ozbay Eedogan, Ahmat oztas, Adil baykasoglu and Haken ozbebek, (2009): “Investigation mix proportions of high strength self compacting concrete by using Taguchi method”, Construction and Building Material, vol. 23, pp. 694-702.

Ozer B. and Ozkul M.H., (2004): “The influence of initial water curing on the strength development of ordinary Portland and pozzolanic cement concretes”, Cement and Concrete Research, Vol. 34, No. 1, pp. 13-18.

Pandey S.P. and Sharma R.L., (2000): “The Influence of Mineral Additives on the Strength and Porosity of OPC Mortar”, Cement and Concrete Research, Vol. 30, pp.19-23.

Papadakis, V.G. and Tsimas, S. (2002): “Supplementary cementing materials in concrete Part I: efficiency and design”, Cement and Concrete Research, Vol. 32, pp. 1525-1532.

Papayianni I. and Anastasia E., (2010): “Production of high-strength concrete using high volume of industrial by-products”, Construction and Building Materials, Vol. 24, pp. 1412-1417.

Park S.B., Lee B.C. and Kim J.H., (2004): “Studies on mechanical properties of concrete containing waste glass aggregate”, Cement and Concrete Research, Vol. 34, No.12, pp. 2181-2189.

Patowari P.K., Saha P. And Mishra P.K., (2010): “Artificial neural network model in surface modification by EDM using tungsten- copper powder metallurgy sintered electrodes”, The International Journal of Advanced Manufacturing Technology, Vol. 51, pp. 627-638.

Pellegrino C. and Gaddo V., (2012): “Mechanical and durability characteristics of concrete containing EAF slag as aggregate”, Cement & Concrete Composites, Vol. 32, pp. 663-671.

Pellegrino C., Cavagnis P., Faleschini F. and Brunelli K., (2013): “Properties of concretes with Black/Oxidizing Electric Arc Furnace slag aggregate”, Cement & Concrete Composites, Vol. 37, No.1, pp. 232-240.

Qasrawi H. Shalabi F. and Asi I., (2009): “Use of low CaO unprocessed steel slag in concrete as fine aggregate”, Construction & Building Material, Vol. 23, pp. 1118-1125.

Radlinski M. and Olek J., (2012): “Investigation into the synergistic effects in ternary cementitious systems containing Portland cement, fly ash and silica fume”, Cement Concrete and Composites, Vol. 34, No. 4, pp. 451-459.

Raif B.A., Ozturk M. and Topcu I.B., (2013): “Using ANN and ANFIS to predict the mechanical and chloride permeability properties of concrete containing GGBFS and CNI”, Composites: Part B, Vol.45, pp. 688-696.

Rashad A.M., (2014): “Recycled waste glass as fine aggregate replacement in cementitious materials based on Portland cement”, Construction and Building Materials, Vol.72, pp. 340-357.

Reddy NRM, (2012): “Back-Propagation Neural Network Model to Predict Split Tensile Strength of Metakaolin Blended Fiber reinforced High-Performance-Concrete “, International Journal of Nonlinear Analysis and Applications (IJNAA), Vol. 5(1), pp. 55-58.

Regev Lior, Ronald L., Merksy and Ayalon Ofira, (2014): "Economic Feasibility of Waste Separation at Source: Case Study of Neighborhoods in Haifa, Israel", Presentation at the Proceedings of the Twenty-Ninth International Conference on Solid Waste Technology and Management. Philadelphia, PA.

Rivera F., Martinez P., Castro J. and Lopez M., (2015): “Massive volume fly-ash concrete: A more sustainable material with fly ash replacing cement and aggregates”, Cement and Concrete Composites, Vol. 63, pp. 104-112.

Rodriguez A., Manso J.M., Aragon A. and Gonzalez J.J., (2009): “Strength and workability of masonry mortars manufactured with ladle furnace slag”, Resource, Conservation &

Recycling, Vol. 53, No.11, pp.645-651.

Ross P. J., (1995): "Taguchi technique for Quality Engineering", 2nd ed. New York: McGraw-Hill.

Roy and R.K., (1990): "A primer on the Taguchi method", Van Nostrand Reinhold, New York, vol. 28, pp. 247

Saez-de-Guinoa Vilaplana A., Ferreira V.J., Lopez-Sabiron A.M., Aranda-Uson A., Lausin-Gonzalez C., Berganza-Conde C. and Ferreira G., (2015): "Utilization of Ladle Furnace slag from a steelwork for laboratory scale production of Portland cement", Construction and Building Materials, Vol. 94, pp. 837-843.

Sahmaran M., Yaman I.O. and Tokyay M., (2009): "Transport and mechanical properties of self consolidating concrete with high volume fly ash", Construction and concrete composites, Vol. 31, pp. 99-106.

Schwarz N. and Neithalath N., (2008): "Influence of a fine glass powder on cement hydration: Comparison to fly ash and modeling the degree of hydration", Cement & Concrete Research, Vol. 38, pp. 429-436.

Setien J., Hernandez D. and Gonzalez, J.J., (2009): "Characterization of ladle furnace basic slag for use as a construction material", Construction and Building Materials, Vol. 23, pp. 1788-1794.

Shaikh, F.U.A. and Supit S.W.M., (2015): "Compressive strength and durability properties of high volume fly ash (HVFA) concretes containing ultrafine fly ash (UFFA)", Construction and Building Materials, Vol. 82, pp. 192-205.

Shayan A. and Xu A., (2004): "Value-added utilisation of waste glass in concrete", Cement & Concrete Research, Vol. 34, pp. 81-89.

Shayan A. and Xu A., (2006): "Performance of glass powder as a pozzolanic material in concrete: A field trial on concrete slabs", Cement & Concrete Research, Vol. 36, pp. 457-468.

Shi C. and Qian J., (2000): "High performance cementing materials from industrial slags-a review", Resources, Conservation and Recycling, Vol. 29, pp. 195-207.

Shi C. and Zheng K., (2007): "A review on the use of waste glasses in the production of cement and concrete", Resource, Conservation & Recycling, Vol. 53, pp.234-247.

Siddique R. and Mohammad I.K., (2011): "Supplementary Cementing Materials", London, New York: Springer Heidelberg Dordrecht.

Siddique R., (2004): "Performance characteristics of high-volume Class F fly ash concrete", Cement & Concrete Research, Vol. 34, pp. 487-493.

Singh S.B., Munjal P. and Thammishetti N., (2015): "Role of Water-Cement Ratio on Strength Development of Cement Mortar (Ref. JOBE48)", Journal of Building Engineering (Elsevier), DOI.10.1016/J.Jobe.2015.09.03.

Taha B. and Nounu G., (2008): "Using lithium nitrate and pozzolanic glass powder in concrete as ASR suppressors", Cement and Concrete Composites, Vol. 30, pp. 497-505.

Thomas M., (2011): "The effect of supplementary cementing materials on alkali-silica reaction: a review", Cement and Concrete Research, Vol. 41, pp. 1224-1231.

Tixier R., Devaguptapu R. and Mobasher, B., (1997): "The effect of copper slag on the hydration and mechanical properties of cementitious mixtures", Cement and Concrete Research, Vol. 27, pp. 1569-80.

Topcu I.B. and Sarıdemir M., (2008): "Prediction of compressive strength of concrete containing fly ash using artificial neural networks and fuzzy logic", Computational Materials Science, Vol. 41, pp. 305-311.

Vaitkevicius V., Serelis E. and Hilbig H., (2014): "The effect of glass powder on the microstructure of ultra high performance concrete", Construction and Building Materials, Vol. 68, pp. 102-109.

Vakhshouri B. and Shami N., (2014): "Application of Adaptive Neuro-Fuzzy Inference System in High Strength Concrete", International Journal of Computer Applications , Vol. 101, No.5.

Vidivelli B. and Jayaranjini A., (2016): "Prediction of compressive strength of high performance concrete containing industrial by products using artificial neural networks", International Journal of Civil Engineering and Technology, Vol. 7, pp. 302-314.

Vivek S. S. and Dhinakaran G., (2017): "Fresh and hardened properties of binary blend high strength self compacting concrete", Engineering Science and Technology, Vol. 20, No. 3, pp. 1173-1179.

Wang Q. and Yan P., (2010): "Hydration properties of basic oxygen furnace steel slag", Construction and Building Material, Vol. 24, No. 7, pp. 1134-1140.

Wang X.Y. and Park K.B., (2015): "Analysis of compressive strength development of concrete containing high volume fly ash", Construction and Building Materials, Vol. 98, pp. 810-819.

Wang Z., (2001): "Influence of fly ash on the mechanical properties of frame concrete", Sustainable Cities & Societies, Vol. 1, pp. 164-169.

Wu W., Zhang W. and Ma G., (2010): "Optimum content of copper slag as a fine aggregate in high strength concrete", Materials & Design, Vol. 31, pp. 2878-2883.

Yang E., Yang Y. and Li V., (2007): “Use of high volumes of Fly Ash to improve ECC Mechanical properties and Material greenness”, ACI Materials Journal, Vol. 104, pp. 6.

Yeih W., Fu T.C., Chang, J.J. and Huang R., (2015): “Properties of pervious concrete made with air-cooling electric arc furnace slag as aggregates”, Construction and Building Materials, Vol. 93, pp. 737-745.

Yixin S., Thibaut L., Shylesh M. and Damian R., (2000): “Studies on concrete containing ground waste glass”, Cement Concrete Research, Vol. 30, pp. 91-100.

Yuan Z, Wang LN, Ji X., (2014): “Prediction of concrete compressive strength: Research on hybrid models genetic based algorithms and ANFIS”, Advances in Engineering Software, Vol. 67, pp. 156-163.